FUNCTIONAL ANALYSIS OF WNT3 IN ZEBRAFISH NEURAL DEVELOPMENT

TEH CATHLEEN
B.Sc (Hons.), NUS
M.Sc, NUS

A THESIS SUBMITTED

FOR THE DEGREE OF DOCTOR OF PHILOSOPHY

INSTITUTE OF MOLECULAR AND CELL BIOLOGY

NATIONAL UNIVERSITY OF SINGAPORE

2005

Acknowledgements

I am indebted to my supervisor A/Prof V. Korzh for taking me as his student and appreciated his guidance and encouragement offered throughout my apprenticeship. In addition I would like to thank past and present research fellows in the Fish Developmental Biology laboratory that include DRs Michael Richardson, Alexander Emelyanov, Inna Sleptsova-Friedrich, Serguei Parinov, Dmitri Bessarab, Svetlana Korzh, Marta Garcia, Gao Rong, Chong Shang Wei and Steven Fong for their invaluable teachings. Equally appreciated are fellow colleagues Ms Poon Kar Lai, Ms Chu Lee Thean, Ms Li Zhen, Ms Nguyen Thi Thu Hang, Ms Erin Lam, Mr Toh Wei Chang, Mr Raymond Ng, Mr Ben Chu, Mr William Go, Mr Igor Kondrychyn and Mr Ke Zhiyuan for their intellectual exchange and friendship. Finally I dedicate this thesis to my mother Mdm Tan Chiat Chee, father, Mr Teh Hee Seang, sister Ms Karen Teh and husband Mr Siow Yeen Ping whose love and support empowered me to pursue my interest in research.

Table of Contents

Page No.

Summary

Several members of the Wnt family are expressed in discrete domains along the A-P and D-V axes of the neural tube. However the role of some of these Wnts in neurogenesis remains unclear. Wnt3 is a signaling molecule broadly expressed in the central nervous system (CNS). The homozygous nonsense mutation of WNT3 in human (Q83X) results in autosomal recessive tetra amelia (loss of four limbs) with affected fetuses exhibiting craniofacial, CNS, pulmonary, skeletal, and urogenital anomalies. This thesis aims to define the role of *wnt3* in neural development of zebrafish to shed light onto malformation of the brain in human WNT3 mutants. We isolated zebrafish *wnt3* and detailed its expression pattern during embryogenesis. The expression in the CNS extends from the spinal cord to the diencephalon, where its expression terminates at the zona limitans intrathalamica. Areas with strong expression lie mainly in dorsal brain and include the ventral epithalamus, dorsal thalamus, optic tectum, cerebellum and hindbrain. The ventral extension of *wnt3* expression to dorsal thalamus is unique when compared to other dorsal midline Wnts such as Wnt1, Wnt3a and Wnt10b (Molven et al., 1990; Krauss et al., 1992). In zebrafish, the expression in the dorsal thalamus remained strong at 7dpf, the last stage of our expression analysis. The persistent expression in the anterior CNS suggests continuous participation in neural patterning events throughout embryo development. Our interest in studying the effect of misexpression of *wnt3* in the anterior CNS led us to develop an in vivo electroporation approach that deliver DNA into the brain of zebrafish embryo (Teh et al., 2003). The electroporation technique allowed us to study later patterning events such as stage-dependent fate determination of precursor cells in the developing brain. Co-electroporation of Wnt3 with TOPflash, a Tcf-reporter construct, shows that Wnt3 acts as a canonical Wnt during neural development. We further showed by electroporation that brain specific over-expression of Wnt3 leads to an increase in neuronal differentiation. Conversely, knockdown of *wnt3* transcripts by pan-embryonic injection of anti-Wnt3 morpholino showed that it is required for development of habenula, dorsal thalamus and optic tectum. Additional patterning defects are observed in the dorsal hindbrain

and craniofacial cartilage of Wnt3 morphants. Three different approaches were adopted to analyze defects that arise upon Wnt3 knockdown. First, marker analysis with *nkx2.2*, *pax6b* and *otx2* riboprobes showed that D-V patterning of the brain, specifically the dorsal thalamic locus and optic tectum were affected in Wnt3 morphants. Second, immunohistochemical experiments conducted on 3dpf larvae further demonstrated that processes of neuronal differentiation (∝-acT and ∝-HuC) and cell proliferation (∝-PCNA) were reduced in the dorsal diencephalon, optic tectum and dorsal hindbrain of Wnt3 morphants. The third approach involved Wnt3 morphant analysis in living color transgenic lines. This method demonstrated that formation of habenula was abnormal in morphants and further verified patterning defects observed in dorsal thalamus, optic tectum, dorsal hindbrain and craniofacial cartilage. Finally these results demonstrated the requirement of Wnt3/β- catenin signaling in the patterning of these regions during zebrafish development.

(494 words)

Page No.

List of Tables

List of Figures

Page No.

Page No.

List of Symbols

AC anterior commissure
A-P anterior-posterior
C cerebellum
CNS central nervous system
D-V dorso-ventral
DT dorsal thalamus
E epiphysis
Fig. figure
FP floor plate
H habenula
hpf hours post fertilization
Hyp hypothalamus
Isl-1 islet-1
MHB midbrain-hindbrain boundary
nMLF nucleus of the medial longitudinal fascicle
nPC nucleus of the posterior commissure
OT optic tectum
P1 prosomeric synencephalon
P2 prosomeric dorsal thalamus
P3 prosomeric ventral thalamus
P4 prosomeric preoptic area
P5 prosomeric hypothalamus
PA pretectal area
PBS phosphate buffered saline
PC posterior commissure
PCNA proliferating cell nuclear antigen
POC post-optic commissure
PT posterior tuberculum
Shh sonic hedgehog
SOT supra-optic tract
T telencephalon
Tg tegmentum
tPC track of the posterior commissure
ZLI zona limitans intrathalamica

Chapter I

Introduction

1. Introduction

1.1 General Introduction to Wnt Signaling

The Wnt family is a group of proteins encoded by seven known genes in *Drosophila* and about 19 genes in mammals (mouse and human). The name Wnt is derived from the *Drosophila* gene *wingless* (wg), which plays a role in segment polarity, and the mouse gene *int-1*, which is required for midbrain and cerebellar formation as well as the generation of neural crest cells (Ikeya et al., 1997; McMahon et al., 1992; McMahon and Bradley, 1990). The size of Wnt proteins varies between 350 and 400 amino acids. They contain around 24 highly conserved cysteine residues most probably involved in disulfide bond formation. Wnt proteins are secreted glycoproteins that signal through Frizzled receptors (Bhanot et al., 1996), a family of seven-pass transmembrane proteins. The receptor (Fz) ligand (Wnt) complex activates Dishevelled (Dvl), a cytoplasmic scaffold protein that brings together components of the pathway for efficient transduction (Wharton, 2003). Downstream of Dvl, the Wnt pathway diverges into at least three branches: the canonical or Wnt/β-catenin pathway, the planar cell polarity (PCP) pathway and the Wnt/calcium pathway.

In the canonical pathway (Fig.1.1a), Wnts control early cell fate decisions through the regulation of gene expression by inducing β-catenin-mediated transcriptional activation. Intracellular mediators of the canonical pathway include Dishevelled and β-catenin (Klingensmith et al., 1994; Noordermeer et al., 1994), which promote pathway activation, and Axin and GSK-3β (Nakamura et al., 1998; Siegfried et al., 1992), which negatively regulate the pathway. In the absence of Wnt ligand, cytoplasmic levels of β-catenin protein remain low, as a result of its association with GSK-3β and Axin, which target it for proteolytic degradation (Aberle et al., 1997). Upon binding of Wnt, GSK-3β is inhibited, and cytoplasmic levels of β-catenin increased (Papkoff et al., 1996). This results in translocation of β-catenin into the nucleus, where it functions as a transcriptional co-activator, commonly associating with members of the LEF/TCF family of transcription factors (Brunner et al., 1997;

McKendry et al., 1997; van de Wetering M. et al., 1997) to activate transcription of target genes (Logan and Nusse, 2004). The interaction of Fz proteins with their co-receptors, low-density lipoprotein receptor-related protein 5 (LRP5) and 6 (LRP6) — single-pass transmembrane proteins — is specifically required for signaling through the canonical pathway (Pinson et al., 2000; Tamai et al., 2000; Wehrli et al., 2000).

The planar cell polarity (PCP) pathway [Fig.1.1b; (Huelsken and Birchmeier, 2001)] controls the orthogonal polarity of cells within an epithelium (Strutt et al., 1997), the convergent extension movements during gastrulation (Heisenberg et al., 2000) and the orientation of cochlear cells in the inner ear (Dabdoub et al., 2003). In *D. melanogaster*, activated Fz signals to Dvl, which, in turn, activates the small GTPase RhoA and c-Jun amino (N)-terminal kinase (JNK) (Strutt et al., 1997). In vertebrates, Dvl can signal through both Rho and Rac1 (another small GTPase) to regulate convergent extension movements during gastrulation (Habas et al., 2003). This role of the Rho GTPases and JNK pathways indicates that both the actin cytoskeleton and microtubules are likely to be affected by activation of the PCP pathway.

The Wnt/calcium pathway (Fig.1.1 c) induces ventral but antagonizes dorsal cell fates in early *Xenopus laevis* embryos (Saneyoshi et al., 2002), and also regulates cell movements during gastrulation and heart development (Sheldahl et al., 2003; Veeman et al., 2003). Binding of specific Wnts to Fz receptors leads to signaling through Dvl to induce calcium influx, and activation of protein kinase C (PKC) and calcium/calmodulin dependent protein kinase II (CaMKII) (Kuhl et al., 2000; Sheldahl et al., 2003).

Seven-pass transmembrane receptors such as Frizzled usually signal through trimeric G proteins. Pharmacological and overexpression studies have indicated that G proteins are involved in Wnt signaling (Liu et al., 2001; Slusarski et al., 1997). Recent loss-of-function (LOF) studies also showed a clear role for G proteins in Wnt signaling. Furthermore,

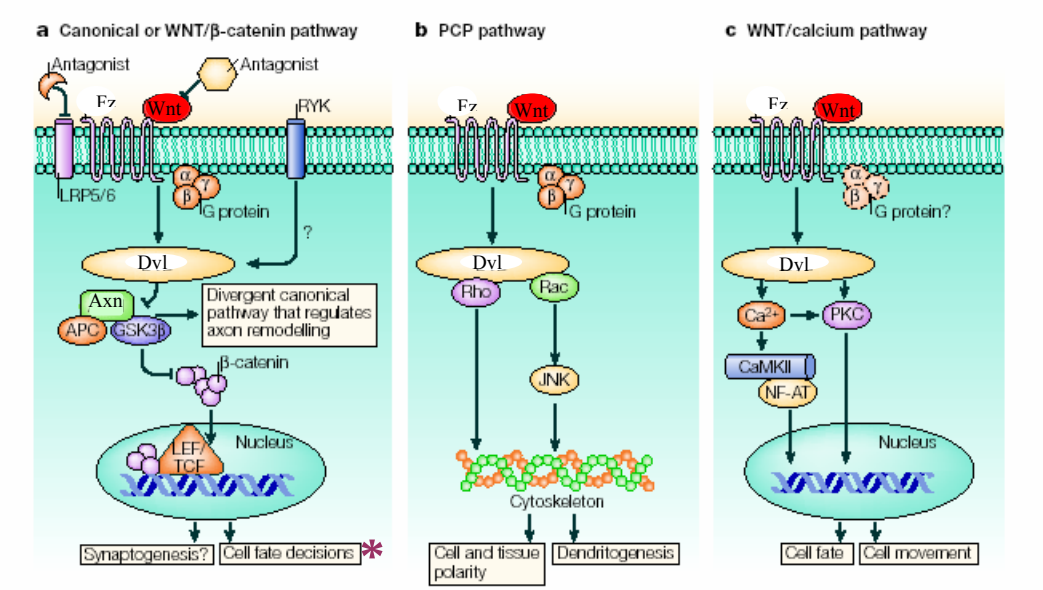

Fig.1.1 | Three main branches of the Wnt signaling pathway. (a) The canonical or Wnt/β-catenin pathway regulates cell fate decisions and possibly synaptogenesis. Binding of WNT to the Frizzled (Fz) and low-density lipoprotein receptor-related protein 5 (LRP5) or LRP6 receptor complexes activates Dishevelled (Dvl). Signaling through Fz requires G-protein activation. Activation of Dvl results in the inhibition of glycogen synthase kinase 3β (GSK3β) and accumulation of β-catenin in the cytoplasm by inducing the disassembly of the destruction complex that is formed by adenomatosis polyposis coli (APC), Axin and GSK-3β. Subsequently, β-catenin translocates to the nucleus where it activates transcription mediated by T-cell specific transcription factor (TCF)/ lymphoid-enhancing factor (LEF). A pathway that diverges downstream of GSK3β has also been shown to control microtubule dynamics. (b) In the planar cell polarity (PCP) pathway, Fz functions through G proteins to activate Dvl, which, in turn, signals to Rho GTPases (Rho or Rac or both). Activation of Rac signals through the c-Jun amino (N)-terminal kinase (JNK). Activation of Rho GTPases induces changes in the cytoskeleton. This pathway has been implicated in cell and tissue polarity and, more recently, in dendritic arborization. (c) In the Wnt/calcium pathway, activation of Dvl induces the release of intracellular calcium and activation of protein kinase C (PKC) and calcium/calmodulin dependent protein kinase II (CaMKII). The role of G proteins is poorly understood. This pathway has been implicated in cell fate and cell movement. NF-AT, nuclear factor of activated T cells (Ciani and Salinas, 2005).

studies in *D. melanogaster* have shown that G proteins are required for the canonical and the PCP pathways (Katanaev et al., 2005). These new findings indicate that G proteins are likely to have a crucial role in Wnt–Fz signaling in vertebrates.

1.2 The Role of Wnt Signaling in Neural Development

Many Wnt ligands and Frizzled receptors are expressed in both the developing and mature nervous systems suggesting their roles in both neural development and function. We focus on the roles of Wnt signaling in the development and maturation of the vertebrate nervous system. The central nervous system (CNS) primordium arises from neural plate, which in turn segregates from embryonic ectoderm and is specified along the anterior–posterior (A-P) and dorso-ventral (D-V) axes in response to inductive signals originating from the underlying dorsal endomesoderm (Lumsden and Krumlauf, 1996). Nieuwkoop proposed a double-gradient model for the A-P specification of neural tube (Nieuwkoop, 1952). According to this model, after the acquisition of neural identity by ectodermal cells, neural tissues are induced to acquire anterior fates. Subsequently, posteriorizing factors induce posterior characteristics in neural tissues that started off with anterior fates. Consequently, a series of morphological vesicles can be distinguished at the anterior end of the neural tube indicating its pattern along the A-P axis. The most anterior end of the neural tube gives rise to the forebrain consisting of the telencephalon and diencephalon, while the more posterior regions form the midbrain, the hindbrain (that is further divided into seven segmental rhombomeres) and the spinal cord. Finally within each of these morphological domains, regional patterning occurs that regulates the formation of specific neural structures with distinct histologies.

The regulation of Wnt signaling for correct A–P specification of the neural tube is accomplished through extracellular antagonists and through intracellular signaling components that are expressed or activated in anterior regions of the neural tube. Several lines of evidence obtained in experiments conducted on animal models ranging from *Xenopus* to mouse indicate that the posteriorizing function of Wnts must be inhibited anteriorly to

generate anterior neural structures. Ectopic expression of Wnts leads to the suppression of anterior fates and the induction of posterior neural markers (Kiecker and Niehrs, 2001). Wnt antagonists are crucial for specification of the anterior neural tube and function by either inhibiting the activity of LRP5/6 or Wnts. For example, the Wnt antagonist DKK1 is expressed by the organizer at the onset of gastrulation and in the anterior axial mesoderm during late gastrulation (Hashimoto et al., 2000). Ectopic expression of DKK1 leads to enlargement of the head, whereas loss of DKK1 function induces microcephaly or loss of anterior structures (Glinka et al., 1998; Kazanskaya et al., 2000; Mukhopadhyay et al., 2001). This function of DKK1 is mediated through its interaction with the LRP6 (MacDonald et al., 2004). In zebrafish, Tlc, a secreted Frizzled-related Wnt antagonist is expressed in the anterior boundary of the neural plate that promote telencephalic fate by antagonizing local Wnt activity at the anterior ectoderm (Houart et al., 2002). Consequently, an enhanced Tlc activity in the anterior margin of the neural plate leads to expansion of telencephalic gene expression into the prospective eye field. Conversely, elimination of Tlc function affects the formation of telencephalon.

The zebrafish *headless* (hdl) mutant illustrates the importance of intracellular signaling components in the canonical pathway. The T-cell factor-3 (Tcf3), a member of the Tcf/Lef family is mutated in this mutant. The wild-type Tcf3 encodes a transcription factor with a β-catenin-binding domain, a single HMG DNA-binding domain and a nuclear localization signal (NLS) motif (Pelegri and Maischein, 1998). The Tcf3 of hdl mutants is truncated. It retains its β-catenin-binding site but lacks the HMG DNA-binding domain as well as the NLS motif. The phenotype is associated with loss of a mechanism that is critical for repressing Wnt signaling. As a result of overt activation of Wnt signaling, zebrafish with maternally and zygotically homozygous *headless* mutations have no eyes or forebrain, and only part of the midbrain, with a concomitant rostral expansion of midbrain and hindbrain markers (Kim et al., 2000). An injection of RNA encoding ΔN-Tcf3 that lacks β-catenin binding but retains its repressor activity, rescued the hdl mutant phenotype.

Subsequent steps after the initial patterning of the early neuroectoderm involve the refinement of initial A/P domains into smaller subdivisions. The cell fate along the D-V axis is known to be controlled by the interplay between dorsally derived factors, such as BMPs and ventrally derived factors, such as Shh (Echelard et al., 1993; Liem et al., 1995). Signaling proteins belonging to the Wnt family (Shimizu et al., 1997; Wong et al., 1994) are also implicated in D-V neural tube patterning. At least 7 vertebrate Wnts are expressed in the embryonic CNS including Wnt1, Wnt3a, Wnt3, Wnt4, Wnt5a, Wnt7a and Wnt7b (Parr et al., 1993), suggesting multiple and complex pattern of Wnt signaling during neural development. *Wnt1* and *Wnt3a* are expressed in extensively overlapping region along the dorsal midline from the diencephalon to the spinal cord. This expression pattern is observed in chick (Cauthen et al., 2001; Hollyday et al., 1995), mouse (McMahon and Bradley, 1990; Parr et al., 1993; Roelink and Nusse, 1991), *Xenopus* (Wolda et al., 1993) and zebrafish (Krauss et al., 1992; Molven et al., 1991), suggesting a conserved role in regional specification of the neural tube. The role of the dorsally expressed *Wnts* in DV neural patterning has been difficult to ascertain through mutagenesis, in part due to overlapping expressions. Still, mutations in these genes do lead to neural patterning defects. *Wnt1*$^{-/-}$ mice fail to develop portions of the midbrain and cerebellum (McMahon et al., 1992; McMahon and Bradley, 1990; Thomas and Capecchi, 1990). However the mutant phenotype is not fully revealed (the spinal cord is normal in *Wnt1*$^{-/-}$ mice) until multiple Wnts are removed. For example *Wnt1*$^{-/-}$*/Wnt3a*$^{-/-}$ mice have additional reduction in the caudal diencephalon, rostral hindbrain, spinal cord and neural crest cells (Ikeya et al., 1997; Ikeya and Takada, 1998; Muroyama et al., 2002). The other indication of a Wnt response in the dorsal neural tube is that β-*catenin*, necessary for the transforming Wnt signal, is transcribed preferentially in the dorsal neural tube (Schmidt et al., 2000). Inactivation of the β-catenin gene in the region of Wnt1 expression resulted in dramatic brain malformation and failure of craniofacial development in mice (Brault et al., 2001). The role of Wnt/β- catenin signaling in neural development is retained in zebrafish as the transgenic Lef1/β- catenin dependent reporter line displays a broad distribution of response in the dorsal

aspect of the neural tube (Dorsky et al., 2002). In contrast to *Wnt1*$^{-/-}$ mice, homozygous mutant embryos from zebrafish line carrying a deficiency allele for *wnt1* and *wnt10b* locus (*Df*^{w5}) are not required for the formation of the midbrain and cerebellum. Relatively mild phenotypic defects such as a greater gap between the medial edges of the MHB constriction and the absence of a fissure between tegmentum and hindbrain in saggital sections are observed instead (Lekven et al., 2003). Hence murine Wnt1 plays a more significant role in neural patterning than their zebrafish counterpart. This suggests that additional genetic redundancy exists amongst other Wnts in zebrafish. The difference in phenotype also highlights the potential functional difference of Wnts between different animal models.

1.3 The Role of Wnt3 in Neural Development

Early neural expression of *Wnt3* has been described in mouse (Bulfone et al., 1993; Roelink and Nusse, 1991; Salinas and Nusse, 1992), *Xenopus* (Christian et al., 1991) and chick (Robertson et al., 2004). When compared to other dorsal midline Wnts such as Wnt1 and Wnt3a, Wnt3 exhibits a broader domain of expression in the dorsal neural tube. However its function as a signaling molecule in neural development remains to be fully addressed. A homozygous nonsense mutation (Q83X) in the *WNT3* gene is identified in 4 fetuses with tetra-amelia that originate from a single family (Niemann et al., 2004). The Q83X mutation truncates WNT3 at its amino terminus and the mutation is associated with the loss of all limbs with concomitant craniofacial and urogenital defects. Neural patterning is also affected in these fetuses with craniofacial defects.

A functional role for Wnt3 in thalamic development has recently been suggested in chick. Exogenous Wnt3 was sufficient to induce the dorsal thalamus marker *Gbx2* in explants isolated posterior to the presumptive zona limitans intrathalamica (zli) (Braun et al., 2003). Until now only Wnt3a has been analyzed in zebrafish development (Buckles et al., 2004). We decided to study the role of zebrafish Wnt3 in development and showed that the expression pattern of the gene is consistent with a role in neural patterning. The expression of *wnt3* is

restricted to the dorsal domain of diencephalon, midbrain, midbrain-hindbrain boundary (mhb), hindbrain and spinal cord of a developing zebrafish embryo. In addition to the dorsal expression in the CNS, *wnt3* expression can also be detected in the anterior floor plate. Dorsal diencephalic expression of *wnt3* is detected at and posterior to zli in the ventral epithalamus and dorsal thalamus. Zli is a local signaling center that was proposed to regulate the acquisition of identity for dorsal and ventral thalamus in chick (Kiecker and Lumsden, 2004). Brain-specific over-expression of Wnt3 via electroporation leads to enhance neuronal differentiation. The knockdown of *wnt3* transcripts by pan-embryonic injection of anti-Wnt3 morpholino showed that it is required for development of the posterior forebrain and midbrain. Specifically, habenula, dorsal thalamus and optic tectum failed to form in Wnt3 morphants. Additional patterning defects are observed in dorsal hindbrain and craniofacial cartilage. Finally, we provide evidence that suggest the involvement of Wnt3/β- catenin signaling in the patterning of above-mentioned regions in the brain.

Chapter II

Materials and Methods

2. Materials and Methods

2.1 DNA Applications

2.1.1 Plasmid Vectors and Host Bacteria

Vectors	**Host Bacteria**
pGem®-Teasy (Promega,USA)	XL1-Blue
pBluescript® SK/KS (Stratagene, USA)	XL1- Blue
pcDNA3.1™(-) (Invitrogen, USA)	DH5α
pEGFP-N2 (BD Biosciences Clontech, USA)	XL1-Blue
pDsRed-Express-C1 (BD Biosciences Clontech, USA)	XL1-Blue
pRL-CMV (Promega, USA)	JM109
TOPflash (Upstate, USA)	XL1-Blue

2.1.2 Bacterial Culture Media

Name	**Descriptions**
Carbenicillin Stock	10 mg carbenicillin sodium salt in 1 ml of water, filter sterilized.
Chloramphenicol Stock	10 mg in 1 ml of methanol, filter sterilized.
Kanamycin Stock	10 mg in 1 ml of water, filter sterilized.
Isopropyl-1-thio-β-D-galactoside (IPTG)	100 mM in sterile water
5-Bromo-4-chloro-3-indolyl-β-D-galactoside (Xgal)	20 mg of Xgal in 1 ml of N,N dimethyl formamide
Luria-Bertani (LB)broth	10 g tryptone 5 g yeast extract 5 g NaCl adjust volume to 1 liter and pH 7.5
LB broth/carbenicillin	75 μg/ml carbenicillin in LB
LB broth/kanamycin	40μg/ml kanamycin in LB
LB broth/glycerol	Transfer 57 ml of 87% glycerol into a beaker and top it up with LB broth to a final volume of 100 ml, filter sterilized.
LB broth agar	15 g agar in 1 liter of LB broth
LB broth agar/ carbenicillin	100 μg/ml ampicillin in LB agar
LB broth agar/ kanamycin	40μg/ml kanamycin in LB agar
LB broth/glycerol	20% (v/v) glycerol in LB broth
TSB solution	85% (v/v) LB broth

	5% (v/v) DMSO 10% (w/v) PEG (Av molecular weight 3,350) 10 mM $MgCl_2$ 10 mM $MgSO_4$
TSBG solution	20 mM glucose in TSB solution

2.1.3 Long-term Storage of Bacteria

Bacterial strains were stored long term at low temperatures (-80°C) in 15 to 40% (v/v) glycerol. A fresh colony was inoculated in 3 ml of LB or LB with specific antibiotics in a 15 ml tube. It was cultured at 37°C until late log or stationary phase (usually overnight). 0.5 ml of LB broth/glycerol was added to 0.5 ml of the bacterial culture (frozen stock will contain 25% glycerol) in a sterile labeled cryovial before being frozen at -80 °C. To revive bacteria from the -80°C stock, a sterile toothpick was used to scrape some of the frozen medium and then streaked on appropriate culture plate e.g. L/A agar. The frozen stocks should not be thawed because each freeze-thaw cycle will result in a 50% loss in cell viability.

2.1.4 Competent Cell Preparation

A single host bacterial colony was inoculated into 3 ml LB and cultured overnight at 240 rpm, 37°C. 0.2 ml of the saturated culture was then inoculated into 50 ml LB in a 500 ml flask. The culture was incubated at 37°C, 240 rpm until it reached exponential phase of approximately A_{600} 0.5 (approximately 3 hrs). The bacterial culture was harvested by centrifugation at 5000 rpm for 10 min at 4°C. The cell pellet was resuspended in 5 ml of ice -cold TSB solution and incubated on ice for 10 minutes before use. 200 µl of the freshly made competent cells was used in each transformation reaction.

2.1.5 Transformation of Bacterial Competent Cells

Transformation was carried out in 1.5 ml Eppendorf tube(s). 20 µl of ligation reaction was added to 200 µl of *E.coli* competent cells. This mixture was then incubated on ice for 30 mins. 800µl TSBG solution was subsequently added into the tube and the entire bacterial cell

suspension was transferred to 10 ml snap-capped tube. The tube was then placed in a 37°C shaker for 1 hr at 240 rpm. The transformation reaction was transferred back to 1.5 ml Eppendorf tubes and spun down using a micro-centrifuge at 6000 rpm for 2 mins at room temperature. The pelleted cells were resuspended in 300 µl of fresh TBSG solution and subsequently plated onto LB agar plates with appropriate antibiotics. For blue/white screening of recombinants, 40 µl of Xgal and 10 µl of IPTG was added to the bacterial suspension before the content was plated onto LB agar plates containing the appropriate antibiotics.

2.1.6 PCR

PCR reaction was carried out in Programmable Thermal Controller PTC-100 (MJ Research Inc. USA). Template DNA (genomic DNA / plasmid / purified DNA) or bacterial culture containing putative transformants (2 µl) were amplified in a reaction volume of 20-100 µl. Each reaction mixture consists of 1× PCR buffer (New England BioLabs Inc), 200 µM of dNTPs, 1 µM of 5'- and 3'- primers and Dynazyme (New England BioLabs Inc, USA) (2 units / 100 µl of PCR reaction). A master mix was usually prepared, dispensed into individual 0.2 ml PCR tubes and respective DNA template was added to each reaction. The reactions were carried out for 35 cycles and each cycle begin with 0.5 min of denaturation at 94°C, followed by 0.5 min annealing at the desired temperature and extension at 72°C for x min (approximately 1 min for each kb of expected amplified product). In order to ensure complete elongation of all PCR products, a 5 min extension of 72 °C was included after the last cycle and the reaction samples were stored at 4 °C until further analysis.

2.1.7 Cloning of PCR Products

To clone PCR products, proper restriction sites were included at the ends of each PCR primer. The restriction sites selected are present in the multiple cloning site of cloning vectors and absent inside the DNA product. To ensure optimal restriction digest of PCR products, flanking nucleotide sequences were added 5' to the restriction site of the primer. The PCR products were separated on agarose gels and the desired DNA fragment was excised and purified with QIAquick® gel extraction kit (Qiagen, USA).

Alternatively, PCR products were amplified by Taq DNA polymerase or Dynazyme (New England BioLabs Inc, USA), purified and directly cloned into pGem®-Teasy vector (Promega Corporation, USA).

2.1.8 Ligation

Traditional Ligation Reaction

T_4 DNA Ligase	1 U
10× T4 DNA Ligase Buffer	2 µl
Vector DNA	1×
Insert DNA	At least 3× that of vector DNA
Autoclaved H_20	Top it up to 20 µl

In order to melt any termini that have re-annealed, vector and insert DNA in H_2O was warmed to 45 °C for 5 min in a sterile microfuge tube before the addition of 10× T4 DNA ligase buffer and the enzyme. Ligation was performed in Programmable Thermal Controller PTC-100 set at 16°C for 16 hr.

Rapid Ligation

T_4 DNA Ligase (3U/ µl)	1
2× Rapid Ligation Buffer	5
Vector DNA	1

Insert DNA	X µl
Autoclaved H_20	Top it up to 10 µl

The rapid ligation reaction (Promega Corporation, USA) was incubated at room temperature for 1 hr or at 4 °C, overnight to obtain maximal number of transformants.

2.1.9 Restriction Digest

There are generally 2 types of restriction digest: a diagnostic and a preparative digest. A diagnostic restriction digest is performed on a small scale to screen for positive recombinants. The larger scale preparative restriction digest is performed to make recombinant constructs that require further manipulations such as sub-cloning into other expression constructs of interest.

The recombinant construct pBluescript SK-EGFP was generated with the aim of making anti-sense EGFP riboprobe. EGFP fragment was obtained from pEGFP-N2 (Clontech, USA) by cutting the latter with SacI and NotI restriction enzymes. The fragment was subsequently subcloned into pBluescript SK (Stratagene, USA) that was similarly treated with SacI and NotI restriction enzymes.

The expression construct pcDNA™3.1(-)-Wnt3 (pExWnt3) was obtained by cutting pGEM®-T Easy-Wnt3 (Michael Richardson, unpublished) with NotI to obtain full-length zebrafish Wnt3 (zfWnt3) DNA fragment of 1537 bp (358 bp 5'UTR, 1068 bp ORF and 74 bp 3'UTR). Similarly, pcDNA™3.1(-) was digested with NotI, dephosphorylated and ligated to NotI digested zfWnt3 fragment. Recombinant clones that contain zfWnt3 inserted in the correct orientation were identified in a typical PCR reaction using T7 and W3R616 reverse primers.

The expression construct pcDNA™3.1(-)-Wnt1 was obtained by cutting pGEM1-Wnt1 (G. Kelly, 1995) with XbaI and HindIII, Wnt1 fragment thus obtained was subsequently

subcloned into similarly cut pcDNA™3.1(-) to give full-length Wnt1 expression construct (pExWnt1)

Diagnostic Digestion (single restriction enzyme)

DNA e.g. plasmid	0.5 µg
10× Reaction Buffer	2 µl
Restriction enzyme	2 units
Autoclaved H_2O	Top up to 20 µl

The contents were added to a microfuge tube in the following order: H2O, buffer, DNA, restriction enzyme. The sample was mixed by pipetting and briefly spun before incubation at the recommended temperature. The standard incubation time is 3 hr. The reaction was stopped by the addition of gel loading buffer and the products were separated by agarose gel electrophoresis.

Preparative Digestion (single restriction enzyme)

DNA	5-20 µg
10× Reaction Buffer	6 µl
Restriction enzymes	10 – 40 units
Autoclaved H_2O	Top up to 60 µl

The above reaction was treated as mentioned for diagnostic digestion and incubated at the recommended temperature (usually 37°C) for a standard period of 3 hr. After incubation, gel loading buffer was added to the reaction mix and the sample was loaded onto an agarose gel. Agarose gel electrophoresis was performed until digested fragments were well separated. The band of interest was cut out of the gel as an agarose block. Purification continued with QIAquick® gel extraction kit (Qiagen, Germany).

2.1.10 Agarose Gel Electrophoresis

Reagent Composition

50× TAE	242 g Tris base 57.1 g glacial acetic acid 100 ml 0.5 M EDTA in H_2O
6× Gel Loading Buffer	0.25% (w/v) Bromophenol blue 0.25% (w/v) Xylene cyanol FF 15% (v/v) Ficoll Type 4000 120 mM EDTA in H_2O
Ethidium Bromide	10 mg/ml in H_2O

To prepare 100 ml of a 1% (w/v) agarose solution, 1 g of agarose was added to 100 ml of 1× TAE and heated in a microwave. The solution was cooled to 55 °C and ethidium bromide was added to a final concentration of 0.5 μg /ml. The gel was allowed to solidify in a gel casting tray. Before loading of samples, the gel was covered with electrophoresis buffer (the same buffer used to prepare the agarose) and 1 μl of 6x gel loading dye was added to every 5 μl of DNA sample. Electrophoresis was performed at 100 volts until dye markers had migrated an appropriate distance. DNA bands in the agarose gel was visualized under UV transilluminator at 304 nm.

2.1.11 Purification of DNA Bands from Agarose Gel

DNA samples were separated by gel electrophoresis and the fragment to be cloned was cut out of the gel and purified by QIAquick® gel extraction kit (Qiagen, Germany). 3 volumes of buffer QG was added to each volume of agarose and incubated at 50 °C until the gel slice had completely dissolved. The sample was applied to QIAquick column to bind DNA. This was then spun down at 14000 rpm for 1 min to allow binding of DNA onto the QIAquick column. The flow through was discarded. Washing was done by the addition of 750 μl PE buffer into

the QIAquick column and spun at 14000 rpm for 1 min. The flow through was discarded. An additional 1 min of centrifugation was carried out to remove any residual ethanol. 40 µl of nuclease-free water was added into the QIAquick column with sterile micro-centrifuge tube and allowed to stand for 1-2 mins. The column was then spun at 14000 rpm for 1 min and the DNA stored at -20°C.

2.1.12 Small-scale Purification of Plasmid DNA

Small-scale preparation of plasmid DNA was carried out using Wizard Miniprep kit (Promega, USA). Overnight bacteria culture in LB medium with the appropriate antibiotic was harvested by centrifugation at 6000 rpm for 2 mins using the 5417C centrifuge (Eppendorf, Germany). After decanting the culture medium, the pellet was resuspended in 250 µl of cell resuspension solution (100 mg/ml RNase A; 10mM EDTA; 25 mM Tris-HCl, pH 7.5). 250 µl of cell lysis solution (0.2 M NaOH; 1% SDS) was added to each sample of the bacterial resuspension and mixed by inverting the Eppendorf tube 4-5 times. 10 µl of alkaline protease solution was added and mixed by inverting 4-5 times. The tubes of mixtures were then left to stand at room temperature for 4-5 mins. 350 µl of Neutralization Buffer (1.32 M KOAc, pH 4.8) was added into each tube and mix by inverting 4-5 times. The neutralized mixture was then spun down at 14000 rpm for 10 mins at room temperature. The supernatant was then decanted into a spin column with a 2 ml collection tube. The spin column with the collection tube was then spun down at 14000 rpm for 1 min at room temperature. The flow through was then discarded. 750 µl of Wash solution with ethanol was added into the spin column. This was spun at 14000 rpm for 1 min at room temperature. The flow through was again discarded. This washing step was repeated with 250 µl of wash solution. This tube was then spun at 14000 rpm for 2 mins at room temperature. The spin column was then transferred to a sterile 1.5 ml micro-centrifuge tube. Plasmid was eluted by the addition of 100 µl of nuclease-free water into the spin column. The tube was allowed to

stand for 1-2 mins before being spun at 14000 rpm for 1 min at room temperature. The spin column was then discarded and DNA stored at -20°C. The DNA was then quantified by optical density reading using spectrophotometer (UV-1601, Shimadzu, Japan).

2.1.13 Large Scale Purification of Plasmid DNA

QIAGEN-tip 100 (midi) or QIAGEN-tip 500 (QIAGEN, Germany) was used to isolate ultrapure plasmid for microinjection or electroporation into zebrafish embryos. *E. coli* cells were lysed by the alkaline/SDS lysis treatment, followed by binding of plasmid DNA to QIAGEN anion-exchange resin. Plasmid DNA was eluted in a high salt buffer and then concentrated and de-salted by isopropanol precipitation. Briefly, 25 ml (midi) or 100 ml (maxi) plasmid containing *E. coli* were lysed with alkali. The cell debris and chromosomal DNA was precipitated with SDS and potassium acetate. After pelleting the debris the plasmid DNA in clarified cell lysate was passed through the pre-equilibrated QIAGEN cartridge by gravity flow. The column was washed twice with Buffer QC and plasmid was eluted with buffer QF. Eluted DNA was precipitated with 0.7 volume of isopropanol at room temperature and centrifuged at 15,000 g, 4°C for 30 min. The DNA pellet was rinsed with 70% (v/v) EtOH and centrifuged for 5 min at 15,000 g, RT. The pellet was dried and suspended in sterile deionized H_2O.

2.1.14 Design of Antisense Oligonucleotides (morpholinos)

Morpholinos (MOs) were obtained from Gene Tools, LLC, USA. The antisense oligonucleotide sequences were designed to bind to the 5'UTR or flanking sequences including the initiation methionine or sequence at exon-intron junctions. To minimize the possibility of non-specific effects, we designed at least two MOs complementary to non-overlapping sequences for each gene. MO sequences are listed in Table 2.2.

MOs were resuspended from lyophilized powder, and then diluted to 1mM stock in 1X Danieau's solution and stored at -80 °C. The MOs were diluted to the appropriate concentration and these were injected into the yolk cell of one to two cell stage embryos using a MPPI-2 pressure injection system (Applied Scientific Instrumentation, Eugene, OR, USA). The designs of MOs used were based on recommendations provided by Gene Tools, LLC (http://www.gene-tools.com).

2.2 RNA Procedures

2.2.1 Isolation of total RNA from zebrafish tissue

Total RNA was isolated from dechorionated zebrafish embryos using RNeasy® mini kit (Qiagen, Germany). Samples were first lysed and homogenized in denaturing guanidine isothiocyanate (GITC) containing buffer which inactivates RNases and thus ensure isolation of intact RNA. Ethanol was added to the lysate to provide appropriate binding condition and then applied to RNeasy mini column for further purification. The zebrafish embryos were collected at desired stages and placed in 1.5 ml Eppendorf tube. Excess liquid was siphoned out from the tube. 350 µl of RLT buffer was added into the tube and the embryos were pulverized. The lysate was then spun down at 14000 rpm, RT, for 3 mins. The supernatant was decanted into a sterile 1.5 ml Eppendorf tube. 350 µl of 70% ethanol was added into the clear lysate and mixed well. This mixture was transferred to an RNeasy mini spin column sitting in a 2 ml collection tube. The column was then spun at 10000 rpm for 15 sec. The flow through was discarded. 350 µl of RW1 buffer was pipetted into the RNeasy column to wash, the column was centrifuged at 10000 rpm for 15 sec. The flow through was discarded. 80 µl of RNase-free DNAse (Qiagen, Germany) incubation mix was then added directly onto the RNeasy silica-gel membrane and allowed to stand on the bench at room temperature for 15 mins. Afterwhich, another 350 µl RW1 buffer was added into the RNeasy column and spun down at 10000 rpm for 15 sec. The flow through was discarded. 500 µl of RPE buffer was

pipetted on the column and spun down at 10000 rpm for 15 sec. The flow through was discarded and the washing step was repeated with another 500 µl of RPE buffer. The column was then spun at 10000 rpm and for 2 mins and the flow through discarded. The column was then spun down for an additional 1 min to remove any residual trace of ethanol. Column was then transferred to a sterile 1.5 ml Eppendorf tube. Total RNA was eluted by the addition of 40 µl of RNase-free water onto the RNeasy membrane and spun for 2 mins. The RNA was then quantified by optical density reading using the spectrophotometer (UV-1601, Shimadzu, Japan).

2.2.2 Quantitation of Total RNA

4 µl of total RNA was diluted with 196µl of water and its absorbance was read at A_{260}. The amount of RNA was quantitated using the following formula:

Total RNA = $(A_{260})^{1} \times (40\ \mu g/ml/A_{260})^{2} \times (50)^{3} \times$ (total sample volume)

1. A_{260} is the absorbance of the solution at 260 nm,

2. 40 $\mu g/ml/A_{260}$ is a fixed conversion factor relating absorbance to concentration for RNA

3. 50 is the dilution factor

2.2.3 One-step RT-PCR

Total RNA (DNAse I treated) was isolated from zebrafish embryos using RNeasy® Mini Kit (Qiagen, Germany). cDNA for RT-PCR analysis was synthesized using Qiagen® OneStep RT-PCR kit (Qiagen, Germany) containing an optimized combination of Omniscript reverse transcriptase, Sensiscript reverse transcriptase and HotStartTaq DNA polymerase and the reaction was carried out according to the manufacturer's instructions. The technique was used to amplify *wnt3* transcripts from wild type and zebrafish embryos injected with *wnt3* morpholino against the exon1 and intron 1 splice site. Primers used are listed in Table 2.1. A typical program used was as follows: cDNA synthesis at 50°C for 30 mins; denaturation at 94°C for 15 mins for 1 cycle followed by 40 cycles of [94°C for 1 min, 61°C for 1 min and

72°C for 1 min] and final extension at 72°C for 5 mins. The annealing temperature wa changed according to the primer design.

Table 2.1. Primers Used in RT-PCR to Detect *wnt*3, *wnt3a* and *β-actin* Transcripts.

Gene name	**Abbreviation**	**Direction**	**Sequence**
wnt3	W3F371	Forward	5'CTGGTTGGATTTCTCATGTGC3'
wnt3	W3R427	Reverse	5'ATAGCCTCCAAGCACCCGAGA3'
wnt3	W3R536	Reverse	5'GGCAGAAGCGCAGCTGTTTT3'
wnt3	W3R616	Reverse	5'ACCACGGAACTGGTGCTGA3'
wnt3	W3R1296	Reverse	5'GCAGGTCACAGCCTTCGAT3'
wnt3	W3*R* 1436	Reverse	5'TTATTTACATGTATGTACGTCGTA3'
wnt3a	Wnt3aF501	Forward	5'CCGAGAGTTTGCTGATGCC3'
wnt3a	Wnt3aR1060	Reverse	5'ACTTGCAGGTGTGAACATCGT3'
Beta-actin	β-actin-F	Forward	5'CTTCCTTCCTGGGTATGGAATC3'
Beta-actin	β-actin-R	Reverse	5'CGCCATACAGAGCAGAAGCCA3'

2.3 Zebrafish

2.3.1 Fish Maintenance

Zebrafish embryos (*Danio rerio*) were obtained from the fish facility of the Institute of Molecular and Cell Biology. The fish were maintained according to the method described by Westerfield (Westerfield, 1995). Fishes were fed three times per day with brine shrimps or brown powder. They were kept under photoperiod cycle set at 14 hrs of daylight and 10 hrs of darkness. Crosses were set after the third meal at 1800 hr with a divider and wire mesh. Divider was removed at desired time to stimulate spawning behavior. Embryos were then collected by a sieve and rinsed thoroughly to remove any waste materials attached to the chorion.

2.3.2 Stages of Embryonic Development

In developmental studies, the accurate staging series is a tool important for defining the timing of various developmental events. The embryos used were raised at 28.5°C and staged according to standard practice (Kimmel et al., 1995). Embryos which were used for analysis at 48 and 72 hpf were treated with 1-phenyl-2-thiourea (PTU; 1.5 mg/ml) at 19 hpf to prevent

the formation of melanin (Westerfield, 1995). The approximate stage of a live embryo was determined by examination under a dissecting stereomicroscope (Leica, Germany).

2.3.3 Microinjection into Blastula Stage Zebrafish Embryos

Morpholinos and plasmid DNA samples for injection were prepared at different concentrations in 1X Danieu solution (58 mM NaCl; 0.7 mM KCl; 0.4 mM $MgSO_4$; 0.6 mM $Ca(NO_3)_2$; 0.5 mM HEPES, pH 7.6). Samples were injected into the cytoplasmic stream of 1-2 cell stage zebrafish embryos using a MPPI-2 pressure injection system (Applied Scientific Instrumentation, USA). Injected zebrafish embryos were raised in 1X egg water (1 ml contains 10% NaCl; 0.3% KCl; 0.4% $CaCl_2$; 1.63% $MgSO_4.7H_2O$).

Table 2.2. A List of Morpholinos Used in This Study.

Gene name	Abbreviation	Sequence	Targeted region	Reference
wnt3	W3-E1I1 MO	5'CTACTCACCACCAGATGGGATAGCC3'	Exon-intron 1	Unpublished
	5'UTRW3 MO	5'GGCAAAGATGGATGCTTGAGAGAAT3'	5'UTR	Unpublished
	W3ctl-MO	5'**T**TACT**G**ACCAC**T**AGATG**T**GATA**C**CC3'	Exon-intron 1	Unpublished

Note: Nucleic acid bases that are underlined – represent intron sequence; nucleic acid bases that are highlighted in bold represent base changes.

2.3.4 Use of Anesthetic to View Embryos

When viewing live embryos after 19hpf, the embryos may twitch or move which affects the process of imaging. Anesthetic was used to facilitate embryo manipulation. Briefly, 400 mg of Tricaine (3-amino benzoic acidethylester) (Sigma, USA) powder was dissolved in 97.9 ml of sterile water and the pH was adjusted to 7 using Tris pH 8.0. Usually, 5 µl of this solution was added in a Petri dish with selected embryos and after a few seconds, the embryos could be transferred for viewing.

2.3.5 Staining with Acridine Orange (AO)

To determine whether there is increased cell death, *in vivo* staining with acridine orange (AO; Calbiochem, USA) which detects DNA double strand breaks in dying cells, was used. AO is a cell-permeable, cationic fluorescent dye that when bound to DNA, it is spectrally very similar to fluorescein, with an excitation maximum at 502 nm and an emission maximum at 525 nm. Dechorionated embryos were placed in glass petri-dish containing AO (150 mg/ml) and incubated for 20min. Afterwhich, the solution in the petri dish was changed three times at 10 min interval. The embryos were then viewed under UV dissecting scope. The dead cells are seen as bright green dots.

2.3.6 Cartilage Staining

The Alcian Blue staining protocol was modified from Neuhauss (Neuhauss et al., 1996). Embryos at 5 dpf (PTU treated) were anesthetized in 0.02% buffered tricaine (Sigma, USA) and fixed overnight in 4% phosphate buffered paraformaldehyde (PFA) at 4°C. After washing in phosphate buffered saline (PBS), embryos were digested with proteinase K (10 μg/ml, 30 min) to better expose the cartilage elements to the dye, briefly fixed with 4% PFA and extensively washed with PBS. The treated embryos were then stained overnight in 0.1% Alcian Blue dissolved in acidic ethanol (70% ethanol, 5% concentrated hydrochloric acid), washed extensively in acidic ethanol, rehydrated and stored in PBS containing 50% glycerol before photography.

2.4 Electroporation into the Anterior Neural Tube of Zebrafish Embryo

2.4.1 Construction of the Electroporation Chamber

The top three quarters of a GenePulser® cuvette (Bio-Rad Laboratories, USA) (Fig. 2.1A) with a 0.4-cm electrode gap was sawed off for convenient manipulation of the embryo. The chamber was half-filled with 1% molten agarose in Hank's buffer (137 mM NaCl, 5.4 mM KCl, 0.25mM Na_2HPO_4, 0.44 mM KH_2PO_4, 1.3mM $CaCl_2$, 1.0 mM $MgSO_4$, 4.2 mM

$NaHCO_3$, pH 7.2). The volume of agarose depends on the age of the embryo, the older the embryo, the longer its A-P axis and the more agarose required. Typically for 24-26 hpf zebrafish embryos the chamber was filled with 3-4 drops of molten 1% agarose in Hanks buffer from a disposable plastic Pasteur pipette (app. 120 μl). The chamber top was sealed with Parafilm®. To cast a well for the embryo, a blunted microinjection capillary [tip diameter, 0.05 mm; outer diameter (o.d.), 1 mm; inner diameter (i.d.), 0.58 mm; length, 100mm] (Sutter Instruments, USA) (the lower capillary on Figure 1B), which functions as a mould, was inserted vertically through parafilm into the center of the chamber containing the molten agarose to the level shown by a line on Fig.2.1B and held in place by parafilm until the agarose had set. The well was formed after removing both capillary and Parafilm® from the electroporation chamber.

The size of the well was further adjusted with the blunt capillary by flicking away excess agarose such that the well could comfortably fit the posterior body of the embryo including the yolk cell. An uninjected embryo was positioned in the well to check the quality of the well. Factors that contribute to well quality include the following:-

1. The agarose well should lightly grip the yolk cell without injuring the embryo.
2. The anterior neural tube should be above agarose level.
3. The position of the embryo in the electroporation chamber should remain unchanged after its exposure to the series of electric pulses.

At least 5 electroporation chambers should be prepared for each session as not all agarose wells would be good enough for electroporation. Besides, an initially optimal well would deteriorate with repeated use. A diagram of the electroporation chamber is shown in Figure 2.1C. The electrode plate is shown in black, and the troughs filled with Hank's buffer are in gray. The embryo was placed in the agarose well (gray circle) surrounded by Hank's buffered agarose (yellow). The orientations of the embryo that resulted in unilateral transgene expression (blue line) or bilateral expression in the cerebellum and telencephalon (brown line) are indicated. Troughs, 1 mm wide (made by the flat end of the blunt capillary with an outer

diameter of 1mm), were made close to the electrode plates, and Hank's buffer was added to fill the electroporation chamber to the top. The height of the well is important; for efficient electroporation into the brain, the head must protrude from the well. Embryo could be manipulated using a blunt capillary under a dissecting microscope with large working distance. The Olympus SZ40 dissecting microscope with transillumination and an additional source of descending light through the gooseneck is particularly suitable for this purpose.

2.4.2 Microinjection of DNA into the Neural Tube of Zebrafish Embryos

Wild type zebrafish embryos 24–48 hours post-fertilization (hpf) were maintained in Hank's buffer containing 0.2 mM PTU, starting from 19 hpf, to inhibit pigment formation. Before microinjection, zebrafish embryos were dechorionated, anesthetized using tricaine and placed dorsal-side up in wedge-shape wells made in 1% agarose and covered by Hank's buffer. For DNA injection into a cavity of a neural tube, a standard microinjection protocol with sharp micropipette (upper capillary, Fig.2.1B) was used. Using the micromanipulator, the injection capillary (micropipette) was inserted into the yolk cell of the embryo approximately at the level of first somite (solid line), then through the floor of the hindbrain near the otic vesicle (broken line) and into the IV ventricle (arrowhead), Fig.2.1D. DNA was injected using the MPPI-2 pressure injection system (Applied Scientific Instrumentation, USA), Fig.2.2, until the neural tube was visibly distended. The injection volume would vary depending on the age of the embryo (Table 2.3). Each injected embryo was immediately transferred into the electroporation chamber filled with Hank's buffer (to prevent damage to the injected embryo that may result during transfer).

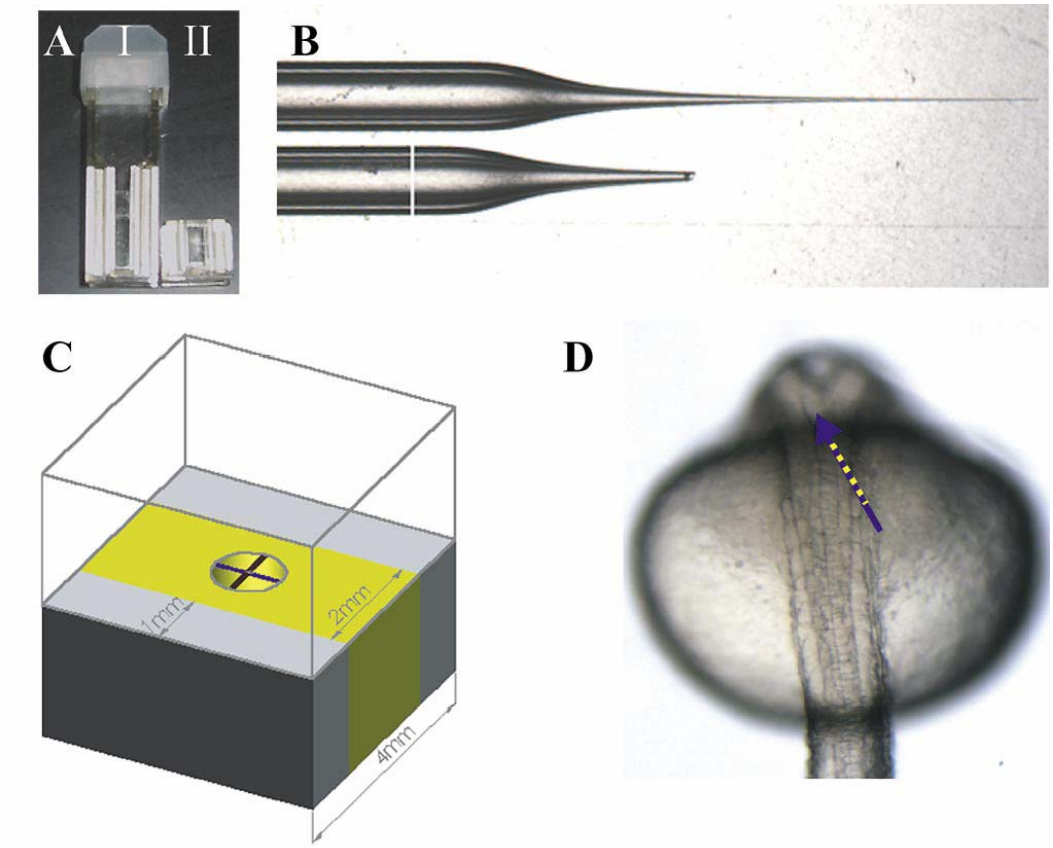

Fig.2.1. Equipment used for in vivo electroporation into zebrafish brain.
(A) The conductivity chamber (II), formed by removing the top three quarters of a Gene Pulser cuvette (I). (B) The sharp microinjection pipette (top) and the blunt micropipette (bottom) as a mould to make the agarose well. The back of the micropipette was used to make 1-mm wide troughs that lined the sides of the electroporation chamber. (C) A diagram of the electroporation chamber. The electrode plate is shown in black, and the troughs filled with Hank's buffer are in gray. The embryo was placed in the agarose well (gray circle) surrounded by Hank's buffered agarose (yellow). The orientations of the embryo that resulted in unilateral transgene expression (blue line) or bilateral expression in the cerebellum and telencephalon (brown line) are indicated. (D) The introduction of DNA into the cavity of the neural tube. Anesthetized wild-type zebrafish embryos (24 h post-fertilization) were placed in wedge shape wells, dorsal-side up. The pipette was pushed into the yolk cell of the embryo flanking the first somite (solid line), through the floor of the hindbrain near the otic vesicle (broken line), and into the IV ventricle (arrowhead).

2.4.3 Electroporation Using Uniform Electric Field

The position of the microinjected embryo was adjusted such that the posterior body including tail and yolk cell was inside the well while its head protruded from the well. Hank's buffer was removed to such a level that it barely covered the head. The electroporation chamber containing the embryo was then clamped tightly between the metal plates of the safety stand. The electro Square Porator ECM 830 (BTX®; Genetronics, USA), (Fig. 2.3) was used to generate square electric pulses phased 1 s apart. Conditions of electroporation depended upon stage of embryo development (Table 2.3). After electroporation, zebrafish embryos were left to recover in small (d=40 mm) glass Petri dishes containing 2.5 ml of Hank's buffer with PTU. This modification of electroporation is used, firstly, for unilateral delivery of DNA into a relatively limited number of cells in experiments that require analysis of cell morphology and, secondly, for massive bilateral DNA delivery into cerebellum (Fig. 2.4, D and E). The above mentioned modification of uniform electroporation into the anterior central nervous system of a zebrafish embryo had been published in BioTechniques (Teh et al., 2003).

Table 2.3. The Effect of Pulse Conditions on Survival and EGFP^{+} Expression in Electroporated Zebrafish Embryos.

Stage of Development	Pulse Conditions	Neuronal and Skin Expression			Total Neuronal^{+}	Skin Only	Deformed Embryos	Total	Injection Vol. / nl
		FB/MB/HB	FB/MB	MB/HB					
24hpf	20V, 5 pulses, 50msec each pulse	6	3	10	19	3	12	34	4-6
24hpf	20V, 2 pulses, 100msec each pulse	3	3	9	15	12	1	28	4-6
30hpf	20V, 5 pulses, 50msec each pulse	1	8	2	11	18	2	31	4-6
36hpf	20V, 5 pulses, 50msec each pulse	0	0	0	0	25	5	30	5-7
36hpf	25V, 5 pulses, 50msec each pulse	2	3	0	5	2	23	30	5-7
42hpf	25V, 5 pulses, 50msec each pulse	0	5	0	5	9	16	30	8-10
48hpf	25V, 5 pulses, 50msec each pulse	2	13	0	15	5	10	30	8-10

Note: Each electroporation condition performed on each developmental stage was completed in a single experiment. Each embryo's anterior neural tube was positioned parallel to the electrode plate. As a result, all zebrafish embryos expressed GFP in a unilateral manner.

Fig. 2.2. Microinjection was performed using the MPPI-2 pressure injection system and dissection microscope Olympus SZ40.

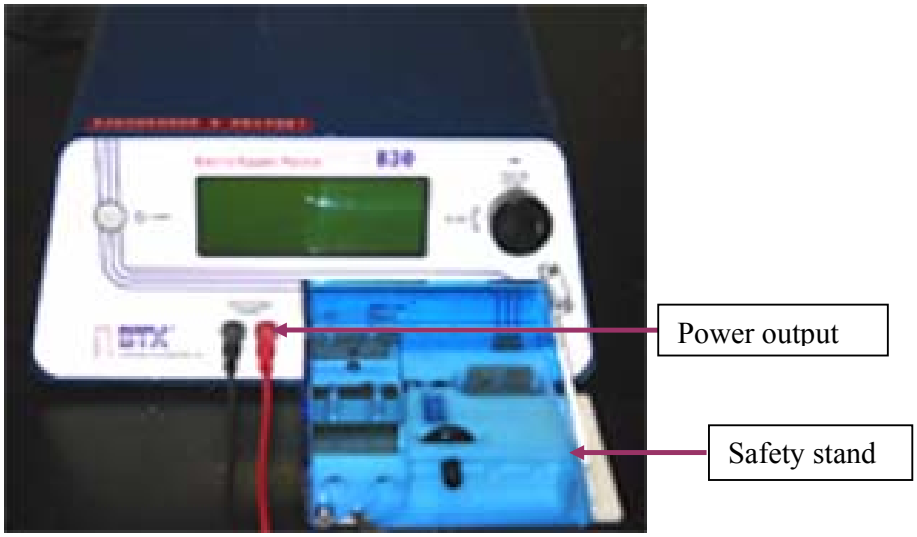

Fig. 2.3. Electro Square Porator ECM 830 with the attached safety stand.

2.4.4 Electroporation Using Converging Electric Field

The electric field becomes non-uniform when electrodes of dissimilar size were used. To generate a converging electric field a plate electrode was used for the cathode and a 1mm rod electrode for the anode. This modification resulted in massive targeted unilateral transgene expression in the neural tube (Teh et al., 2005). The setup is similar to that for electroporation using uniform electric field but requires an additional pair of electrodes. A pair of electrodes with L-shaped shaft configuration and an electrode length of 1mm (Genetrodes, model 516; Genetronics, USA) were connected to the power output of the Electro Square Porator ECM 830. The 3mm gap between the electrodes was maintained by the Genetrode holder with an adjustable distance that varies between 1-10mm (Genetronics, USA). In order to generate a converging electric field, the Genetrode holder was positioned such that the negative electrode touched the electrode plate of the electroporation chamber while the positive electrode was placed 1mm from the neural tube of the embryo (Fig. 2.5). 19-24 hpf zebrafish embryos were optimally electroporated with 4 pulses (spaced 1sec apart) of 17 volts, with pulse duration of 50msec each. After electroporation, the embryos recovered in Petri dishes containing Hank's buffer with PTU.

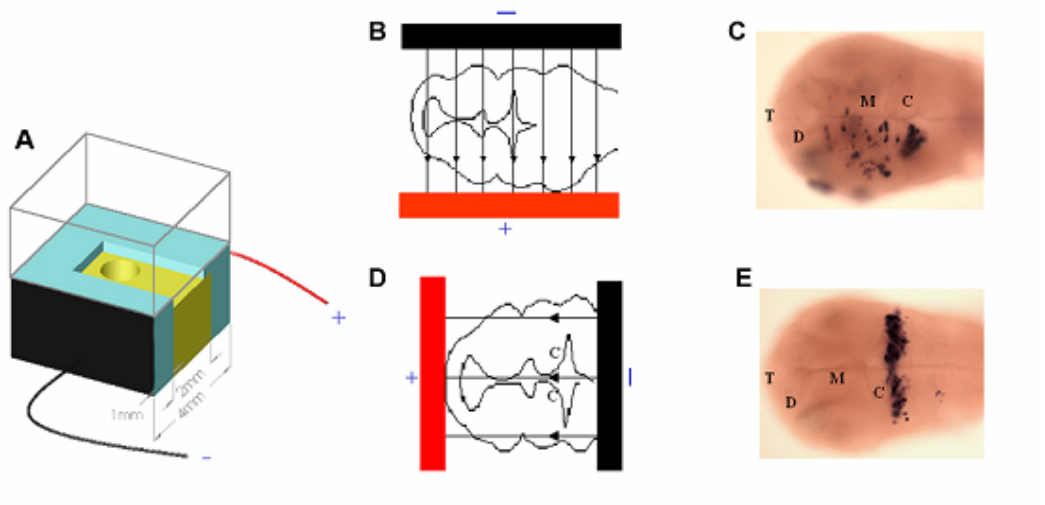

Fig. 2.4. Electroporation using uniform electric field**.** A –electroporation chamber, B – scheme of unilateral electroporation [medial to lateral (M-L) axis]**,** C – typical outcome of unilateral electroporation along M-L axis, GFP mRNA is detected by whole mount *in situ* hybridization in the brain of 48 hpf embryo shown in dorsal view, D – scheme of electroporation along anterior to posterior (A-P) axis, E – typical outcome of electroporation along A-P axis, GFP mRNA is detected by whole mount *in situ* hybridization in the cerebellum of 48 hpf embryo.

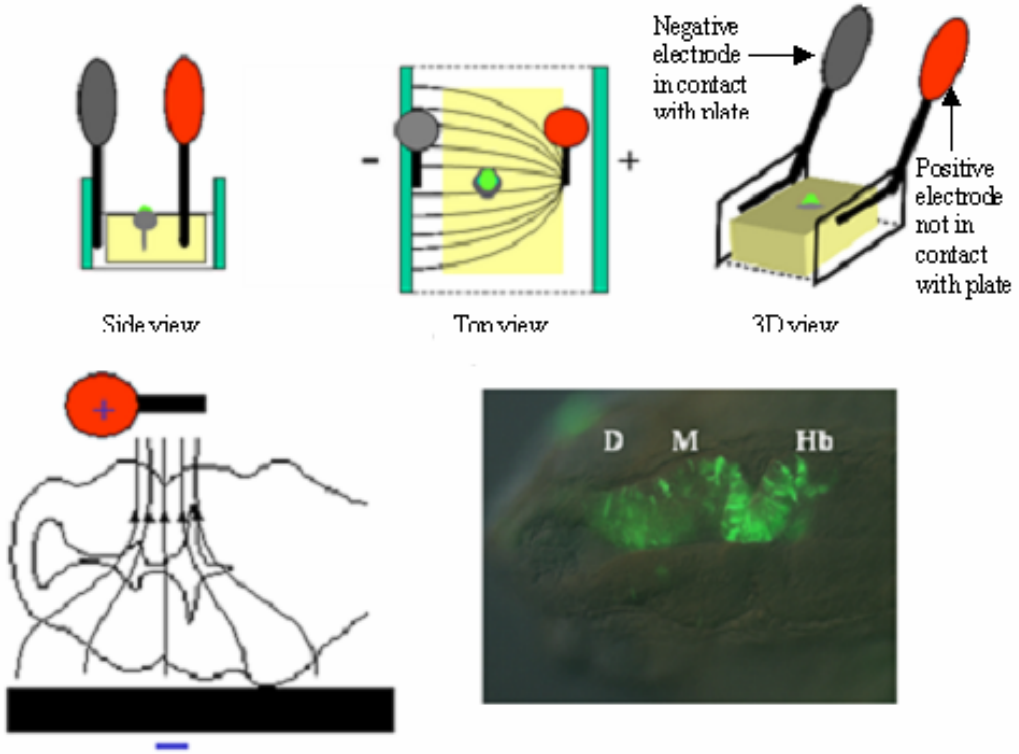

Fig.2.5. Electroporation using converging electric field. The anterior neural tube of electroporated embryo massively express GFP on the right hand side 12 hrs post electroporation as observed under fluorescent microscope (d – diencephalon, m – midbrain, hb – hindbrain).

2.5 *In situ* Hybridization

2.5.1 Antisense Probe Synthesis

5 μg of plasmid DNA was linearized at the 5' end of the cDNA insert by a preparative restriction enzyme at 37°C for 3 hrs. 1μg of linearized DNA was used to synthesize the DIG/fluorescein probe. The reaction was performed at 37°C for 2 hrs in a total volume of 20 μl containing 2 μl of 10X transcription buffer (Ambion, USA), 2 μl of DIG/Fluorescein-NTP mix [10 mM ATP, 10 mM CTP, 10 mM GTP, 6.5 mM UTP and 3.5 mM DIG/Fluorescein-UTP (Boehringer Mannheim, Germany)], 1 μl of RNase inhibitor (40U/ μl) (Promega, USA). 2 μl of RNase-free DNase I was used to digest the DNA template at 37°C for 15 mins following this reaction. The probes used in this study are listed in Table 2.4.

Table 2.4. A List of Molecular Markers Used in this Study.

Marker	Plasmid	Linearizing enzyme	RNA polymerase	References
egfp	pBluescript	SacI	T7	Teh et al, Chapter 2
wnt3	pGem®-Teasy	SalI	T7	Teh et al, unpublished
wnt3a	pGem®-Teasy	SmaI	T7	(Dorsky et al., 1998)
wnt1	pGEMI	EcoRI	Sp6	(Kelly and Moon, 1995)
nkx2.2	pBluescript	BamH1	T7	(Barth and Wilson, 1995)
otx2	pBluescript	BamH1	T7	(Mori et al., 1994)
pax6b	pBluescript	EcoRI	T7	(Nornes et al., 1998)

2.5.2 Probe Clean Up

Sample was adjusted to a volume of 100 μl with RNAse-free water. 10 μl of β-mercaptoethanol was added to 1 ml of RLT buffer. This was followed by the addition of 350 μl of the RLT buffer to the diluted RNA sample that was subsequently mixed with 250 μl of 96-100% ethanol. This whole volume was then transferred to an RNeasy mini spin column that had been inserted into a collection tube. The spin column and collection tube was spun at 10000 rpm for 15 sec. The flow through was then discarded. 500 μl of RPE buffer was pipetted into the spin column and spun at 10000 rpm for 15 sec. Flow through was discarded and replaced with another 500 μl of RPE buffer. The column was spun at 10000 rpm for

another 2 min. The RNeasy column was then removed and placed onto a new 1.5 ml Eppendorf tube and 30-50 µl of Rnase-free water was added into the RNeasy column and allowed to stand for 1 min. RNA probe was then eluted out by micro-centrifuging the column at 10000 rpm for 1 min. The RNA probe was then stored at -80°C.

2.5.3 Preparation of Staged Zebrafish Embryos

Embryos were dechorionated manually using a pair of 26 gauge hypodermic needles and fixed overnight at room temperature. Staged embryos were fixed in 4% PFA (paraformaldehyde) /PBS (0.8% NaCl; 0.02% KCl; 0.0144% Na_2HPO4; 0.024% KH_2PO4, pH 7.4) for 12 to 24 hrs at room temperature or overnight at 4°C. Embryos younger than 15hpf were fixed before dechorionation and the chorion was removed afterwards. Embryos older than 16hpf were dechorionated before fixation. After fixation, the embryos were washed in PBST (0.1% Tween-20 in PBS) twice for 1 min each, followed by four times for 20 mins each on a nutator at room temperature.

2.5.4 Proteinase K Treatment

This step is carried out for embryos that are older than 14 somites (>16 hpf). Embryos were treated with 10 µg/ml of proteinase K in PBST at room temperature. The time of exposure to proteinase K is dependent on the stage of the embryos and the specific activity of proteinase K, which vary from batch to batch. In general, the guidelines are listed in Table 2.5. To stop the proteinase K reaction, the proteinase K solution was completely removed, and the embryos were fixed again in 4% PFA/PBS for 20 mins at room temperature. Embryos were then washed in PBST twice for 1 min each and four times for 20 mins each.

Table 2.5. Permeabilization of Zebrafish Embryos and Larvae by Proteinase K.

Stage of Embryo Development/hpf	Time of Proteinase K Treatment/ min
< 24	3
24-32	5
33-36	10
37-40	15
41 <	20

2.5.5 Prehybridization

Prehybridization was performed by replacing PBST with prehybridization buffer [50% formamide; 5X SSC; 50 μg/ml heparin; 500 μg/ml tRNA; 0.1% Tween-20; pH 6.0 (adjusted by citric acid)]. And the tube was placed at 68°C for at least 4 hrs.

2.5.6 Hybridization

2 - 4 μl of DIG-labeled probe (signal intensity dependent) was diluted in 200 μl of hybridization buffer and denatured at 70°C for 5 mins, followed by 5 mins on ice. Selected embryos were placed in a 1.5 ml Eppendorf tube with the original prehybridization solution removed and replaced with probe added in prehybridization solution. The reaction was incubated overnight at 68°C in a circulating water bath. The next morning, the embryos were incubated in four changes of washing solution containing decreasing percentage of formamide in 2X SSCT. The four washing solutions contained stepwise decrease in formamide from 50% formamide in 2X SSCT at the first wash to 12.5% of formamide in 2X SSCT at the last wash. All washings were conducted in the 68°C water bath for a period of 15 min per wash. This was followed by the fifth wash with 2X SSCT without formamide for 15 min. And the final wash of 0.2X SSCT at 68°C for 1 hr.

2.5.7 Preparation of Preabsorbed Anti-DIG and Anti-Fluorescein Antibody

Commercial anti-DIG and anti-Fluorescein-AP antibodies (Boehringer Mannheim, Germany) should be preincubated with intact biological specimen, to decrease the staining background

and to increase signal-to-noise ratio. In the study, sheep anti-DIG-AP and anti-Fluorescein-AP antibodies (Boehringer Mannheim, Germany) were diluted to 1:200 and 1:50 respectively in PBS containing 5% blocking reagent (Roche, Germany) and incubated with 4% PFA fixed zebrafish embryos on a nutator at 4°C overnight. After that, the antibody solution was transferred to a new tube and diluted to 1:2000 and 1:500 with PBS in 5% blocking reagent, 10 µl of 0.5 M EDTA (pH 8.0) and 5 µl of 10% sodium azide in a final volume of 10 ml to prevent bacterial growth. The preabsorbed antibody was stored at 4°C and can be reused several times.

2.5.8 Incubation with Preabsorbed Antibodies

After hybridization and post hybridization washes, the embryos were incubated in PBS containing blocking solution for a minimum of 1 hr at room temperature to remove background signal generated from non-specific binding of antibodies. After removing the blocking solution, the embryos were incubated with preabsorbed anti-DIG-AP antibody at 4°C overnight.

2.5.9 DIG or Fluorescein Staining

After antibody incubation, embryos were washed 4X 20 min in PBS followed by 2X 15 min in detection buffer (100 mM Tris pH9.5, 5 mM Mg Cl2, 100 mM NaCl). NBT/BCIP color substrate development was performed in the presence of 0.3375 µg/ml of nitroblue tetrazolium (NBT) (Sigma-Aldrich, USA) and 0.175 µg/ml of 5-bromo, 4-chloro, 3-indolil phosphate (BCIP) (Sigma-Aldrich, USA) dissolved in detection buffer. Fast red staining was prepared by dissolving 1/2 of the fast red tablet (Roche Biochemicals, Switzerland) in 1ml detection buffer (100 mM Tris pH8.2, 5 mM Mg Cl2, 100 mM NaCl). The content was clarified by centrifugation and mixed with equal part of Naphthol AS-MX phosphate (Sigma, MO, USA) solution (500 µg/ml in fast red detection buffer). Color development was allowed

to proceed in the dark and monitored occasionally under light microscopy until the desired intensities were achieved. For control and experimentally injected sets of embryos, the staining procedures were initiated and stopped at the same time. The staining reaction was stopped by a 2X 5 min PBS wash followed by 4% PFA fixation for a minimum period of 30 min before storing the appropriately stained embryos in PBS containing 50% glycerol.

2.5.10 Two-color Whole Mount *In Situ* Hybridization

In two-color whole mount *in situ* hybridization, two distinct RNA probes labeled with DIG or Fluorescein were applied to the same embryos in equal ratio. After incubation at 68°C overnight, the probe in hybridization solution was removed and washing was carried out as stated in section 2.5.6. The DIG detection was carried out first and the procedure is as described in section 2.5.9.

Following the DIG staining with NBT/BCIP, the embryos were washed with MA buffer (0.15 M maleic acid; 0.1 M NaCl; pH 7.5) twice for 10 mins. To remove the phosphatase activity of first antibody, the embryos were incubated with glycine buffer (0.1 M, pH 2.2) for 30 mins at room temperature. After that, the embryos were washed with PBST four times for 10 mins each and then incubated in blocking buffer (5% Blocking reagent in MA buffer, Roche, Germany) at room temperature for 1 hr. Embryos were subsequently incubated with anti-Fluorescein-AP antibody overnight at 4°C.

To detect the fluorescein signal, the embryos were washed with MA buffer (50 mM maleic acid; 100 mM NaCl) at room temperature for 4X 20 min. Afterwhich, the MA buffer was replaced with fast-red staining as stated in section 2.5.9.

2.6 Cryostat Sectioning

2.6.1 Mounting Specimen for Cryostat Sectioning

Fixed or stained embryos were first transferred into molten 1.5% bactoagar - 5% sucrose in a detached Eppendorf cap at 50°C. A syringe needle was used to adjust the embryo in a desired orientation in a gradually hardening agar. After the agar block solidified, a small block was cut with razor blade to mount the sample in the proper position. The block was then transferred into 30% sucrose solution and allowed to stand at 4°C overnight.

2.6.2 Freezing and Collecting Sectioned Specimens

Subsequently, the block was placed on the frozen surface of a layer of frozen tissue freezing medium (Reichert-Jung, Germany) on a prechilled tissue holder. The block was then coated with one drop of freezing medium and frozen in liquid nitrogen until the block had solidified completely. The frozen block was placed into a cryostat chamber (Leica, Germany) for 30 mins to be equilibrated with temperature of chamber that is at -25°C. Normally, 10 μm thick sections were cut and collected on a Leica CM1900 Cryostat (Leica, Germany) and the sections were transferred onto warmed subslides. The slides were dried at 42°C on the hotplate for 30 mins. The sections were rinsed briefly with PBST and cover slips were placed on the slides with several drops of 50% glycerol/PBS. The slides were sealed with nail polish and ready for observation under microscope.

2.6.3 DAPI Staining

Some sections were further analyzed by staining with 1.5 ml of diluted 3.5 μM DAPI (4', 6-diamidine-2-phenylidole-dihydrochloride) and incubated in the dark for 20 mins. Afterwhich, the slides were tilted to remove the staining solution. Washing was carried out using PBST for 2X 20 mins. Once washing was completed, coverslip was mounted as described in section2.6.2.

2.7 Protein Applications

2.7.1 Immunohistochemical staining

2.7.1.1 Primary Antibody Incubation

Fresh embryos were collected at appropriate stages and were fixed in Histochoice (AMRESCO Inc.,USA) overnight at RT. The next morning, the embryos were washed in MA buffer pH 7.4 for 4X 20 min each and blocked with 5% blocking reagent (Roche, Germany) for 1 hr on a nutator at RT. Primary antibodies were non-preadsorbed. They were diluted to the desired titer in MA buffer containing blocking solution and incubated with embryos on a nutator at 4°C overnight. All antibodies were used at 1:200 dilutions. The following day, the embryos were washed 4X 20 min in MA buffer, pH7.4 and incubated overnight at 4°C with the appropriately tagged and pre-adsorbed secondary antibodies (1: 200 dilution) in MA blocking solution. The embryos were then washed 4X with MA buffer, pH7.4 on a nutator at RT.

To detect the signal of secondary peroxidase conjugated antibodies the staining solution containing 1 tablet of diamino benzidine (DAB) was incubated with the embryos. The staining solution was prepared by dissolving a DAB tablet (Sigma, USA) in 5 ml of water and the solution was clarified by centrifugation. DAB staining was initiated by the addition of 1 µl of 33% hydrogen peroxide (H_2O_2) to every 1 ml of DAB staining solution. The staining was observed under a stereomicroscope and stopped when an appropriate staining level was reached. To stop the reaction, the embryos were rinsed in water and then washed in PBS containing 0.1% Tween20. Embryos were prepared for viewing and photography as stated in section 2.5.9.

2.7.1.2 Immunostaining on cryosections

Embryos of desired stages were fixed and sectioned as described in sections 2.6.1 and 2.6.2. After the slides were heated at 42°C for ½ hr, the slides were placed in a plastic container

with a modified stage. The slides were rinsed twice with PBST (0.8% NaCl; 0.02% KCl; 0.0144% Na_2HPO_4, 0.024% KH_2PO_4, pH 7.4; and 0.1% Tween 20). Afterwhich, blocking was carried with 5% blocking reagent (Roche, Germany) in PBS at RT for a period of 1 hr. The primary antibody was diluted to the appropriate titer, added to each slide and incubated at 4°C overnight. The primary antibody was subsequently removed from the slides and washing was carried out with PBS for 4X 5 min in a washing chamber with a 50 ml capacity. Pre-adsorbed secondary antibodies (Alexa Fluor 488; Alexa Fluor 594, Molecular Probes, USA) diluted 1:200 in PBS containing 5% blocking reagent was applied to the slides and incubated at room temperature for 4 hr. The washing with PBS was repeated for 4X 5 min. Once washing was completed, a coverslip was mounted onto each slide using 50% glycerol/ 50% PBS as the mounting medium. The specimen was overlaid with coverslip and sealed with nail polish. The slides were kept in a slide carrier in the dark.

2.7.2 Dual-Luciferase® Reporter Assay

Promega's Dual-Luciferase® Reporter (DLR™) Assay System sequentially measures the activities of firefly (Photinus pyralis) and Renilla (Renilla reniformis, also known as sea pansy) luciferases in the same sample. The kit was used in TOPFLASH (TCF reporter plasmid, Upstate, USA)) luciferase analysis where following expression constructs pEGFPN2, TOPFLASH, pRL-CMV (Promega, USA), pExWnt1 or pExWnt3 were concomitantly electroporated into 24hpf neural tube of zebrafish embryo. Zebrafish embryos that were successfully electroporated upon and hence misexpressed the cocktail of expression vectors in the neural tube were identified under Olympus SZX12 stereomicroscope (Olympus, Japan) equipped with the ultraviolet lamp and GFP filter 12 hours post electroporation. Embryos that positively misexpressed EGFP reporter in the neural tube were pooled into groups of three and lysed in 50µl of T-PER (Pierce Biotechnology, USA), containing c∅mplete protease inhibitor cocktail (Roche Diagnostics GmbH, Germany) using pestle in 1.5 ml microcentrifuge tubes. The firefly luciferase reporter activity that was activated upon

binding of TCF (T- Cell factor) to its recognition sites in TOPflash was assayed by adding 20µl of embryo lysate to 100µl of Luciferase Assay Reagent II. Quenching of firefly luciferase luminescence and concomitant activation of Renilla luciferase (from pRL-CMV) was accomplished by adding 100µl of Stop & Glo® Reagent to the same sample tube immediately after quantitation of the firefly luciferase reaction. Luciferase activity obtained from *Renilla* function functioned as the reporter for electroporation efficiency. All luminescence data points obtained were normalized against Renilla luciferase activity and measured with a manual luminometer.

2.8 Microscopy

2.8.1 Mounting and Photography Using Upright Light Microscope

Stained embryos were fixed in 4% PFA for 1hr at room temperature and selected embryos were washed with PBST twice for 15 mins each and transferred to 50% glycerol/PBS, equilibrated at room temperature for several hours. A single chamber was made by placing stacks of 1-5 small cover glasses on both side of a 25.4 X 76.2 mm microscope slide to facilitate whole mount examination. Stacks of small cover slips became tightly bound to one another 1 hr after placing a drop of Permount between them. The selected embryo was transferred to the chamber in small drop of 50% glycerol/PBS and oriented by a needle. A 22X44 mm cover slip with a small drop of the same buffer covered the chamber. The orientation of the embryo can be adjusted by gently moving the cover slip.

For flat specimen, the yolk of the selected embryo was removed completely with needles. The de-yolked embryo was then placed onto a slide with a small drop of 50% glycerol /PBS and adjusted to a proper orientation by a needle. Excess liquid was removed with tissue paper. A small fragment of cover slip (a little bit bigger in size then the specimen) was put onto the embryo. This was done carefully to avoid air bubbles being trapped. A drop of 50% glycerol/PBS was added to fill the space under the cover glass. The specimen was sealed with nail polish along the edge of the cover glass to prevent it from drying. Photos were taken

using a camera mounted to an AX-70 microscope (Olympus, Japan) or Axiophot2 photomicroscope (Zeiss, Germany) with software supplied by the manufacturers or Kodak Gold 400ASA films were used during photo sessions. Overlapping of images and measuring of relative areas were performed using Adobe® Photoshop 5.5.

2.8.2 Confocal Microscopy and Imaging

EGFP expression in live transgenic embryos was monitored under a Leica MZ FLIII stereomicroscope equipped for UV epifluorescence viewing. For detailed analysis, embryos were anesthetized as described in Section 2.3.4. A viewing chamber was made by cutting a 12.5 mm diameter hole at the bottom of a 35 mm plastic petri dish and placing a coverslip outside to cover the hole. The coverslip was secured to the base of the petri dish using clear adhesive. 0.8% agarose was poured into the chamber and cut glass micro-capillaries of 0.8 cm were placed into the agarose to make lined spaces. Confocal images were acquired using Zeiss LSM510 scanning laser (Carl Zeiss Inc., Germany) using 488 nm excitation and 510-550 nm band-pass filters. Serial optical sections were taken at desired intervals using a 10X Plan-Neofluar 0.3 objective. Raw image collection and processing were performed using the LSM510 Software (Carl Zeiss Inc., Germany). Combined images were made on Adobe® Photoshop5.5.

Chapter III

Results

3. Results

3.1 Expression Pattern of Zebrafish Wnt3

A cDNA clone containing the full length coding region corresponding to zebrafish *wnt3* was obtained in this laboratory by 5'- and 3'-RACE and a complete cDNA, 1537 bp in length was subsequently amplified as a single PCR product (Michael Richardson, unpublished data). Sequence analysis of the amplified clone shows that it is related to other vertebrate Wnt3 orthologs (Fig.3.1). Vertebrate Wnt3 sequences are highly conserved with amino acid identities of approximately 90% between species. Homology analysis of Wnt3 and Wnt3a orthologs supports the assignment of the zebrafish protein as Wnt3 (Fig. 3.2). In comparison, DNA sequence identities between the open reading frames are less conserved between zebrafish and the mammalian *Wnt3*. Pair distance analyses conducted between zebrafish and human and between zebrafish and mouse generate percent identities of 75.4 and 76.0 respectively (data not shown). In contrast, zebrafish *wnt3a* transcript only shares 72% DNA sequence identity in the open reading frame with *wnt3* (Fig.3.3). RT-PCR analysis detected the presence of *wnt3* transcripts from 100% epiboly that reach maximal expression by neurula stage. In comparison, *wnt3a* exhibits an earlier onset of transcription at 6hpf (Fig. 3.4).

The early neural tube of a vertebrate embryo consists of four regions, the forebrain, midbrain, hindbrain and spinal cord. The forebrain consists of the telencephalon and diencephalon. Several major subdivisions could be distinguished in the diencephalon; epithalamus, dorsal thalamus, ventral thalamus and hypothalamus. Caudal to the thalamus are the pretectum dorsally and posterior tuberculum ventrally. These regions lie in a transition zone between diencephalon and midbrain. The midbrain consists of the optic tectum dorsally and tegmentum ventrally. The hindbrain subdivides into seven segmental rhombomeres encompassing the cerebellum at anterior rhombomere 1 followed by rhombomeres 2-7 at the posterior end. We will describe patterns of *wnt* gene expression and discuss results obtained from our functional analyses with reference to the above subdomains of the brain.

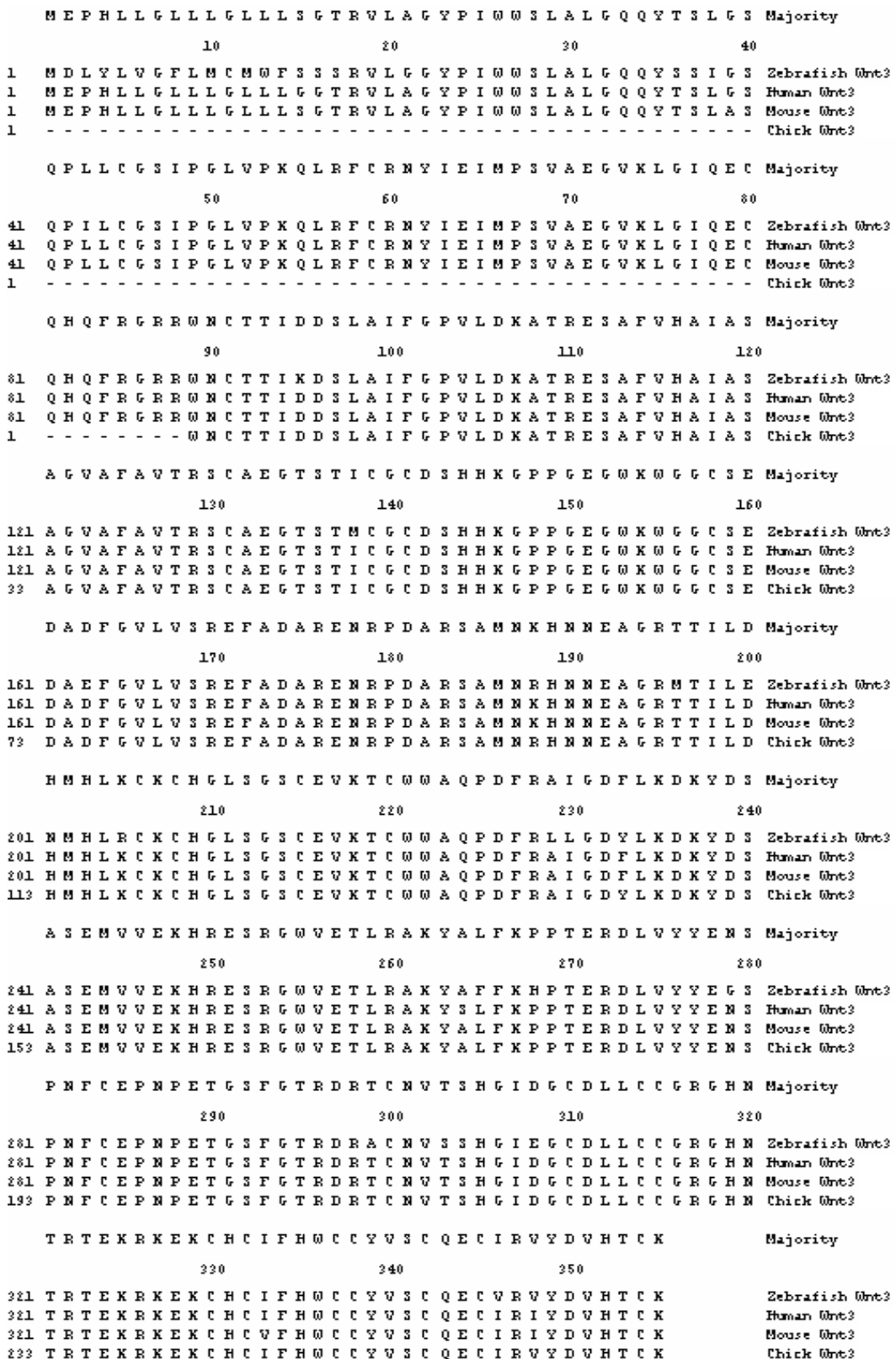

Fig.3.1 ClustalW alignment of zebrafish Wnt3 with human, mouse and chickWnt3.

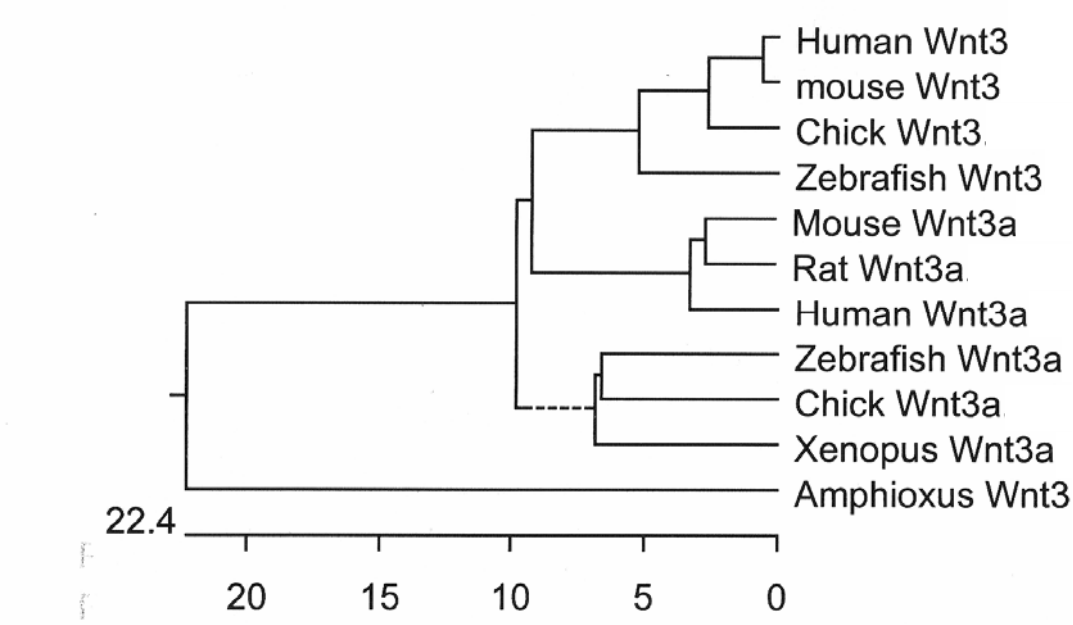

Fig.3.2 Homology analysis of vertebrate Wnt3 and Wnt3a protein sequences. Zebrafish Wnt3 clusters with other vertebrate Wnt3 orthologs.

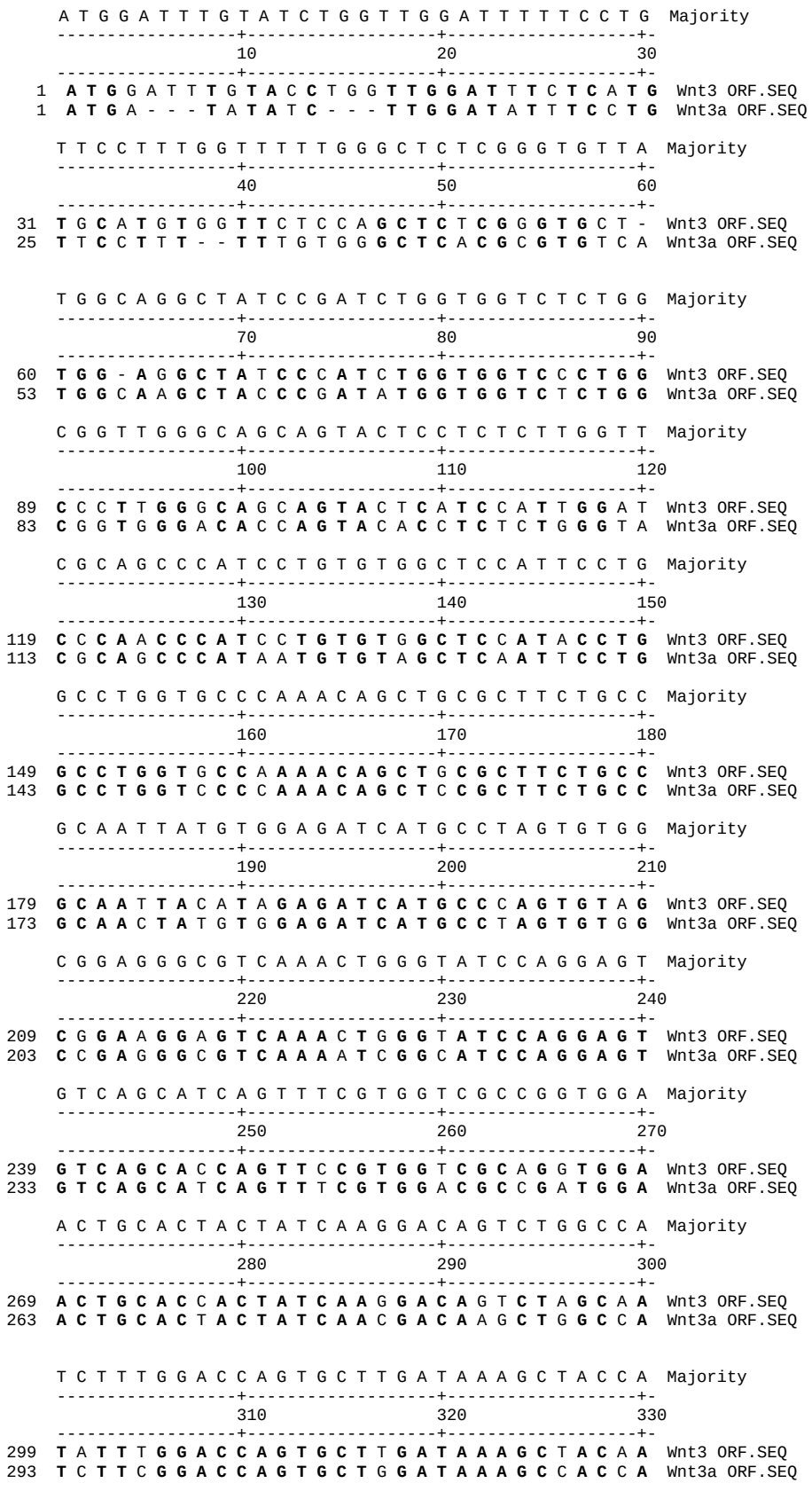
A T G G A T T T G T A T C T G G T T G G A T T T T T C C T G Majority
10 20 30
1 ATGGATTTGTACCTGGTTGGATTTCTCATG Wnt3 ORF.SEQ
1 ATGA---TATAT---TTGGATATTTCCTG Wnt3a ORF.SEQ
T T C C T T T G G T T T T T G G G C T C T C G G G T G T T A Majority
40 50 60
31 TGCATGTGGTTCTCCAGCTCTCGGGTGCT- Wnt3 ORF.SEQ
25 TTCCTTT--TTGTGGGCTCACGCGTGTCA Wnt3a ORF.SEQ
T G G C A G G C T A T C C G A T C T G G T G G T C T C T G G Majority
70 80 90
60 TGG-AGGCTATCCCATCTGGTGGTCCCTGG Wnt3 ORF.SEQ
53 TGGCAAGCTACCCGATATGGTGGTCTCTGG Wnt3a ORF.SEQ
C G G T T G G G C A G C A G T A C T C C T C T C T T G G T T Majority
100 110 120
89 CCCTTGGGCAGCAGTACTCATCCATTGGAT Wnt3 ORF.SEQ
83 CGGTGGGACACCAGTACACCTCTCTGGGTA Wnt3a ORF.SEQ
C G C A G C C C A T C C T G T G T G G C T C C A T T C C T G Majority
130 140 150
119 CCCAACCCCATCCTGTGTGTGGCTCCATACCTG Wnt3 ORF.SEQ
113 CGCAGCCCCATAATGTGTGTAGCTCAATTCCTG Wnt3a ORF.SEQ
G C C T G G T G C C C A A A C A G C T G C G C T T C T G C C Majority
160 170 180
149 GCCTGGTGCCCAAAACAGCTGCGCTTCTGCCC Wnt3 ORF.SEQ
143 GCCTGGTCCCCAAACAGCTCCGCTTCTGCCC Wnt3a ORF.SEQ
G C A A T T A T G T G G A G A T C A T G C C T A G T G T G G Majority
190 200 210
179 GCAATTATACATAGAGATCATGCCCAGTGTAG Wnt3 ORF.SEQ
173 GCAACTATGTGGAGATCATGCCTAGTGTGG Wnt3a ORF.SEQ
C G G A G G G C G T C A A A C T G G G T A T C C A G G A G T Majority
220 230 240
209 CGGAAGGAGTCAAACTGGGTATCCAGGAGT Wnt3 ORF.SEQ
203 CCGAGGGCGTCAAAAATCGGCATCCAGGAGT Wnt3a ORF.SEQ
G T C A G C A T C A G T T T C G T G G T C G C C G G T G G A Majority
250 260 270
239 GTCAGCACCAGTTCCGTGGTCGCAGGTGGA Wnt3 ORF.SEQ
233 GTCAGCATCAGTTTCGTGGACGCCGATGGA Wnt3a ORF.SEQ
A C T G C A C T A C T A T C A A G G A C A G T C T G G C C A Majority
280 290 300
269 ACTGCACCCACTATCAAGGACAGTCTAGCAA Wnt3 ORF.SEQ
263 ACTGCACTACTATCAACGACAAGCTGGCCA Wnt3a ORF.SEQ
T C T T T G G A C C A G T G C T T G A T A A A G C T A C C A Majority
310 320 330
299 TATTTGGACCAGTGCTTGATAAAGCTACAA Wnt3 ORF.SEQ
293 TCTTCGGACCAGTGCTGGATAAAGCCACCA Wnt3a ORF.SEQ

```
    G G G A A T C T G C G T T T G T T C A T G C T A T T G C C T  Majority
    -----------------+------------------+------------------+-
                     340                350                360
    -----------------+------------------+------------------+-
329 G G G A A T C T G C A T T T G T T C A T G C G A T T G C C T  Wnt3 ORF.SEQ
323 G A G A A T C G G C G T T C G T G C A T G C T A T A G C C T  Wnt3a ORF.SEQ

    C G G C T G G G G T A G C C T T T G C T G T G A C C C G T T  Majority
    -----------------+------------------+------------------+-
                     370                380                390
    -----------------+------------------+------------------+-
359 C A G C T G G A G T A G C A T T T G C A G T A A C C C G T T  Wnt3 ORF.SEQ
353 C G G C G G G G G T A G C C T T C G C T G T G A C A C G G G  Wnt3a ORF.SEQ

    C T T G T G C G G A G G G G T C C T C C A C T A T G T G T G  Majority
    -----------------+------------------+------------------+-
                     400                410                420
    -----------------+------------------+------------------+-
389 C A T G T G C A G A G G G G A C C T C C A C T A T G T G T G  Wnt3 ORF.SEQ
383 C T T G T G C G G A A G G C T C A G C C A C C A T C T G C G  Wnt3a ORF.SEQ

    G C T G T G A C T G C C G T C G T A A A G G C C C G C C G G  Majority
    -----------------+------------------+------------------+-
                     430                440                450
    -----------------+------------------+------------------+-
419 G C T G T G A C T C C C A T C A T A A A G G C C C A C C G G  Wnt3 ORF.SEQ
413 G C T G T G A C A G C C G G A G G A A A G G A C C G C C G G  Wnt3a ORF.SEQ

    G C G A G G G C T G G A A G T G G G G T G G C T G C A G T G  Majority
    -----------------+------------------+------------------+-
                     460                470                480
    -----------------+------------------+------------------+-
449 G A G A A G G A T G G A A G T G G G G T G G C T G C A G T G  Wnt3 ORF.SEQ
443 G C G A G G G C T G G A A G T G G G G T G G C T G C A G T G  Wnt3a ORF.SEQ

    A G G A T G T T G A G T T T G G G G T T T T G G T G T C T C  Majority
    -----------------+------------------+------------------+-
                     490                500                510
    -----------------+------------------+------------------+-
479 A A G A T G C T G A A T T T G G G G T T T T G G T A T C T C  Wnt3 ORF.SEQ
473 A G G A T G T G G A G T T C G G C A G C A T G G T G T C C C  Wnt3a ORF.SEQ

    G A G A G T T T G C T G A T G C T C G T G A G A A T C G G C  Majority
    -----------------+------------------+------------------+-
                     520                530                540
    -----------------+------------------+------------------+-
509 G A G A G T T T G C A G A C G C T C G T G A G A A C C G G C  Wnt3 ORF.SEQ
503 G A G A G T T T G C T G A T G C C C G C G A G A A T C G C C  Wnt3a ORF.SEQ

    C C G A T G C T C G G T G T G C T A T G A A T C G G C A C A  Majority
    -----------------+------------------+------------------+-
                     550                560                570
    -----------------+------------------+------------------+-
539 C A G A T G C T C G G A G T G C C A T G A A C A G G C A C A  Wnt3 ORF.SEQ
533 C C G A T G C C C G C T C T G C T A T G A A T C G A C A C A  Wnt3a ORF.SEQ

    A C A A T G A G G C T G G A C G T T T G T C C A T C T T T G  Majority
    -----------------+------------------+------------------+-
                     580                590                600
    -----------------+------------------+------------------+-
569 A C A A T G A G G C A G G A C G A A T G A C C A T A T T G G  Wnt3 ORF.SEQ
563 A C A A T G A A G C T G G A C G T T C G T C A A T C A C T G  Wnt3a ORF.SEQ


    A G C A C A T G T A C C T G C G C T G T A A G T G T C A T G  Majority
    -----------------+------------------+------------------+-
                     610                620                630
    -----------------+------------------+------------------+-
599 A G A A C A T G C A C C T G C G C T G T A A A T G C C A T G  Wnt3 ORF.SEQ
593 A C C A C A T G T A C C T G A A A T G C A A G T G T C A C G  Wnt3a ORF.SEQ

    G G C T T T C G G G C A G C T G T G A G G T G A A G A C G T  Majority
    -----------------+------------------+------------------+-
                     640                650                660
    -----------------+------------------+------------------+-
629 G G C T G T C A G G C A G C T G T G A A G T G A A G A C G T  Wnt3 ORF.SEQ
623 G G C T T T C G G G C A G C T G C G A G G T G A A A A C C T  Wnt3a ORF.SEQ
```

```
    G C T G G T G G T C T C A G C C T G A C T T C C G G G T G T  Majority
    -----------------+-----------------+-----------------+-
                     670               680               690
    -----------------+-----------------+-----------------+-
659 G C T G G T G G G C G C A G C C T G A C T T C A G A C T G T  Wnt3 ORF.SEQ
653 G C T G G T G G T C T C A G C C G G A C T T C C G G G T G A  Wnt3a ORF.SEQ

    T G G G G A C T A C C T G A A G G A C A A G T A C G A C A  Majority
    -----------------+-----------------+-----------------+-
                     700               710               720
    -----------------+-----------------+-----------------+-
689 T G G G G A C T A C C T G A A A G A C A A G T A C G A C A  Wnt3 ORF.SEQ
683 T C G G C G A C T A C A T G A A G G A C A A G T A C G A C A  Wnt3a ORF.SEQ

    G C G C C T C T G A G A T G G T G G T T G A G A A A C A T C  Majority
    -----------------+-----------------+-----------------+-
                     730               740               750
    -----------------+-----------------+-----------------+-
719 G C G C C T C T G A G A T G G T G G T G G A G A A A C A C C  Wnt3 ORF.SEQ
713 G C G C A T C G G A A A T G G T G G T T G A G A A A C A T C  Wnt3a ORF.SEQ

    G G G A G T C G C G A G G T T G G G T T G A A A C C C T A C  Majority
    -----------------+-----------------+-----------------+-
                     760               770               780
    -----------------+-----------------+-----------------+-
749 G G G A G T C C A G A G G C T G G G T G G A A A C A C T A C  Wnt3 ORF.SEQ
743 G G G A A T C G C G A G G T T G G G T T G A A A C C C T A C  Wnt3a ORF.SEQ

    G G G C C A A G T A C G C C T T C T T C A A G C C T C C C A  Majority
    -----------------+-----------------+-----------------+-
                     790               800               810
    -----------------+-----------------+-----------------+-
779 G A G C C A A A T A C G C C T T C T T C A A G C A T C C C A  Wnt3 ORF.SEQ
773 G G C C A A A G T A C C C C T A C T A C A A A C C A C C A A  Wnt3a ORF.SEQ

    C T G A G C G C G A C C T G G T C T A C T A T G A G G G C T  Majority
    -----------------+-----------------+-----------------+-
                     820               830               840
    -----------------+-----------------+-----------------+-
809 C T G A G C G A G A C C T G G T A T A C T A T G A G G G A T  Wnt3 ORF.SEQ
803 C A G A A A C C G A C C T C G T C T A C T A T G A A A G C T  Wnt3a ORF.SEQ

    C G C C C A A C T T C T G T G A G C C C A A C C C A G A G A  Majority
    -----------------+-----------------+-----------------+-
                     850               860               870
    -----------------+-----------------+-----------------+-
839 C A C C C A A C T T C T G C G A G C C A A A C C C A G A G A  Wnt3 ORF.SEQ
833 C G C C C A A C T T C T G T G A A C C C A A C C C A G A G A  Wnt3a ORF.SEQ

    C G G G T T C C T T C G G C A C C C G T G A C C G T G C C T  Majority
    -----------------+-----------------+-----------------+-
                     880               890               900
    -----------------+-----------------+-----------------+-
869 C G G G C T C A T T C G G C A C C C G T G A C C G T G C C T  Wnt3 ORF.SEQ
863 C C G G T T C C T T C G G C A C A C G T G A C C G T A C A T  Wnt3a ORF.SEQ

    G T A A C G T G T C G T C G C A C G G C A T C G A C G G C T  Majority
    -----------------+-----------------+-----------------+-
                     910               920               930
    -----------------+-----------------+-----------------+-
899 G C A A C G T G T C G T C G C A C G G C A T C G A A G G C T  Wnt3 ORF.SEQ
893 G T A A C C T G A C G T C G C A C G G C A T A G A C G G C T  Wnt3a ORF.SEQ

    G T G A T T T G C T G T G C T G T G G C C G T G G T C A T A  Majority
    -----------------+-----------------+-----------------+-
                     940               950               960
    -----------------+-----------------+-----------------+-
929 G T G A C C T G C T G T G C T G T G G C C G T G G C C A T A  Wnt3 ORF.SEQ
923 G C G A T T T G C T G T G C T G C G G C A G A G G T C A C A  Wnt3a ORF.SEQ

    A C A C T C G G A C T G A G A A G C G C A A A G A G A A G T  Majority
    -----------------+-----------------+-----------------+-
                     970               980               990
    -----------------+-----------------+-----------------+-
959 A C A C A C G G A C A G A A A A G C G C A A A G A G A A A T  Wnt3 ORF.SEQ
953 A C A C T C G A A C T G A G A A G C G C A A A G A A A A G T  Wnt3a ORF.SEQ
```

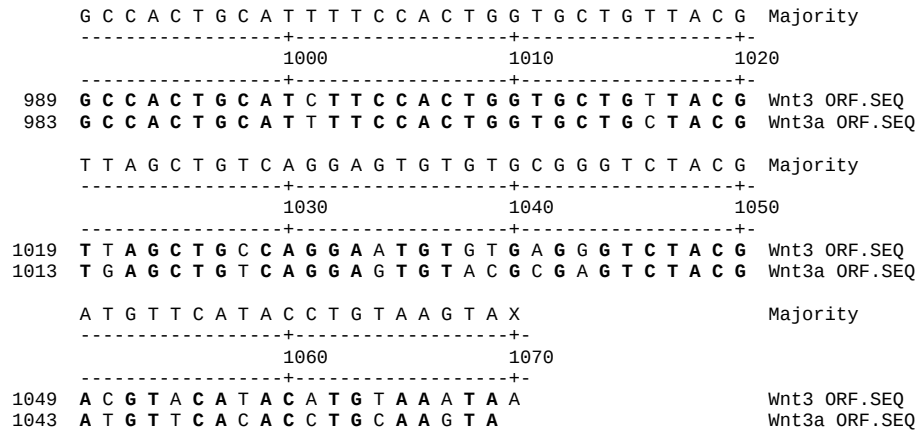

Fig.3.3 Pair wise comparison of zebrafish *wnt3* DNA sequence with respect to that of zebrafish *wnt3a* at the open reading frame.

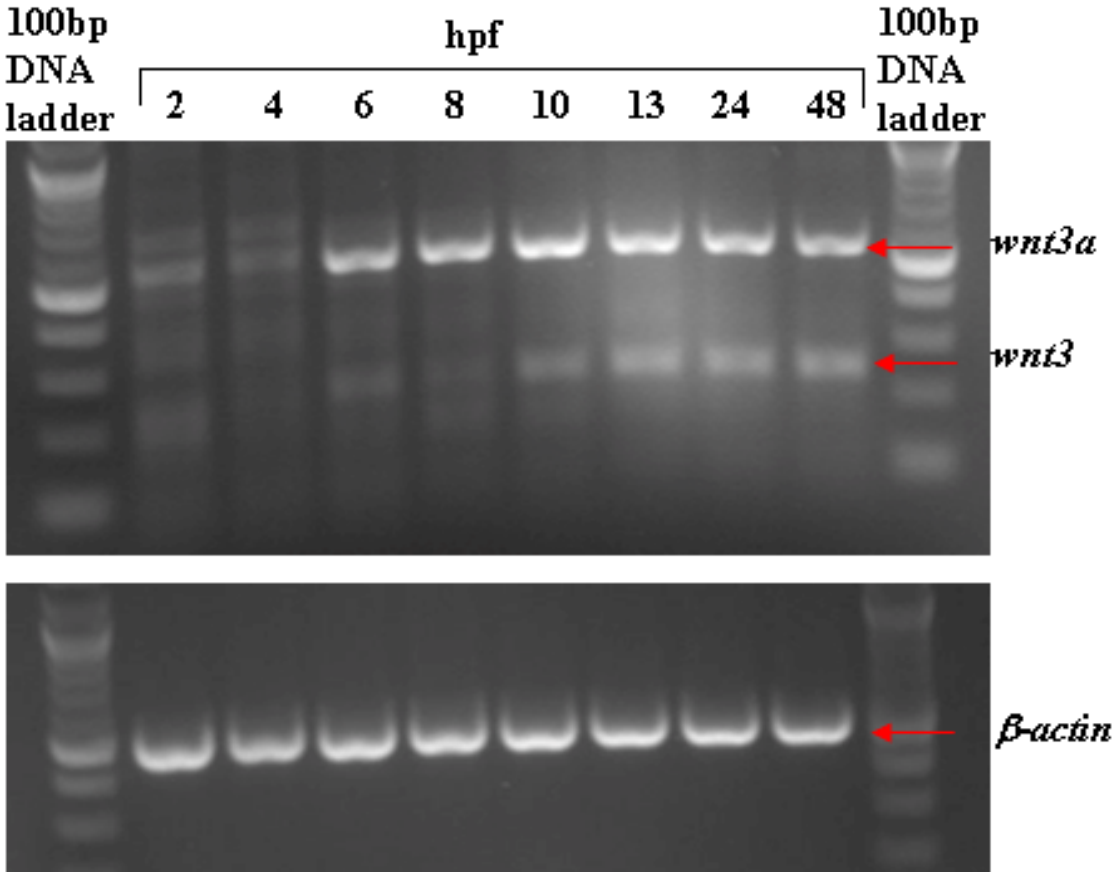

Fig.3.4 Reverse transcription (RT)-PCR detects the presence of *wnt3* and *wnt3a* transcripts from gastrula stage to larval stage zebrafish embryos. *Wnt3* mRNA is first detected at a low level during late gastrula and, its expression level starts to increase from the early neurula stage (see Fig.3.5). On the other hand *wnt3a* transcripts are strongly expressed from 5hpf.

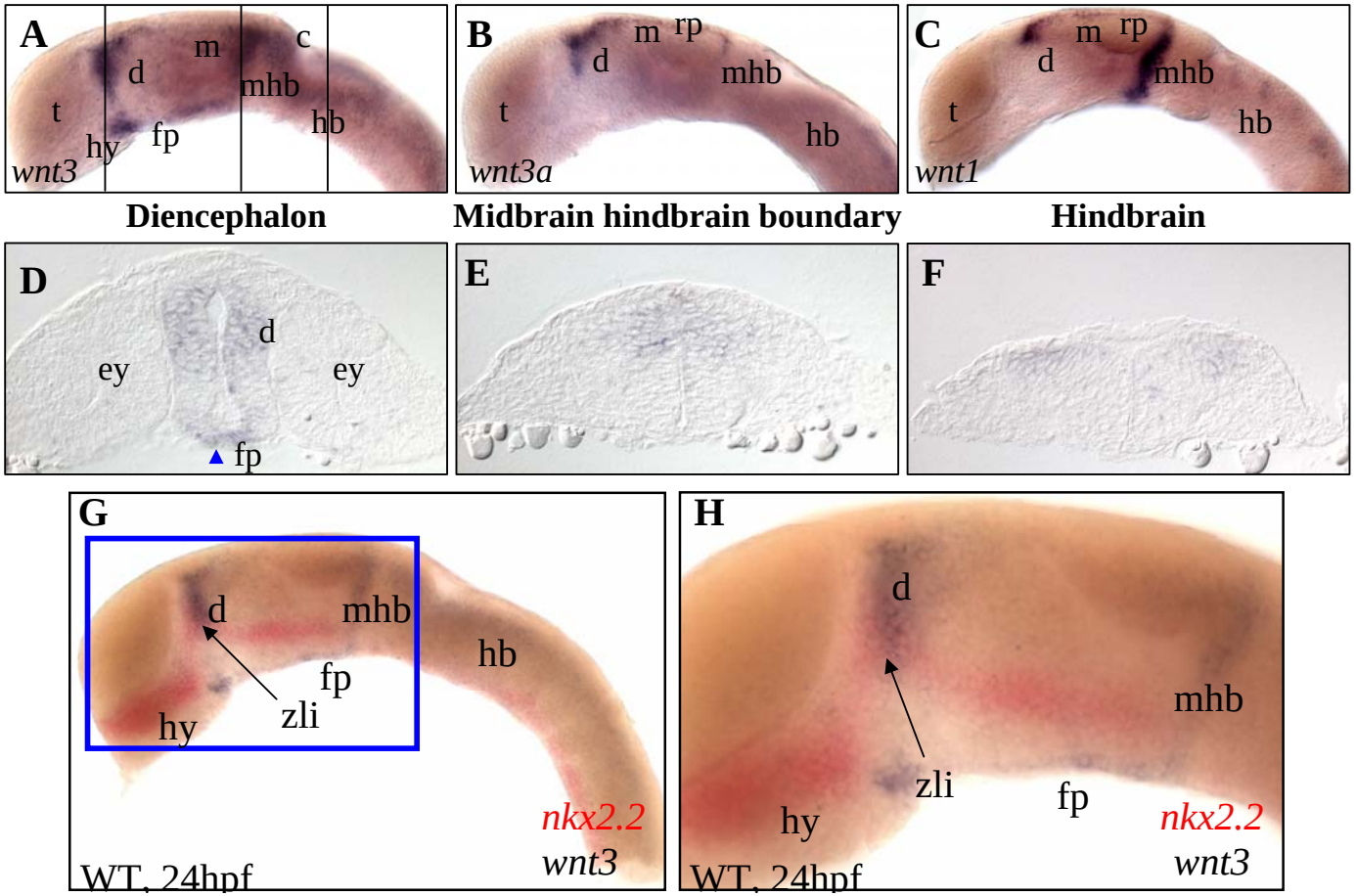

Fig.3.5 Analysis of *wnt3* expression pattern at 24hpf. (A – C) Comparison of *wnt3*, *wnt3a* and *wnt1* expression patterns. In situ hybridization was used to detect *wnt3* (A), *wnt3a* (B) and *wnt1* (C) transcripts at 24hpf. Black bars in (A) show the positions of cross sections illustrated in panels D to F at the level of (D) diencephalon, (E) midbrain hindbrain boundary (mhb) and (F) hindbrain. The ventral extension at diencephalon is deeper than that in either *wnt3a* or *wnt1* with an additional unique expression domain in the floorplate (blue arrowhead, D). In contrast to other midline Wnts, expression of *wnt3* in the hindbrain (F) is restricted to the lateral part of the neural tube and not at the midline. (G-H) The anterior domain of of *wnt3* expression abuts zona limitans intrathalamica (zli) posteriorly. Double *in situ* hybridization was used to detect transcripts of *wnt3* (black) and *nkx2.2* (red) in 24hpf embryos. Abbreviations: d, diencephalon; ey, eye; fp, floorplate; hb, hindbrain; hy, hypothalamus; m, midbrain; mhb, midbrain-hindbrain boundary; rp, roof plate; t, telencephalon and zli, zona limitans intrathalamica.

We compared the expression patterns of *wnt3* with two other canonical Wnts, w*nt3a* and *wnt1* in 24hpf embryos. Despite some similarities, expressions patterns of these genes are distinct. During somitogenesis, *wnt3a* (Fig. 3.5B) and *wnt1* (Fig. 3.5C) are expressed at the dorsal midline of the midbrain extending to the prospective epiphysis anteriorly and to the dorsal midline of the hindbrain posteriorly. At this stage, *wnt3* expression pattern is distinct due to domains in the more ventral diencephalon and anterior floor plate (Fig. 3.5A and D). This is further illustrated by transverse cryosections that shows the extensive ventral extension of *wnt3* expression in the diencephalon and presence of the transcripts in the anterior floor plate (blue arrowhead, Fig, 3.5D). Expression in the hindbrain is also unlike that of *wnt3a* and *wnt1* and extends much more laterally (Fig. 3.5F). Notably, *wnt3* is less strongly expressed in the ventral region of the midbrain-hindbrain boundary (mhb) than that in *wnt1* but more than that of *wnt3a*. We proceed to check if ventral extension of *wnt3* expression in the diencephalon co-localizes with zona limitans intrathalamica (zli), a border between the prospective ventral thalamus and dorsal thalamus. Recent efforts have demonstrated that zli functions as a diencephalic signaling center (Kiecker and Lumsden, 2004; Zeltser, 2005). Shh is expressed within the zli (Echelard et al., 1993; Krauss et al., 1993), the extent of its activity from zli is defined by the expression of *nkx2.2*, a target gene of Shh pathway (Barth and Wilson, 1995). Nkx2.2 is a homeodomain transcription factor. Transcripts of *nkx2.2* can be analyzed as three distinct bands: a rostral band extending from the posterior pre-optic area (pPOA) to zli, an intermediate band from dorsal thalamus to the ventral portion of the midbrain-hindbrain boundary (mhb) and a caudal band from ventral portions of the hindbrain to the spinal cord. Double *in situ* hybridization with antisense probes against digoxygenin labeled *wnt3* and fluorescein labeled *nkx2.2* colocalized in regions at and immediately posterior to zli (Fig.3.5 G-H). This suggests that *wnt3*, like *shh* could participate in patterning of the diencephalon. Having established *wnt3* expression pattern in the brain, we proceed to analyze how this pattern emerged and changed during neural development. The expression of *wnt3* was first

detected at the beginning of neurulation and is confined to the anterior CNS with distinct expression in the dorsal midline, diencephalon and midbrain-hindbrain boundary (mhb) by 13hpf (Fig. 3.6 A). No *wnt3* expression was detected by whole mount in situ hybridization at earlier stages of development. By 16hpf *wnt3* is present in the floor and roof plate, diencephalon and mhb. Thus its expression effectively surrounds a large part of the brain that includes posterior diencephalon and midbrain. The dorsal domain of expression continues from diencephalon and terminates posteriorly at the dorsal anterior hindbrain (Fig. 3.6 B). By 30hpf expression is enhanced in all these areas and cerebellum (Fig. 3.6C). Wnt3 expression can now be distinguished in the ventral epithalamus and dorsal thalamus. Interestingly, the expression in the dorsal thalamus remains strong at the last embryonic stage of analysis at 7dpf (Fig. 3.6G). The hindbrain is a region with dynamic expression of *wnt3*. Here expression is first detected at 13hpf (Fig. 3.6A), reached a peak at 30hpf (Fig. 3.6D) and become restricted to a few dorsal clusters of cells by 72hpf (data not shown). Similarly dynamic changes in *wnt3* expression pattern occurred in the anterior floor plate (Fig. 3.6 B-G). Here expression is initially present underlying the diencephalon and midbrain (Fig. 3.6B-C) but the location of the expression domain changes as a result of unequal proliferation maxima. This causes the neural tube to bend in the midsaggital plane generating a ventral inflexion at the caudal end of the forebrain called the cephalic flexure (Puelles, 2001). This folding event in the brain brought the two ventral domains derived from the floor plate (in the hypothalamus and ventral posterior midbrain) together (Fig. 3.6D) and extend them dorsal up towards the optic tectum (Fig. 3.6 E-F).

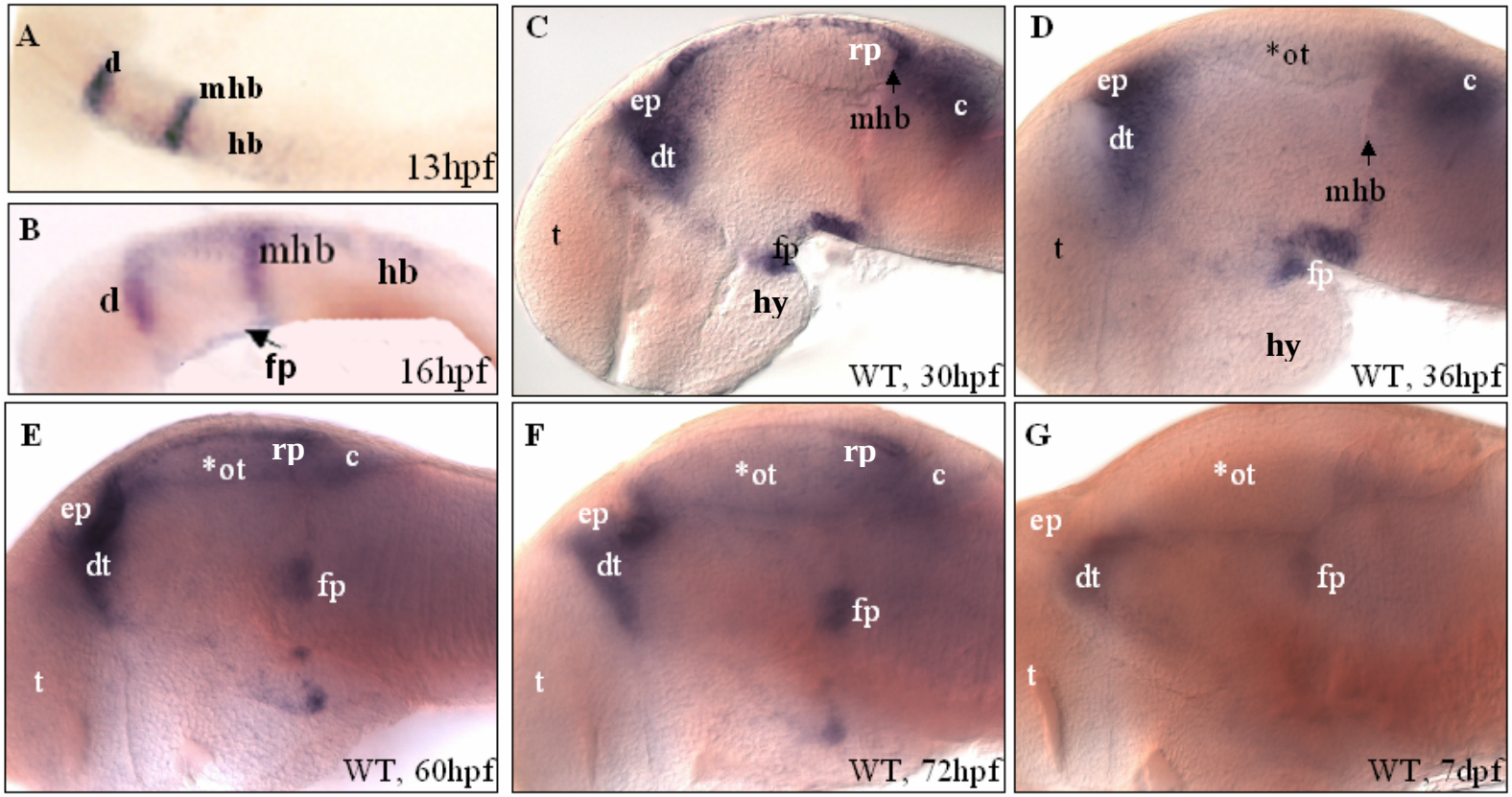

Fig.3.6 Neural expression pattern of zebrafish *wnt3* in the anterior CNS at various stages of development. Eyes and mesodermal tissues are removed from the specimens C-F. (A) 13hpf, (B) 16hpf, (C) 30hpf, (D) 36hpf, (E) 60hpf, (F) 72hpf and (G) 7dpf. Fig.3.5A shows dorsal view of an embryo. Fig.3.5B-G show lateral views with anterior to the left. (A) *Wnt3* transcripts are observed in the anterior neural keel and forms distinct bands at the prospective midbrain and the hindbrain. (B) At 16 h transcripts of *wnt3* appeared in the anterior floor plate (arrow) and the expression now extends ventrally in the diencephalon and the MHB. (C) By 30hpf *wnt3* transcripts are detected in the ventral epithalamus, dorsal thalamus and cerebellum and the anterior floor plate expression persists only most anteriorly in the hypothalamus and most posteriorly in the floor of the midbrain. (D) Floor plate expression converged at the midbrain. (E-F) By 60hpf cephalic flexure of the brain results in the dorsal ventral extension of the floor plate in the tegmentum, additional expression in the optic tectum can be observed by this stage. (G) Expression in the dorsal thalamus and floor plate remains detectable by 7dpf (the last stage of analysis). Abbreviations: c, cerebellum; d, diencephalon; dt, dorsal thalamus; ep, epithalamus; fp, floorplate; hb, hindbrain; hy, hypothalamus; mhb, midbrain-hindbrain boundary; ot, optic tectum; rp, roofplate; t, telencephalon.

Wnt3 is also expressed in domains other than the brain that include spinal cord, branchial arches, ear, notochord and lymphoid cells. In the posterior CNS *wnt3* is dynamically expressed in the spinal cord (Fig.3.7A-C). Its expression is initially limited to the anterior spinal cord at 30hpf (Fig. 3.7A) but can be seen extending posterior-wards throughout the development of the embryo such that by 72hpf it almost reach the posterior end of the spinal cord (Fig.3.7C). This domain of expression disappears by 7dpf (data not shown). The expression of *wnt3* in the branchial arches can be detected at 48-72hpf (Fig.3.7D-F). From 48hpf *wnt3*'s expression is detected in the ear (Fig. 3.7D-F) and notochord (Fig.3.7B-C). Both domains of expression remain at least until 7dpf. Finally, *wnt3* expression in the lymphoid cells can be observed at 7dpf (Fig.3.7G). The latter correlate with the finding that Wnt3 is expressed in B cells and become overexpressed in chronic lymphocytic leukemia that is characterized by a progressive expansion of apparently quiescent B cells (Lu et al., 2004).

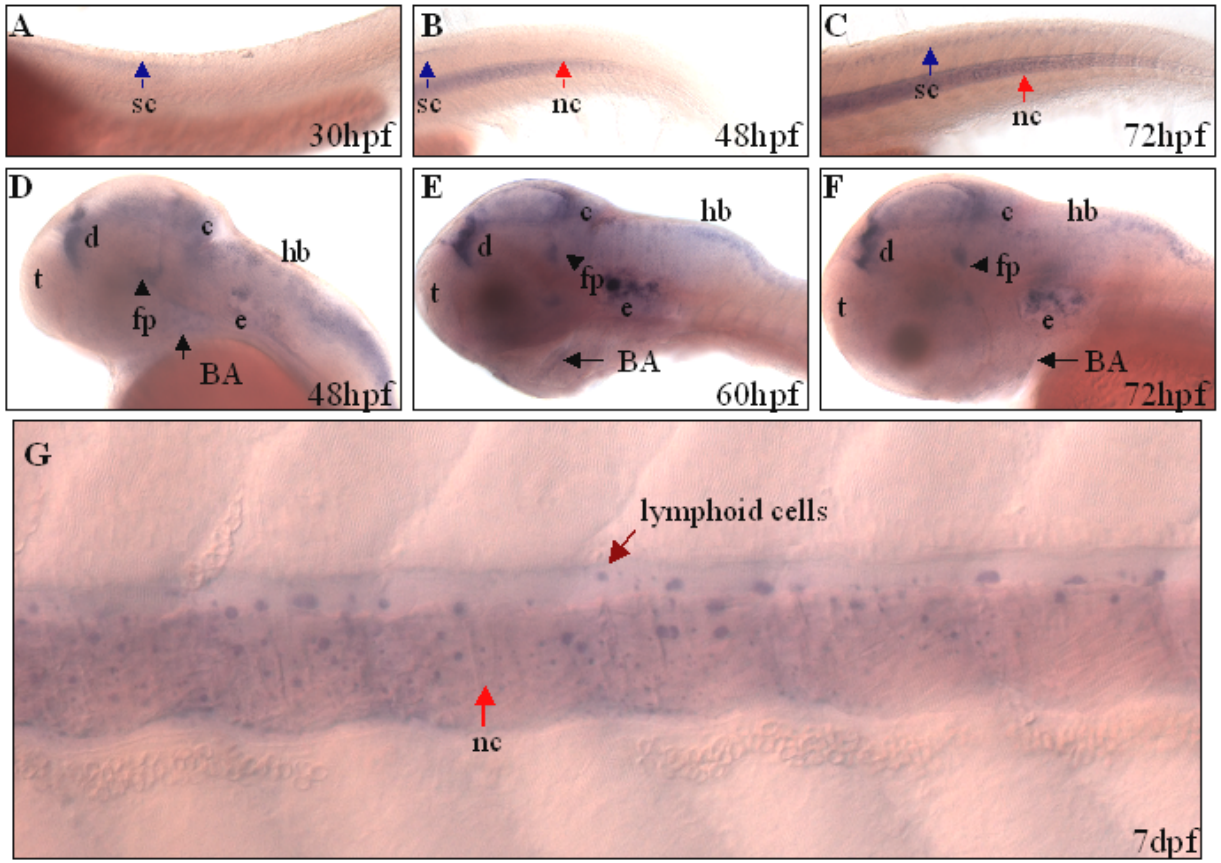

Fig.3.7 Expression pattern of zebrafish *wnt3* in domains other than the anterior central nervous system. Whole mount *in situ* hybridization was performed on zebrafish embryos aged between 1 to 7 dpf with antisense Dig labeled *wnt3* probe. (A-C) *Wnt3* expression in the spinal cord (blue arrow) extended posterior wards from 30-72hpf. Notochordal expression (red arrow) can be detected from 48hpf and persisted until the last stage of analysis at 7dpf. (D-F) Additional domains of expression in the ear appeared from 48hpf. Weak staining in the branchial arches are transient and can be detected from 48 to 72hpf. (G) Staining in the lymphoid cells (brown arrow) can be observed by 7dpf. All panels show lateral view of the embryo with anterior to the left. Abbreviations: BA, branchial arches; c, cerebellum; d, diencephalon; e, ear; fp, floorplate; hb, hindbrain; mhb, midbrain-hindbrain boundary; nc, notochord; o, optic tectum; rp, roofplate; sc, spinal cord; t, telencephalon.

3.2 Wnt3 is Involved in Canonical Signaling During Neural Tube Development

In order to determine in which signaling pathway Wnt3 is involved in during neural development, we developed the electroporation technique to deliver DNA into the anterior CNS of zebrafish embryo (Teh et al., 2003). The methodology was discussed in section 2.4 of Materials and Methods in the thesis. In vivo electroporation is an attractive misexpression approach that allows targeted delivery of expression construct(s). It permits the manipulation of gene expression within a biological context and allows temporal and spatial control of DNA misexpression (Swartz et al., 2001). We decided to co-electroporate two or more expression constructs in all our misexpression experiments, one of which being a fluorescent reporter vector. The stage of misexpression was fixed to 22-24hpf. This stage was chosen as cavitation in the hindbrain is complete while surrounding neuroepithelial cells remain highly proliferative (Wullimann and Knipp, 2000). First we co-electroporated equimolar quantities of two independent fluorescent reporter constructs pEGFPN2 and pDsRed-Express-C1 (BD Biosciences Clontech, USA) into the anterior neural tube. The two fluorescent proteins predominantly colocalized with one another in the brain of an electroporated embryo imaged at 2 days post electroporation (Fig. 3.8). We decided to use the expression construct pEGFPN2 as our fluorescent reporter as GFP fluorescence in the neural tube can be detected 4 hours post-electroporation. In comparison, the fluorescence from pDsRed-Express-C1 can only be observed a day after electroporation. Hence the coelectroporation experiment stated above showed that fluorescent reporter such as GFP can be used to demarcate the region that predominantly misexpress non-tagged expression constructs such as pExWnt3.

Several assays are used to demonstrate the ability of Wnts to activate canonical signaling. One of these uses a LEF/TCF reporter gene construct (TOPflash) to measure activation of the canonical Wnt pathway (Korinek et al., 1998). A cocktail of expression constructs were electroporated into the neural tube. The endogenous activity of canonical Wnt pathway was detected by electroporating a mastermix of EGFP control containing 2μl pEGFP-N2 (4 μg/ μl), 1μl pRLCMVLuc (*Renilla* luciferase reporter under a CMV promoter, 4 μg/ μl)

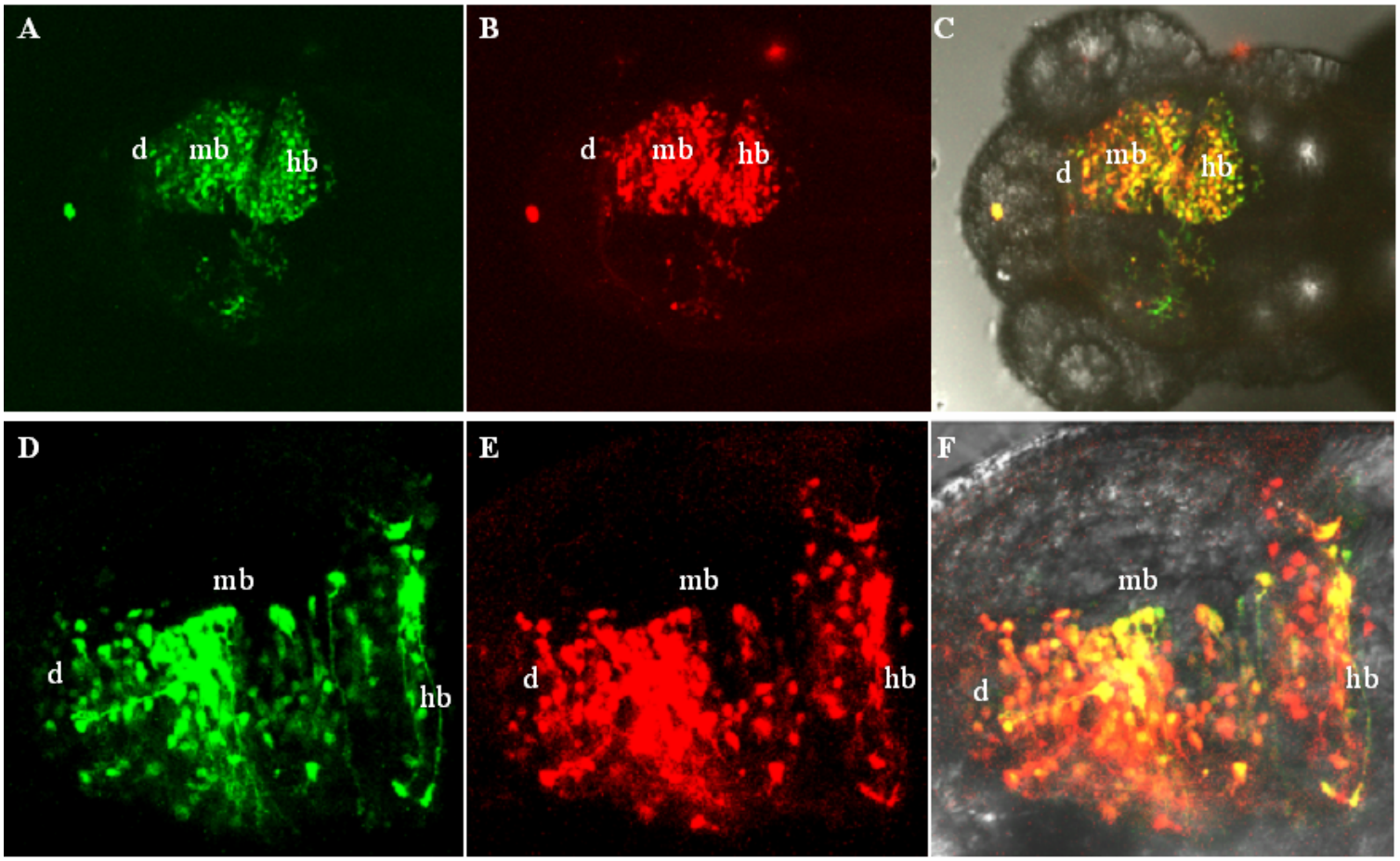

Fig.3.8 Two independent co-electroporated fluorescent reporters predominantly co-localized with one another in the brain of an electroporated embryo. 24hpf wild type zebrafish embryos were microinjected with 6nl of pEGFPN2 and pDsRed-Express-C1 expression constructs before exposing the anterior neural tube to 4 electric pulses of 17 volts, each of 50 msec duration and delivered 1 second apart. (A-C) Dorsal and (D-F) lateral views of an electroporated embryo imaged by confocal microscopy two days post electroporation. (A, D) Panels illustrating EGFP expression, (B, E) DsRed expression and (C,F) triple merged images of acquired under fluorescent and bright field. Abbreviations: d, diencephalon; hb, hindbrain and mb, midbrain.

and 3µl TOPflash (*Photinus* luciferase reporter under the regulation of TCF binding sites, 1 µg/ µl). The total amount of DNA delivered to all treatments were made identical and effect of Wnt1 or Wnt3 on canonical signaling was tested by electroporating a mastermix of 1µl pExWnt1 (4µg/ µl), 1µl pEGFP-N2 (4 µg/ µl), 1µl pRLCMVLuc (4 µg/ µl) - and 3µl TOPflash (1 µg/ µl) or 1µl pExWnt3 (4µg/ µl), 1µl pEGFP-N2 (4 µg/ µl), 1µl pRLCMVLuc (4 µg/ µl) - and 3µl TOPflash (1 µg/ µl) respectively into the neural tube of zebrafish embryos. In all experiments 6nl of the mastermix was first microinjected into the neural cavity of the zebrafish before exposing the embryo to the electric pulses stated in section 2.4 of this thesis. Transgenes were successfully electroporated into the neural tube of the embryos as shown by unilateral misexpression of EGFP 12 hours post electroporation. These embryos were photographed, pooled into groups of three and lysed in 50µl T-PER (Pierce Biotechnology, USA) containing complete protease inhibitor cocktail (Roche Diagnostics GmbH, Penzberg, Germany). 20µl of the embryo lysate was subsequently used in the Dual-Luciferase® Reporter Assay to measure *Photinus* luciferase activity from the TCF reporter, TOPflash. *Renilla* luciferase activity from pRLCMVLuc was used to normalize the extent of electroporation that vary between embryos. The result showed that like *wnt1*, *wnt3* is involved in canonical signaling during zebrafish neural tube development; both Wnts induced at least 7 fold more firefly luciferase activity than EGFP, a protein not known to activate the canonical pathway (Fig. 3.9). Upon examining values obtained from each experiment series, firefly luciferase activity induced by overexpression of Wnt3 is almost always higher than that induced by Wnt1 (4 out of 5 experiments). However since Wnt3 expression construct contain both 5' and 3'UTRs (section 2.1.9) while Wnt1 doesn't (only Wnt1 ORF), the observed difference may be attributed to differences in translation efficiency or RNA stability. Importantly, this series of experiments showed that during neural development Wnt3 acts within a context of the canonical pathway.

A

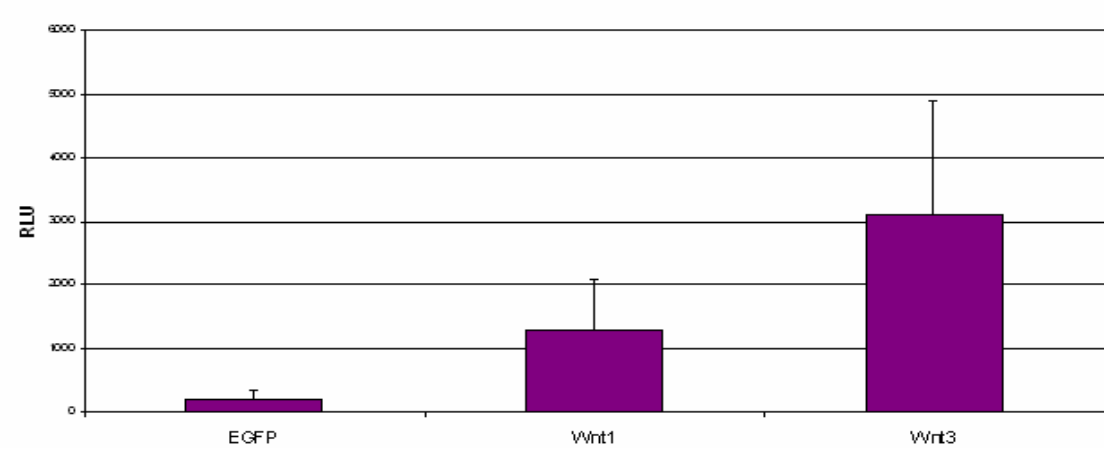

Mastermix	pEGFP-N2 (4 µg/ µl) - 2µl pRLCMVLuc (4 µg/ µl) -1µl TOPflash (1 µg/ µl) - 3µl	pExWnt1 (4 µg/ µl) -1µl pEGFP-N2 (4 µg/ µl) - 1µl pRLCMVLuc (4 µg/ µl) -1µl TOPflash (1 µg/ µl) - 3µl	pExWnt3 (4 µg/ µl) -1µl pEGFP-N2 (4 µg/ µl) - 1µl pRLCMVLuc (4 µg/ µl) -1µl TOPflash (1 µg/ µl) - 3µl

B

	EGFP	Wnt1	Wnt3
Series1	19.4	1466	2142
Series 2	563	934	6821
Series3	327	3573	564
Series4	260	300	4490
Series5	236	1511	3942
Average	281.08	1556.8	3591.8

Fig.3.9 Zebrafish *wnt3* acts within the context of canonical Wnt signaling during neural tube development. 24hpf zebrafish embryos were microinjected with 6nl of expression constructs that can be grouped into the EGFP control, zebrafish *wnt1* positive control or zebrafish *wnt3* experimental sample before exposing the anterior neural tube to 4 electric pulses of 17 volts, each of 50 msec duration and delivered 1 second apart. Positively electroporated embryos from each group were gathered into groups of three, lysed and firefly luciferase activity from the TCF-reporter, TOPflash were quantified using a manual luminometer. The above data were obtained from five different experimental sets and normalized against *Renilla* luciferase activity from reporter vector pRLCMVLuc. Both *wnt3* and *wnt1* have significantly higher luciferase activity than the EGFP control indicating that both Wnts are involved in the canonical signaling pathway. A) A bar chart of the Topflash analysis conducted on EGFP, Wnt1 or Wnt3 electroporated embryos, each bar represents an average of 5 independent experiments. B) The actual data set obtained from each experiment series.

3.3 Overexpression of Wnt3 by Electroporation Induced Cell Proliferation and Overt Neuronal Differentiation in Zebrafish Brain

We have shown that Wnt3 acts as a canonical Wnt and proceed to verify if it can induce proliferation during neural development. Indications that overexpression of Wnt3 may lead to an enhanced cell proliferation come from the fact that this gene is one of the six genetic loci altered in mouse mammary tumors induced by integration of mouse mammary tumor virus (MMTV) (Roelink et al., 1990; Tekmal and Keshava, 1997). An increase in Wnt3 expression has also been reported in chronic lymphocytic leukemia (Lu et al., 2004) . To avoid the effect of Wnt3 expression construct on gastrulation and limit this treatment to specific region of the brain we used electroporation as a method of DNA delivery into the neural tube of wild type zebrafish embryo. We assayed for the effect of cell proliferation with an antibody against the M phase cell cycle marker phospho-Histone H3 (∝-pH3) on embryos co-electroporated with pExWnt3 and pEGFPN2. In all experiments 6nl of mastermix was first microinjected into the neural cavity of the zebrafish before exposing the embryo to the electric pulses as described in section 2.4 of this thesis. Immunohistochemistry with primary antibodies (mouse ∝-GFP and rabbit ∝-pH3) and secondary antibodies [Alexa Fluor® 488 f(ab')2 fragment of goat anti-mouse IgG and Alexa Fluor® 594 f(ab')2 fragment of goat anti-rabbit IgG] was performed on 10μm thick cryo-sections. Cells labeled in green and red represent expression of GFP and pH3 respectively. Based on data obtained from three separate experiments, analysis from sequential cryosections of an electroporated embryo showed that on average the number of proliferating cells doubled on the side of the brain that overexpressed Wnt3. Only one set of data is illustrated in this thesis (Fig.3.10). Cells in the M- phase of the cell cycle in the region where Wnt3 was misexpressed were quantitated and their numbers were compared to the opposite part of the brain (used as an internal control). The effect becomes less obvious when Wnt3 is occasionally misexpressed on both sides of the brain (Fig.3.9F).

Fig.3.10 Electroporation of *wnt3* expression construct induces proliferation on the side of the brain that ectopically express Wnt3. 24hpf wild type zebrafish embryos were microinjected with 6nl of *wnt3* and EGFP reporter expression constructs before exposing the anterior neural tube to 4 electric pulses of 17 volts, each of 50 msec duration and delivered 1 second apart. Positively electroporated embryos marked by unilateral EGFP expression in the neural tube were fixed with 4% PFA, 12 hours post electoporation and cryo-sectioned. Immunohistochemistry with primary antibodies (rabbit ∝-GFP and mouse ∝-pH3) and secondary antibodies [Alexa Fluor® 488 f(ab')2 fragment of goat anti-rabbit IgG and Alexa Fluor® 594 f(ab')2 fragment of goat anti-mouse IgG] was performed on the 10μm thick sections. The figure comprises of 6 serial tissue slices marked A-F of an electroporated embryo. Each panel consists of 2 images taken of the same section. The image on the left of each panel represents a triple merged photograph of images taken under the green, red and bright field filters. The image on the right of each panel represents a double merged photograph of the same section taken under the red and bright field filters. Cells labeled in green and red represent expression of GFP and pH3 respectively. The site of GFP misexpression correlates with ectopic expression of *wnt3* by electroporation. An increase in mitotic cells marked by pH3 expression can be seen in the side of the brain where *wnt3* is misexpressed. Wnt3 Overexpression = 11.0 ± 2.2; Non-electroporated side = 5.2 ± 1.8. Abbreviations: 3rd v, third ventricle; c, cerebellum; dt, dorsal thalamus; hb, hindbrain; hyp, hypothalamus; ot, optic tectum; pr, pretectum; pt, posterior tuberculum; t, telencephalon; tg, tegmentum and vt, ventral thalamus.

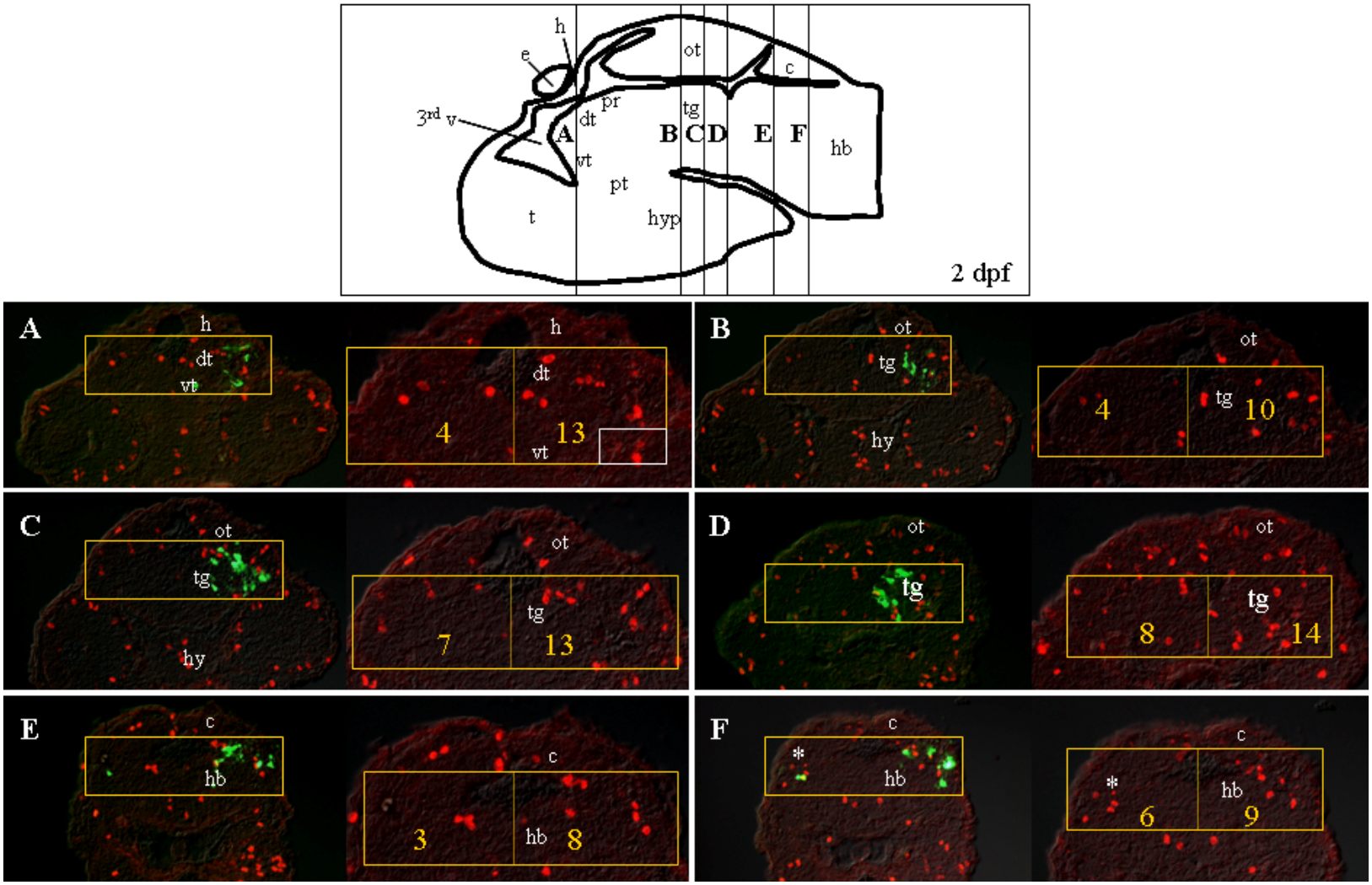
h
e
ot
c
3rd v
dt
pr
tg
A
B C D
E
F
hb
vt
pt
t
hyp
2 dpf
A
h
dt
vt
4
13
B
ot
tg
hy
10
C
7
D
8
14
E
hb
3
8
F
*
6
9

We next checked for the effect on neuronal differentiation upon Wnt3 overexpression by immunostaining for Hu-proteins. The presence of Hu proteins serves as a marker for newly committed neuronal cells as well as for mature neurons of the CNS (Barami et al., 1995; Marusich et al., 1994). Transgenes successfully introduced into the embryonic neural tube were detected by unilateral misexpression of EGFP 12 hours post electroporation. These embryos were fixed overnight at 4°C with 4% PFA and processed for cryosections. Immunohistochemistry with primary antibodies (rabbit ∝-GFP and mouse ∝-HuC/D) and secondary antibodies [Alexa Fluor® 488 f(ab')2 fragment of goat anti-rabbit IgG and Alexa Fluor® 594 f(ab')2 fragment of goat anti-mouse IgG] was performed on 10μm thick sections. The effect of overexpression of *wnt3* on neuronal differentiation is indicated by comparing the number of HuC/D+ cells in both electroporated and non-electroporated side (control) of the brain. Cells labeled in green and red represent expression of GFP and HuC / D respectively. The site of GFP expression correlates with ectopic expression of *wnt3* induced by electroporation. Both ventricular (a layer of cells surrounding the ventricle) and subventricluar zones contain progenitor cells. Ectopically positioned neurons marked by HuC/D+ expression can be seen in the ventricular zone on the side where *wnt3* is misexpressed (Fig.3.11). This phenomenon is not observed on the control side of the brain. The situation is reversed in the cerebellum (Fig.3.11 E-F) where overexpression of *wnt3* results in less neuronal differentiation. This effect seemes to be limited to the dorsal part of the brain as enhanced neuronal differentiation remained in the ventral hindbrain where Wnt3 is misexpressed. Hence these results demonstrate a potential role of Wnt3 in neuronal differentiation of the diencephalon, midbrain and hindbrain. An increase in HuC/D+ cells may be explained in part by an increase in cell proliferation (Fig.3.10). It remains unclear why HuC positive cells are found within the ventricular and subventricular zones. Perhaps Wnt3 expression affected cell migration from proliferative regions or alternatively the process of cell proliferation and migration is tightly coupled and excessive cell proliferation overwhelmed the machinery of cell migration.

Fig.3.11 Electroporation of *wnt3* expression construct induces ectopic neuronal differentiation. 24hpf wild type zebrafish embryos were microinjected with 6nl of *wnt3* and EGFP reporter expression constructs before exposing the anterior neural tube to 4 electric pulses of 17 volts, each of 50 msec duration and delivered 1 second apart. Positively electroporated embryos marked by unilateral EGFP expression in the neural tube were fixed with 4% PFA, 12 hours post electoporation and cryo-sectioned. Immunohistochemistry with primary antibodies (rabbit ∝-GFP and mouse ∝-HuC) and secondary antibodies [Alexa Fluor® 488 f(ab')2 fragment of goat anti-rabbit IgG and Alexa Fluor® 594 f(ab')2 fragment of goat anti-mouse IgG] was performed on 10μm thick sections. The figure comprises of 6 serial tissue slices marked A-F of an electroporated embryo. Each panel consists of 2 images taken of the same section. The image on the left of each panel represents a triple merged photograph of images taken under the green, red and bright field filters. The image on the right of each panel represents a double merged photograph of the same section taken under the red and bright field filters. Cells labeled in green and red represent expression of GFP and HuC/D respectively. The site of GFP misexpression correlates with ectopic expression of *wnt3* by electroporation. Ectopically positioned post-mitotic neurons marked by HuC/D expression can be seen in the ventricular and sub ventricular zone on the side where Wnt3 is misexpressed. The opposite is seen in the cerebellum where misexpression of Wnt3 results in less neuronal differentiation. Abbreviations: 3rd v, third ventricle; c, cerebellum; dt, dorsal thalamus; e, eye; hb, hindbrain; hyp, hypothalamus; ot, optic tectum; pr, pretectum; pt, posterior tubercle; t, telencephalaon; tg, tegmentum and vt, ventral thalamus.

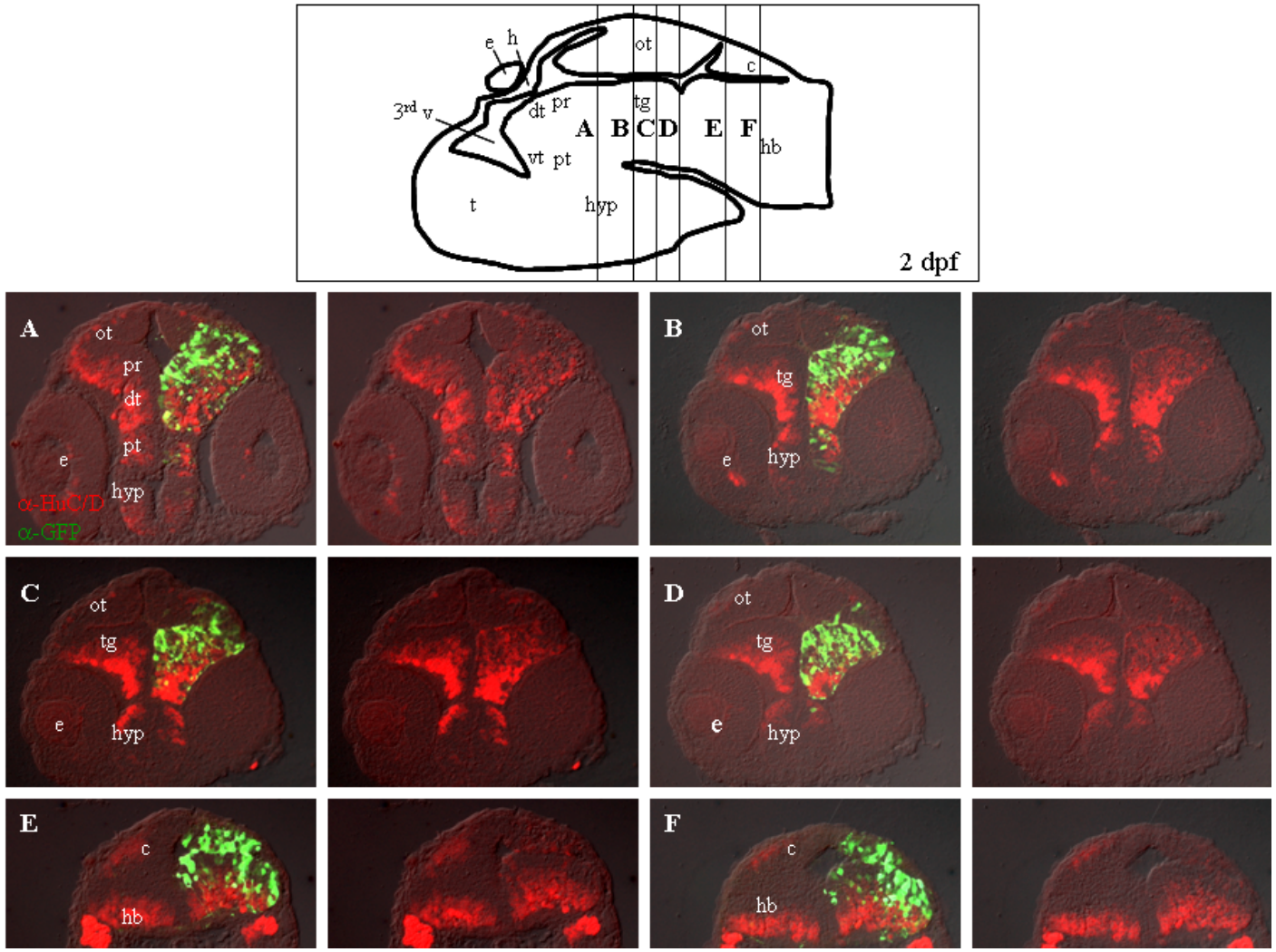
e
h
ot
c
3rd v
dt
pr
tg
A
B
C
D
E
F
hb
vt
pt
t
hyp
2 dpf
A
ot
pr
dt
pt
e
hyp
α-HuC/D
α-GFP
B
ot
tg
e
hyp
C
ot
tg
e
hyp
D
ot
tg
e
hyp
E
c
hb
F
c
hb

3.4 Morpholino Knockdown of Wnt3 Results in Enhanced Apoptosis in the Brain

Antisense morpholino oligonucleotides (MO) have been used successfully in zebrafish to knockdown gene function by gene-specific inhibition of mRNA translation (Ekker, 2000). In addition to their ability to block cytosolic processes, MO can enter the nucleus (Partridge et al., 1996) and have been shown to be effective inhibitors of pre-mRNA splicing in zebrafish embryos (Draper et al., 2001). Splice-blocking MOs had the advantage that the efficacy of gene knockdown can be quantified without the use of antibodies, and that they specifically target zygotic, and not maternal, transcripts. The *wnt3* exon/intron structure had previously been determined in our laboratory by Michael Richardson (unpublished data). The four exons are distributed along a genomic locus of 43585 bp with the intronic region between the first and second exon being the longest (30757 bp). A morpholino of 25-mer complementary to the splice site between exon 1 and the flanking intron (designated W3E1I1) was designed based on the above sequence. This MO spanned the exon/intron junction, including the most conserved residues of the splice donor consensus sequence. We first asked whether splice site blocking MO can alter splicing of *wnt3* mRNA. Using reverse transcriptase polymerase chain reaction (RT-PCR), we found that injection of the W3E1I1 MO into early zebrafish embryos results in elimination of *wnt3* transcripts (Fig. 3.12A). To check for possible inhibition of splicing of *wnt3* pre-mRNA, RT-PCR reactions using a fixed forward *wnt3* primer with varying *wnt3* reverse primers were performed. The forward primer (21-mer) used defines the first exon and will anneal to complementary sequences 13bp downstream from the start codon whereas the series of reverse primers will anneal to various complementary sequence downstream from exon 2 to exon 4 (Fig. 3.12B). We failed to detect any wild-type *wnt3* transcript from RNA samples isolated from 30hpf splice morphants in the resulting RT-PCR

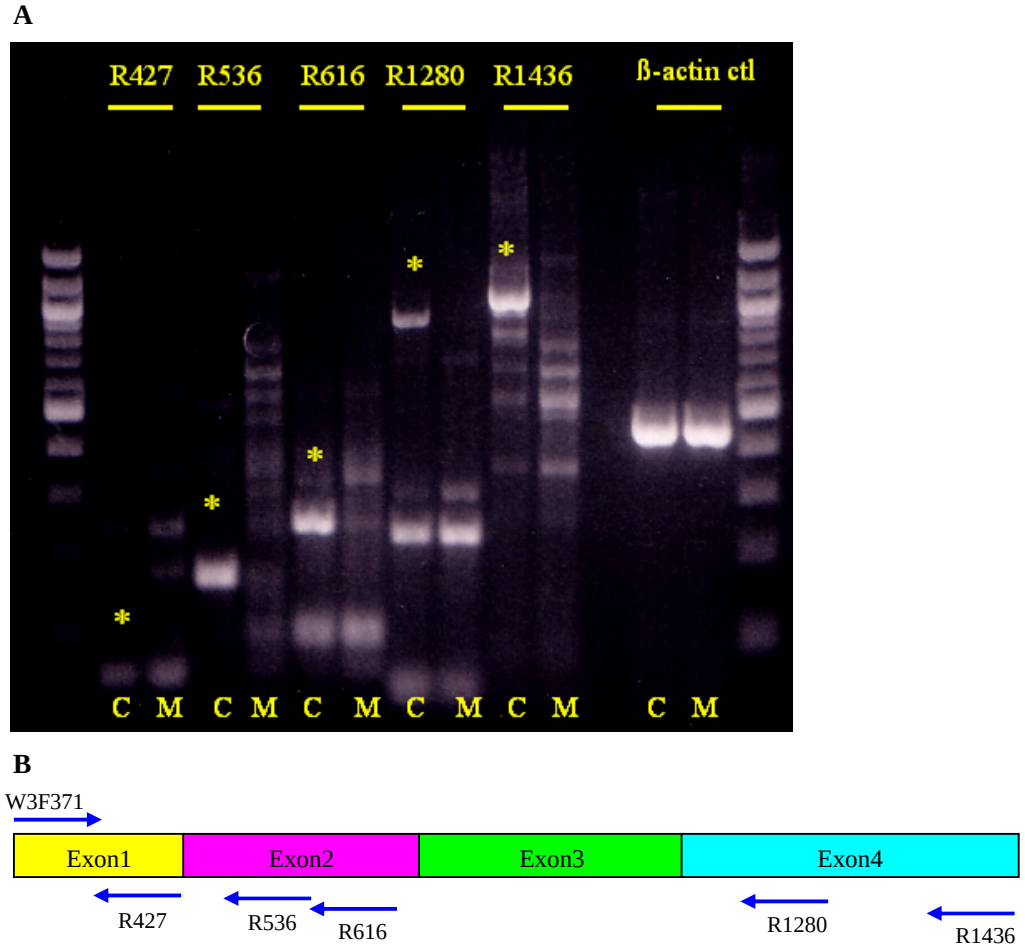

Fig.3.12 Reverse transcription (RT)-PCR analysis of *wnt3* mRNA structure in wild-type and W3E1I1 MO-injected embryos. (A) RT-PCR fails to detect the presence of *wnt3* transcripts from RNA isolated from the splice morphants. Reverse primers used are shown above lanes. Lanes marked with both C and asterick (*) represent control RT-PCR performed on wild type zebrafish embryos whereas lanes marked M represent RT-PCR performed on similarly staged splice morphants. (B) The annealing positions along *wnt3* open reading frame of various primers used in the RT-PCR analysis are illustrated in this figure.

analysis despite the use of various primer pairs. This suggests that W3E1I1 MO had successfully interfered with the splicing of *wnt3* transcript such that no wild-type mRNA copies can be detected by RT-PCR.

In order to minimize the possibilities of analyzing nonspecific abnormalities that result from injection of morpholino oligos, another anti-Wnt3 morpholino oligonucleotide was designed. 5'UTRW3 MO is a 25mer oligonucleotide complementary to the 5'UTR of *wnt3* transcript, 85 bp upstream from the translational start site. As sequence information in the 5'UTR is less conserved than the coding region, the chance of the morpholino oligonucleotide blocking incorrect mRNA nonspecifically is less. An additional control is the use of a mismatched morpholino oligonucleotide W3Ctl MO that contains random modification of 5 bases along the 25mer sequence of W3E1I1 MO. The dosage of Wnt3 morpholinos was previously titrated at 0.05 pmol, 0.1 pmol, 0.2 pmol, 0.5 pmol and 1 pmol. The optimal dosage for W3E1I1 is 0.2 pmol, no morphant phenotype was observed at 0.05 pmol, a 50% penetrance was observed at 0.1 pmol while 100% penetrance was seen at 0.2 pmol. A dosage of 0.05-0.075 pmol will give 100% penetrance of Wnt3 morphnat phenotype in embryos injected with 5'UTRW3 MO. Statistics to verify the penetrance of the phenotype was re-confirmed using transgenic lines (elaborated in Section 3.10). Any dose higher than that in the optimal range of both Wnt3 morpholinos (W3E1I1 and 5'UTRW3) will lead to enhanced lethality in injected embryos. We next analyzed the phenotype of Wnt3 morphants. The process of gastrulation was not affected, however, defects in eye, midbrain and hindbrain can be clearly seen in Wnt3 morphants (embryos injected with either 0.2 pmol of W3E1I1 MO or 0.05 pmol of 5'UTRW3 MO) but not after injection of 0.2 pmol of W3Ctl MO by 30hpf (Fig. 3.13A-C). The embryos were stained for apoptotic cells with the vital dye Acridine Orange at 48hpf. The dye permeates inside acidic lysosomal vesicles and becomes fluorescent, thus marking cells dying by apoptosis. Embryos were analyzed under a fluorescence microscope and exposed only once to UV light during photography. Apoptotic cells were marked as bright green dots under the fluorescent microscope. The result showed that both Wnt3 morphants exhibit

enhanced levels of apoptosis in the diencephalon, midbrain and hindbrain but not in the telencephalon, a region where *wnt3* is not expressed (Fig.3.13E-F). In comparison, very few apoptotic cells were detected in the control morphant (Fig. 3.13D).

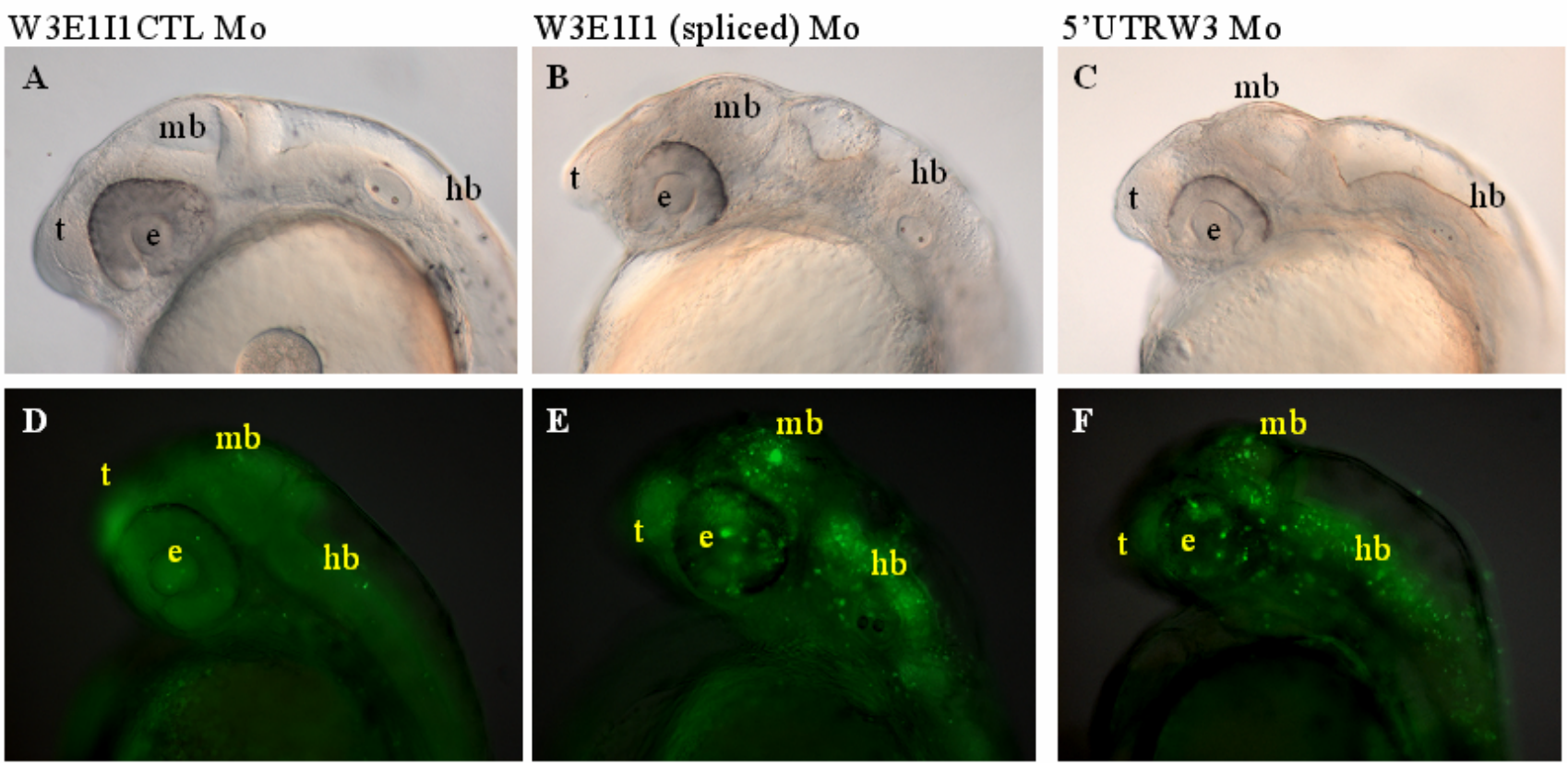

Fig.3.13 Absence of *wnt3* activity leads to increased levels of apoptosis in diencephalon, midbrain and hindbrain. (A) Bright field imaging of the control morphant and (B-C) *wnt3* morphant embryos at 30hpf. (D) Detection of dying cells by Acridine Orange staining of control morphant and (E-F) *wnt3* morphants embryos at 48 hpf (lateral views). Abbreviations: e, eye; hb, hindbrain; mb, midbrain and t, telencephalon.

3.5 The Phenotype of Wnt3 Morphants in Craniofacial Cartilage Mimics that Observed in Human Mutant

We have shown that both Wnt3 morphants are similar in phenotype upon knockdown of Wnt3 function. Hence the observed phenotype could be specific. Ideally the phenotypic defects should be similar to phenotype of known mutants. While Wnt3 mutant in zebrafish is not available, mice homozygous for null allele of Wnt3 exhibit gastrulation defect (Liu et al., 1999). The homozygous nonsense mutation of WNT3 gene in human (Q83X) results in abnormal fetal development, affected fetuses displayed autosomal recessive tetra amelia (loss of four limbs) and exhibit craniofacial, nervous system, pulmonary, skeletal, and urogenital anomalies. The Q83X mutation truncates WNT3 at its amino terminus, suggesting that loss of its function is the most likely cause of disorder (Niemann et al., 2004). First, we proceed to examine whether Wnt3 morphants recapitulate craniofacial anomalies exhibited by the loss of function phenotype in human. We explored the requirement for Wnt3 signaling in the development of cartilage elements in the head by performing cartilage staining with Alcian blue on 4% paraformaldehyde fixed, proteinase K treated, 5dpf wild type, control morphant or the two respective Wnt3 morphants. Both wild type embryos and control morphant have 7 pharyngeal arches in the head (Fig.3.14A-B). Embryos injected with 0.2 pmol of the *wnt3* splice morpholino, W3E1I1 have a normal Meckel's cartilage (the first pharyngeal arch), a somewhat dysmorphic second pharyngeal arch and the complete absence of elements derived from arches 3-7(Fig.3.14C). Embryos injected with 0.05 pmol of *wnt3* morpholino targeted at the 5' UTR (5'UTRW3) have a more severe craniofacial defect, in addition to the absence of pharyngeal arches numbered 3-7, the Meckel's cartilage is also absent in this morphant (Fig.3.14D). Hence similar to requirement of WNT3 for normal craniofacial development in human, morpholino knockdown on zebrafish Wnt3 demonstrated that it is required for the development of craniofacial cartilage. We have decided to focus our project analysis on brain development in Wnt3 morphants of zebrafish to shed light into malformation of the brain that exists but not characterized in human WNT3 mutants.

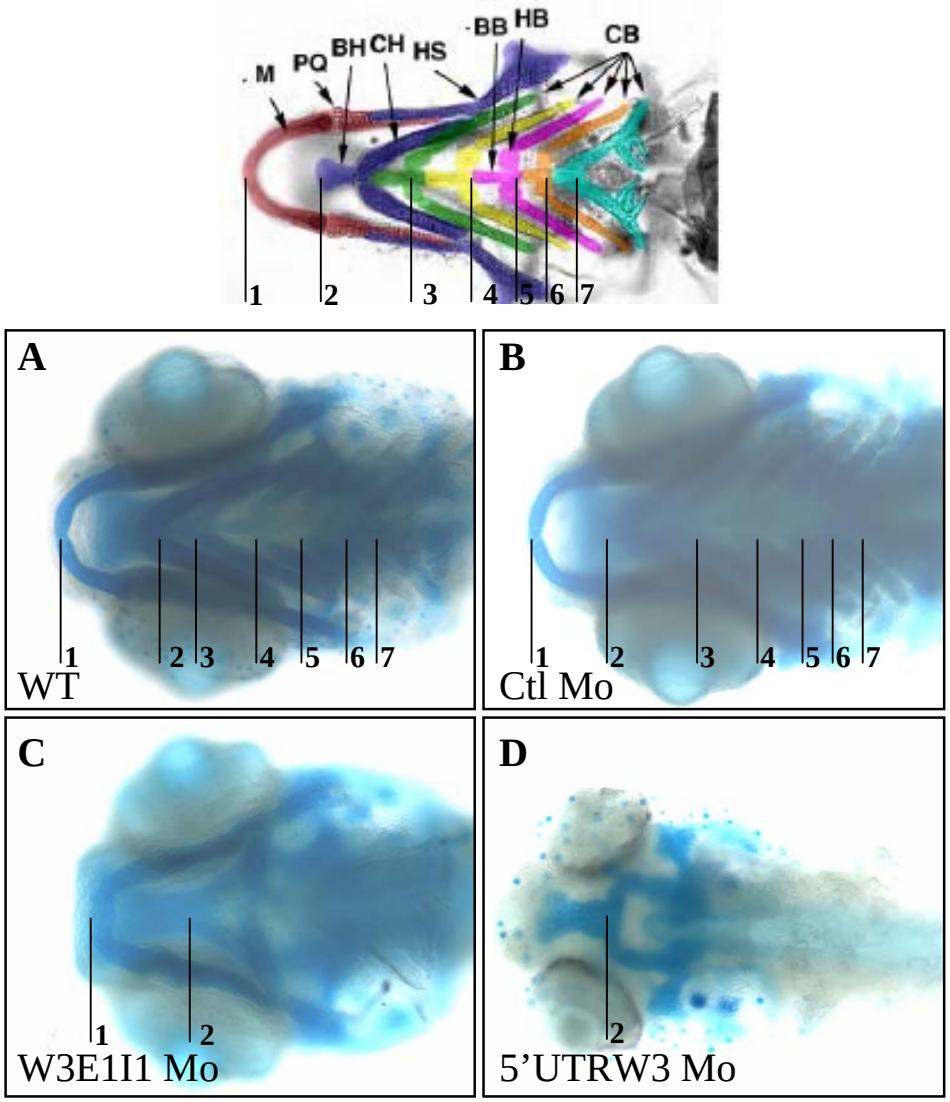

Fig.3.14 Wnt3 is required for formation of pharyngeal arches. Ventral views of zebrafish embryo stained for cartilage at 5 days of development. (A) Wild type and (B) embryo injected with 5bp mismatched *wnt3* control morpholino showed wild type phenotype. (C-D) *wnt3* morphants showed loss of cartilage derivatives of pharyngeal arches 3-7 (C) or 1, 3-7, (D) following inhibition of *wnt3* function. M, Meckel's cartilage: PQ, palatoquadrate; BH, basihyal; CH, ceratohyal; HS, hyosymplectic; BB, basibranchial; HB, hypobranchial; CB, ceratobranchials.

3.6 Wnt3 Functions in Patterning Of Diencephalon

The vertebrate forebrain develops from the anterior-most part of the neural tube, the prosencephalon and consists of the telencephalon (anterior forebrain) and diencephalon (posterior forebrain). Based on topological comparisons of various genes expressions in subregions of the forebrain and morphological data of intersegmental and intrasegmental relationships between diencephalon and telencephalon, the forebrain is thought to give rise to six subregions called prosomeres numbered p1-p6 in a caudal to rostral fashion (Rubenstein et al., 1994). The spatially restricted expression of genes encoding several signaling molecules and transcription factors has been noted in diencephalon (Bulfone et al., 1993; Krauss et al., 1991; Nornes et al., 1998; Puschel et al., 1992).We have decided to use *pax6*, a gene broadly expressed in the diencephalon, to see if its expression is affected in the diencephalon of Wnt3 morphants. Pax6 is a transcription factor that contains two DNA binding domains, the N-terminally located paired domain and the paired-type homeodomain. The expression pattern of *pax6* has been reported in zebrafish (Krauss et al., 1991; Puschel et al., 1992)**.** Detailed immunochemical analysis of Pax6 protein has also been performed in the zebrafish brain (Wullimann and Rink, 2001). In the diencephalon, many Pax6+ cells are observed in the pretectal region (p1), some Pax6+ cells are seen in the subventricular zone of anterior dorsal thalamus (p2) and a large Pax6+ domain is present in the ventral thalamus (p3). There are two *pax6* genes in zebrafish (Nornes et al., 1998) and *pax6b* is the orthologue of human PAX6 gene (zebrafish nomenclature committee). Hence we have decided to use this marker in our Wnt3 morphant analysis.

By 30hpf, *pax6b* is extensively expressed in the telencephalon, ventral thalamus, dorsal thalamus and pretectal region of wild type embryos. However, the expression in dorsal thalamus becomes much reduced in Wnt3 morphants (Fig. 3.15B-C).

Zli forms the interface between the future anteriorly located ventral thalamus (vt) and the posteriorly located dorsal thalamus (dt). It is the only true compartment boundary found with restricted cell lineage and border cell properties in the diencephalon (Larsen et al., 2001). We

have shown in Figure 3.4 that diencephalic expression of *wnt3* lies at and immediately posterior to that of zli and co-localizes with *nkx2.2* at the dorsal thalamus. We next examined if the dorsal thalamic expression of *nkx2.2* flanking zli is affected in Wnt3 morphants by performing whole mount *in situ* hybridization with riboprobes against *nkx2.2* on 30hpf zebrafish embryos. Comparison with wild type embryos clearly indicated that *nkx2.2* expression in the dorsal thalamus is decreased in both Wnt3 morphants (Fig. 3.15E-F). Thus *in situ* hybridization with antisense *pax6b* and *nkx2.2* riboprobes show that dorsal thalamus is greatly reduced in embryos deficient in Wnt3.

Besides the diencephalon, the midbrain is another region with enhanced apoptosis in Wnt3 morphants (Fig. 3.13D-F). We decide to analyze the expression of *otx2* whose expression is restricted to the diencephalon and midbrain of wild-type embryos (Millet et al., 1996; Mori et al., 1994; Simeone et al., 1993). Otx2 is a member of Otx homeobox gene family and is a well-characterized vertebrate homolog of *Drosophila* orthodenticle (otd). Comparison of *otx2* expressions in wild type embryos and Wnt3 morphants showed that expression of this gene becomes dysmorphic in the midbrain by 30hpf (Fig. 3.16B-C). Expression in the dorsal thalamus is also reduced in Wnt3 morphants by this stage (white asterick). By 48hpf, *otx2* expression in the optic tectum becomes strongly deficient in both Wnt3 morphants (Fig. 3.16 E-F). It was demonstrated that TCF regulates the expression of *Otx2* in mouse (Kurokawa et al., 2004). We speculate that Wnt3 could activate the canonical pathway that in turn regulates *otx2* expression via TCF mediated transactivation. This may account for the great reduction of *otx2* expression seen in diencephalon and midbrain of Wnt3 morphants.

In summary, through *in situ* hybridization analysis with different marker genes we concluded that Wnt3 is required for the formation of diencephalon and midbrain. We have noted that the formation of dorsal thalamus could be particularly sensitive to the lack of Wnt3.

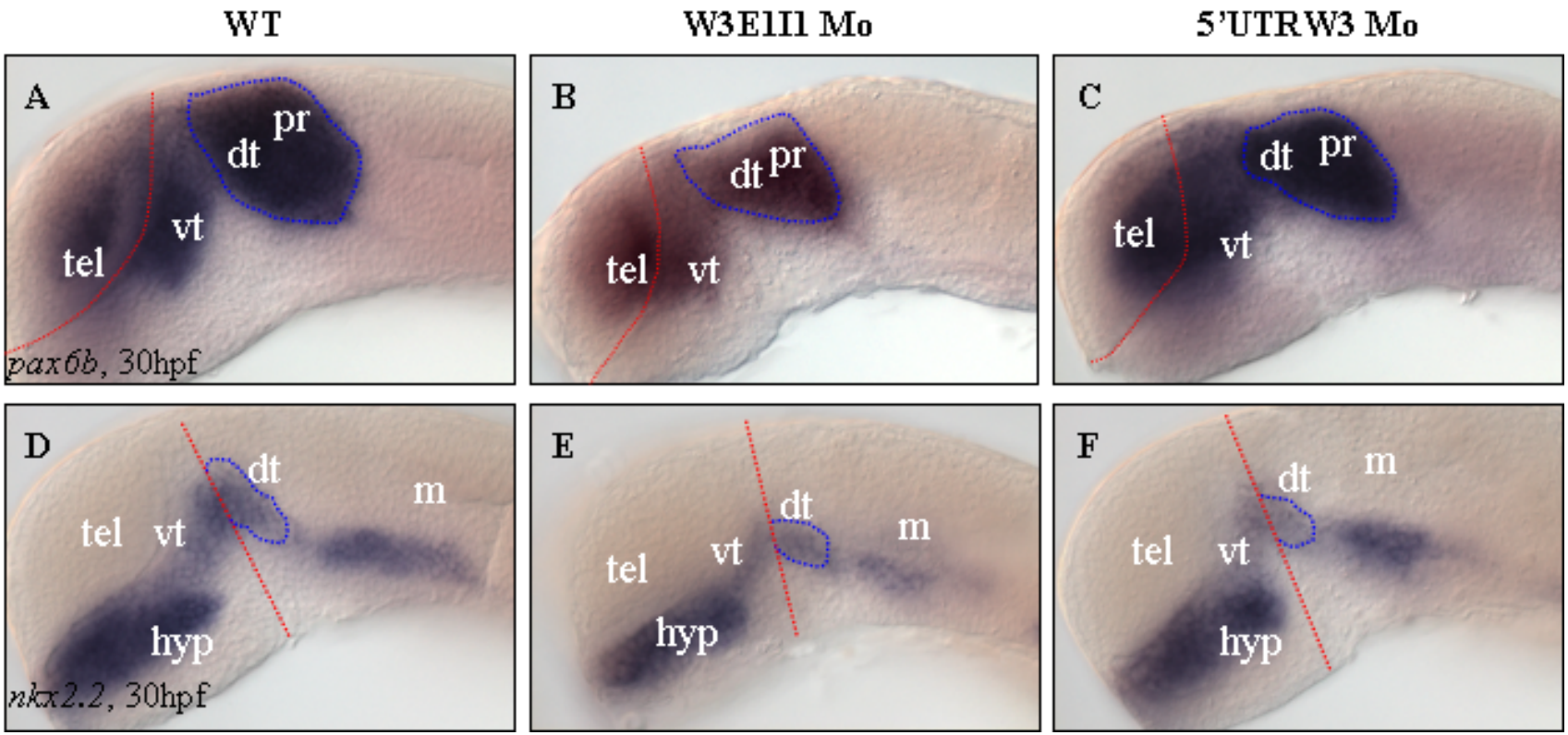

Fig.3.15 The formation of dorsal thalamus is deficient in Wnt3 morphants. In situ hybridization was used to detect *pax6b* and *nkx2.2* transcripts in (A, D), wild type, (B, E) Wnt3 morpholino against the splice site and (C, F) Wnt3 morpholino against the 5'UTR at 30hpf respectively. (A-C) The red serrated line differentiates *pax6b* telencephalic expression from that of diencephalon. The blue serrated line encircles *pax6b* expression in the dorsal thalamus and pretectal region. The expression in dorsal thalamus is reduced in both Wnt3 morphants (B-C). (D-F) *Nkx2.2* expression in dorsal thalamus, demarcated by the blue serrated line is reduced in Wnt3 morphants (E-F). All six images represent lateral view of the embryo with anterior to the left. Abbreviations: dt, dorsal thalamus; hyp, hypothalamus; m, midbrain; pr, pretectal region; tel, telencephalon and vt, ventral thalamus.

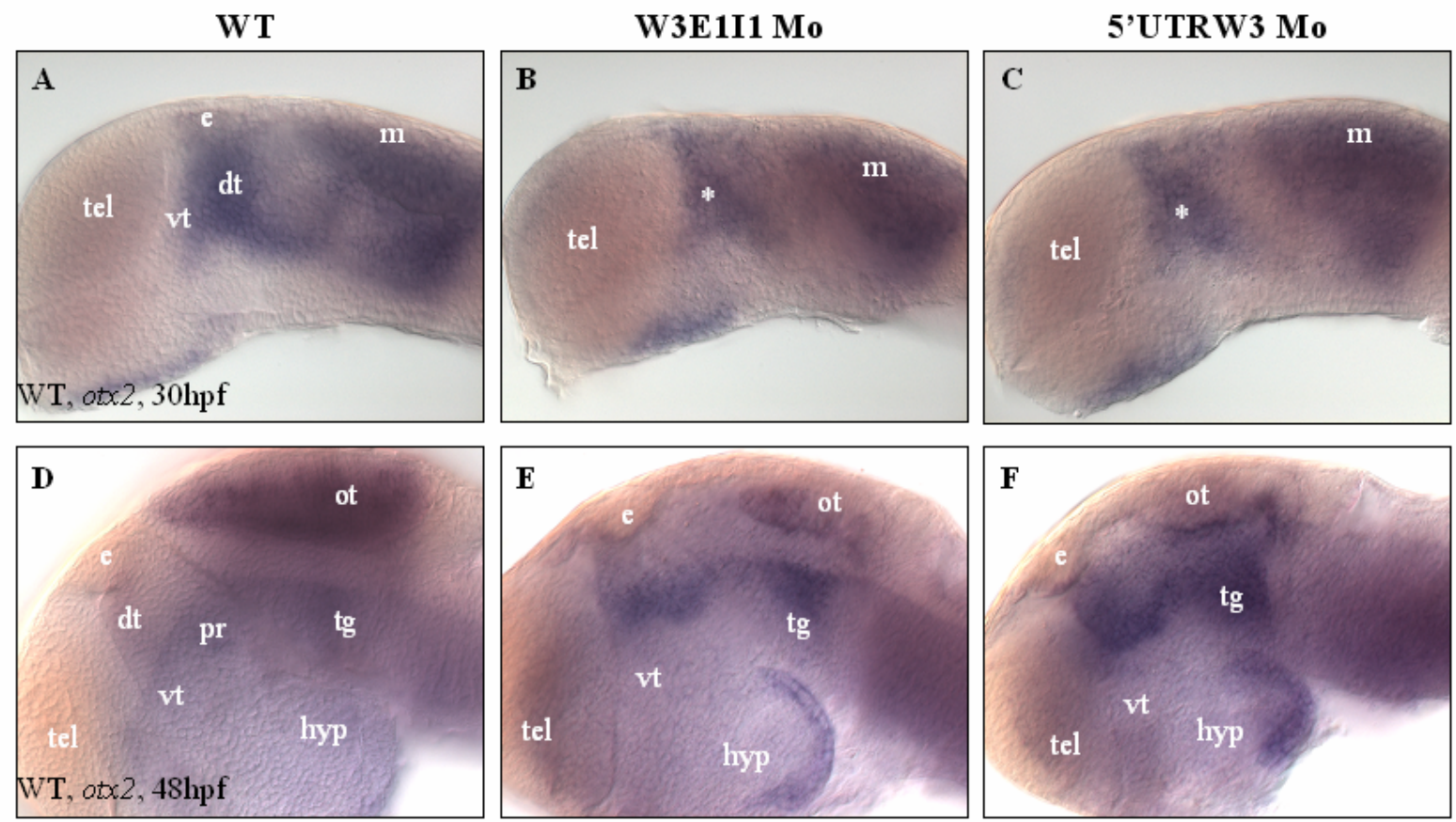

Fig.3.16 Formation of optic tectum is severely reduced in Wnt3 morphants. In situ hybridization was used to detect *otx2* transcripts in (A, D), wild type, (B, E) Wnt3 morpholino against the splice site and (C, F) Wnt3 morpholino against the 5'UTR at 30 and 48hpf respectively. (A-C) The white ∗ (B-C) highlights reduced diencephalic expression in Wnt3 morphants at 30hpf. (D-F) The expression of *otx2* in the optic tectum is greatly reduced in Wnt3 morphants (E-F) by 48hpf. All six images represent lateral view of the embryo with anterior to the left. Abbreviations: dt, dorsal thalamus; e, epithalamus; hyp, hypothalamus; ot, optic tectum; pta, pretectal area; tel, telencephalon; tg, tegmentum and vt, ventral thalamus.

3.7 Wnt3 is Required for Axonogenesis in Dorsal Diencephalon, Optic Tectum and Cerebellum

Several axonal tracts, confined to segmental boundaries, exist within the area of the brain affected by Wnt3 knockdown. To check if the boundary between diencephalon and midbrain is affected in Wnt3 morphants, we examined the nervous system of wild type embryos, control morphants and Wnt3 morphants at 72 hpf with the anti-acetylated tubulin (∝-acT) antibody, which stains developing axon tracts (Chitnis and Kuwada, 1990; Ross et al., 1992; Wilson et al., 1990). The tract of posterior commissure (TPC), a neuroanatomic landmark for the boundary between diencephalon and midbrain is not affected in Wnt3 morphants. However the dorsoventral diencephalic tract (DVDT) and axons emanating from midbrain and cerebellum are missing in Wnt3 morphants (Fig. 3.17 C-D). Since DVDT joins the tract of postoptic commissure (TPOC) midway through the diencephalon, the absence of DVDT suggests that diencephalic regionalization may be affected in Wnt3 morphants. This could be due to the fact that the epithalamus and dorsal thalamus, i.e. regions that DVDT transversed, are defective or underdeveloped in Wnt3 morphants. The absence of ∝-acT staining in the optic tectum and the cerebellar commissure indicate that neuronal differentiation in these and adjacent sites could also be affected. The defect in neuronal differentiation in the optic tectum is apparent in Wnt3 morphants from 48hpf (Fig. 3.16) and they remain unable to initiate axonogenesis by 72hpf. In general, it seems that dorsal structures of diencephalon, midbrain and hindbrain are most affected by the deficiency of Wnt3 function.

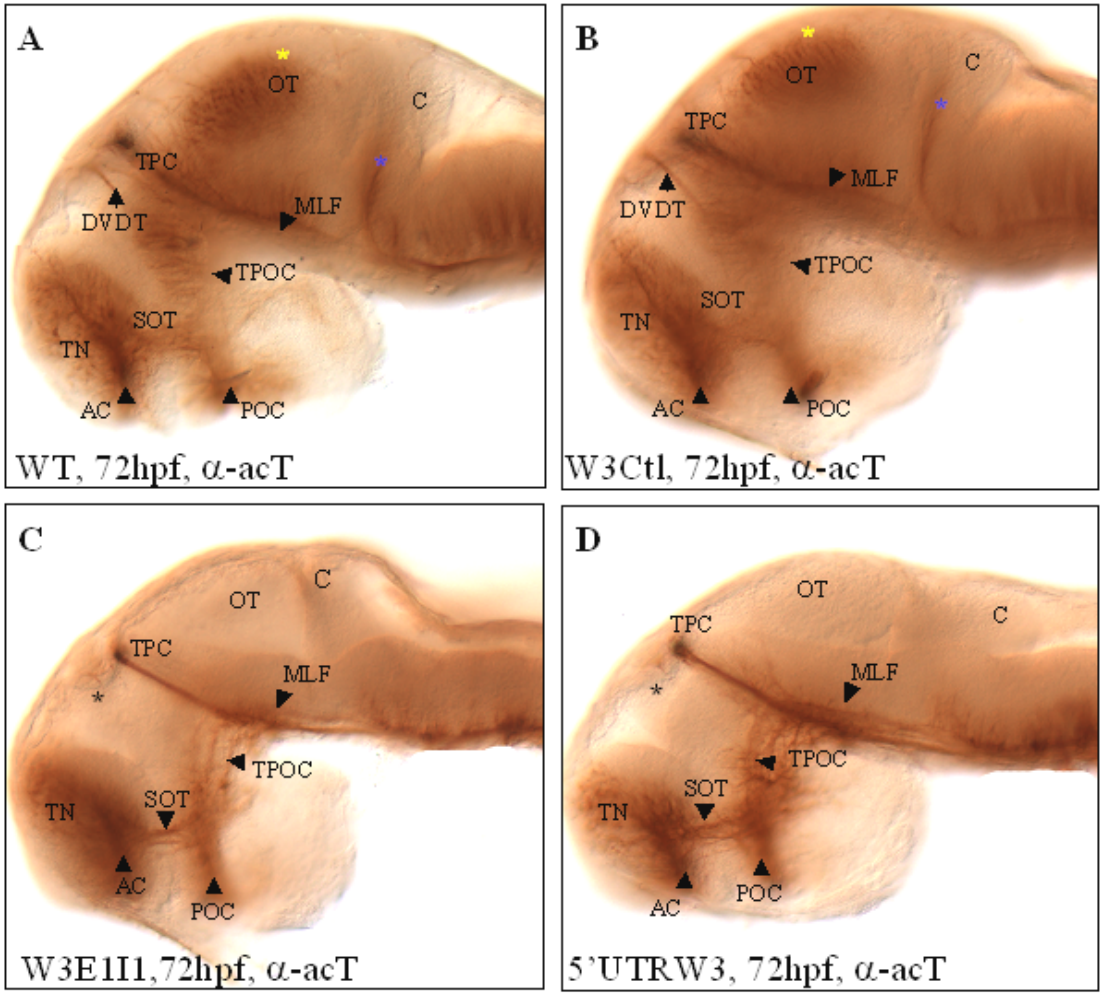

Fig.3.17 The dorsoventral diencephalic tract (DVDT), the optic tectum and cerebellar commissure are absent in Wnt3 morphants. (A-D) Immunochemical labelling of acetylated tubulin was used to study axon formation in 72hpf embryos, oriented anterior to the left. (C-D) DVDT, axons of the optic tectum and cerebellar commissure are absent in both Wnt3 morphants. Abbreviations: AC, anterior commissure; C, cerebellum; DVDT, dorsoventral diencephalic tract; OT, optic tectum; MLF, medial longitudinal fascicle; POC, postoptic commissure; SOT, supraoptic tract; TN, telencephalic nucleus; TPC, tract of the posterior commissure; TPOC, tract of the postoptic commissure.

To see if *wnt3* plays a role in neural differentiation we subjected control embryos and Wnt3 morphants at two stages of development to immunohistochemistry using monoclonal antibody 16A11 (∝-HuC / HuD; Molecular Probes, Oregon, USA), an early marker for differentiating neurons. At 36hpf, the pattern of neural differentiation within the diencephalon, midbrain and hindbrain is affected in Wnt3 morphants (Fig. 3.18 B-C). By 72hpf, the dorsal brain remains largely depleted of HuC/D+ cells (Fig. 3.18 E, F). In comparison, differentiated neurons appear less affected in the telencephalon and ventral brain. Hence whole mount immunohistochemical analysis with ∝-acT and ∝-HuC/D showed that Wnt3 is required for neuronal differentiation in the dorsal brain. Interestingly in the posterior forebrain only DVDT that originates from the dorsal diencephalon but not TPC that derives from the dorsally positioned nucleus of the posterior commissure, located between pineal gland and the anterior border of the optic tectum (Chitnis and Kuwada, 1990), is affected in Wnt3 morphants. This suggests that Wnt3 may have a more important function in the formation of dorsal diencephalon, particularly the dorsal thalamus, a region transversed by DVDT. In addition, deficiency of axonal tracts could be attributed to earlier neuronal differentiation defect observed in Wnt3 morphants, suggesting a role of Wnt3 in early neurodifferentiation of the dorsal brain.

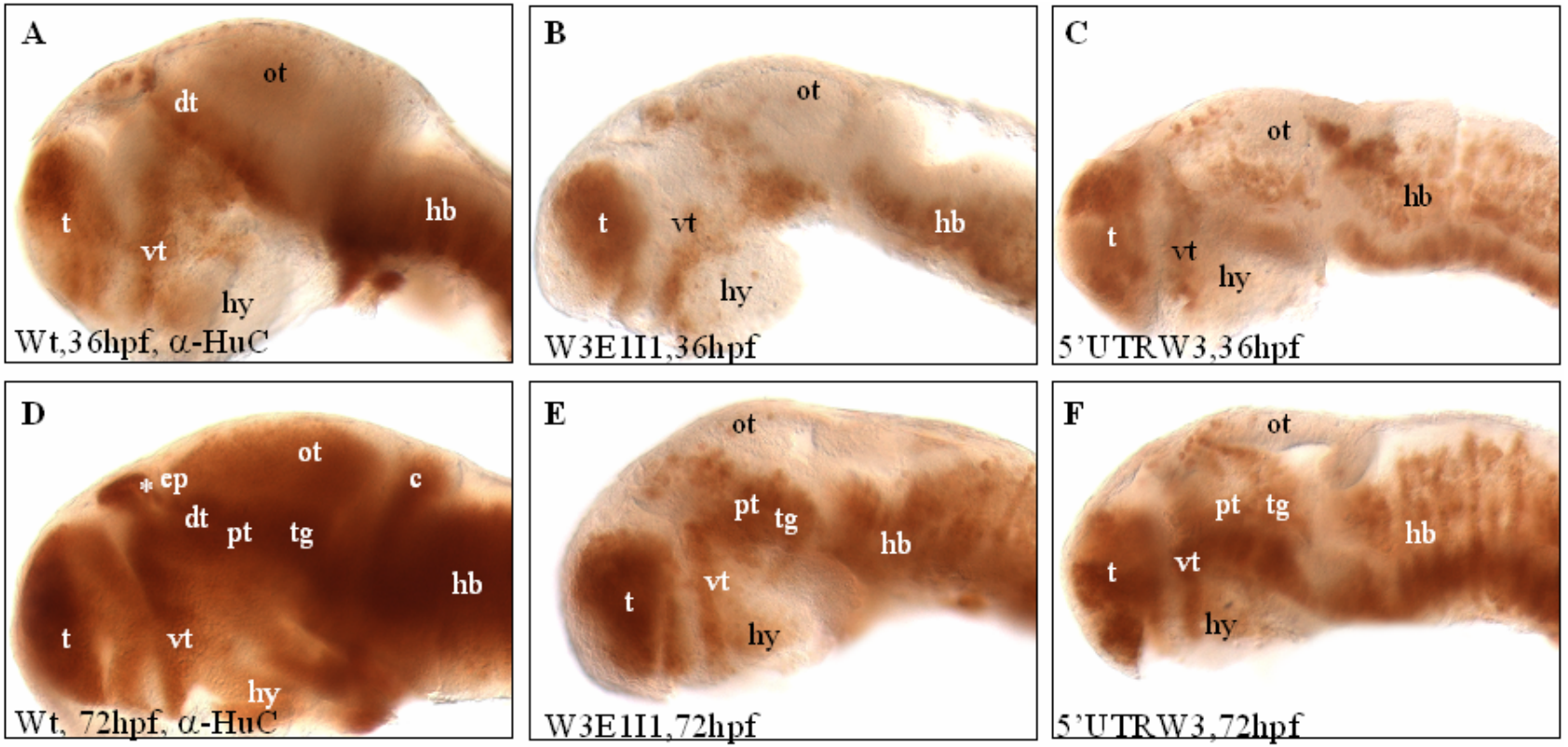

Fig.3.18 Neuronal differentiation in the diencephalon and midbrain are affected in Wnt3 morphants. Immunohistochemistry was performed with monoclonal antibody against HuC on both wild type embryos and *wnt3* morphants at the stages of 36 (A-C) and 72hpf(D-F). (A-C). Neuronal differentiation in the dorsal brain is reduced by 36hpf in *wnt3* morphants (B, C). (D-F) By 72hpf the process of neuronal differentiation in the dorsal diencephalon and midbrain remain affected in *wnt3* morphants (E, F). Abbreviations: c, cerebellum; dt, dorsal thalamus; ep, epithalamus; hb, hindbrain; hy, hypothalamus;pt, posterior tuberculum; t, telencephalon; tg, tegmentum and vt, ventral thalamus.

3.8 Wnt3 is Required for Cell Proliferation

Most events of early neural differentiation occur close to the ventricular zone from where the newborn postmitotic cells migrate to more peripheral mantle zone of the neural tube. We have previously shown that overexpression of Wnt3 induces proliferation in the brain (Fig. 3.10) and decided to investigate the contribution of cell proliferation deficiency on differentiation defects observed in Wnt3 morphants. Comparative immunohistochemical study of the CNS was conducted with monoclonal antibody against Proliferating Cell Nuclear Antigen (α-PCNA) on both wild type and morphants after injection of MO against *wnt3* splice site (Fig.3.19). PCNA is the auxiliary protein of DNA polymerase-δ (Bravo et al., 1987; Mathews et al., 1984) and is essential for mitosis. PCNA-immunoreactive cells can be seen in distinct zones of proliferation of the anterior CNS by 72hpf (Wullimann and Knipp, 2000). In the wild type embryo, large clusters of proliferative cells are detected in the telencephalon, habenula, dorsal thalamus, ventral thalamus, pretectal area, preoptic area, hypothalamus, optic tectum, midbrain-hindbrain boundary and cerebellum. In the Wnt3 morphant, PCNA+ cells cannot be detected in dorsal parts of the brain including the optic tectum and cerebellum. Since *wnt3* is expressed in a similar manner in both regions (Fig.3.6), we suggest that Wnt3 is essential for cell proliferation in both optic tectum and cerebellum. In addition, cell proliferation is reduced but not absent in dorsal diencephalon of Wnt3 morphant (Fig. 3.19 D). This implies that factor(s) other than absence of proliferation may contribute to reduce differentiation observed in this part of the brain or presence of proliferation in this area could be due to incomplete knockdown revealing a dose-dependent effect of anti-sense Wnt3 morpholino oligonucleotides.

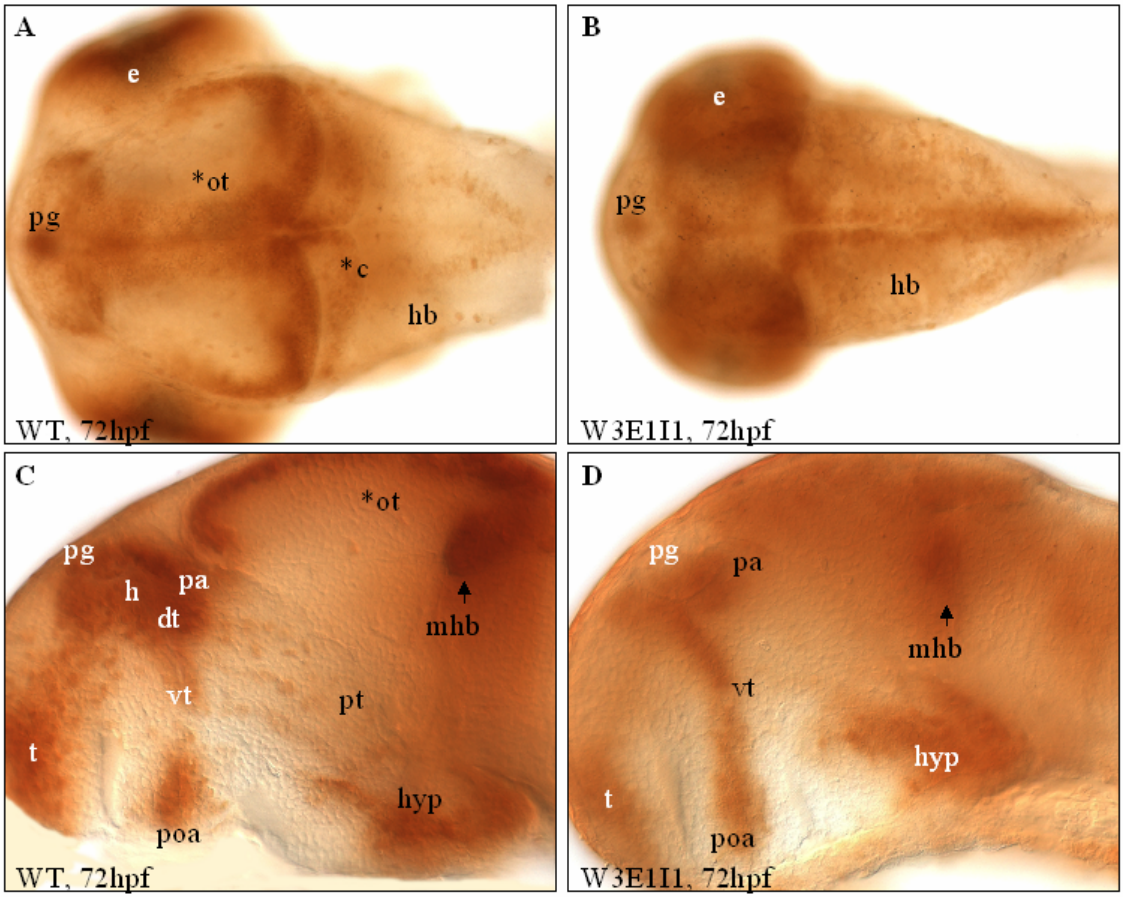

Fig.3.19 Cell proliferations in dorsal diencephalon, optic tectum and cerebellum are affected in Wnt3 morphant. Dorsal (A-B) and lateral views (C-D) of 3dpf PCNA stained zebrafish embryos. Immunohistochemistry was performed with polyclonal antibody against PCNA on both wild type (A, C) and Wnt3 morphant (B, D) at the stage of 72hpf. Cell proliferation in the dorsal diencephalon is reduced in Wnt3 morphant (D). In addition no PCNA staining is detected in the vicinity of the cerebellum (B) and optic tectum (D). Abbreviations: c, cerebellum; dt, dorsal thalamus; h, habenula; hb, hindbrain; hyp, hypothalamus; mhb, midbrain-hindbrain boundary; pa, pretectal area; pg, pineal gland; poa, preoptic area; pt, posterior tuberculum; t, telencephalon and vt; ventral thalamus.

3.9 Islet-1^{+} Neurons in the Diencephalon are Specifically Reduced in Wnt3 Morphants

We have used α-16A11 as an early neuronal marker to examine neuronal differentiation defects in Wnt3 morphants. In this section we proceed to check if neuronal-type specific factors that regulate differential properties of neurons, such as axon projection pattern are affected in Wnt3 morphants. Examples of neuron-type specific factors are the LIM family of transcription factors, expressed in combinations in different motor neuron populations (Appel et al., 1995; Thor et al., 1999; Thor and Thomas, 1997; Tosney et al., 1995; Tsuchida et al., 1994). Islet-1 (Isl1) is a member of the Isl family of LIM-homeodomain transcription factors and is expressed in a defined subsets of neurons during vertebrate embryogenesis (Ericson et al., 1992; Gong et al., 1995; Inoue et al., 1994; Korzh et al., 1993). In the anterior CNS of rat Isl1 is expressed in neurons of the caudate-putamen, septal nuclei, and in nuclei of basal telencephalon. In the diencephalon, a particularly high expression of Isl1 can be detected in the pineal gland, dorsal thalamus, ventral thalamus and hypothalamus (Thor et al., 1991). Islet-1 is expressed in several clusters of primary neurons in zebrafish (Korzh et al., 1993). Later developmental analysis of zebrafish islet-1 transgenic line revealed that Islet-1 is also expressed in motor neurons of cranial nerves III, IV, in the midbrain and V, VII, IX and X in the hindbrain (Higashijima et al., 2000). Islet-1 expression is only partially reflected in this transgenic line. In particular, the dorsal Islet-1 positive clusters do not express GFP in this transgenic line.

We decided to stain 72hpf embryos with anti- Isl1 polyclonal antibody (∝-Isl-1) to visualize Isl1+ neurons in the dorsal neural tube of both wild type embryos (Fig.3.20 A, D) and Wnt3 morphants (Fig.3.20 B-C, E-F). We show that neurons in the diencephalon, particularly those in the dorsal thalamus and ventral thalamus are almost absent upon knockdown of Wnt3 (Fig.3.20 B-C). In contrast, the Isl1+ neurons in the telencephalic nuclei and cranial motor nerves are less affected (Fig.3.20 B-C, E-F). Hence whole-mount immunochemical labeling with ∝-Isl-1 suggests that neuronal differentiation in both dorsal and ventral thalamus is defective in Wnt3 morphants.

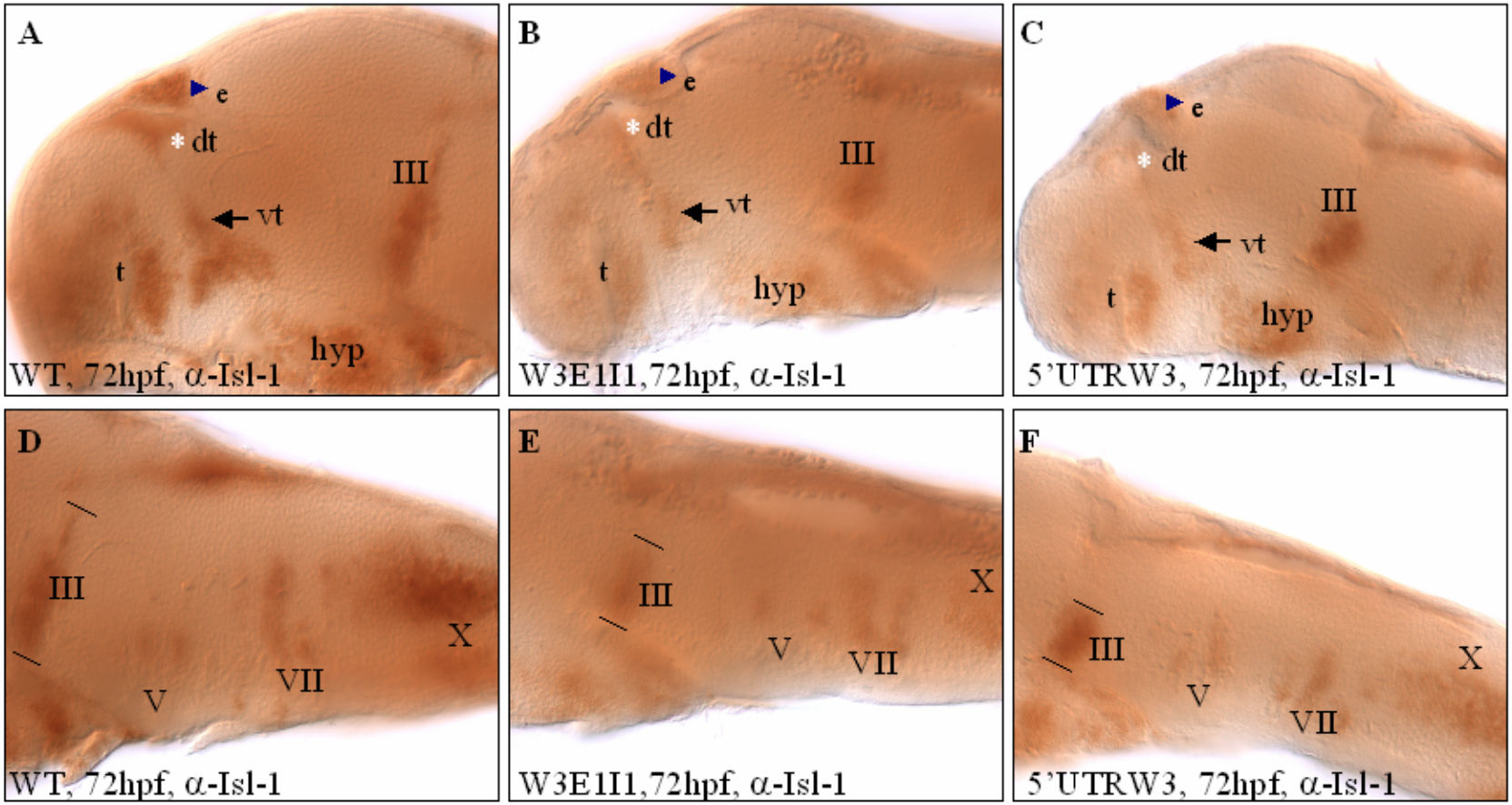

Fig.3.20 Whole-mount immunochemical labeling of 72hpf embryos with anti-Isl1 polyclonal antibody (∝-Isl-1). The approach was used to visualize subsets of neurons involved in motor, autonomic and endocrine control in both wild type (A, D) and Wnt3 morphants (B, E and C, F). Lateral views of rostral (A-C) and caudal (D-F) segment of the anterior CNS in 72hpf zebrafish embryos. Both ventral (black arrow) and dorsal thalamus (white asterisk) are almost absent in Wnt3 morphants (B, C). In comparison, Wnt3 morphants retain Islet-1^{+} expression in cranial nerves III, V, VII and X (B, E and C, F). Dorsoventral extension of the cranial nerves is reduced in Wnt3 morphants (E,F) as exemplified by oculomotor nerve. Abbreviations: dt, dorsal thalamus; e, epiphysis; hyp, hypothalamus; t, telencephalic nucleus; vt, ventral thalamus; III, oculomotor nerve; V, trigeminal nerve; VII, facial nerve and X, vagus nerve.

We verified the effect of Wnt3 on cranial motor nerves by microinjecting control or Wnt3 MO into 1-4 cell stage embryos collected from Isl1-GFP transgenic line (Higashijima et al., 2000). The expression of GFP by the motor neurons in the transgenic fish enabled visualization of the cell bodies and main axons, of the cranial nerves. Motor neurons of cranial nerves III, V and VII though reduced are present in Wnt3 morphants (Fig. 3.21 C-D). However most of the axonal projections seen in wild type embryos and Wnt3 control morphant that emanate from labeled cranial nerves (Fig. 3.21 A-B) are absent in Wnt3 morphants (Fig. 3.21 C-D). The absence of axonal tract suggests that motor neurons of cranial nerves III, V, VII and X are functionally deficient or their development is delayed in Wnt3 morphants.

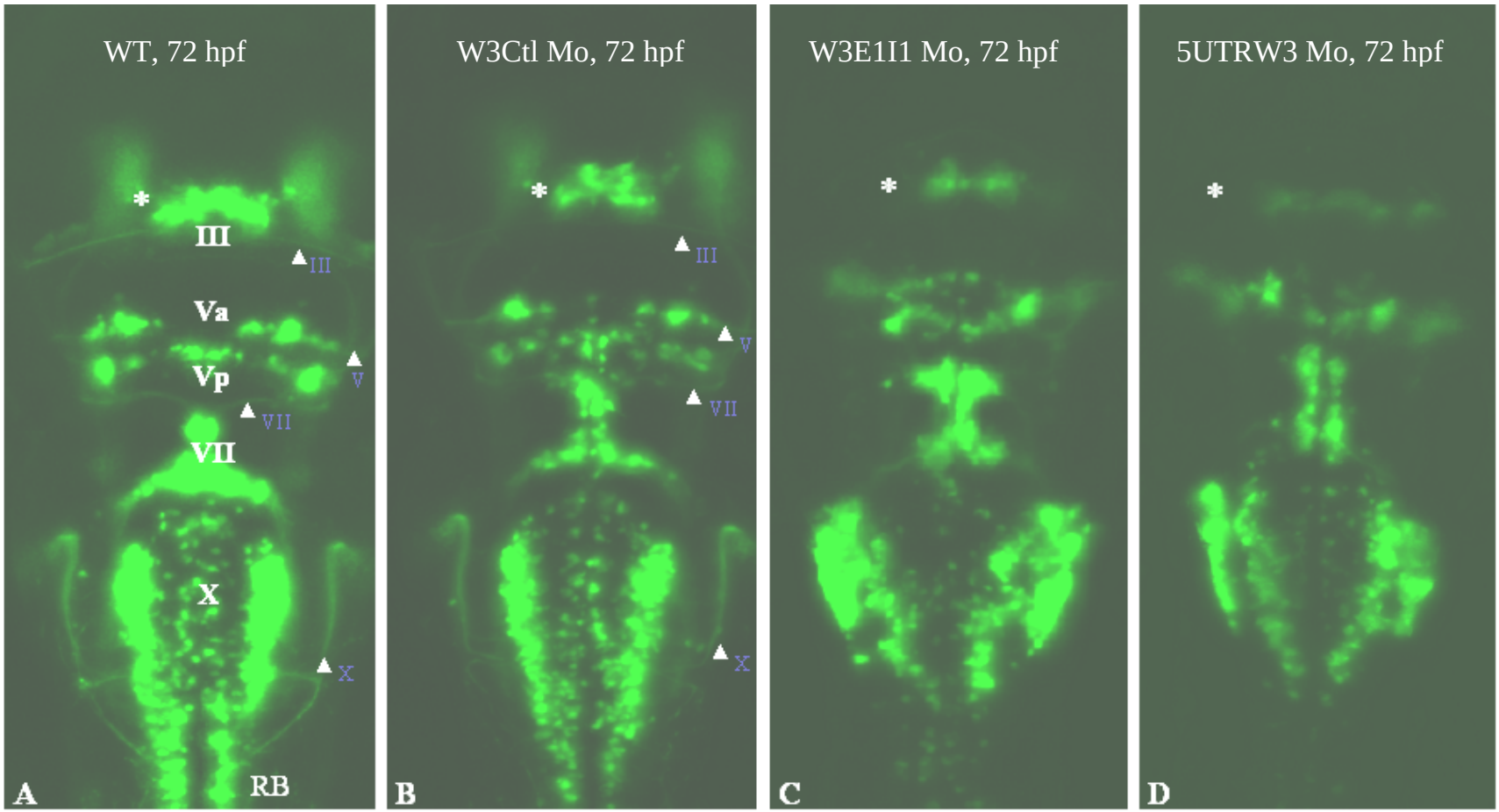

Fig.3.21 GFP expression in cranial motor neurons in the Isl1-GFP transgenic line is present in Wnt3 morphants. (A-D) Dorsal view of the midbrain (*) and the hindbrain of 72 hpf embryos. Notice the absence of axonal tracts associated with all labeled cranial nerves. Abbreviations: III, oculomotor nerve (eye muscles); V, trigeminal nerve (jaw muscles); VII, Facial nerve (facial muscles); X, vagus nerve (viscera of thorax and abdomen). A white arrowhead with corresponding cranial cluster labeled in blue marks the axonal tract emanating from each cranial nerve.

3.10 Wnt3 Morphants Specifically Affect the Formation of Habenula, Dorsal Thalamus and Optic Tectum

Analyses with ∝-acT (Fig. 3.17) and ∝-16A11 (Fig. 3.18) indicated that neuronal differentiation in the dorsal brain is particularly affected in Wnt3 morphants. Our final approach to characterize differentiation defects in Wnt3 morphants involved living color transgenic lines, with special interest in the diencephalon and midbrain. Zebrafish embryos are optically transparent thus making transgenic lines with tissue-specific distribution of fluorescent reporter great markers for anatomical studies. The following enhancer trapped transgenic lines ET11, ET16, ET22-1 and ET27 are used to further characterize defects that arise in the absence of Wnt3. These transgenic lines are part of a panel of enhancer trap (ET) transgenic lines generated in this laboratory by insertion of modified Tol2 transposable element (Parinov et al., 2004). Complex GFP expression patterns were detected in the anterior CNS of these transgenic lines. We characterized GFP expression pattern in the diencephalon and the midbrain by merging lateral views of fluorescent and bright field images of 72hpf larvae of these lines and compared the region of GFP expression with a map of zebrafish anterior CNS at 72hpf (Fig. 3.22).

Overlapping subdomains of the epithalamus can be clearly segregated by comparing GFP expression from transgenic lines ET11, ET16 and ET22-1. The epithalamus in dorsal diencephalon is constituted by two sets of neuronal conglomerates: the habenula and the pineal complex. In zebrafish, the more dorsal pineal complex situated along the caudal part of the diencephalic roof plate gives rise to a pair of tubular evaginations known as the pineal gland and the parapineal organ (Concha and Wilson, 2001), the pineal gland developing earlier and is located in more posterior position than the parapineal organ. The more ventral habenula is formed by a bilateral set of nuclei that aligned the third ventricle dorsally. The dorsoventral patterning of the epithalamus can be seen upon anatomical comparison

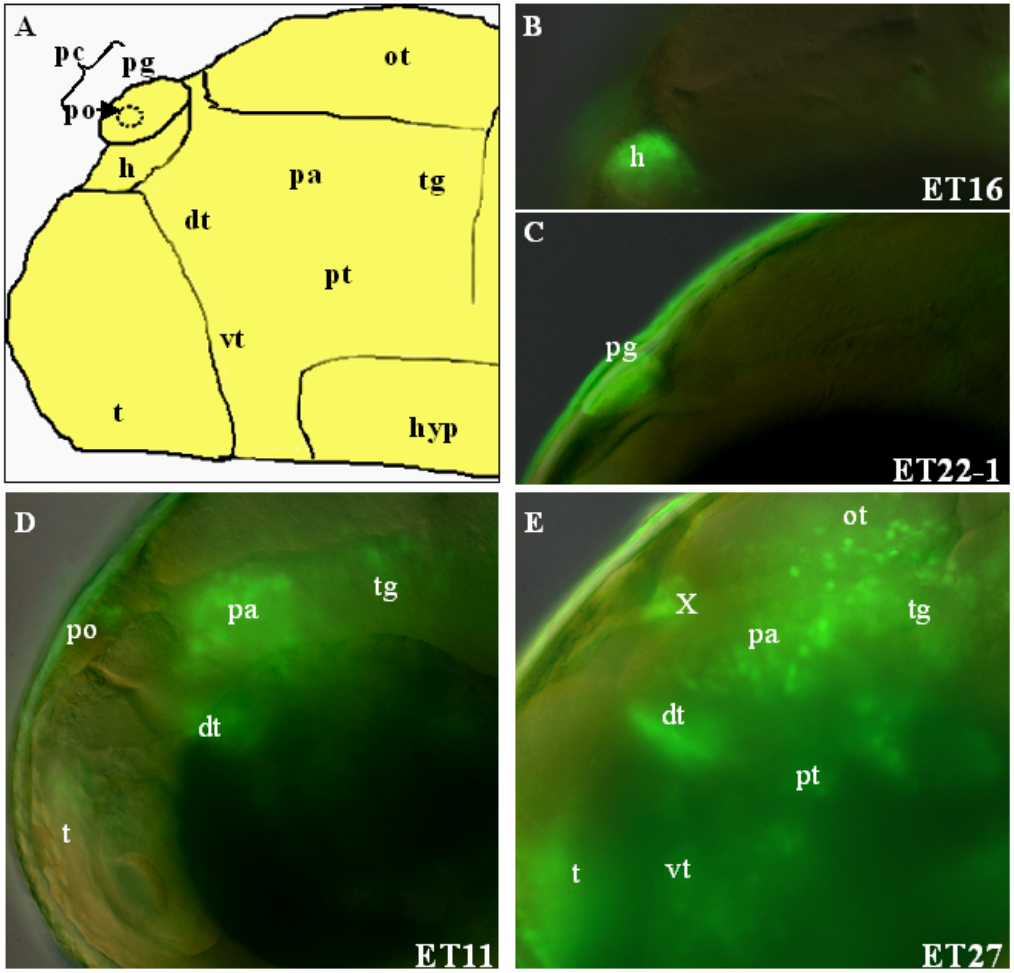

Fig.3.22 Summary of GFP expression in ET lines 11,16, 22-1 and 27 at 72hpf. (A) A diagram demarcating subdomains of the anterior CNS in a zebrafish embryo at 72hpf. (B-E) Lateral views of wild type72 hpf transgenic embryos from (B) ET16, (C) ET22-1, (D) ET11 and (E) ET27. Images displayed in (B-E) are obtained by merging bright field and fluorescent views of the respective embryo at 200X magnification. Abbreviations: dt, dorsal thalamus; h, habenula; hyp, hypothalamus; ot, optic tectum; pa, pretectal area; pc, pineal complex; pg, pineal gland; po, parapineal organ; pt, posterior tuberculum; t, telencephalon; tg, tegmentum; vt, ventral thalamus and X, undefined structure in pretectal area.

of GFP+ cells in ET11, ET16 and ET22-1 where GFP+ habenula in ET16 (Fig.3.22B) is located ventral to that of GFP+ pineal gland and parapineal organ of ET22-1 (Fig.3.22C) and ET11 (Fig.3.22D), respectively. In addition to the parapineal organ, an asymmetrically left-sided structure within the epithalamus, ET11 also expresses GFP in the dorsal thalamus, pretectal region and tegmentum (Fig. 3.22D). More complex expression is seen in ET27 where GFP+ cells are found in the telencephalon, dorsal thalamus, ventral thalamus, pretectal region, posterior tuberculum, optic tectum and tegmentum (Fig. 3.22E).

Our preliminary characterization of GFP expression in ET lines showed that the pineal gland, parapineal organ and habenula, subdomains of the epithalamus, are differentially labeled in three of the transgenic lines. We decided to characterize GFP+ habenula in greater detail. The habenula is a relatively complex structure that relays information from the telencephalon to the midbrain through stria medullaris and the habenular-interpeduncular tract, respectively. The habenular complex is a bilaterally asymmetrical organ located ventral to the pineal gland and is further divided into the medial and lateral nuclei (Aizawa et al., 2005; Kim and Chang, 2005). The habenula by 72hpf is asymmetrical (Fig.3.23A) and relays information to the midbrain via the habenular-interpeduncular tract (Aizawa et al., 2005). In rat, the medial habenular nucleus is characterized by a remarkable high density of cells (Kim and Chang, 2005) and thus can be differentiated from the lateral nucleus. A similar observation is made in sections of Nissl-stained zebrafish embryo in Fig. 3.23B (Lam, 2002). Transverse cryo-section at the level of habenula of ET16 embryo showed that the *gfp* expression is restricted to the lateral habenular nuclei (LHN; Fig. 3.23C).

We proceed to investigate the status of neuronal differentiation in the epithalamus by injecting both control and *wnt3* MO into GFP transgenic lines that specifically tagged the pineal gland (ET22-1) or lateral habenular nuclei (ET16). The pineal gland, the dorsal most

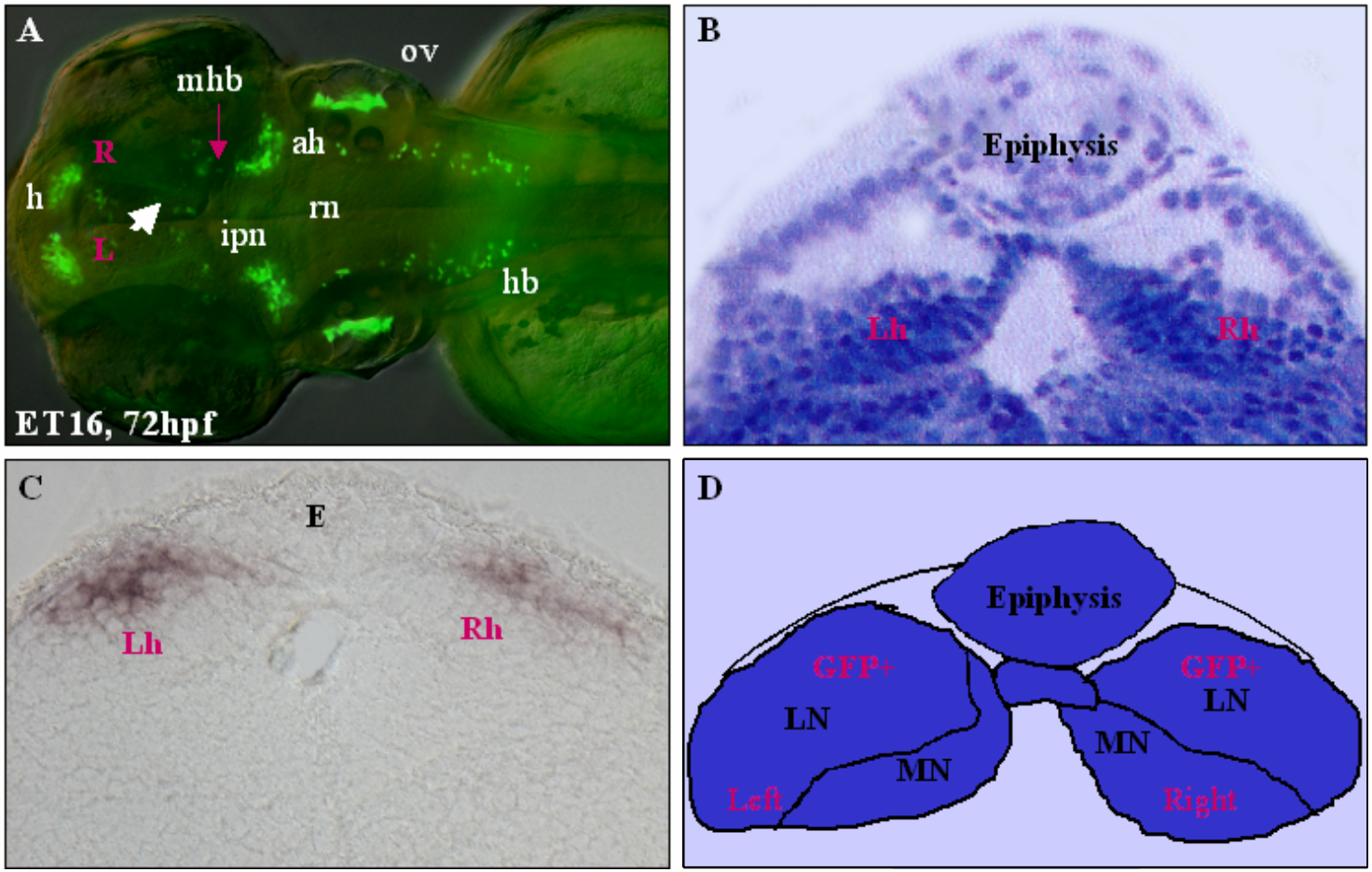

Fig.3.23 The enhancer trap transgenic line ET16 expresses EGFP in the lateral nucleus of the habenula. (A) Dorsal view of ET16 at 72hpf showing GFP labeling of the entire length of the habenulo-interpeduncular projection (white arrow). (B) Nissl-stained embryo at 72hpf on transverse cryo-sections at the level of bilateral lobes of the habenular nucleus. (C) Transverse cryo-section at the level of bilateral lobes of the habenular nucleus of a 72hpf ET16 stained with Dig labeled anti-*EGFP* probe. (D) Summary schematic of habenula organization indicating GFP expression of ET16 with respect to medial and lateral nuclei of habenula in a transverse section of a 72hpf embryo. Abbreviations: ah, anterior hindbrain; h, habenula; hb, hindbrain; ipn, inter peduncular nucleus; Lh, left habenula; LN, lateral nucleus of the habenula; MN, medial nucleus of the habenula; Rh, right habenula and rn, raphe nucleus.

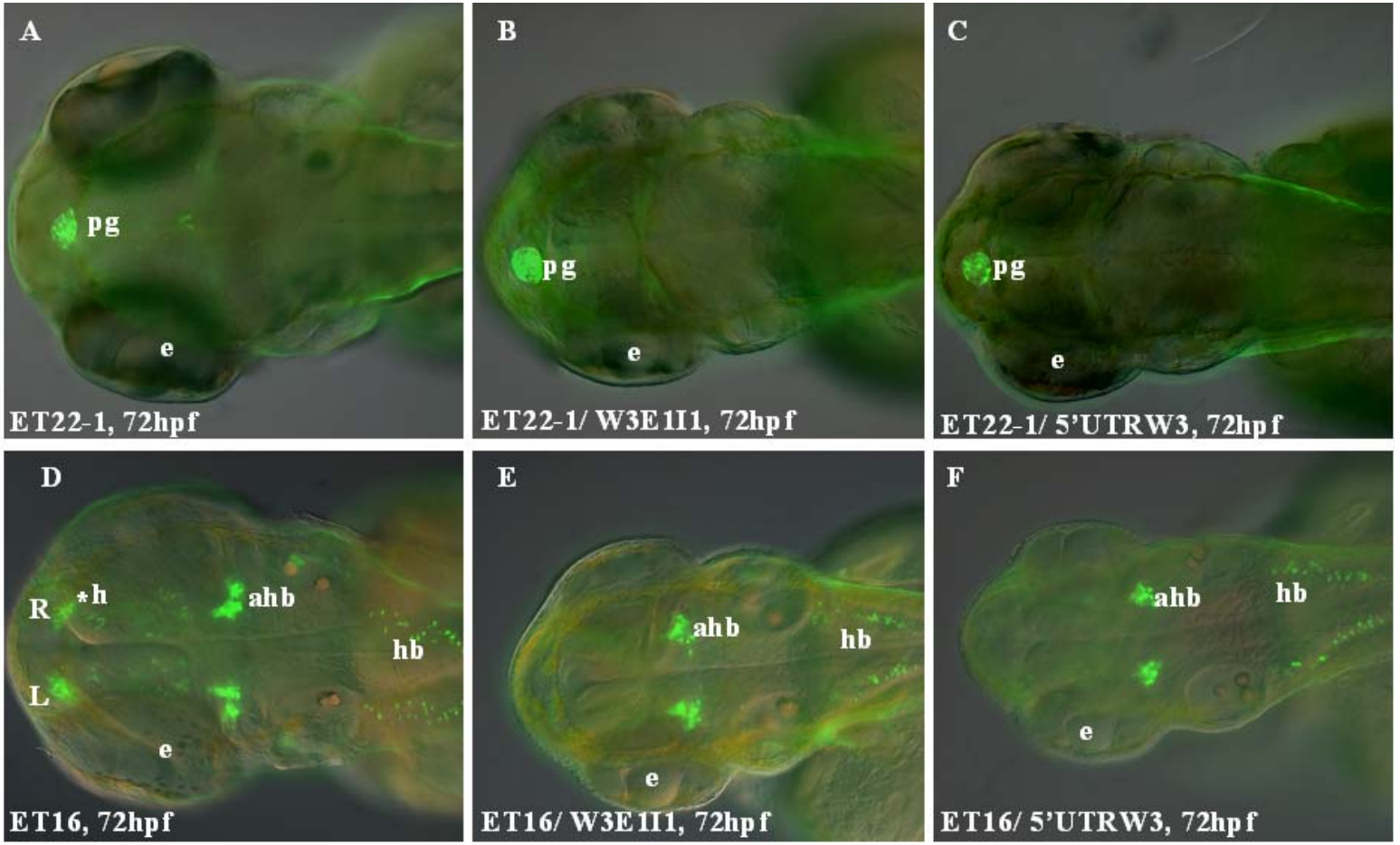

Fig.3.24 Habenula is affected in Wnt3 morphants. (A-F) Dorsal views of 72 hpf embryos from ET22-1 (A-C) and ET16 (D-F). Control (A, D) or embryos microinjected at 1-4 cell stage with anti-*wnt3* morpholino (B-C, E-F) are illustrated in the above panels. (B, C) The integrity of pineal gland is not affected in *wnt3* morphants. (E, F) The bilateral asymmetrical habenula is absent in *wnt3* morphants. Images displayed are obtained by merging bright field and fluorescent views of the embryo using Adobe Photoshop. Abbreviations: ahb, anterior hindbrain; e, eye; h, habenula; hb, hindbrain; L, left habenula; pg, pineal gland and R, right habenula.

structure in the diencephalon is unaffected in ET22-1 transgenic line injected with Wnt3 MO (W3E1I1 MO, 20/20; 5UTRW3 MO, 20/20; Fig.3.24 A-C). However, the more ventral habenula is absent in both Wnt3 morphants (W3E1I1 MO, 30/30; 5UTRW3 MO, 30/30; Fig.3.24 E-F). This observation is confirmed in lateral views of Wnt3 morphant (Fig. 3.25 D-F). In addition to the lateral habenular nuclei, GFP+ cells are detected in the telencephalon, anterior hindbrain, otic vesicle, rhombomere 5 and anterior spinal cord of ET16 transgenic line. GFP expression in the otic vesicle and rhombomere 5 were also abolished upon Wnt3 knockdown while clusters of GFP+ cells in the anterior hindbrain and spinal cord remain unaffected. Hence Wnt3 is required for the formation of habenula, otic vesicle and rhombomere 5 but not the pineal gland or ventral neurons in anterior hindbrain and spinal cord.

We continue our analysis in ET11 to check if the parapineal organ and other GFP+ structures labeled in the transgenic line are affected upon Wnt3 knockdown. GFP+ cells can be detected in the telencephalon, parapineal organ, eye, dorsal thalamus, pretectal area, hindbrain, anterior spinal cord and branchial arches of 72hpf ET11 embryo. Many of these structures are affected upon Wnt3 knockdown and include dorsal thalamus, eye, tegmentum, hindbrain and branchial arches (W3E1I1 MO, 30/30; 5UTRW3 MO, 26/26). GFP expression in the telencephalon, parapineal organ, pretectal area and anterior spinal cord remained unaffected in Wnt3 morphant (Fig. 3.26 D-F). Hence combined analyses from ET11, ET16 and ET22-1 demonstrated that habenular differentiation is specifically affected in Wnt3 morphant. The absence of GFP+ cells in the dorsal thalamus and hindbrain agrees with abnormal differentiation found in the dorsal brain of Wnt3 morphants (Fig. 3.18). We verified differentiation defects observed in the dorsal thalamus, midbrain, hindbrain and branchial arches by incorporating ET27 into our final morphant analysis. GFP+ cells are present in the telencephalon, dorsal thalamus, ventral thalamus, pretectal region, posterior tuberculum, optic tectum, tegmentum, hindbrain, anterior spinal cord and branchial arches. Regions affected in ET27 upon Wnt3 knockdown included the eye, dorsal thalamus, ventral thalamus, optic

tectum, hindbrain and branchial arches (W3E1I1 MO, 20/20; 5UTRW3 MO, 22/22). Common differentiation defects caused by Wnt3 knockdown were detected in the eye, dorsal thalamus, hindbrain and branchial arches of ET11 and ET27. In fact a distinctly labeled horn-like structure (*) in the dorsal thalamus of wild type embryo (Fig.3.27 A-C) is absent in Wnt3 morphant (Fig.3.27 D-F). The dorsal midbrain is specifically affected, as neuronal differentiation in the optic tectum is absent in ET27 transgenic line microinjected with *wnt3* MO (Fig.3.27 D-F). The absence of neuronal differentiation in the hindbrain is similar to that observed in ET11 (Fig. 3.26). Wnt3 activity seems to be limited to the brain, as neuronal differentiation in the more posterior spinal cord remained unaffected in Wnt3 morphant. Hence based on morphant analysis conducted with transgenic lines ET11, ET16, ET22-1 and ET27 we conclude that Wnt3 activity is required for the development of the habenula, dorsal thalamus, ventral thalamus, optic tectum and hindbrain of zebrafish embryo.

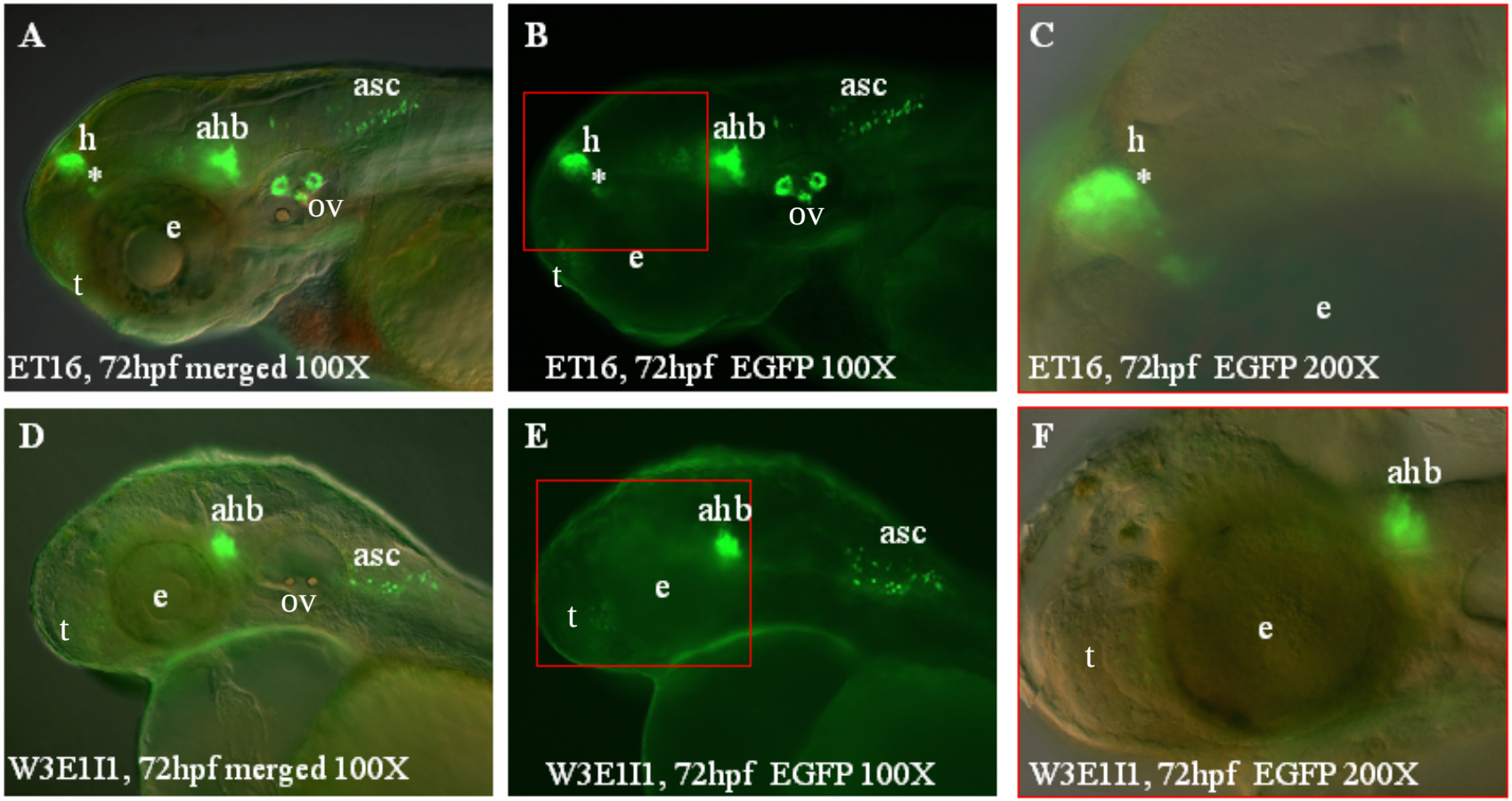

Fig.3.25 The habenula is affected in Wnt3 morphant. Lateral views of 72 hpf embryos from ET16 control (A-C) or microinjected at 1-2 cell stage with W3E1I1 Mo (D-F). Images displayed in (A, D) are obtained by merging bright field and fluorescent views of the respective embryo using Adobe Photoshop; (B, E) are the fluorescent images and (C, F) are the enlarged merged images boxed in (B, E) and taken under 200X magnification. Abbreviations: ahb, anterior hindbrain; asc, anterior spinal cord; e, eye; h, habenula; ov, otic vesicle and t, telencephalon.

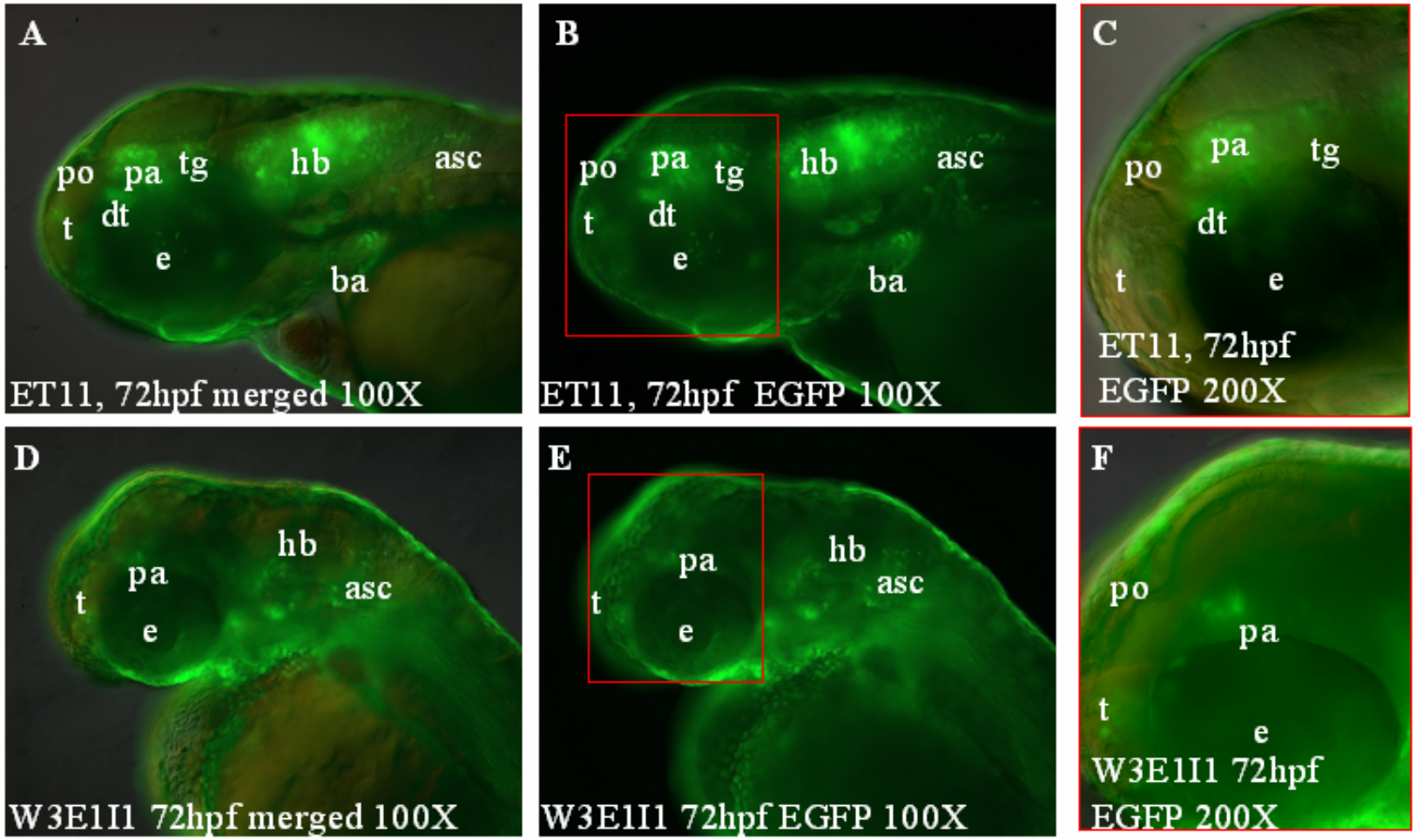

Fig.3.26 The dorsal thalamus is affected in Wnt3 morphants. Lateral views of 72 hpf embryos from ET11, that are control (A-C) or microinjected at 1-2 cell stage with W3E1I1 Mo (D-F). Images displayed in (A, D) are obtained by merging bright field and fluorescent views of the respective embryo using Adobe Photoshop; (B, E) are the fluorescent images and (C, F) are the enlarged merged images boxed in (B, E) and taken under 200X magnification. Abbreviations: asc, anterior spinal cord; ba, branchial arches; dt, dorsal thalamus; e, eye; hb, hindbrain; pa, pretectal area; po, parapineal organ, t, telencephalon and tg, tegmentum.

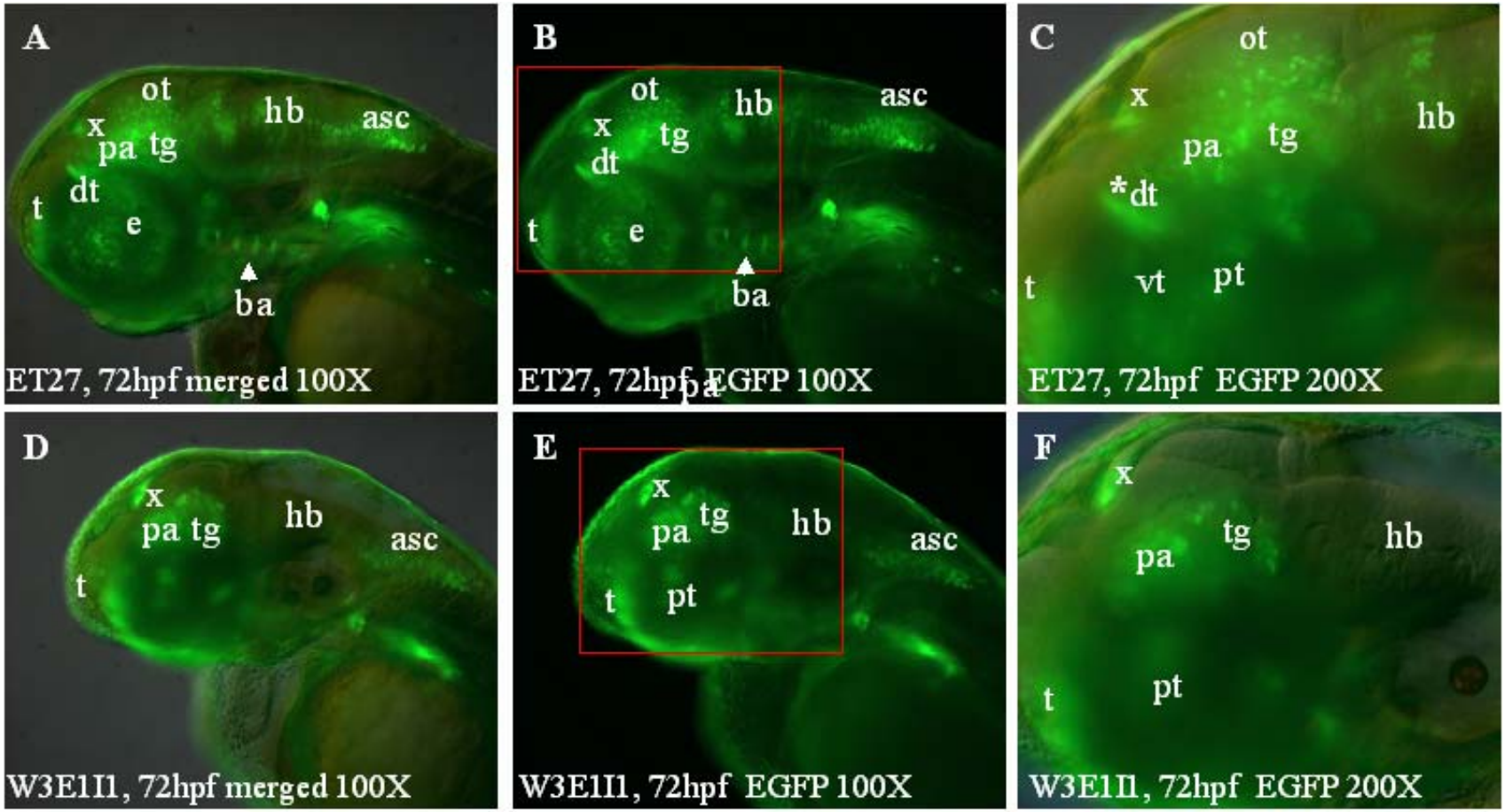

Fig.3.27 The dorsal thalamus and optic tectum are affected in Wnt3 morphant. Lateral views of 72 hpf embryos from ET27, that are control (A-C) or microinjected at 1-2 cell stage with W3E1I1 Mo (D-F). Images displayed in (A, D) are obtained by merging bright field and fluorescent views of the respective embryo using Adobe Photoshop; (B, E) are the fluorescent images and (C, F) are the enlarged merged images boxed in (B,E) and taken under 200X magnification. Abbreviations: asc, anterior spinal cord; ba, branchial arches; dt, dorsal thalamus; e, eye; hb, hindbrain; ot, optic tectum; pa, pretectal area; pt, posterior tuberculum; t, telencephalon; tg, tegmentum; vt, ventral thalamus and X (undefined structure in pretectal area).

Chapter IV

Discussion

4. Discussion

Several members of the Wnt family are expressed in discrete domains along the A-P and D-V axes of the neural tube. However the role of some of these Wnts in neurogenesis remains unclear. This thesis aims to define the role of *wnt3* in neural development of zebrafish.

4.1 Expression Pattern of *wnt3* in Zebrafish

We analyzed the expression pattern of zebrafish *wnt3* in the neural tube to define areas where the gene could be active. We have shown that zebrafish *wnt3* is expressed in a pattern that is similar to that reported in chick (Robertson et al., 2004) and mouse (Bulfone et al., 1993; Parr et al., 1993; Roelink and Nusse, 1991) and summarized the respective expression patterns in Table 4.1. The expression in the CNS extends from the spinal cord to the diencephalon, where its expression terminates at the zona limitans intrathalamica. Areas with strong expression lie mainly in dorsal brain and include the ventral epithalamus, dorsal thalamus, optic tectum, cerebellum and hindbrain. The continuous expression from ventral epithalamus to dorsal thalamus has resulted in the use of *wnt3* as a neuromeric molecular marker for prosomere 2 of diencephalon (Bulfone et al., 1993). Additional expression domains include the midbrain-hindbrain boundary (MHB), zona limitans intrathalamica (ZLI), and anterior floor plate. These regions together with expression in the dorsal domains form a *wnt3*+ zone that surrounds the territory of posterior diencephalon and midbrain. The ventral extension of *wnt3* expression in zli towards anterior floor plate is unique when compared to other dorsal midline Wnts such as Wnt1, Wnt3a and Wnt10b (Buckles et al., 2004; Lekven et al., 2003). Transverse cryosection showed that *wnt3* is detected in both the ventricular zone and mantle of dorsal thalamus. This implies that *wnt3* is expressed in the mitotically active precursor cells as well as differentiating cells of the dorsal thalamus. Similar observations were made in chick and mouse (Bulfone et al., 1993; Robertson et al., 2004) that suggested a putative role of Wnt3 in patterning the developing dorsal thalamus. In zebrafish, the expression in the dorsal thalamus remained strong at 7dpf, the last stage of our expression analysis.

Table 4.1. A Comparative Study of *wnt3* Expression Domains in Zebrafish, Chick and Mouse.

	Zebrafish	Chick	Mouse
Primitive Streak *	-	-	+
Anterior Floor Plate	+	-	-
Diencephalon			
Zona limitans intrathalamica	+	+	+
Ventral epithalamus	+	+	+
Dorsal thalamus	+	+	+
Midbrain			
Optic Tectum	+	+	+
Midbrain-hindbrain boundary	+	-	+
Hindbrain			
Cerebellum	+	+	+
Posterior dorsal hindbrain	+	+	+
Spinal cord	+	+	+
Branchial arches	+	+	+
Limb buds **	-	+	+

Note: The expression in the primitive streak is unique to mouse (*). The absence of *wnt3* expression in the fin buds is unique to zebrafish (**).

Divergence in expression pattern arises in the domains of anterior floorplate and fin buds. The expression domain of *wnt3* in the anterior floorplate, the ventral-most part of the neural tube, seems to be unique to zebrafish. In addition, ectodermal staining of the limb buds that were detected in chick and mouse (Parr et al., 1993; Robertson et al., 2004), are absent in the fin buds of zebrafish. Similar to chick, we do not detect any expression of zebrafish *wnt3* during primary gastrulation. The earliest *wnt3* signal detected by WISH is at 13hpf and is confined to the anterior CNS with distinct expression in the dorsal midline, diencephalon and MHB. This is in contrast to high levels of *Wnt3* expression seen in the mouse primitive streak (Liu et al., 1999). In fact analysis of *Wnt3* knockout mouse makes it clear that this gene is critical for murine gastrulation. Current data obtained from homozygous mutation of this gene in human (Niemann et al., 2004) as well as expression analysis conducted in chick (Robertson et al., 2004) and zebrafish (this study) suggest that a role of Wnt3 during gastrula stage may be unique to mouse. Hence both evolutionary conserved and species-specific characteristics exist in the expression pattern of zebrafish *wnt3*.

4.2 Electroporation as a Method for Targeted Misexpression of Genes

We have shown that *wnt3* is expressed in the developing CNS. The persistent expression in the anterior CNS suggests continuous participation in neural patterning events throughout embryo development. Functional studies in zebrafish are generally carried out by loss of function experiments including mutant analysis and / or inhibition of gene function by the injection of antisense morpholino oligonucleotides into 1-4 cell staged embryo. These efficient approaches are unfortunately limited to the earliest phase of gene activity as it is difficult to disentangle different biological functions of the gene that could play multiple roles at closely spaced periods of development. Gain of function experiments such as panembryonic microinjection of mRNA or DNA could provide some information about gene activity (Holder and Xu, 1999; Xu, 1999). In addition, effects of these experiments could be slightly delayed by microinjection into a single cell or late blastomere limiting changes in

gene activity to individual cell or small clones of cells with distinct fates (Fong et al., 2005; Strehlow et al., 1994). Electroporation, a relatively new technology, is another way to locally misexpress any gene of interest at any time during development. While it allows us to analyze late patterning events while keeping earlier functions intact (Nakamura and Funahashi, 2001; Osumi and Inoue, 2001; Tabata and Nakajima, 2001), it was not developed to be readily applied to zebrafish embryos.

Our interest in studying the effect of misexpression of *wnt3* in the anterior CNS led us to develop an *in vivo* electroporation approach that allows delivery of DNA into the brain of zebrafish embryo (Teh et al., 2003). Our method involves microinjecting DNA into the neural cavity. After that, the injected embryo is placed into an an agarose well in the electroporation chamber. The embryo position is adjusted such that only the neccessary region of the neural tube is exposed to the full strength of the electric field. A further refinement of the technique that was introduced later on involves variations in types of electrodes used. When electrodes of dissimilar size are used, the electric field becomes non-uniform. This resulted in substantial enhancement of transgene expression (Teh et al., 2005). This approach allowed us to study the effect of Wnt3 misexpression in specific regions of the brain.

4.3 Wnt3 Signals through the Canonical Pathway during Neural Development

Three major pathways have been identified in Wnt signaling, (i) the Wnt/ β-catenin pathway (canonical pathway) in which β-catenin is involved; (ii) the Frizzled/planar cell polarity (Fz/PCP) pathway, and (iii) the Ca2+ pathway. Distinct sets of Wnt and Frizzled ligand-receptor pairs can activate each of these pathways that lead to unique cellular responses. The Wnt/ β-catenin pathway primarily regulates cell proliferation and cell fate determination during development. The major function of the Fz/PCP pathway involves regulation of cytoskeletal organization. The biological function of the Ca2+ pathway is more complex and encompasses both cell fate determination and regulation of cell movement (Ciani and Salinas, 2005; Miller, 2002). Various assays were used to classify Wnts into distinct functional

classes. For example, overexpression studies in ventral blastomeres of *Xenopus* have shown that XWnt1, XWnt3a, XWnt8 and XWnt8b can stimulate axis duplication whereas XWnt4, XWnt5a and XWnt11 cannot. A second assay involves transfecting various Wnts into murine mammary epithelial cells. Three categories of Wnt genes could be described based on their transformation activity. Wnt1, Wnt3a and Wnt7a are highly transforming, Wnt2, Wnt5b and Wnt7b are intermediate in their transformation activities and Wnt4, Wnt5a and Wnt6 are unable to transform these cells (Wong et al., 1994). Wnts that cause axis duplication in *Xenopus* or transform murine mammary epithelial cells are deemed to act via the Wnt/ β-catenin pathway. Wnts that failed to do so activate the non-canonical pathways (Moon et al., 1997; Wodarz and Nusse, 1998). Although we can classify Wnts into two functional classes the relationship between specific Wnts and the intracellular pathways they use are not fixed. For example, overexpression of XWnt5a in combination with human FZ5 in Xenopus embryos results in activation of Wnt/ β-catenin pathway (He et al., 1997). This suggests that in vivo activities of Wnts also depend on the repertoire of Fz receptors present on the cell surface.

Neither the axis duplication assay in *Xenopus* nor transformation capabilities in murine mammary epithelial cells are suitable approaches for deciphering the signaling pathway Wnt3 adopts during neural development of zebrafish. Since activation of the canonical pathway requires the association of β-catenin with LEF/TCF family of transcription factors, we decide to assay for the effect of Wnt stimulation on activation of Tcf reporter plasmid(Korinek et al., 1997), TOPflash (Upstate, USA), during neural development. TOPflash plasmid contains 3 copies of TCF binding sites, a thymidine kinase (TK) minimal promoter and a luciferase ORF. Wnts that signal through the canonical pathway will activate the transcription of luciferase in the Tcf reporter plasmid. We therefore assay for canonical Wnt activity by electroporating expression constructs TOPflash, pExWnt3 or pExWnt1, pRLCMVLuc (loading control) and pEGFPN2 (fluorescent reporter) into the neural tube. The activation of canonical Wnt pathway is quantitated by luciferase activity upon overexpressing Wnt1 or

Wnt3 *in vivo*. Similar to Wnt1 and Wnt3a (Holmen et al., 2002), Wnt3 strongly activates TOPflash. Hence Wnt3 acts as a canonical Wnt during neural development. However we do not exclude the potential of Wnt3 in activating non-canonical pathways. Other experiments such as the effect on Ca^{2+} fluxes upon overexpression of Wnt3 need to be done before a full understanding of signaling pathway(s) downstream of Wnt3 can be achieved.

4.4 Gain of Function Experiments Conducted by Electroporation Indicate Patterning Potential of Wnt3

The electroporation technique that we developed allows studies of later patterning events such as stage-dependent fate determination of precursor cells in the brain. The brain of a 24hpf zebrafish embryo is already regionalized and contains progenitors with distinct developmental potentials (Simeone, 2002). Some fates, such as neuronal or glial, may be determined when a cell is actively proliferating. Other decisions, such as the phenotype of a mature neuron are determined post-mitotically (Ohnuma et al., 2001). A potential role of Wnt3 in neural patterning was suggested when transverse cryosection showed that this gene is expressed in both dividing and differentiating cells of the dorsal thalamus. To determine if Wnt3 acts as a mitogen for precursor cells in the brain, we co-electroporated pEGFP-N2 and pExWnt3 into the developing neural tube and measured the effect on cell proliferation. Ectopic expression of Wnt3 doubled the number of M-phase cells (pH3+) in the brain suggesting that Wnt3 acts as a mitogenic Wnt during neural development.

With the exception of dorsal roof plate and the ventral floor plate, the medial portion of the neural tube represents an epithelium composed entirely of mitotically active multipotent precursor cells. The exit from the cell cycle is marked by lateral migration of cells from the ventricular zone to the mantle zone, which is composed of post-mitotic, differentiating neurons and glia. To examine the developmental role of Wnt3, we overexpress Wnt3 at 24hpf by unilateral electroporation. Hu proteins are neuronal markers that identify both proliferating neuronal precursor cells as well as mature neurons (Barami et al., 1995; Marusich et al.,

1994). Over-expression of Wnt3 is sufficient to increase the number of HuC/D+ neuronal cells. In fact ectopic neuronal precursor cells are observed in the ventricular zone with enhanced Wnt3 activity. The strongest effect is seen in the dorsal thalamus and tegmentum. In comparison, increased HuC/D+ cells induced by ectopic expression of Wnt3 in the hindbrain remain restricted to the subventricular domain. Finally, overexpression of Wnt3 does not initiate neuronal differentiation in the cerebellum. Hence neuronal differentiation can be determined not only by the expression of differentiation-inducing factors, but also by the responsiveness of the cells to these factors.

Gain of function studies by electroporation showed that Wnt3 possesses both mitogenic and neurogenic properties. The two somewhat contradictory effects of Wnt3 may be due to the induction of excess neuronal precursor cells that have yet to exit their cell cycle. Alternatively, Wnt3 increase proliferation in the progenitor pool that later exit the cell cycle and move out of the progenitor areas. Consequently, the increase in HuC/D+ cells is a result of increase in cell proliferation. Ectopic HuC/D+ cells observed in the ventricular zone of dorsal thalamus and tegmentum may result from cells adopting a neuronal fate prior to their migration into the mantle zone or simply due to migration defect that results from enhanced Wnt3 activity. All these possibilities can be verified by assaying the effect on proliferation, differentiation and migration at various time points after misexpression of Wnt3. Our current data obtained from a fixed time point of 12 hours post-electroporation should be extended to cover a wider range of developmental stages to address these issues. However we favour a role of Wnt3 in the induction of neuronal precursor cells as enhanced Wnt3 signalling in vivo increased adult hippocampal neurogenesis of mice and rat by controlling neuronal fate committment and proliferation of neuronally committed precursor cells (Lie et al., 2005).

4.5 Wnt3 is Required for the Specification of Prosomere 2 of Diencephalon

The prosomeric model of brain development divides the developing forebrain into neuromeric divisions called prosomeres arrayed in an A-P manner in the neuroaxis (Rubenstein et al., 1994). In this schema the diencephalon arises from components of prosomeres p1 (pretectum), p2 (dorsal thalamus and epithalamus), p3 (ventral thalamus) and hypothalamus. It has been shown in chick that zli acts as a local signaling center that regulates the development of adjacent thalamic regions via Hedgehog signaling (Kiecker and Lumsden, 2004). Similarly, by default of its expression in zli and the flanking p2, Wnt3 like Shh may participate in thalamic patterning. An important functional role for Wnt signaling in thalamic development has been suggested in chick, where Wnt signals were shown to be required at early stages to induce a posterior forebrain marker in the diencephalon and then again at later stages to induce dorsal thalamic markers within this posterior forebrain domain (Braun et al., 2003). Importantly, the study conducted in chick explants have shown that exogenous Wnt3 or Wnt3a were sufficient to induce the dT marker *Gbx2* in explants isolated posterior to the presumptive zli (Braun et al., 2003).

Recent work on zebrafish *wnt3a* showed that depletion of Wnt3a through injection of either a translation blocking or splice blocking morpholinos is insufficient to interfere with development of wild type embryos. Extensive apoptosis in the midbrain and cerebellum can only be observed in the absence of Wnt3a, Wnt1 and Wnt10b (Buckles et al., 2004). Our work with zebrafish *wnt3* showed that this gene is functionally less redundant than *wnt3a*. Knockdown studies conducted with the injection of either a translation blocking or splice blocking morpholinos into wild type embryos resulted in extensive apoptosis (Fig.3.13) as well as patterning defects in the diencephalon, midbrain and hindbrain (discussed below). Three different approaches were adopted to analyze defects that arise upon Wnt3 knockdown. Marker analysis in Wnt3 morphants with *nkx2.2* and *pax6b* showed that D-V patterning is affected, specifically with the loss of the dorsal thalamic locus (Fig. 3.15). Immunohistochemical experiments conducted on 3dpf embryos substantiated the data as

processes of neuronal differentiation (∝-acT and ∝-HuC) and cell proliferation (∝-PCNA) are reduced in the dorsal diencephalon of Wnt3 morphants. The absence of DVDT showed that defect in formation of dorsal thalamus first indicated by patterning defects observed with *nkx2.2* and *pax6b* probes is still present in 3dpf Wnt3 morphants. The final approach involved Wnt3 morphant analysis on living color transgenic lines. Zebrafish embryos are optically transparent thus making transgenic lines with tissue-specific distribution of fluorescent reporter great living markers for anatomical studies. Wnt3 morphant studies in ET11 and ET27 transgenic lines re-affirmed the absence of dorsal thalamus or its great reduction (Fig. 3.26 and Fig. 3.27). Hence we showed through morphant analysis that zebrafish *wnt3* is required for the specification of dorsal thalamus. This requirement is an evolutionary conserved feature of Wnt3 as the formation of dorsal thalamus is also Wnt3-dependent in chick.

Wnt3 is expressed in the epithalamus from 30hpf. In order to see which part of the epithalamus depends on Wnt3, we used transgenic lines ET11, ET16 and ET22-1as our living anatomical markers for the pineal gland, parapineal organ and habenula respectively. Morphant analysis showed that Wnt3 is differentially required in the epithalamus. The habenula in ET-16 is specifically obliterated by morpholino injection while the pineal gland and parapineal organ in the dorsal epithalamus (Fig.3.24 and Fig.3.26) are less affected. Given that habenular nuclei originate from ventral epithalamic cells (Concha et al., 2003), we suggest that Wnt3 activity is required for the specification of ventral epithalamus.

Since Wnt3 functions as a canonical Wnt during neural development, we further proposed that activation of the Wnt/β-catenin pathway is involved in the specification of prosomere 2. This is supported by the knockout phenotype of Wnt coreceptor, low-density lipoprotein receptor-related protein-6 (LRP6). LRP6 acts along with members of the Frizzled family to transduce Wnt signals through the Wnt/β-catenin pathway (Pinson et al., 2000; Tamai et al., 2000; Wehrli et al., 2000). Mice with mutation in LRP6 have a severely disorganized dorsal thalamus (Zhou et al., 2004). Specifically the epithalamic and most dorsal thalamic neurons

are missing resulting in rostral displacement of the ventral thalamus, a phenotype similar to that observed in Wnt3 morphants. Hence the loss of habenula and dorsal thalamus may be a reflection of cell autonomous loss of Wnt/β-catenin signaling in prosomere 2 of diencephalon.

4.6 Wnt3 is Required for Patterning of Dorsal Midbrain and Hindbrain

The expression of more than one Wnt gene in a given region raises the possibility of functional redundancy between different family members. Comparative WISH analysis in zebrafish (Fig.3.5) showed that *wnt3* overlaps with domain of *wnt1*, *wnt3a* and *wnt10b* expression in the roofplate of the midbrain. Expression of *wnt3* in the hindbrain overlaps with that of *wnt10b* in the prospective cerebellum (Lekven et al., 2003). Deficiency of *wnt3a*, *wnt1* and *wnt10b* causes extensive apoptosis in the midbrain and cerebellum anlagen, which results in the absence of a significant portion of the midbrain and cerebellum (Buckles et al., 2004). We noted that Wnt3 is functionally less redundant than Wnt1, Wnt3a and Wnt10b. Knockdown of Wnt3 alone is sufficient to cause extensive apoptosis in the midbrain and cerebellum (Fig.3.13) and changes the expression pattern of *otx2*. In fact *otx2* expression in the optic tectum become greatly reduced in Wnt3 morphants (Fig.3.16). Neuronal differentiation in the optic tectum and cerebellum is also severely affected in Wnt3 morphants. ∝-acT that stains developing axon tracts indicate their absence in the optic tectum as well as cerebellar commissure in Wnt3 morphants, concomitantly, the lack of HuC/D+ neuronal cells is observed in similar domains of the brain. We failed to detect any PCNA+ cells in the optic tectum and cerebellum (Fig.3.19) of Wnt3 morphant. This suggests that the lack of neuronal differentiation observed in both regions could be due to deficiency of precursor cells. Finally the lack of neuronal differentiation in the optic tectum is re-affirmed in the living marker transgenic line ET27 (Fig.3.27). In addition neuronal differentiation in the dorsal hindbrain is defective in ET11 and ET27. The effect is limited to the dorsal hindbrain as ventral neurons remain in Isl1-GFP and ET16 transgenic lines (Fig.3.21 and Fig.3.25).

Consistent with defective differentiation in the dorsal hindbrain, craniofacial cartilage is defective in Wnt3 morphants (Fig.3.14). Cranial neural crest cells migrate in three streams from the hindbrain to form craniofacial cartilage (Halloran and Berndt, 2003). The most anterior stream arises from hindbrain rhombomeres 2 and 3 and predominantly populates the first (mandibular) pharyngeal arch. The second stream arises from rhombomeres 4 and 5 and populates the second (hyoid) pharyngeal arch. The most posterior stream arises from rhombomeres 5, 6 and more posterior region and migrates to the third and more posterior pharyngeal arches. Cartilage derivatives of pharyngeal arches 3-7 are missing; suggesting that migration of cranial neural crest cells from the most posterior stream is absent in Wnt3 morphants.

The formation of midbrain, cerebellum and craniofacial cartilage had been shown to be dependent on Wnt/β-catenin pathway. Mutant mice with specific inactivation of β-catenin in the region of *Wnt1* expression had a malformed forebrain. The midbrain, cerebellum and craniofacial structures are also absent in this conditional mutant (Brault et al., 2001). Wnt3 morphant phenotype largely resembles that of Wnt1-Cre mediated deletion of β-catenin mutant mice. Our functional analysis involving site-specific overexpression of Wnt3 and panembryonic knockdown of its function by morpholino demonstrated that Wnt3 is required for formation of prosomere 2, optic tectum, cerebellum and branchial arches and further suggest that these developmental processes required the activation of Wnt3/β-catenin signaling pathway.

Reference List

Aberle,H., Bauer,A., Stappert,J., Kispert,A., and Kemler,R. (1997). beta-catenin is a target for the ubiquitin-proteasome pathway. *EMBO J* **16,** 3797-3804.

Aizawa,H., Bianco,I.H., Hamaoka,T., Miyashita,T., Uemura,O., Concha,M.L., Russell,C., Wilson,S.W., and Okamoto,H. (2005). Laterotopic representation of left-right information onto the dorso-ventral axis of a zebrafish midbrain target nucleus. *Curr Biol* **15,** 238-243.

Appel,B., Korzh,V., Glasgow,E., Thor,S., Edlund,T., Dawid,I.B., and Eisen,J.S. (1995). Motoneuron fate specification revealed by patterned LIM homeobox gene expression in embryonic zebrafish. *Development* **121,** 4117-4125.

Barami,K., Iversen,K., Furneaux,H., and Goldman,S.A. (1995). Hu protein as an early marker of neuronal phenotypic differentiation by subependymal zone cells of the adult songbird forebrain. *J Neurobiol.* **28,** 82-101.

Barth,K.A. and Wilson,S.W. (1995). Expression of zebrafish nk2.2 is influenced by sonic hedgehog/vertebrate hedgehog-1 and demarcates a zone of neuronal differentiation in the embryonic forebrain. *Development* **121,** 1755-1768.

Bhanot,P., Brink,M., Samos,C.H., Hsieh,J.C., Wang,Y., Macke,J.P., Andrew,D., Nathans,J., and Nusse,R. (1996). A new member of the frizzled family from Drosophila functions as a Wingless receptor. *Nature* **382,** 225-230.

Brault,V., Moore,R., Kutsch,S., Ishibashi,M., Rowitch,D.H., McMahon,A.P., Sommer,L., Boussadia,O., and Kemler,R. (2001). Inactivation of the beta-catenin gene by Wnt1-Cre-mediated deletion results in dramatic brain malformation and failure of craniofacial development. *Development* **128,** 1253-1264.

Braun,M.M., Etheridge,A., Bernard,A., Robertson,C.P., and Roelink,H. (2003). Wnt signaling is required at distinct stages of development for the induction of the posterior forebrain. *Development* **130,** 5579-5587.

Bravo,R., Frank,R., Blundell,P.A., and Macdonald-Bravo,H. (1987). Cyclin/PCNA is the auxiliary protein of DNA polymerase-delta. *Nature* **326,** 515-517.

Brunner,E., Peter,O., Schweizer,L., and Basler,K. (1997). pangolin encodes a Lef-1 homologue that acts downstream of Armadillo to transduce the Wingless signal in Drosophila. *Nature* **385,** 829-833.

Buckles,G.R., Thorpe,C.J., Ramel,M.C., and Lekven,A.C. (2004). Combinatorial Wnt control of zebrafish midbrain-hindbrain boundary formation. *Mech Dev* **121,** 437-447.

Bulfone,A., Puelles,L., Porteus,M.H., Frohman,M.A., Martin,G.R., and Rubenstein,J.L. (1993). Spatially restricted expression of Dlx-1, Dlx-2 (Tes-1), Gbx-2, and Wnt-3 in the embryonic day 12.5 mouse forebrain defines potential transverse and longitudinal segmental boundaries. *J Neurosci.* **13,** 3155-3172.

Cauthen,C.A., Berdougo,E., Sandler,J., and Burrus,L.W. (2001). Comparative analysis of the expression patterns of Wnts and Frizzleds during early myogenesis in chick embryos. *Mech Dev* **104,** 133-138.

Chitnis,A.B. and Kuwada,J.Y. (1990). Axonogenesis in the brain of zebrafish embryos. *J Neurosci.* **10,** 1892-1905.

Christian,J.L., Gavin,B.J., McMahon,A.P., and Moon,R.T. (1991). Isolation of cDNAs partially encoding four Xenopus Wnt-1/int-1-related proteins and characterization of their transient expression during embryonic development. *Dev Biol* **143,** 230-234.

Ciani,L. and Salinas,P.C. (2005). WNTs in the vertebrate nervous system: from patterning to neuronal connectivity. *Nat Rev Neurosci.* **6,** 351-362.

Concha,M.L., Russell,C., Regan,J.C., Tawk,M., Sidi,S., Gilmour,D.T., Kapsimali,M., Sumoy,L., Goldstone,K., Amaya,E. et al. (2003). Local tissue interactions across the dorsal midline of the forebrain establish CNS laterality. *Neuron* **39,** 423-438.

Concha,M.L. and Wilson,S.W. (2001). Asymmetry in the epithalamus of vertebrates. *J Anat.* **199,** 63-84.

Dabdoub,A., Donohue,M.J., Brennan,A., Wolf,V., Montcouquiol,M., Sassoon,D.A., Hseih,J.C., Rubin,J.S., Salinas,P.C., and Kelley,M.W. (2003). Wnt signaling mediates reorientation of outer hair cell stereociliary bundles in the mammalian cochlea. *Development* **130,** 2375-2384.

Dorsky,R.I., Moon,R.T., and Raible,D.W. (1998). Control of neural crest cell fate by the Wnt signalling pathway. *Nature* **396,** 370-373.

Dorsky,R.I., Sheldahl,L.C., and Moon,R.T. (2002). A transgenic Lef1/beta-catenin-dependent reporter is expressed in spatially restricted domains throughout zebrafish development. *Dev Biol* **241,** 229-237.

Draper,B.W., Morcos,P.A., and Kimmel,C.B. (2001). Inhibition of zebrafish fgf8 pre-mRNA splicing with morpholino oligos: a quantifiable method for gene knockdown. *Genesis.* **30,** 154-156.

Echelard,Y., Epstein,D.J., St Jacques,B., Shen,L., Mohler,J., McMahon,J.A., and McMahon,A.P. (1993). Sonic hedgehog, a member of a family of putative signaling molecules, is implicated in the regulation of CNS polarity. *Cell* **75,** 1417-1430.

Ekker,S.C. (2000). Morphants: a new systematic vertebrate functional genomics approach. *Yeast* **17,** 302-306.

Ericson,J., Thor,S., Edlund,T., Jessell,T.M., and Yamada,T. (1992). Early stages of motor neuron differentiation revealed by expression of homeobox gene Islet-1. *Science* **256,** 1555-1560.

Fong,S., Emelyanov,A., Teh,C., and Korzh,V. (2005). Wnt signalling mediated by Tbx2b regulates cell migration during formation of the neural plate. *Development* **In Press**.

Glinka,A., Wu,W., Delius,H., Monaghan,A.P., Blumenstock,C., and Niehrs,C. (1998). Dickkopf-1 is a member of a new family of secreted proteins and functions in head induction. *Nature* **391,** 357-362.

Gong,Z., Hui,C.C., and Hew,C.L. (1995). Presence of isl-1-related LIM domain homeobox genes in teleost and their similar patterns of expression in brain and spinal cord. *J Biol Chem* **270,** 3335-3345.

Habas,R., Dawid,I.B., and He,X. (2003). Coactivation of Rac and Rho by Wnt/Frizzled signaling is required for vertebrate gastrulation. *Genes Dev* **17,** 295-309.

Halloran,M.C. and Berndt,J.D. (2003). Current progress in neural crest cell motility and migration and future prospects for the zebrafish model system. *Dev Dyn.* **228,** 497-513.

Hashimoto,H., Itoh,M., Yamanaka,Y., Yamashita,S., Shimizu,T., Solnica-Krezel,L., Hibi,M., and Hirano,T. (2000). Zebrafish Dkk1 functions in forebrain specification and axial mesendoderm formation. *Dev Biol* **217,** 138-152.

He,X., Saint-Jeannet,J.P., Wang,Y., Nathans,J., Dawid,I., and Varmus,H. (1997). A member of the Frizzled protein family mediating axis induction by Wnt-5A. *Science* **275,** 1652-1654.

Heisenberg,C.P., Tada,M., Rauch,G.J., Saude,L., Concha,M.L., Geisler,R., Stemple,D.L., Smith,J.C., and Wilson,S.W. (2000). Silberblick/Wnt11 mediates convergent extension movements during zebrafish gastrulation. *Nature* **405,** 76-81.

Higashijima,S., Hotta,Y., and Okamoto,H. (2000). Visualization of cranial motor neurons in live transgenic zebrafish expressing green fluorescent protein under the control of the islet-1 promoter/enhancer. *J Neurosci.* **20,** 206-218.

Holder,N. and Xu,Q. (1999). Microinjection of DNA, RNA, and protein into the fertilized zebrafish egg for analysis of gene function. *Methods Mol Biol* **97,** 487-490.

Hollyday,M., McMahon,J.A., and McMahon,A.P. (1995). Wnt expression patterns in chick embryo nervous system. *Mech Dev* **52,** 9-25.

Holmen,S.L., Salic,A., Zylstra,C.R., Kirschner,M.W., and Williams,B.O. (2002). A novel set of Wnt-Frizzled fusion proteins identifies receptor components that activate beta -catenin-dependent signaling. *J Biol Chem* **277,** 34727-34735.

Houart,C., Caneparo,L., Heisenberg,C., Barth,K., Take-Uchi,M., and Wilson,S. (2002). Establishment of the telencephalon during gastrulation by local antagonism of Wnt signaling. *Neuron* **35,** 255-265.

Huelsken,J. and Birchmeier,W. (2001). New aspects of Wnt signaling pathways in higher vertebrates. *Curr Opin Genet Dev* **11,** 547-553.

Ikeya,M., Lee,S.M., Johnson,J.E., McMahon,A.P., and Takada,S. (1997). Wnt signalling required for expansion of neural crest and CNS progenitors. *Nature* **389,** 966-970.

Ikeya,M. and Takada,S. (1998). Wnt signaling from the dorsal neural tube is required for the formation of the medial dermomyotome. *Development* **125,** 4969-4976.

Inoue,A., Takahashi,M., Hatta,K., Hotta,Y., and Okamoto,H. (1994). Developmental regulation of islet-1 mRNA expression during neuronal differentiation in embryonic zebrafish. *Dev Dyn.* **199,** 1-11.

Katanaev,V.L., Ponzielli,R., Semeriva,M., and Tomlinson,A. (2005). Trimeric G protein-dependent frizzled signaling in Drosophila. *Cell* **120,** 111-122.

Kazanskaya,O., Glinka,A., and Niehrs,C. (2000). The role of Xenopus dickkopf1 in prechordal plate specification and neural patterning. *Development* **127,** 4981-4992.

Kelly,G.M. and Moon,R.T. (1995). Involvement of wnt1 and pax2 in the formation of the midbrain-hindbrain boundary in the zebrafish gastrula. *Dev Genet* **17,** 129-140.

Kiecker,C. and Lumsden,A. (2004). Hedgehog signaling from the ZLI regulates diencephalic regional identity. *Nat Neurosci.* **7,** 1242-1249.

Kiecker,C. and Niehrs,C. (2001). A morphogen gradient of Wnt/beta-catenin signalling regulates anteroposterior neural patterning in Xenopus. *Development* **128,** 4189-4201.

Kim,C.H., Oda,T., Itoh,M., Jiang,D., Artinger,K.B., Chandrasekharappa,S.C., Driever,W., and Chitnis,A.B. (2000). Repressor activity of Headless/Tcf3 is essential for vertebrate head formation. *Nature* **407,** 913-916.

Kim,U. and Chang,S.Y. (2005). Dendritic morphology, local circuitry, and intrinsic electrophysiology of neurons in the rat medial and lateral habenular nuclei of the epithalamus. *J Comp Neurol.* **483,** 236-250.

Kimmel,C.B., Ballard,W.W., Kimmel,S.R., Ullmann,B., and Schilling,T.F. (1995). Stages of embryonic development of the zebrafish. *Dev Dyn.* **203,** 253-310.

Klingensmith,J., Nusse,R., and Perrimon,N. (1994). The Drosophila segment polarity gene dishevelled encodes a novel protein required for response to the wingless signal. *Genes Dev* **8,** 118-130.

Korinek,V., Barker,N., Morin,P.J., van Wichen,D., de Weger,R., Kinzler,K.W., Vogelstein,B., and Clevers,H. (1997). Constitutive transcriptional activation by a beta-catenin-Tcf complex in APC-/- colon carcinoma. *Science* **275,** 1784-1787.

Korinek,V., Barker,N., Willert,K., Molenaar,M., Roose,J., Wagenaar,G., Markman,M., Lamers,W., Destree,O., and Clevers,H. (1998). Two members of the Tcf family implicated in Wnt/beta-catenin signaling during embryogenesis in the mouse. *Mol Cell Biol* **18,** 1248-1256.

Korzh,V., Edlund,T., and Thor,S. (1993). Zebrafish primary neurons initiate expression of the LIM homeodomain protein Isl-1 at the end of gastrulation. *Development* **118,** 417-425.

Krauss,S., Concordet,J.P., and Ingham,P.W. (1993). A functionally conserved homolog of the Drosophila segment polarity gene hh is expressed in tissues with polarizing activity in zebrafish embryos. *Cell* **75,** 1431-1444.

Krauss,S., Johansen,T., Korzh,V., Moens,U., Ericson,J.U., and Fjose,A. (1991). Zebrafish pax[zf-a]: a paired box-containing gene expressed in the neural tube. *EMBO J* **10,** 3609-3619.

Krauss,S., Korzh,V., Fjose,A., and Johansen,T. (1992). Expression of four zebrafish wnt-related genes during embryogenesis. *Development* **116,** 249-259.

Kuhl,M., Sheldahl,L.C., Park,M., Miller,J.R., and Moon,R.T. (2000). The Wnt/Ca2+ pathway: a new vertebrate Wnt signaling pathway takes shape. *Trends Genet* **16,** 279-283.

Kurokawa,D., Kiyonari,H., Nakayama,R., Kimura-Yoshida,C., Matsuo,I., and Aizawa,S. (2004). Regulation of Otx2 expression and its functions in mouse forebrain and midbrain. *Development* **131,** 3319-3331.

Lam,E. Embryonic neuroanatomy and the localization of Tyrosine Hydroxylase immunoreactive neurons in the zebrafish, *Danio rerio*. 2002. National University of Singapore.
Ref Type: Thesis/Dissertation

Larsen,C.W., Zeltser,L.M., and Lumsden,A. (2001). Boundary formation and compartition in the avian diencephalon. *J Neurosci.* **21,** 4699-4711.

Lekven,A.C., Buckles,G.R., Kostakis,N., and Moon,R.T. (2003). Wnt1 and wnt10b function redundantly at the zebrafish midbrain-hindbrain boundary. *Dev Biol* **254,** 172-187.

Lie,D.C., Colamarino,S.A., Song,H.J., Desire,L., Mira,H., Consiglio,A., Lein,E.S., Jessberger,S., Lansford,H., Dearie,A.R. et al. (2005). Wnt signalling regulates adult hippocampal neurogenesis. *Nature* **437,** 1370-1375.

Liem,K.F., Tremml,G., Roelink,H., and Jessell,T.M. (1995). Dorsal differentiation of neural plate cells induced by BMP-mediated signals from epidermal ectoderm. *Cell* **82,** 969-979.

Liu,P., Wakamiya,M., Shea,M.J., Albrecht,U., Behringer,R.R., and Bradley,A. (1999). Requirement for Wnt3 in vertebrate axis formation. *Nat Genet* **22,** 361-365.

Liu,T., DeCostanzo,A.J., Liu,X., Wang,H., Hallagan,S., Moon,R.T., and Malbon,C.C. (2001). G protein signaling from activated rat frizzled-1 to the beta-catenin-Lef-Tcf pathway. *Science* **292,** 1718-1722.

Logan,C.Y. and Nusse,R. (2004). The Wnt signaling pathway in development and disease. *Annu Rev Cell Dev Biol* **20,** 781-810.

Lu,D., Zhao,Y., Tawatao,R., Cottam,H.B., Sen,M., Leoni,L.M., Kipps,T.J., Corr,M., and Carson,D.A. (2004). Activation of the Wnt signaling pathway in chronic lymphocytic leukemia. *Proc Natl Acad Sci U S A* **101,** 3118-3123.

Lumsden,A. and Krumlauf,R. (1996). Patterning the vertebrate neuraxis. *Science* **274,** 1109-1115.

MacDonald,B.T., Adamska,M., and Meisler,M.H. (2004). Hypomorphic expression of Dkk1 in the doubleridge mouse: dose dependence and compensatory interactions with Lrp6. *Development* **131,** 2543-2552.

Marusich,M.F., Furneaux,H.M., Henion,P.D., and Weston,J.A. (1994). Hu neuronal proteins are expressed in proliferating neurogenic cells. *J Neurobiol.* **25,** 143-155.

Mathews,M.B., Bernstein,R.M., Franza,B.R., Jr., and Garrels,J.I. (1984). Identity of the proliferating cell nuclear antigen and cyclin. *Nature* **309,** 374-376.

McKendry,R., Hsu,S.C., Harland,R.M., and Grosschedl,R. (1997). LEF-1/TCF proteins mediate wnt-inducible transcription from the Xenopus nodal-related 3 promoter. *Dev Biol* **192,** 420-431.

McMahon,A.P. and Bradley,A. (1990). The Wnt-1 (int-1) proto-oncogene is required for development of a large region of the mouse brain. *Cell* **62,** 1073-1085.

McMahon,A.P., Joyner,A.L., Bradley,A., and McMahon,J.A. (1992). The midbrain-hindbrain phenotype of Wnt-1-/Wnt-1- mice results from stepwise deletion of engrailed-expressing cells by 9.5 days postcoitum. *Cell* **69,** 581-595.

Miller,J.R. (2002). The Wnts. *Genome Biol* **3,** REVIEWS3001.

Millet,S., Bloch-Gallego,E., Simeone,A., and Alvarado-Mallart,R.M. (1996). The caudal limit of Otx2 gene expression as a marker of the midbrain/hindbrain boundary: a study using in situ hybridisation and chick/quail homotopic grafts. *Development* **122,** 3785-3797.

Molven,A., Njolstad,P.R., and Fjose,A. (1991). Genomic structure and restricted neural expression of the zebrafish wnt-1 (int-1) gene. *EMBO J* **10,** 799-807.

Moon,R.T., Brown,J.D., and Torres,M. (1997). WNTs modulate cell fate and behavior during vertebrate development. *Trends Genet* **13,** 157-162.

Mori,H., Miyazaki,Y., Morita,T., Nitta,H., and Mishina,M. (1994). Different spatio-temporal expressions of three otx homeoprotein transcripts during zebrafish embryogenesis. *Brain Res Mol Brain Res* **27,** 221-231.

Mukhopadhyay,M., Shtrom,S., Rodriguez-Esteban,C., Chen,L., Tsukui,T., Gomer,L., Dorward,D.W., Glinka,A., Grinberg,A., Huang,S.P. et al. (2001). Dickkopf1 is required for embryonic head induction and limb morphogenesis in the mouse. *Dev Cell* **1,** 423-434.

Muroyama,Y., Fujihara,M., Ikeya,M., Kondoh,H., and Takada,S. (2002). Wnt signaling plays an essential role in neuronal specification of the dorsal spinal cord. *Genes Dev* **16,** 548-553.

Nakamura,H. and Funahashi,J. (2001). Introduction of DNA into chick embryos by in ovo electroporation. *Methods* **24,** 43-48.

Nakamura,T., Hamada,F., Ishidate,T., Anai,K., Kawahara,K., Toyoshima,K., and Akiyama,T. (1998). Axin, an inhibitor of the Wnt signalling pathway, interacts with beta-catenin, GSK-3beta and APC and reduces the beta-catenin level. *Genes Cells* **3,** 395-403.

Neuhauss,S.C., Solnica-Krezel,L., Schier,A.F., Zwartkruis,F., Stemple,D.L., Malicki,J., Abdelilah,S., Stainier,D.Y., and Driever,W. (1996). Mutations affecting craniofacial development in zebrafish. *Development* **123,** 357-367.

Niemann,S., Zhao,C., Pascu,F., Stahl,U., Aulepp,U., Niswander,L., Weber,J.L., and Muller,U. (2004). Homozygous WNT3 mutation causes tetra-amelia in a large consanguineous family. *Am J Hum Genet* **74,** 558-563.

Nieuwkoop,P.D. (1952). Activation and organisation of the central nervous system in amphibians. *Journal of Experimental Zoology* **120,** 1-108.

Noordermeer,J., Klingensmith,J., Perrimon,N., and Nusse,R. (1994). dishevelled and armadillo act in the wingless signalling pathway in Drosophila. *Nature* **367,** 80-83.

Nornes,S., Clarkson,M., Mikkola,I., Pedersen,M., Bardsley,A., Martinez,J.P., Krauss,S., and Johansen,T. (1998). Zebrafish contains two pax6 genes involved in eye development. *Mech Dev* **77,** 185-196.

Ohnuma,S., Philpott,A., and Harris,W.A. (2001). Cell cycle and cell fate in the nervous system. *Curr Opin Neurobiol.* **11,** 66-73.

Osumi,N. and Inoue,T. (2001). Gene transfer into cultured mammalian embryos by electroporation. *Methods* **24,** 35-42.

Papkoff,J., Rubinfeld,B., Schryver,B., and Polakis,P. (1996). Wnt-1 regulates free pools of catenins and stabilizes APC-catenin complexes. *Mol Cell Biol* **16,** 2128-2134.

Parinov,S., Kondrichin,I., Korzh,V., and Emelyanov,A. (2004). Tol2 transposon-mediated enhancer trap to identify developmentally regulated zebrafish genes in vivo. *Dev Dyn.* **231,** 449-459.

Parr,B.A., Shea,M.J., Vassileva,G., and McMahon,A.P. (1993). Mouse Wnt genes exhibit discrete domains of expression in the early embryonic CNS and limb buds. *Development* **119,** 247-261.

Partridge,M., Vincent,A., Matthews,P., Puma,J., Stein,D., and Summerton,J. (1996). A simple method for delivering morpholino antisense oligos into the cytoplasm of cells. *Antisense Nucleic Acid Drug Dev* **6,** 169-175.

Pelegri,F. and Maischein,H.M. (1998). Function of zebrafish beta-catenin and TCF-3 in dorsoventral patterning. *Mech Dev* **77,** 63-74.

Pinson,K.I., Brennan,J., Monkley,S., Avery,B.J., and Skarnes,W.C. (2000). An LDL-receptor-related protein mediates Wnt signalling in mice. *Nature* **407,** 535-538.

Puelles,L. (2001). Brain segmentation and forebrain development in amniotes. *Brain Res Bull* **55,** 695-710.

Puschel,A.W., Gruss,P., and Westerfield,M. (1992). Sequence and expression pattern of pax-6 are highly conserved between zebrafish and mice. *Development* **114,** 643-651.

Robertson,C.P., Braun,M.M., and Roelink,H. (2004). Sonic hedgehog patterning in chick neural plate is antagonized by a Wnt3-like signal. *Dev Dyn.* **229,** 510-519.

Roelink,H. and Nusse,R. (1991). Expression of two members of the Wnt family during mouse development--restricted temporal and spatial patterns in the developing neural tube. *Genes Dev* **5,** 381-388.

Roelink,H., Wagenaar,E., Lopes,d.S., and Nusse,R. (1990). Wnt-3, a gene activated by proviral insertion in mouse mammary tumors, is homologous to int-1/Wnt-1 and is normally expressed in mouse embryos and adult brain. *Proc Natl Acad Sci U S A* **87,** 4519-4523.

Ross,L.S., Parrett,T., and Easter,S.S., Jr. (1992). Axonogenesis and morphogenesis in the embryonic zebrafish brain. *J Neurosci.* **12,** 467-482.

Rubenstein,J.L., Martinez,S., Shimamura,K., and Puelles,L. (1994). The embryonic vertebrate forebrain: the prosomeric model. *Science* **266,** 578-580.

Salinas,P.C. and Nusse,R. (1992). Regional expression of the Wnt-3 gene in the developing mouse forebrain in relationship to diencephalic neuromeres. *Mech Dev* **39,** 151-160.

Saneyoshi,T., Kume,S., Amasaki,Y., and Mikoshiba,K. (2002). The Wnt/calcium pathway activates NF-AT and promotes ventral cell fate in Xenopus embryos. *Nature* **417,** 295-299.

Schmidt,M., Tanaka,M., and Munsterberg,A. (2000). Expression of (beta)-catenin in the developing chick myotome is regulated by myogenic signals. *Development* **127,** 4105-4113.

Sheldahl,L.C., Slusarski,D.C., Pandur,P., Miller,J.R., Kuhl,M., and Moon,R.T. (2003). Dishevelled activates Ca2+ flux, PKC, and CamKII in vertebrate embryos. *J Cell Biol* **161,** 769-777.

Shimizu,H., Julius,M.A., Giarre,M., Zheng,Z., Brown,A.M., and Kitajewski,J. (1997). Transformation by Wnt family proteins correlates with regulation of beta-catenin. *Cell Growth Differ* **8,** 1349-1358.

Siegfried,E., Chou,T.B., and Perrimon,N. (1992). wingless signaling acts through zeste-white 3, the Drosophila homolog of glycogen synthase kinase-3, to regulate engrailed and establish cell fate. *Cell* **71,** 1167-1179.

Simeone,A. (2002). Towards the comprehension of genetic mechanisms controlling brain morphogenesis. *Trends Neurosci.* **25,** 119-121.

Simeone,A., Acampora,D., Mallamaci,A., Stornaiuolo,A., D'Apice,M.R., Nigro,V., and Boncinelli,E. (1993). A vertebrate gene related to orthodenticle contains a homeodomain of the bicoid class and demarcates anterior neuroectoderm in the gastrulating mouse embryo. *EMBO J* **12,** 2735-2747.

Slusarski,D.C., Corces,V.G., and Moon,R.T. (1997). Interaction of Wnt and a Frizzled homologue triggers G-protein-linked phosphatidylinositol signalling. *Nature* **390,** 410-413.

Strehlow,D., Heinrich,G., and Gilbert,W. (1994). The fates of the blastomeres of the 16-cell zebrafish embryo. *Development* **120,** 1791-1798.

Strutt,D.I., Weber,U., and Mlodzik,M. (1997). The role of RhoA in tissue polarity and Frizzled signalling. *Nature* **387,** 292-295.

Swartz,M., Eberhart,J., Mastick,G.S., and Krull,C.E. (2001). Sparking new frontiers: using in vivo electroporation for genetic manipulations. *Dev Biol* **233,** 13-21.

Tabata,H. and Nakajima,K. (2001). Efficient in utero gene transfer system to the developing mouse brain using electroporation: visualization of neuronal migration in the developing cortex. *Neuroscience* **103,** 865-872.

Tamai,K., Semenov,M., Kato,Y., Spokony,R., Liu,C., Katsuyama,Y., Hess,F., Saint-Jeannet,J.P., and He,X. (2000). LDL-receptor-related proteins in Wnt signal transduction. *Nature* **407,** 530-535.

Teh,C., Chong,S.W., and Korzh,V. (2003). DNA delivery into anterior neural tube of zebrafish embryos by electroporation. *Biotechniques* **35,** 950-954.

Teh,C., Parinov,S., and Korzh,V. (2005). New ways to admire zebrafish: progress in functional genomics research methodology. *Biotechniques* **38,** 897-906.

Tekmal,R.R. and Keshava,N. (1997). Role of MMTV integration locus cellular genes in breast cancer. *Front Biosci.* **2,** d519-d526.

Thomas,K.R. and Capecchi,M.R. (1990). Targeted disruption of the murine int-1 proto-oncogene resulting in severe abnormalities in midbrain and cerebellar development. *Nature* **346,** 847-850.

Thor,S., Andersson,S.G., Tomlinson,A., and Thomas,J.B. (1999). A LIM-homeodomain combinatorial code for motor-neuron pathway selection. *Nature* **397,** 76-80.

Thor,S., Ericson,J., Brannstrom,T., and Edlund,T. (1991). The homeodomain LIM protein Isl-1 is expressed in subsets of neurons and endocrine cells in the adult rat. *Neuron* **7,** 881-889.

Thor,S. and Thomas,J.B. (1997). The Drosophila islet gene governs axon pathfinding and neurotransmitter identity. *Neuron* **18,** 397-409.

Tosney,K.W., Hotary,K.B., and Lance-Jones,C. (1995). Specifying the target identity of motoneurons. *Bioessays* **17,** 379-382.

Tsuchida,T., Ensini,M., Morton,S.B., Baldassare,M., Edlund,T., Jessell,T.M., and Pfaff,S.L. (1994). Topographic organization of embryonic motor neurons defined by expression of LIM homeobox genes. *Cell* **79,** 957-970.

van de Wetering M., Cavallo,R., Dooijes,D., van Beest,M., van Es,J., Loureiro,J., Ypma,A., Hursh,D., Jones,T., Bejsovec,A. et al. (1997). Armadillo coactivates transcription driven by the product of the Drosophila segment polarity gene dTCF. *Cell* **88,** 789-799.

Veeman,M.T., Slusarski,D.C., Kaykas,A., Louie,S.H., and Moon,R.T. (2003). Zebrafish prickle, a modulator of noncanonical Wnt/Fz signaling, regulates gastrulation movements. *Curr Biol* **13,** 680-685.

Wehrli,M., Dougan,S.T., Caldwell,K., O'Keefe,L., Schwartz,S., Vaizel-Ohayon,D., Schejter,E., Tomlinson,A., and DiNardo,S. (2000). arrow encodes an LDL-receptor-related protein essential for Wingless signalling. *Nature* **407,** 527-530.

Westerfield,M. (1995). *The Zebrafish Book*. University of Oregon Press.

Wharton,K.A. (2003). Runnin' with the Dvl: proteins that associate with Dsh/Dvl and their significance to Wnt signal transduction. *Dev Biol* **253,** 1-17.

Wilson,S.W., Ross,L.S., Parrett,T., and Easter,S.S., Jr. (1990). The development of a simple scaffold of axon tracts in the brain of the embryonic zebrafish, Brachydanio rerio. *Development* **108,** 121-145.

Wodarz,A. and Nusse,R. (1998). Mechanisms of Wnt signaling in development. *Annu Rev Cell Dev Biol* **14,** 59-88.

Wolda,S.L., Moody,C.J., and Moon,R.T. (1993). Overlapping expression of Xwnt-3A and Xwnt-1 in neural tissue of Xenopus laevis embryos. *Dev Biol* **155,** 46-57.

Wong,G.T., Gavin,B.J., and McMahon,A.P. (1994). Differential transformation of mammary epithelial cells by Wnt genes. *Mol Cell Biol* **14,** 6278-6286.

Wullimann,M.F. and Knipp,S. (2000). Proliferation pattern changes in the zebrafish brain from embryonic through early postembryonic stages. *Anat. Embryol. (Berl)* **202,** 385-400.

Wullimann,M.F. and Rink,E. (2001). Detailed immunohistology of Pax6 protein and tyrosine hydroxylase in the early zebrafish brain suggests role of Pax6 gene in development of dopaminergic diencephalic neurons. *Brain Res Dev Brain Res* **131,** 173-191.

Xu,Q. (1999). Microinjection into zebrafish embryos. *Methods Mol Biol* **127,** 125-132.

Zeltser,L.M. (2005). Shh-dependent formation of the ZLI is opposed by signals from the dorsal diencephalon. *Development* **132,** 2023-2033.

Zhou,C.J., Pinson,K.I., and Pleasure,S.J. (2004). Severe defects in dorsal thalamic development in low-density lipoprotein receptor-related protein-6 mutants. *J Neurosci.* **24,** 7632-7639.

Appendices

DNA delivery into anterior neural tube of zebrafish embryos by electroporation

Cathleen Teh, Shang Wei Chong, and Vladimir Korzh
Institute of Molecular and Cell Biology, Singapore

BioTechniques 35:950-954 (November 2003)

The zebrafish is widely used for functional studies of vertebrate genes. It is accessible to manipulations during all stages of embryogenesis because the embryo develops externally and is optically transparent. However, functional studies conducted on the zebrafish have been generally limited to the earliest phase of activity of the gene of interest, which is a limitation in studies of genes that are expressed at various stages of embryonic development. It is therefore necessary to develop methods that allow for the modulation of gene activity during later stages of zebrafish development while leaving earlier functions intact. We have successfully electroporated the green fluorescent protein (GFP) reporter gene into the neural tube of the zebrafish embryo in a unidirectional or bilateral manner. This approach can be used for the functional analysis of the late role of developmental genes in the neural tube of zebrafish embryo and larvae.

INTRODUCTION

Following the completion of genome sequencing projects for human and several other model organisms, efforts were under way to assign a function to specific genes. To understand the function of genes, their overexpression or inhibition is widely used. The zebrafish is a model system that is particularly suitable for such an approach because the large-scale rapid delivery of genetic constructs into the semitransparent embryos is possible. This allows for developmental analysis at a high level of resolution. The zebrafish has already become a useful system for the study of vertebrate genetics and development (1,2), human hereditary diseases (3), and infectious diseases (4). In zebrafish, functional studies have relied on mutant analysis and/or inhibition of gene function by the injection of antisense morpholino oligonucleotides into the one-cell stage embryo (5). While these approaches are very efficient, they are unfortunately limited to the analysis of early gene activity.

For studying later gene activity, electroporation is an attractive approach because early gene function can be bypassed. Initially, electroporation was limited to cells in culture (6); however, subsequently, electroporation conditions have been optimized, including the usage of square wave pulses of low voltage and long duration. This approach resulted in improved survival of chick retinal explants (7) and has been adapted for in vivo studies (8).

Electroporating zebrafish embryos is not new, but previous attempts have been limited to early development or adult stages. Strategies to electroporate DNA into a whole embryo or sperm to generate transgenic zebrafish have been described (9,10); however, for various reasons, these methods are not widely used. Recently, DNA electroporation into the zebrafish fin has been introduced (11).

In contrast, effective in vivo electroporation of DNA into cells of the neural tube was established in chick and mouse embryos and more recently in Xenopus tadpoles (12–14). In this case, the neural cavity was used as a DNA reservoir. The success of this approach has prompted electroporation of zebrafish genes into chick embryos (15). Thus, a need to develop an efficient system of electroporation of DNA into specific regions of the late zebrafish embryo became apparent. The challenge for performing electroporation on zebrafish embryos is to ensure the successful delivery of DNA into target tissue without damaging the yolk cell (6). Using the microinjection of DNA into the brain ventricles of the zebrafish embryo and performing electroporation in a modified conductivity chamber, where the position of the brain with respect to the electrode plate determines the direction of electroporation, we succeeded in expressing green fluorescent protein (GFP) in the brain with a high survival rate. This method provides another useful addition to the quickly growing list of attractive methodological approaches that make zebrafish an even better model for developmental studies.

MATERIALS AND METHODS

Materials

The plasmid was prepared using the QIAGEN Plasmid Maxi kit (Qiagen, Hilden, Germany), solubilized in water, and its concentration adjusted to 0.5 µg/µL.

Electroporation Chamber

The top three quarters of a Gene Pulser® cuvette (Bio-Rad Laboratories, Hercules, CA, USA) (Figure 1A) with a 0.4-cm electrode gap were removed to improve the manipulation of the embryo. The chamber was half-filled with 1% molten agarose in Hank's buffer (137 mM NaCl, 5.4 mM KCl, 0.25 mM Na_2HPO_4, 0.44 mM KH_2PO_4, 1.3 mM $CaCl_2$, 1.0 mM $MgSO_4$, 4.2 mM $NaHCO_3$, pH 7.2). To cast a well for the embryo, a blunt microinjection pipet (Figure 1B) was inserted vertically into the center of the chamber and held in place by Parafilm®, which sealed the top of the chamber [tip diameter, 0.05 mm; outer diameter (o.d.), 1 mm; inner diameter (i.d.), 0.58 mm; length, 100 mm] (Sutter Instruments, Novato, CA, USA). After the agarose had set, the injection needle and Parafilm were removed. Troughs that were 1 mm wide were constructed adjacent to the electrode plates, and Hank's buffer was added to fill them (Figure 1C). The height of the well is important; for efficient electroporation into the brain, the head must protrude from the well.

Microinjection of DNA into the Neural Tube of Zebrafish Embryos

Wild-type zebrafish embryos at 24–48 hours post-fertilization (hpf) were

grown in Hank's buffer (full-strength) containing 0.2 mM 1-phenyl-2-thiourea (PTU) (Sigma, St. Louis, MO, USA) to inhibit pigment formation (16). Before microinjection, zebrafish embryos were anesthetized with tricaine (Sigma) and placed dorsal-side up in wedge-shape wells made in 1% agarose and covered by Hank's buffer. For injection, we used a pipet (tip diameter, 0.02 mm) pulled from a glass microcapillary (o.d., 1 mm; i.d., 0.58 mm; length, 100 mm) (Sutter Instruments). Using the micromanipulator, the pipet was inserted as described in the Figure 1D legend. DNA was injected using the MPPI-2 pressure injection system (Applied Scientific Instrumentation, Eugene, OR, USA) until the neural tube was visibly distended. The injection volume depended on the age of the embryo (Table 1). Each injected embryo was immediately transferred to the electroporation chamber.

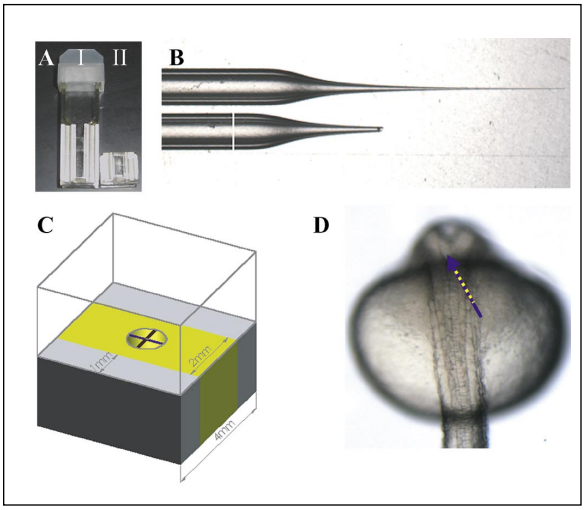

Figure 1. Equipment used for in vivo electroporation into zebrafish brain. (A) The conductivity chamber (II), formed by removing the top three quarters of a Gene Pulser cuvette (I). (B) The sharp microinjection pipet (top) and the blunt micropipet (bottom) as a mould to make the agarose well. The back of the micropipet was used to make 1-mm wide troughs that lined the sides of the electroporation chamber. (C) A diagram of the electroporation chamber. The electrode plate is shown in black, and the troughs filled with Hank's buffer are in gray. The embryo was placed in the agarose well (gray circle) surrounded by Hank's buffered agarose (yellow). The orientations of the embryo that resulted in unilateral transgene expression (blue line) or bilateral expression in the cerebellum and telencephalon (brown line) are indicated. (D) The introduction of DNA into the cavity of the neural tube. Anesthetized wild-type zebrafish embryos (24 h post-fertilization) were placed in wedge-shape wells, dorsal-side up. The pipet was pushed into the yolk cell of the embryo flanking the first somite (solid line), through the floor of the hindbrain near the otic vesicle (broken line), and into the IV ventricle (arrowhead).

Electroporation

Excess Hank's buffer was removed until it barely covered the head. The electroporation chamber was clamped tightly between the metal plates of the safety stand. The electro Square Porator ECM 830 (BTX®; Genetronics, San Diego, CA, USA) was used to generate square electric pulses (Figure 1F), phased 1 s apart. The conditions of electroporation are age-dependent (Table 1). After electroporation, the embryos recovered in 40 × 12 mm (o.d. × height) soda-lime glass Petri dishes (Schott Glaswerke, Mainz, Germany) containing 2.5 mL of Hank's buffer with PTU.

Fluorescence Microscopy

The initial examination of the embryos was performed using the Olympus SZX12 stereomicroscope (Olympus, Tokyo, Japan) equipped with the ultraviolet lamp and GFP filter. For a detailed examination, the embryos expressing GFP were anesthetized in tricaine, mounted in 0.5% low melting agarose (CAMBREX, Rockland, ME, USA), and examined using the Axioplan 2 upright epifluorescence microscope (Carl Zeiss Light Microscopy, Göttingen, Germany) with a GFP filter. Images were taken with an AxioCam HRC digital camera (Carl Zeiss Vision GmbH, Hallbergmoos, Germany). High-resolution images were taken with an LSM510 confocal laser-scanning microscope (Carl Zeiss Vision GmbH).

Whole-Mount In Situ Hybridization

Embryos were processed for whole-mount in situ hybridization (17) using a digoxigenin-labeled (Roche Applied

Table 1. The Effect of Pulse Conditions on Survival and Enhanced Green Fluorescent Protein (EGFP) Expression in Electroporated Zebrafish Embryos

Stage of Development (hpf)	Pulse Conditions	Neuronal and Skin Expression			Total Neuronal	Skin Only	Deformed Embryos	Total	Injection Volume/nL
		FB/MB/HB	FB/MB	MB/HB					
24	20 V, 5 pulses, 50 ms each	6	3	10	19	3	12	34	4–6
24	20 V, 2 pulses, 100 ms each	3	3	9	15	12	1	28	4–6
30	20 V, 5 pulses, 50 ms each	1	8	2	11	18	2	31	4–6
36	20 V, 5 pulses, 50 ms each	0	0	0	0	25	5	30	5–7
36	25 V, 5 pulses, 50 ms each	2	3	0	5	2	23	30	5–7
42	25 V, 5 pulses, 50 ms each	0	5	0	5	9	16	30	8–10
48	25 V, 5 pulses, 50 ms each	2	13	0	15	5	10	30	8–10

Note that each electroporation condition performed on each developmental stage was completed in a single experiment. Each embryo's anterior neural tube was positioned parallel to the electrode plate. As a result, all zebrafish embryos expressed EGFP in a unilateral manner. V, volts; hpf, hours post-fertilization; FB, forebrain; MB, midbrain; HB, hindbrain.

Science, Mannheim, Germany) antisense GFP RNA probe. For cryosectioning, the embryos were embedded in molten Bacto™ agar (Difco, Detroit, MI, USA) and sectioned (18).

RESULTS AND DISCUSSION

Optimization of Electroporation

Embryos (24 hpf) were used to optimize conditions for in vivo electroporation into the brain. To analyze transfection efficiency, we used pEGFPN2, a plasmid carrying the GFP gene downstream of the ubiquitous cytomegalovirus (CMV) promoter. By this stage, the neural tube is hollow and contains wider ventricles in the brain and a narrower central canal in the spinal cord. Therefore, after a single injection of DNA, which fills these cavities, the reporter vector could be electroporated anywhere in the brain. To determine the electroporation efficiency and embryo viability, embryos between 24–48 hpf were exposed to varying electroporation conditions (Table 1). Successful electroporation into the brain was observed only when square pulses of 20 volts (V) or more were used. Lower voltage caused GFP expression in the skin only (data not shown). Maximal GFP expression in the nervous tissue was observed when 24 hpf embryos were electroporated. In this case, more than half of the embryos displayed intense expression (Table 1). To electroporate 36–48 hpf embryos, the voltage was increased from 20 to 25 V. In these embryos, expression was more localized (data not shown).

GFP Expression After Electroporation

GFP signals were detected in the skin 2 h after electroporation, while GFP expression in the brain appeared after 4 h (data not shown). Maximal GFP expression was detected 12 hpf in the forebrain to hindbrain (Figure 2A), midbrain to hindbrain (Figure 2B), and forebrain to midbrain (Figure 2, C–F). GFP was expressed in a unilateral manner in all embryos (Figure 2, F–J). The telencephalon was not targeted due to electroporation along the medial-lateral axis of the neural tube. GFP expression in the telencephalon can be seen when electroporation is applied along the anterior-posterior axis (22 V, 5 pulses, 55 ms/pulse) such that the telencephalon faced the anode. Telencephalic expression is often accompanied by intense bilateral GFP expression in the cerebellum. Overall, 18 embryos of 20 survived this operation. Seventy-seven percent of the embryos (14 of 18) expressed GFP in the telencephalon, and close to 40% (7 of 18) expressed GFP in the cerebellum. However, no expres-

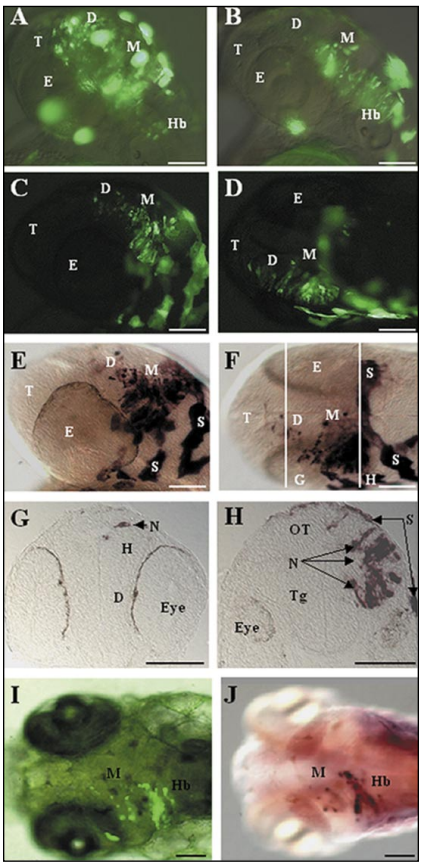

Figure 2. The range of green fluorescent protein (GFP) expression in electroporated embryos. (A and B) GFP was expressed in (A) the forebrain to hindbrain or (B) the midbrain and hindbrain 12 h after the electroporation of embryos that were 24 h post-fertilization. The merged bright-field and fluorescence photographs present embryos in side view with anterior to the left. (C and D) GFP expression in the forebrain and midbrain. The embryo is shown in side view (C) with the anterior to the left and (D) dorsal view. The majority of GFP expression was observed on the left side of the embryo that was adjacent to the anode during electroporation. (E and F) The embryo shown in panels C and D was stained by whole-mount in situ hybridization using anti-*gfp* RNA probe and presented in the same orientation. The expression pattern of *gfp* transcripts is the same as that of GFP protein detected by fluorescence microscopy. The white bars show the positions of cross sections shown in panels G and H. (G and H) Cross sections of the embryo shown in panels C–F at the level of (G) the forebrain and (H) the midbrain demonstrated the expression of *gfp* in the neurons and skin. (I and J) The electroporation of GFP does not affect the development of the embryo. GFP expression in the brain can be detected 10 days after electroporation. (I) The merged bright-field and fluorescence photograph present an embryo in dorsal view with anterior to the left. The same embryo was processed for whole-mount in situ hybridization using (J) anti-*gfp* RNA probe. Scale bar = 100 µm. Abbreviations: D, diencephalons; E, eye; H, habenula; Hb, hindbrain; M, midbrain; N, neuron; OT, optic tectum; S, skin; T, telencephalon; Tg, tegmentum.

sion was seen in the anterior spinal cord when the embryo was placed in the opposite orientation, with the hindbrain facing the anode. Thus, our conditions favor electroporation into the brain.

Whole-mount in situ hybridization using a digoxigenin-labeled anti-GFP riboprobe (Figure 2, E and F) recapitulated the pattern of GFP expression detected by fluorescent microscopy (Figure 2, C and D). The same embryo was sectioned, and *gfp* transcripts were detected in the dorsal diencephalon, including the left habenula (Figure 2G), and more posteriorly in the optic tectum and tegmentum of the midbrain (Figure 2H). This means that the midbrain was electroporated at all levels along the dorsoventral axis. In addition, the

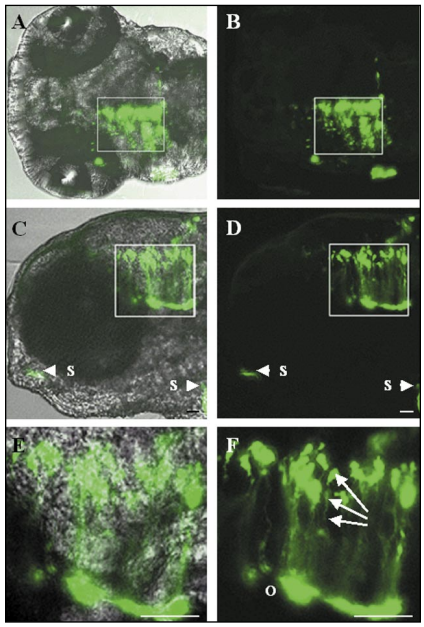

Figure 3. Confocal imaging of zebrafish embryo 4 days post-electroporation. (A and B) One-sided green fluorescent protein (GFP) expression in the brain 4 days post-electroporation. The dorsal view with anterior to the left. GFP expression was confined to the left side of the brain. (A) Merged bright-field and fluorescence and (B) the corresponding fluorescent image. (C and D) The same embryo in lateral view with anterior to the left. GFP is expressed in the midbrain and hindbrain. (E) Merged bright-field image and fluorescent image and (F) the corresponding fluorescent image. (E and F) The enlarged view of the boxed regions in panels C and D, respectively. (E) Merged bright-field image and fluorescent image and (F) the corresponding fluorescent image. Arrows indicate a cell body in the ventricular zone with long processes. Scale bar: 50 µm. Abbreviations: O, outer region of the neural tube; S, skin.

cells of the skin were also *gfp*-positive (Figure 2H). These cells demonstrated a typical morphology of epithelial cells. In general, the fluorescence signal in the neural tube started to decline 3 days after electroporation. However, in a small subset of embryos, GFP fluorescence remained visible 10 days after electroporation (Figure 2, I and J).

The morphology of embryos expressing GFP was examined under the confocal microscope 4 days post-electroporation (Figure 3). In this sample, the left side of the brain was targeted, and GFP-positive cells extended from the midbrain to the hindbrain (Figure 3, A–D). GFP-positive cells were detected in the medial and lateral region of the dorsal hindbrain (Figure 3F). We noticed that some of these cells had long processes (Figure 3F, arrows). This region of the brain contains premigratory neuroblasts and radial glial cells (RGCs). RGCs are characterized by long processes directed ventrally (19). Therefore, in this case, the GFP-positive cells probably represent neuroblasts and RGCs. A second region of GFP expression was found ventrally in the region known to contain postmigratory differentiating neurons (18). Therefore, expression of GFP was detected in the early and late neurons as well as RGCs. Thus, a combination of electroporation and 3-D in vivo imaging represents a powerful approach to study the differentiation of neurons and glial cells in zebrafish development.

The modification to the in vivo electroporation method presented here is substantially different from earlier attempts to use electroporation in the zebrafish. First, a DNA solution is injected into the brain. Second, the embryo is not in direct contact with the electrode plate. Importantly, only a small part of the embryo is exposed to the electric pulse so that only cells within the exposed region are transformed. The rest of the embryo remains within the agarose well, thus minimizing the effect of the electric field on the embryo. Using this method, multiple constructs can be delivered simultaneously into the embryo. Further complexity could be achieved by the introduction of bicistronic vectors used previously for injection into one-cell stage embryos (20).

In summary, we have developed an efficient procedure for the electroporation of DNA into the brain of the zebrafish embryo. The success and reproducibility of our experiments were determined by four factors, (*i*) usage of a modified electroporation chamber instead of electrodes; (*ii*) the optimized injection volume; (*iii*) the ability to rotate the embryo within the well; and (*iv*) electroporation that immediately followed microinjection.

ACKNOWLEDGMENTS

We thank Steven Fong, Alexander Emelyanov, and Jonathan Clarke for their helpful discussions. This project was supported by a research grant from the Agency for Science, Technology and Research (A-STAR) of Singapore (V.K.).

REFERENCES

1. **Kimmel, C.B., W.W. Ballard, S.R. Kimmel, B. Ullmann, and T.F. Schilling.** 1995. Stages of embryonic development of the zebrafish. Dev. Dyn. *203*:253-310.
2. **Haffter, P., M. Granato, M. Brand, M.C. Mullins, M. Hammerschmidt, D.A. Kane, J. Odenthal, F.J. van Eeden, et al.** 1996. The identification of genes with unique and essential functions in the development of the zebrafish. Development *123*:1-36.
3. **Dooley, K. and L.I. Zon.** 2000. Zebrafish: a model system for the study of human disease. Curr. Opin. Genet. Dev. *10*:252-256.
4. **Davis, J.M., H. Clay, J.L. Lewis, N. Ghori, P. Herbomel, and L. Ramakrishnan.** 2002. Real-time visualization of mycobacterium-macrophage interactions leading to initiation of granuloma formation in zebrafish embryos. Immunity *17*:693-702.
5. **Nasevicius, A. and S.C. Ekker.** 2000. Effective targeted gene "knockdown" in zebrafish. Nat. Genet. *26*:216-220.
6. **Swartz, M., J. Eberhart, G.S. Mastick, and C.E. Krull.** 2001. Sparking new frontiers: using *in vivo* electroporation for genetic manipulations. Dev. Biol. *233*:13-21.
7. **Pu, H. and A.P. Young.** 1990. Glucocorticoid-inducible expression of a glutamine synthetase-CAT-encoding fusion plasmid after transfection of intact chick retinal explant cultures. Gene *89*:259-263.
8. **Muramatsu, T., Y. Mizutani, and J. Okumura.** 1996. Live detection of the firefly luciferase gene expression by bioluminescence in incubating chick embryos. Ann. Sci. Technol. *67*:906-909.
9. **Buono, R.J. and P.J. Linser.** 1992. Transient expression of RSVCAT in transgenic zebrafish made by electroporation. Mol. Mar. Biol. Biotechnol. *1*:271-275.
10. **Patil, J.G. and H.W. Khoo.** 1996. Nuclear internalization of foreign DNA by zebrafish spermatozoa and its enhancement by electroporation. J. Exp. Zool. *274*:121-129.
11. **Tawk, M., D. Tu, Y. Torrente, S. Vriz, and D. Paulin.** 2002. High-efficiency gene transfer into adult fish: a new tool to study fin regeneration. Genesis *32*:27-31.
12. **Nakamura, H. and J. Funahashi.** 2001. Introduction of DNA into chick embryos by *in ovo* electroporation. Methods *24*:43-48.
13. **Saito, T. and N. Nakatsuji.** 2001. Efficient gene transfer into the embryonic mouse brain using *in vivo* electroporation. Dev. Biol. *240*: 237-246.
14. **Haas, K., W.C. Sin, A. Javaherian, Z. Li, and H. Cline.** 2001. Single-cell electroporation for gene transfer in vivo. Neuron *29*: 583-591.
15. **Müller, F., S. Albert, P. Blader, N. Fischer, M. Hallonet, and U. Strähle.** 2000. Direct action of the nodal-related signal cyclops in induction of sonic hedgehog in the ventral midline of the CNS. Development *127*:3889-3897.
16. **Westerfield, M.** 1995. The Zebrafish Book: A Guide for the Laboratory Use of Zebrafish (*Brachydanio rerio*). University of Oregon Press, Eugene, OR.
17. **Oxtoby, E. and T. Jowett.** 1993. Cloning of the zebrafish krox-20 gene (krx-20) and its expression during hindbrain development. Nucleic Acids Res. *21*:1087-1095.
18. **Korzh, V., T. Edlund, and S. Thor**. 1993. Zebrafish primary neurons initiate expression of the LIM homeodomain protein Isl-1 at the end of gastrulation. Development *118*:417-425.
19. **Trevarrow, B., D.L. Marks, and C.B. Kimmel.** 1990. Organization of hindbrain segments in the zebrafish embryo. Neuron *4*: 669-679.
20. **Wang, X., H. Wan, V. Korzh, and Z. Gong.** 2000. Use of an IRES bicistronic construct to trace expression of exogenously introduced mRNA in zebrafish embryos. BioTechniques *29*:814-818.

Received 10 July 2003; accepted 15 September 2003.

Address correspondence to Vladimir Korzh, Institute of Molecular and Cell Biology, 1 Research Link, Singapore, 117604. e-mail: vlad@imcb.a-star.edu.sg

New ways to admire zebrafish: progress in functional genomics research methodology

Cathleen Teh, Serguei Parinov, and Vladimir Korzh

BioTechniques 38:897-906 (June 2005)

The main challenge of the post-genomic era is to functionally characterize genes identified by the genome sequencing projects. Model organisms, including zebrafish, are indispensable for this demanding task. Zebrafish has been successfully incorporated into large-scale genetic screens due to the optical clarity of the embryos and their accessibility to various experimental techniques throughout development. The attractiveness of the zebrafish as a model organism is enhanced by the availability of continuously improving genomic tools and methodologies for functional characterization of the gene. This article will highlight the current techniques used in the field, with the focus on transgenesis.

INTRODUCTION

Since the human genome project was completed several years ago, the next daunting task ahead will be the annotation of genes about whose function scientists may have little knowledge. This task could be accomplished efficiently by using model animals and large-scale approaches. However, not all animal models are suitable for large-scale functional characterization. For example, identifying large numbers of mutations in mice is hampered by inherent limitations of this model system such as a small litter size, intrauterine development, and the relatively expensive supporting laboratory facilities. In contrast, zebrafish has been successfully incorporated into large-scale forward genetic screens in which mutants with phenotypic defects are identified before the identity of the gene is known (1). The attractiveness of zebrafish as a model organism can be attributed to its relatively small genome size, short generation time, external development, and optical clarity of the embryos. In particular, the latter two features allow for direct monitoring of developmental processes and their manipulation using chemical, genetic, and mechanical approaches. The ease of such manipulations when coupled to the continuously improving genomic tools developed with the support of the National Institutes of Health (NIH; Bethesda, MD, USA) funding (2) facilitates the process of gene annotation and accelerates mutant identification.

The more we learn about the zebrafish, the more we admire this tiny vertebrate. It was recently discovered that the zebrafish genome contains more genes than the human one due to an additional round of genome duplication (3,4). The analysis of zebrafish mutants affecting some of the duplicated genes led us to appreciate the resulting functional dissection of genes because each of these duplicated genes perform only a subset of functions when compared to their single mammalian homologs (5,6). As a result, zebrafish mutations affecting either of the two homologous genes usually give rise to milder phenotypes. Furthermore, even lethal mutants survive longer; for instance, zebrafish embryos resort to passive gaseous exchange to survive a mutation-induced blood circulation defect (7). A combination of these factors favors a comparatively longer period of development of zebrafish mutants. During this extended period, some developmental genes could be reused over and over again, which presents the possibility of studying much later gene function than in other vertebrate models. All this contributes to the fact that currently zebrafish is a well-established model system to study human diseases and heredity (7–9).

Importantly, zebrafish stands out as a model animal because it represents the teleost, a class of bony fishes that encompasses half of all vertebrate species on the planet. Thus, zebrafish is probably a good representative of vertebrates, and it is easy to envision that methodological advances in zebrafish biology may help to establish experimental approaches that could be applied to studies in other teleost species. A good example is the large-scale mutant screen repeated on another fish model, medaka (10).

This review will highlight current techniques used in the field of zebrafish biology, with the focus on transgenesis. Given that interest in zebrafish as a vertebrate model originates from its successful incorporation in large-scale genetic screens (11,12), we will briefly discuss various approaches used toward mutagenesis and then move on to current knockdown methodologies

National University of Singapore, Singapore

used in zebrafish research. The article will then focus on recent advances made in the field of both stable and transient transgenesis and conclude with a brief discussion on transient misexpression of secreted proteins and small molecules via implantation of carrier beads.

MUTAGENESIS SCREENS

Traditional Approaches Toward Cloning a Mutated Gene

Large-scale mutagenesis screens in zebrafish generated mutant phenotypes that result from random point mutations induced by ethylnitrosourea (ENU)-mediated chemical mutagenesis (11,12). This led to the identification of over 2000 developmentally important loci (13). Only a small fraction of the discovered mutants have been molecularly characterized, as cloning of the ENU-mutated gene remains a laborious task. Nevertheless, this process continues to accelerate with the refinement of genetic and physical maps of the zebrafish genome (www.ncbi.nlm.nih.gov/genome/guide/zebrafish/index.html). Currently, chemically mutated genes are cloned either by the candidate gene approach or via positional cloning (14). The majority of genes cloned from chemical mutagenesis screens have been identified by the candidate gene approach (1). However, this approach is limited to those genes previously shown to act in the process of interest (1). Positional cloning is still required to identify novel mutated genes. It involves high-resolution genetic mapping of the mutation, assembly of a set of contiguous genomic clones spanning the region of the mutated gene, cataloging the genes in the region, and narrowing down the list of genes until the mutated gene is identified. Positional cloning of ENU-mutated genes is a laborious process. Efforts made to facilitate rapid mapping of new zebrafish mutations generated through mutagenesis screens include the development of highly polymorphic inbred lines and the derivation of such polymorphisms into reliable markers that can be used in bulk segregant analysis to rapidly identify map positions of new mutations (15). In practice, however, there is a growing demand for mutations in a selected gene of interest. Current progress made in sequencing genomes will help to set the stage for reverse genetics.

Target-Selected Mutagenesis

A reverse genetic methodology has been developed to identify more mutated genes. During the process of target-selected mutagenesis (16,17), carriers of mutations in genes of interest were identified before their mutant phenotype. In this method, also known as targeting induced local lesions in genome (TILLING), male zebrafish are mutagenized with ENU and used to generate F_1 progeny with multiple random heterozygous mutations in their genomes. DNA from fin clips undergoes PCR amplification with target gene-specific primers followed by CEL-I-mediated heteroduplex cleavage to detect mutations in target genes of interest. Potential mutations in genes of interest are reconfirmed by sequencing. Alternatively, direct sequence analysis can be carried out on mutagenized DNA with target gene-specific primers. Identified carriers can then be used in large-scale outcrosses to generate the F_2 generation, and homozygous F_3 mutants can be identified by incrossing sexually mature F_2 zebrafish.

Insertional Mutagenesis

To accelerate the cloning process while retaining the unbiased approach toward identification of the target gene, an insertional mutagenesis screen using a genetically modified retrovirus that could infect zebrafish cells was performed (18,19). Identification of the mutated gene is greatly simplified by the presence of the exogenous molecular tag within the gene it mutates. This improvement comes at a price because the efficiency of mutagenesis is 7- to 8-fold lower than that from the ENU screen (20). Nevertheless, the ease of cloning the mutated gene makes this method attractive enough to be performed on a large scale. Besides, it complements the approach undertaken via chemical mutagenesis (21). The insertional mutagenesis screen resulted in the isolation of 525 insertional mutants and the identification of 315 genes essential for early zebrafish development (22). Although the transgenic efficiency of retroviruses is acceptable for large-scale insertional mutagenesis, its usage as a routine approach for transgenesis is limited by the requirement to produce retroviruses of high titer (20).

This problem, together with safety concerns associated with the use of retrovirus in insertional mutagenesis screens, can be circumvented by applications based on transposon-mediated systems (23,24). Transposons have been used as tools for insertional mutagenesis and germline transgenesis in various model organisms (25,26). Initial reports describing the use of transposons for insertional mutagenesis in vertebrates indicated its low efficiency (27,28). However, some improvements are being made to increase the efficiency. For example, the *Sleeping Beauty* (SB) transposon system had its transposition efficiency increased with the use of improved SB transposon vectors (29,30), and transposition using these vectors was successfully demonstrated in zebrafish (31). Furthermore, preliminary results with the *Tol2* transposon suggest that the transposition rate should be high enough to make the large-scale mutagenesis screen a reality (32,33). The increased rate of transposition will promote the use of transposons in future insertional mutagenesis screens. In particular, transposons can be used as "launching pads" for local saturating mutagenesis in the genomic regions surrounding the donor sites (34).

GENE KNOCKDOWN METHODOLOGIES

Classical methods of inactivating the gene function using antisense and dominant negative RNA microinjection are now complemented by newer techniques. Currently, the most widely used reverse genetics method in zebrafish is undoubtedly the use of morpholino phosphorodiamidate oligonucleotides (morpholinos) to effectively knockdown a specific gene

function in zebrafish (35). Translation-blocking morpholinos (MOs) are designed to target the 5′-untranslated region (UTR) of messenger RNA (mRNA) or the first 20–25 nucleotides of the open reading frame (ORF) of the mRNA of interest (36). MOs can also be designed against splice acceptor or splice donor sites of pre-mRNA (37). The splice-blocking MOs interfere with the function of the spliceosome, leading to exon skipping or usage of cryptic splice sites that result in aberrantly spliced mRNA. Currently, delivery of the antisense oligonucleotide involves microinjection into embryos. Although popular, this knockdown approach may produce several nonspecific defects if high doses of MOs are employed. Proper specificity controls are therefore essential for the fruitful interpretation of the results (36).

Another approach to inhibit protein translation uses the negatively charged homo-oligomers of alternating trans-4-hydroxy-L-proline/phosphonate polyamides with DNA bases (HypNA-pPNA). This type of homo-oligomer also displays excellent hybridization properties toward DNA and RNA, while preserving the mismatch discrimination, nuclease resistance, and protease resistance of peptide nucleic acids (PNAs; References 38 and 39). A different approach toward gene silencing involves the use of short interfering RNA (siRNA). While it seems that this technique may not be applicable to the analysis of all genes (40), perhaps it could be used selectively (41–43). Moreover, siRNA technology allows for the possibility of controlled interference of the target gene by expressing short double-stranded RNA under various tissue- or stage-specific promoters (43). The availability of three different approaches for transient interference with gene expression makes it easier to choose the correct method and/or to design proper controls to validate experimental results. In particular, techniques that interfere with gene expression provide a useful means of verifying the identity of the target genes isolated in the mutagenesis screens.

TRANSGENESIS

Transgenesis is another approach used to decipher the complex mechanisms that transform a unicellular zygote into a functional multicellular organism. The combination of rapidly dividing embryos and fluorescent reporter technology (44) allows for changes in gene expression and detailed morphogenetic movement to be visualized in the developing embryo. Thus, the living color transgenic zebrafish system has been widely used in the studies of tissue-specific gene regulation, cell migration, and targeted misexpression (45,46). With the help of stable transgenic lines expressing fluorescent reporter genes in a tissue-restricted manner, mutagenesis screens performed on a transgenic background will probably unveil mutants in previously uncharacterized genes (13).

Approaches Toward Transgenesis

Many laboratories generate transgenic lines by direct transgenesis, whereby DNA is microinjected into the cell of 1–4 cell stage embryos. The injected construct usually contains a tissue-specific promoter that drives the expression of a reporter gene. This method, although simple, gives low frequency of germline transgenic founders, and the integration event usually results from the insertion of concatemers of the transgene. Such complex integration events may result in intrachromosomal recombination that changes the gene expression profile (46). Alternative methods with improved germline transgenesis characterized by a single integration event have been explored. These include the use of pseudotyped retroviruses (20) or transposons (28,31). Both methods molecularly tag the integration loci, which facilitates subsequent genomic analysis. Retroviral-mediated transgenesis, although efficient with an average of 25 independently segregating single copy insertions per transgenic founder (20), requires the construction, packaging, titering, and injection of virus into the 512–2000 cell stage embryos (19) and is thus less practical for the routine generation of transgenic zebrafish compared to DNA microinjection. Transposon-mediated transgenesis requires the same preparation time as the regular DNA microinjection technique, and transposons can accommodate large transgene constructs. In addition, the titer of the construct could be selected in such a way that most carriers will have just a few insertions, making a generation of single insertion lines an easier task.

Transposon-Mediated Transgenesis

Transposons are DNA sequences that can move from one locus in the genome to another. They can produce heritable mutations by inserting into genes and interrupting their regulatory and coding sequences, resulting in abnormal mRNA splicing or expression (47). The sequence of the surrounding region can easily be isolated and the affected gene identified. Transposable elements can carry reporter genes and can be engineered into enhancer and gene traps (32,33,48,49). They can also be used as vectors for high-efficiency transgenesis. Transposons are thus powerful tools for reverse genetics. All transposable elements can be divided into two classes: autonomous and nonautonomous (28). The former encodes transposase enzyme, which is required for transposition, while the latter lacks the transposase gene and can only be mobilized in the presence of autonomous transposons because transposase acts *in trans*. Therefore, to mobilize a nonautonomous element, the transposase gene can be located on the same DNA molecule as the transposon, supplied on another DNA molecule, or applied as either mRNA or protein. It has been demonstrated that several heterologous elements are capable of transposition in zebrafish (27,28,31–33,50–52). However, to date, only *Tol2* (28,32,33) and SB (31,48) were successfully used to generate stable transgenic zebrafish lines producing reliable transgene expression.

SB belongs to a superfamily of *Tcl/mariner* transposable elements. Its

transposase was reconstructed from consensus sequence derived from nonautonomous salmonoid *Tc1*-like elements (53). The SB transposon contains two terminal inverted repeat/direct repeat sequences that are required for transposition. SB transposition occurs by a cut-and-paste mechanism where the transposase binds to the inverted repeat sequence, excises the element from the donor molecule, and integrates it into new site(s) containing TA dinucleotide, carrying the sequence flanked by inverted repeats. Thus, the synthetic SB transposon system consists of two elements: the transposase and a transposon vector containing the inverted repeat/direct repeat sequences. Transposon-mediated transgenesis is performed by co-injecting transposase mRNA and the transposon DNA into 1–2 cell stage zebrafish embryos. A 6-fold increase in transgenesis was observed when compared to the standard plasmid injection-based approach (31). Enhancer trapping using the SB transposon system has also been demonstrated in zebrafish (54).

The *Tol2* element was isolated from the medaka fish, *Oryzias latipes*. It belongs to the hAT family of transposons (*hobo/Ac/Tam3*). Modified nonautonomous *Tol2* element can transpose in the genome of zebrafish germ cell lineage when co-injected with *Tol2* transposase (28). This methodology has been developed further for enhancer (32) and gene trap (33) such that the insertion reveals the expression of the trapped gene. In our laboratory, we used *Tol2* transposon for a pilot transgenic enhancer trap screen. We observed a transgenic efficiency of 16%, which resulted in the identification of more than 30 transgenic lines. The enhancer trap construct used in our study carried the enhanced green fluorescent protein (*EGFP*) gene controlled by a partial promoter from the keratin 8 gene expressed in epithelium. This construct was very effective in detecting enhancer elements in the genome of transgenic zebrafish. In fact, characteristic tissue-specific expression of the reporter gene was found among 75% of the founders. Although enhancer trap lines often reflect only a subset of gene-specific expression, they produce an endless variety of tissue- and cell-specific expression patterns (Figure 1). In addition, cytoplasmic distribution of GFP allows detailed analysis of cellular architecture, including fine processes and neurites. Thus, enhancer trap lines are great tools for detailed anatomical studies and have been used to identify anatomical structures previously unknown in zebrafish, such as the corpuscles of Stannius, which act as a parathyroid gland (32). The identification of insertion site is also relatively straightforward because thermal asymmetric interlaced PCR (TAIL-PCR) was efficiently used to identify DNA sequences that flank the site of transposon insertion.

The number of enhancer trap lines is continuously increasing because these lines are being used as "launching pads" to initiate transposon jumps into new sites by injecting transposase mRNA (32). This proves to be a novel and efficient approach for the generation of additional transgenic lines. Given the ease of identifying the insertion sites, we can now map the regulatory elements in the genome. Thus, this approach expands our knowledge about the noncoding genome, which, until recently, has been characterized as "junk DNA."

The gene trap element usually carries a promoterless reporter gene with splice acceptor sequences in front of the coding region to allow for fusion with the tagged gene (33). The expression of the tagged gene is detected when it is inserted inside genes in the correct orientation. The trapping efficiency of the gene trap approach is lower than that of an enhancer trap; however, it is expected that it should better reflect the expression patterns of the tagged genes and be more mutagenic because it can affect the tagged gene by splicing its RNA with a reporter one (55). To date, a medium-scale screen using this approach has not illustrated its mutagenicity (33). Nevertheless, given the fact that this approach is very new and its potential will be further explored and developed, it would be premature to rule out its usefulness for mutagenesis.

Sperm Nuclear Transplantation

A common characteristic among plasmid DNA injection, transposon, and retroviral-mediated gene transfer is that DNA integration occurs after several rounds of cell division. This results in a mosaic expression of the gene in the F_0 population. Sperm-mediated gene transfer was carried out in zebrafish to resolve the issue of mosaic gene expression (56). The technique was first used in *Dictyostelium* and had been successfully adopted in the generation of nonmosaic transgenic frogs. In this method, transgenes are integrated into sperm nuclei before they are injected into nonfertilized eggs. To show that the transgene introduced by sperm-mediated gene transfer can be transmitted to the germline and expressed in a cell type-specific manner, a plasmid containing EGFP fused to a 3.2-kb HuC promoter was used. Zebrafish generated by this method expressed EGFP in a pattern similar to HuC mRNA in the F_0 generation. Progeny of the embryos that were grown to adulthood express EGFP in a similar manner, which demonstrates that the technique can be used to generate transgenic lines (56).

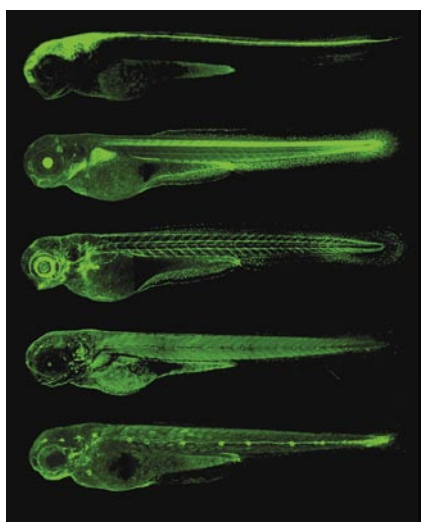

Figure 1. Enhancer trap transgenic zebrafish embryos generated by insertion of *Tol2* transposon. Using insertional transgenesis mediated by a *Tol2* transposon that contains the gene encoding the green fluorescent protein (GFP) expressed under control of the minipromoter of keratin 8, more then 30 different transgenic lines were generated. Here 5-day-old larvae of the lines ET33, ET5, ET37, ET20, ET4 (from top to bottom) demonstrate different expression patterns detected in vivo under the confocal microscope.

Transgenesis-Mediated by *I-SceI* Meganuclease

Another approach that promotes a higher germline transmission rate is *I-SceI* meganuclease-mediated transgenesis. *I-SceI* is an intron-encoded homing endonuclease with an 18-bp recognition site that is expected to be found only once in 7×10^{10} bp of random DNA sequence. Consequently, co-injection of plasmids bearing meganuclease recognition sites with the meganuclease will only digest the injected DNA and not run the risk of fractionating the genome. This methodology of generating transgenic fish was applied to medaka with 30.5% efficiency (57). More impressively, the germline transmission rate reached an optimum of 50% in most lines generated by meganuclease co-injection. This suggests that a single integration event at the one cell stage occurred in a nonmosaic heterozygous fish that transmits the transgene to 50% of its offspring. The co-injected meganuclease likely counteracts the endogenous ligase activity, preventing the generation of long concatemers found upon injection of circular or linear DNA. This results in the availability of more recombination ends, which facilitates integration into the genome. The consequence is an increase in transgenic founders identified at the F_0 generation with a high germline transmission rate. A similar approach has been applied to zebrafish, and an average transgenic frequency of 30% was observed (J. Shin, H.-C. Park, and B. Appel, personal communication).

TRANSIENT TRANSGENESIS

Transient assays remain a complementary approach to generating stable transgenic lines (46,58). The effect of a gene on development can be studied by targeted misexpression. This can be achieved through the use of tissue- or stage-specific promoters (46). If misexpression of the gene results in abnormalities that affect reproduction or embryo viability, a stable misexpressing line cannot be generated. The alternative is transient misexpression of the gene. Tissue-specific ectopic expression of a gene can be achieved by microinjecting plasmids containing tissue-specific regulatory elements into a single blastomere of zebrafish embryos at later stages (16–128 cells). As the injected plasmid gets distributed in a mosaic manner to descendants of the injected cell, only a limited number of cells will eventually express the transgene (46). Alternative methods have been devised to transiently increase the level of transgene expression and are mentioned below.

Gal4-VP16-Mediated Misexpression

The Gal4-VP16 activator/effector system was used to amplify transgene expression in zebrafish embryos. When compared to promoter-driven misexpression in conventional expression vectors, a significantly higher number of cells that express a transgene at detectable levels were observed (59). For the system to function, a combination of the activator and effector components is required. The Gal4-VP16 transcriptional activator is a fusion of the Gal4-DNA binding domain with the herpes simplex virus transcriptional activation domain VP16. Either tissue- or stage-specific promoters can regulate the expression of the activator while the effector expresses the gene of interest under the control of an upstream activating sequence (UAS). Less mosaic expression can be obtained if the activator and effector units are placed in a single injection construct. Furthermore, Gal4-VP16 can drive the expression of two effector cassettes efficiently from the same construct, resulting in simultaneous coexpression of both genes (59). Therefore, EGFP coexpressed with any transgene of interest can act as a reporter for transgene-expressing cells. This allows for the in vivo imaging of the behavior of transgene-expressing cells in real time. The system, although attractive, requires empirical optimization of the concentration of Gal4-VP16 activator constructs. Overt misexpression of the activator could result in developmentally retarded and malformed embryos. This is due to a phenomenon called squelching as the Gal4-VP16 activator can bind to and titrate out other transcription factors, thereby down-regulating the general transcription machinery. Thus, a balance between maximal activation and minimal squelching must be found (59).

HSP70-Mediated Transgenesis

Tissue-specific regulation of ectopic transgene expression or its dominant negative forms allows the possibility of directly addressing a gene function during any time point in any tissue of interest provided that promoters for each pattern of interest are cloned. In the absence of such regulatory elements, one can regulate misexpression by expressing genes under the control of the heat shock promoter *hsp70*. Inducibility is desirable for transgenic systems because the level of the transgenic product could be affected at will. For instance, transgenes with adverse effects could be turned on and off and, in this way, used to study gene activity during the later stages of development. Currently *hsp70* promoters from mouse, *Xenopus*, tilapia, and zebrafish (60–62) have been cloned and shown to mediate heat shock-induced expression of a reporter gene in zebrafish embryos. The *hsp70* constructs allow for temporal control over gene expression because the promoter can be activated at any time by increasing the temperature. Control of both spatial and temporal expression was demonstrated by focusing a sublethal laser microbeam onto specific cells in *hsp70* zebrafish transgenic lines (62). The laser beam was focused through a ×50 objective; the cells were visualized under differential interference contrast (DIC) optics and heat shocked with a 2-min burst of 4-ns laser pulses, delivered at a frequency of 3–4 Hz. After the laser heat shock, embryos recover for 4–24 h at 28.5°C. By taking advantage of the accessibility and optical clarity of zebrafish embryos, targeted cells expressing laser-induced GFP appear to develop normally. The usefulness of laser-targeted expression was further demonstrated in a transgenic line where the *hsp70* promoter regulates the expression of *sema3A1*. In the transient misexpression study, early motor axons were retarded by laser-induced Sema3A1 in muscle cells upon which they normally extend (62).

Despite the attractiveness of the system, the zebrafish *hsp70* promoter is

slightly leaky. This method of induction was improved on when novel artificial synthetic heat-inducible promoter consisting of multimerized heat shock elements (HSEs) used in medaka fish demonstrated a high signal-to-noise ratio (63).

In Vivo Electroporation

Another transient transgenesis approach that targets gene delivery into a specific tissue at any time point of interest is electroporation. The attractiveness of this technique lies in the ability to have spatial and temporal control over gene expression and gives a quick readout of the effects caused by gene misexpression. In vivo electroporation involves the injection of plasmid DNA into the target tissue, followed by the administration of an electric field. Application of the electric pulse temporarily disrupts membrane stability, creating pores or holes in the plasma membrane through which DNA is driven as a result of its negative charge. The difficulty in applying this approach to living organisms had been that the electric pulses often damaged cells and resulted in substantial cell death. Optimization of conditions for electroporation is required before successful DNA delivery that results in ectopic gene expression in the living embryo can occur. A compromise must be struck between efficient DNA delivery and toxicity that results from the application of the electric field. Permeabilization is the main cause of toxicity as the cytoplasmic composition is modified by the diffusion of the external media.

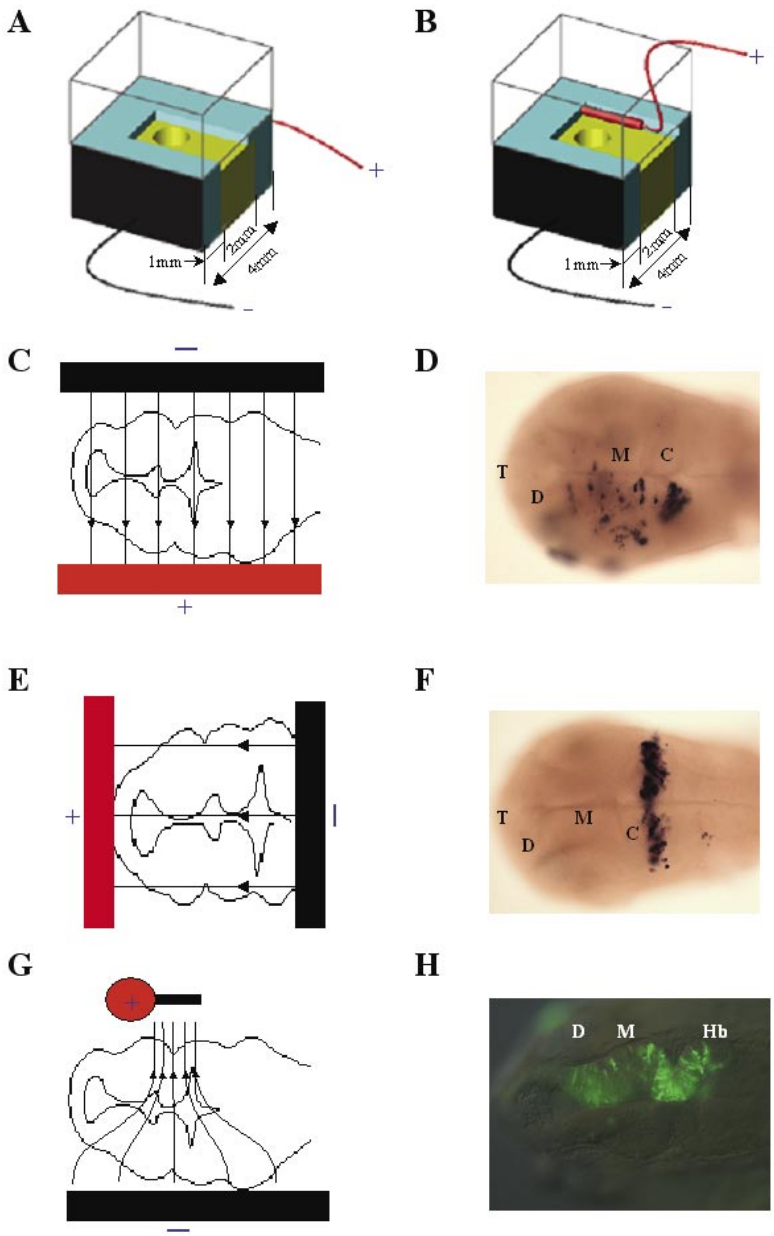

Figure 2. Electroporation into zebrafish embryos. (A) Diagram of an electroporation chamber that generates uniform electric field through plates of similar size. The negative electrode plate is shown in black, and the troughs filled with Hank's buffer are in cyan. A zebrafish embryo with DNA microinjected into the cavity of the neural tube will be placed in the agarose well (yellow) and covered with Hank's buffer. The positive electrode on the other side of the chamber is not depicted in this illustration. A section of the overlying Hank's buffer had been removed to reveal the agarose well underneath for both panels A and B. (B) Diagram of an electroporation chamber that generates a converging electric field through plates of dissimilar size. The negative electrode plate is shown in black while the positive rod-shaped electrode appears in red. (C) Diagram of the embryo during electroporation for unilateral expression of the transgene. The anterior-posterior (A-P) axis of the embryo is positioned parallel to the electrode plate; negatively charged DNA in the cavity of the neural tube is targeted toward the positive electrode. (D) Whole-mount in situ hybridization with an anti-*gfp* RNA probe of an embryo electroporated as in panel C. The hybridization was performed 1 day after electroporation. The embryo is shown in dorsal view with the anterior to the left. GFP is expressed in a unilateral manner in the forebrain, midbrain, and cerebellum. (E) Diagram of the embryo during electroporation for bilateral expression of the transgene. The A-P axis of the embryo is perpendicular to the electrode plates. Negatively charged DNA molecules in the cavity of the neural tube are attracted to the positive electrode and efficiently transfect cerebellar tissue at the narrow midbrain-hindbrain boundary. (F) Whole-mount in situ hybridization with an anti-*gfp* RNA probe of an embryo electroporated as in panel E. The hybridization was performed 1 day after electroporation. The embryo is shown in dorsal view with the anterior to the left. GFP is expressed in a bilateral manner in the cerebellum. (G) Diagram of the embryo during electroporation for increased unilateral expression of the transgene using a converging electric field. The A-P axis of the embryo is parallel to the electrode plate, and negatively charged DNA in the cavity of the neural tube is targeted to the tissue adjacent to the smaller positive electrode. (H) GFP was expressed at high levels (compare to panel D) in the forebrain, midbrain, and hindbrain 12 h after electroporation of a 19 hpf stage embryo. The merged bright-field and fluorescence images present the embryo in dorsal view with anterior to the left. GFP expression was observed on the right side of the embryo, which, during electroporation, was adjacent to the positive electrode. GFP, green fluorescent protein; hpf, hours post-fertilization; C, cerebellum; D, diencephalon; Hb, hindbrain; M, midbrain; and T, telencephalon.

Other toxicity effects include the induction of free radicals, inflammation, and vascular defects (64).

The whole embryo electroporation approach was first introduced to the field of zebrafish research as a means of gene delivery to generate transgenic fish (65). However, this method was essentially abandoned due to the high lethality rate. Later, its modification for sperm-mediated DNA transfer was reported (66). This was followed by a more recent report on the electroporation of DNA into the fin of adult zebrafish (67). But DNA delivery into internal organs of embryonic zebrafish remained impossible until recently, when in vivo electroporation was adapted in our laboratory to the study of neural development in zebrafish (68). The neural tube is particularly easy to target because the gene expression vector can be introduced into its lumen, which permits the directed transfer of DNA to tissue on the side of the positive electrode.

Effective in vivo electroporation into the neural tube is an established technique in chick, mouse, and *Xenopus* (69–72). The challenge of performing electroporation on zebrafish embryos is to ensure successful DNA delivery without damaging the yolk cell. We circumvented the limitation by positioning the injected embryo in an electroporation chamber containing an agarose well (Figure 2A; Reference 68) such that only the injected region of the neural tube is exposed to the full strength of the electric field. To minimize embryo toxicity that results from microinjection, DNA was microinjected through the floor of the neural tube. Because the yolk cell is adjacent to the site of injection, this minimized diffusion of external media through the puncture site. Leakage of injected DNA from the neural tube can be minimized when electroporation is carried out immediately after microinjection. The uniform electric field is conducted through the plates of a shortened 4-mm wide electroporation chamber, which houses the embryo in an agarose well surrounded by Hank's buffer. Using this method, DNA can be delivered and expressed in cells of the anterior neural tube of 24–48 hours post-fertilization (hpf) zebrafish. By changing embryo position with respect to the electrodes in the electroporation chamber, various regions of the anterior neural tube can be targeted (Figure 2, C–F).

A further refinement of the electroporation approach arises from variation in types of electrodes used. The shape of electrode could vary from a fine point to a long wire or even a plate. Large electrodes (e.g., plate electrodes) pass more electric current and generate electric field of higher intensity compared to fine electrodes. This results in massive transgene expression. The electric field becomes nonuniform when electrodes of dissimilar size are used (Figure 2B). For example, we generated a converging electric field that concentrated the current flow to the neural tube by using a plate electrode for the cathode and a 1-mm rod electrode for the anode. This resulted in substantial enhancement of transgene expression (Figure 2, G and H). In theory, using this method, DNA can be delivered into any hollow organ of the embryonic zebrafish. In practice, it remains to be seen how successful this technique would be in targeting DNA into more ventral organs located closer to the yolk cell, such as the intestine.

At the other extreme, localized electroporation with very fine electrodes to target specific groups of cells has been performed in both *Xenopus* tadpoles and chick embryos (71,73). It is achieved by restricting both the DNA and the electric field to the tip of a glass micropipet. Using this modification of microionophoresis previously used to trace the movement of individual zebrafish cells during early development (74), both dyes and mRNA have been successfully delivered into a few cells of the neural tube of the zebrafish embryo (75,76).

Implantation of Carrier Beads

Bead implantation into zebrafish embryos is another transient "misexpression" approach used for the targeted delivery of proteins, which was initially established in other model animals and recently applied to zebrafish (77,78). In our laboratory, Lam et al. (79) showed that beads coated with fibroblast growth factor 8 (*FGF8*) or bone morphogenetic protein 4 (*BMP4*) can be loaded into beveled capillaries and implanted using an aspirator tube assembly into the midbrain, hindbrain, or the endoderm at 20 hpf without affecting embryo viability. Using this method, the formation of noradrenergic neurons in the *acerebellar* (*ace*) mutant was rescued by providing exogenous *FGF8* with the implanted bead. For now, this method is limited to the study of secreted proteins and small molecules. However, given the importance of these molecules in development, this method represents a powerful technique to modulate activity of signaling pathways in vivo and provides a valuable tool to the rapidly expanding field of chemical genetics.

CONCLUSION

In recent years, zebrafish has been transformed from an unremarkable ornamental fish into an indispensable model of developmental biology whose studies attract increasing numbers of multimillion dollar research grants (80). Its popularity as a vertebrate model for functional genomics also can be attributed to the methodological tools recently developed for mutagenesis, reverse genetics, transgenesis, and micromanipulations. These technical advantages coupled with its small size, short generation time, external development, and optical clarity make the zebrafish an increasingly popular model to study human diseases and drug development. These tools can be almost instantaneously used to study many other teleosts and expand our knowledge in molecular evolutionary biology, physiology, and neurobiology, where fish other than zebrafish are widely used for research. Further development of these tools will provide us with new means to admire zebrafish.

ACKNOWLEDGMENTS

We are grateful to Raymond Ng and Siow Yeen Ping for their contributions to the drawings shown in the manuscript, Ms. Chu Lee Thean for her comments, and the fish laboratories of the Institute of Molecular and Cell Biology for their collaboration and continuous

support. The V.K. Laboratory is supported by a grant from the Agency for Science, Technology, and Research of Singapore.

COMPETING INTERESTS STATEMENT

The authors declare no competing interests.

REFERENCES

1. **Mullins, M.C.** 2002. Building-blocks of embryogenesis. Nat. Genet. *31*:125-126.
2. **Rasooly, R.S., D. Henken, N. Freeman, L. Tompkins, D. Badman, J. Briggs, and A.T. Hewitt.** 2003. Genetic and genomic tools for zebrafish research: the NIH zebrafish initiative. Dev. Dyn. *228*:490-496.
3. **Postlethwait, J.H., Y.L. Yan, M.A. Gates, S. Horne, A. Amores, A. Brownlie, A. Donovan, E.S. Egan, et al.** 1998. Vertebrate genome evolution and the zebrafish gene map. Nat. Genet. *18*:345-349.
4. **Gates, M.A., L. Kim, E.S. Egan, T. Cardozo, H.I. Sirotkin, S.T. Dougan, D. Lashkari, R. Abagyan, et al.** 1999. A genetic linkage map for zebrafish: comparative analysis and localization of genes and expressed sequences. Genome Res. *9*:334-347.
5. **Sampath, K., A.L. Rubinstein, A.M. Cheng, J.O. Liang, K. Fekany, L. Solnica-Krezel, V. Korzh, M.E. Halpern, et al.** 1998. Induction of the zebrafish ventral brain and floorplate requires cyclops/nodal signalling. Nature *395*:185-189.
6. **Feldman, B., M.A. Gates, E.S. Egan, S.T. Dougan, G. Rennebeck, H.I. Sirotkin, A.F. Schier, and W.S. Talbot.** 1998. Zebrafish organizer development and germ-layer formation require nodal-related signals. Nature *395*:181-185.
7. **North, T.E. and L.I. Zon.** 2003. Modeling human hematopoietic and cardiovascular diseases in zebrafish. Dev. Dyn. *228*:568-583.
8. **Dooley, K. and L.I. Zon.** 2000. Zebrafish: a model system for the study of human disease. Curr. Opin. Genet. Dev. *10*:252-256.
9. **Amatruda, J.F., J.L. Shepard, H.M. Stern, and L.I. Zon.** 2002. Zebrafish as a cancer model system. Cancer Cell *1*:229-231.
10. **Furutani-Seiki, M., T. Sasado, C. Morinaga, H. Suwa, K. Niwa, H. Yoda, T. Deguchi, Y. Hirose, et al.** 2004. A systematic genome-wide screen for mutations affecting organogenesis in Medaka, Oryzias latipes. Mech. Dev. *121*:647-658.
11. **Haffter, P., M. Granato, M. Brand, M.C. Mullins, M. Hammerschmidt, D.A. Kane, J. Odenthal, F.J. van Eeden, et al.** 1996. The identification of genes with unique and essential functions in the development of the zebrafish, Danio rerio. Development *123*:1-36.
12. **Driever, W., L. Solnica-Krezel, A.F. Schier, S.C. Neuhauss, J. Malicki, D.L. Stemple, D.Y. Stainier, F. Zwartkruis, et al.** 1996. A genetic screen for mutations affecting embryogenesis in zebrafish. Development *123*:37-46.
13. **Patton, E.E. and L.I. Zon.** 2001. The art and design of genetic screens: zebrafish. Nat. Rev. Genet. *2*:956-966.
14. **Talbot, W.S. and N. Hopkins.** 2000. Zebrafish mutations and functional analysis of the vertebrate genome. Genes Dev. *14*:755-762.
15. **Rawls, J.F., M.R. Frieda, A.R. McAdow, J.P. Gross, C.M. Clayton, C.K. Heyen, and S.L. Johnson.** 2003. Coupled mutagenesis screens and genetic mapping in zebrafish. Genetics *163*:997-1009.
16. **Wienholds, E., S. Schulte-Merker, B. Walderich, and R.H. Plasterk.** 2002. Target-selected inactivation of the zebrafish rag1 gene. Science *297*:99-102.
17. **Wienholds, E., F. van Eeden, M. Kosters, J. Mudde, R.H. Plasterk, and E. Cuppen.** 2003. Efficient target-selected mutagenesis in zebrafish. Genome Res. *13*:2700-2707.
18. **Amsterdam, A., S. Burgess, G. Golling, W. Chen, Z. Sun, K. Townsend, S. Farrington, M. Haldi, et al.** 1999. A large-scale insertional mutagenesis screen in zebrafish. Genes Dev. *13*:2713-2724.
19. **Amsterdam, A.** 2003. Insertional mutagenesis in zebrafish. Dev. Dyn. *228*:523-534.
20. **Chen, W., S. Burgess, G. Golling, A. Amsterdam, and N. Hopkins.** 2002. High-throughput selection of retrovirus producer cell lines leads to markedly improved efficiency of germ line-transmissible insertions in zebra fish. J. Virol. *76*:2192-2198.
21. **Golling, G., A. Amsterdam, Z. Sun, M. Antonelli, E. Maldonado, W. Chen, S. Burgess, M. Haldi, et al.** 2002. Insertional mutagenesis in zebrafish rapidly identifies genes essential for early vertebrate development. Nat. Genet. *31*:135-140.
22. **Amsterdam, A., R.M. Nissen, Z. Sun, E.C. Swindell, S. Farrington, and N. Hopkins.** 2004. Identification of 315 genes essential for early zebrafish development. Proc. Natl. Acad. Sci. USA *101*:12792-12797.
23. **Danos, O. and J.M. Heard.** 1992. Recombinant retroviruses as tools for gene transfer to somatic cells. Bone Marrow Transplant. *9*(*Suppl 1*):131-138.
24. **Izsvak, Z. and Z. Ivics.** 2004. Sleeping beauty transposition: biology and applications for molecular therapy. Mol. Ther. *9*:147-156.
25. **Kempken, F. and F. Windhofer.** 2001. The hAT family: a versatile transposon group common to plants, fungi, animals, and man. Chromosoma *110*:1-9.
26. **Ivics, Z., C.D. Kaufman, H. Zayed, C. Miskey, O. Walisko, and Z. Izsvak.** 2004. The Sleeping Beauty transposable element: evolution, regulation and genetic applications. Curr. Issues Mol. Biol. *6*:43-55.
27. **Raz, E., H.G. van Luenen, B. Schaerringer, R.H. Plasterk, and W. Driever.** 1998. Transposition of the nematode Caenorhabditis elegans Tc3 element in the zebrafish Danio rerio. Curr. Biol. *8*:82-88.
28. **Kawakami, K., A. Shima, and N. Kawakami.** 2000. Identification of a functional transposase of the Tol2 element, an Ac-like element from the Japanese medaka fish, and its transposition in the zebrafish germ lineage. Proc. Natl. Acad. Sci. USA *97*:11403-11408.
29. **Cui, Z., A.M. Geurts, G. Liu, C.D. Kaufman, and P.B. Hackett.** 2002. Structure-function analysis of the inverted terminal repeats of the sleeping beauty transposon. J. Mol. Biol. *318*:1221-1235.
30. **Geurts, A.M., Y. Yang, K.J. Clark, G. Liu, Z. Cui, A.J. Dupuy, J.B. Bell, D.A. Largaespada, et al.** 2003. Gene transfer into genomes of human cells by the sleeping beauty transposon system. Mol. Ther. *8*:108-117.
31. **Davidson, A.E., D. Balciunas, D. Mohn, J. Shaffer, S. Hermanson, S. Sivasubbu, M.P. Cliff, P.B. Hackett, et al.** 2003. Efficient gene delivery and gene expression in zebrafish using the Sleeping Beauty transposon. Dev. Biol. *263*:191-202.
32. **Parinov, S., I. Kondrichin, V. Korzh, and A. Emelyanov.** 2004. Tol2 transposon-mediated enhancer trap to identify developmentally regulated zebrafish genes in vivo. Dev. Dyn. *231*:449-459.
33. **Kawakami, K., H. Takeda, N. Kawakami, M. Kobayashi, N. Matsuda, and M. Mishina.** 2004. A transposon-mediated gene trap approach identifies developmentally regulated genes in zebrafish. Dev. Cell *7*:133-144.
34. **Smith, D., Y. Yanai, Y.G. Liu, S. Ishiguro, K. Okada, D. Shibata, R.F. Whittier, and N.V. Fedoroff.** 1996. Characterization and mapping of Ds-GUS-T-DNA lines for targeted insertional mutagenesis. Plant J. *10*:721-732.
35. **Nasevicius, A. and S.C. Ekker.** 2000. Effective targeted gene "knockdown" in zebrafish. Nat. Genet. *26*:216-220.
36. **Heasman, J.** 2002. Morpholino oligos: making sense of antisense? Dev. Biol. *243*:209-214.
37. **Draper, B.W., P.A. Morcos, and C.B. Kimmel.** 2001. Inhibition of zebrafish fgf8 pre-mRNA splicing with morpholino oligos: a quantifiable method for gene knockdown. Genesis *30*:154-156.
38. **Urtishak, K.A., M. Choob, X. Tian, N. Sternheim, W.S. Talbot, E. Wickstrom, and S.A. Farber.** 2003. Targeted gene knockdown in zebrafish using negatively charged peptide nucleic acid mimics. Dev. Dyn. *228*:405-413.
39. **Chen, E., P.B. Hackett, and S.C. Ekker.** 2004. Gene "knockdown" approaches using unconventional antisense oligonucleotides, p. 454-475. *In* Z. Gong and V. Korzh. (Eds.), Molecular Aspects of Fish and Marine Biology. World Scientific, Singapore.
40. **Oates, A.C., A.E. Bruce, and R.K. Ho.** 2000. Too much interference: injection of double-stranded RNA has nonspecific effects in the zebrafish embryo. Dev. Biol. *224*:20-28.
41. **Wargelius, A., S. Ellingsen, and A. Fjose.** 1999. Double-stranded RNA induces specific developmental defects in zebrafish embryos. Biochem. Biophys. Res. Commun. *263*:156-161.
42. **Boonanuntanasarn, S., G. Yoshizaki, and T. Takeuchi.** 2003. Specific gene silencing using small interfering RNAs in fish embryos. Biochem. Biophys. Res. Commun. *310*:1089-1095.
43. **Dodd, A., S.P. Chambers, and D.R. Love.** 2004. Short interfering RNA-mediated gene targeting in the zebrafish. FEBS Lett. *561*:89-93.
44. **Finley, K.R., A.E. Davidson, and S.C. Ekker.** 2001. Three-color imaging using fluorescent proteins in living zebrafish embryos. BioTechniques *31*:66-72.
45. **Gong, Z., B. Ju, and H. Wan.** 2001. Green fluorescent protein (GFP) transgenic fish and their applications. Genetica *111*:213-225.

46. **Udvadia, A.J. and E. Linney.** 2003. Windows into development: historic, current, and future perspectives on transgenic zebrafish. Dev. Biol. *256*:1-17.
47. **Hamer, L., T.M. DeZwaan, M.V. Montenegro-Chamorro, S.A. Frank, and J.E. Hamer.** 2001. Recent advances in large-scale transposon mutagenesis. Curr. Opin. Chem. Biol. *5*:67-73.
48. **Balciunas, D., A.E. Davidson, S. Sivasubbu, S.B. Hermanson, Z. Welle, and S.C. Ekker.** 2004. Enhancer trapping in zebrafish using the Sleeping Beauty transposon. BMC Genomics *5*:62.
49. **Clark, K.J., A.M. Geurts, J.B. Bell, and P.B. Hackett.** 2004. Transposon vectors for gene-trap insertional mutagenesis in vertebrates. Genesis *39*:225-233.
50. **Fadool, J.M., D.L. Hartl, and J.E. Dowling.** 1998. Transposition of the mariner element from Drosophila mauritiana in zebrafish. Proc. Natl. Acad. Sci. USA *95*:5182-5186.
51. **Szabo, M., F. Muller, J. Kiss, C. Balduf, U. Strahle, and F. Olasz.** 2003. Transposition and targeting of the prokaryotic mobile element IS30 in zebrafish. FEBS Lett. *550*:46-50.
52. **Miskey, C., Z. Izsvak, R.H. Plasterk, and Z. Ivics.** 2003. The Frog Prince: a reconstructed transposon from Rana pipiens with high transpositional activity in vertebrate cells. Nucleic Acids Res. *31*:6873-6881.
53. **Ivics, Z., P.B. Hackett, R.H. Plasterk, and Z. Izsvak.** 1997. Molecular reconstruction of Sleeping Beauty, a Tc1-like transposon from fish, and its transposition in human cells. Cell *91*:501-510.
54. **Balciunas, D., A.E. Davidson, S. Sivasubbu, S.B. Hermanson, Z. Welle, and S.C. Ekker.** 2004. Enhancer trapping in zebrafish using the Sleeping Beauty transposon. BMC Genomics *5*:62.
55. **Stanford, W.L., J.B. Cohn, and S.P. Cordes.** 2001. Gene-trap mutagenesis: past, present and beyond. Nat. Rev. Genet. *2*:756-768.
56. **Jesuthasan, S. and S. Subburaju.** 2002. Gene transfer into zebrafish by sperm nuclear transplantation. Dev. Biol. *242*:88-95.
57. **Thermes, V., C. Grabher, F. Ristoratore, F. Bourrat, A. Choulika, J. Wittbrodt, and J.S. Joly.** 2002. I-SceI meganuclease mediates highly efficient transgenesis in fish. Mech. Dev. *118*:91-98.
58. **Gong, Z., Y.L. Wu, S.P. Mudumana, and S. Lin.** Transgenic fish for developmental biology studies, p. 476-516. *In* Z. Gong and V. Korzh. (Eds.), Molecular Aspects of Fish and Marine Biology. World Scientific, Singapore.
59. **Koster, R.W. and S.E. Fraser.** 2001. Tracing transgene expression in living zebrafish embryos. Dev. Biol. *233*:329-346.
60. **Adam, A., R. Bartfai, Z. Lele, P.H. Krone, and L. Orban.** 2000. Heat-inducible expression of a reporter gene detected by transient assay in zebrafish. Exp. Cell Res. *256*:282-290.
61. **Molina, A., F. Biemar, F. Muller, A. Iyengar, P. Prunet, N. Maclean, J.A. Martial, and M. Muller.** 2000. Cloning and expression analysis of an inducible HSP70 gene from tilapia fish. FEBS Lett. *474*:5-10.
62. **Halloran, M.C., M. Sato-Maeda, J.T. Warren, F. Su, Z. Lele, P.H. Krone, J.Y. Kuwada, and W. Shoji.** 2000. Laser-induced gene expression in specific cells of transgenic zebrafish. Development *127*:1953-1960.
63. **Bajoghli, B., N. Aghaallaei, T. Heimbucher, and T. Czerny.** 2004. An artificial promoter construct for heat-inducible misexpression during fish embryogenesis. Dev. Biol. *271*:416-430.
64. **Bigey, P., M.F. Bureau, and D. Scherman.** 2002. In vivo plasmid DNA electrotransfer. Curr. Opin. Biotechnol. *13*:443-447.
65. **Buono, R.J. and P.J. Linser.** 1992. Transient expression of RSVCAT in transgenic zebrafish made by electroporation. Mol. Mar. Biol. Biotechnol. *1*:271-275.
66. **Patil, J.G. and H.W. Khoo.** 1996. Nuclear internalization of foreign DNA by zebrafish spermatozoa and its enhancement by electroporation. J. Exp. Zool. *274*:121-129.
67. **Tawk, M., D. Tuil, Y. Torrente, S. Vriz, and D. Paulin.** 2002. High-efficiency gene transfer into adult fish: a new tool to study fin regeneration. Genesis *32*:27-31.
68. **Teh, C., S.W. Chong, and V. Korzh.** 2003. DNA delivery into anterior neural tube of zebrafish embryos by electroporation. BioTechniques *35*:950-954.
69. **Nakamura, H. and J. Funahashi.** 2001. Introduction of DNA into chick embryos by in ovo electroporation. Methods *24*:43-48.
70. **Saito, T. and N. Nakatsuji.** 2001. Efficient gene transfer into the embryonic mouse brain using in vivo electroporation. Dev. Biol. *240*:237-246.
71. **Haas, K., W.C. Sin, A. Javaherian, Z. Li, and H.T. Cline.** 2001. Single-cell electroporation for gene transfer in vivo. Neuron *29*:583-591.
72. **Haas, K., K. Jensen, W.C. Sin, L. Foa, and H.T. Cline.** 2002. Targeted electroporation in Xenopus tadpoles in vivo—from single cells to the entire brain. Differentiation *70*:148-154.
73. **Atkins, R.L., D. Wang, and R.D. Burke.** 2000. Localized electroporation: a method for targeting expression of genes in avian embryos. BioTechniques *28*:94-100.
74. **Warga, R.M. and C.B. Kimmel.** 1990. Cell movements during epiboly and gastrulation in zebrafish. Development *108*:569-580.
75. **Lyons, D.A., A.T. Guy, and J.D. Clarke.** 2003. Monitoring neural progenitor fate through multiple rounds of division in an intact vertebrate brain. Development *130*:3427-3436.
76. **Dorsky, R.I., R.T. Moon, and D.W. Raible.** 1998. Control of neural crest cell fate by the Wnt signalling pathway. Nature *396*:370-373.
77. **Reifers, F., E.C. Walsh, S. Leger, D.Y. Stainier, and M. Brand.** 2000. Induction and differentiation of the zebrafish heart requires fibroblast growth factor 8 (fgf8/acerebellar). Development *127*:225-235.
78. **Hyatt, G.A., E.A. Schmitt, N. Marsh-Armstrong, P. McCaffery, U.C. Drager, and J.E. Dowling.** 1996. Retinoic acid establishes ventral retinal characteristics. Development *122*:195-204.
79. **Lam, C.S., I. Sleptsova-Friedrich, A.D. Munro, and V. Korzh.** 2003. SHH and FGF8 play distinct roles during development of noradrenergic neurons in the locus coeruleus of the zebrafish. Mol. Cell Neurosci. *22*:501-515.
80. **Bradbury, J.** 2004. Small fish, big science. PLoS Biol. *2*:E148.

Received 6 September 2004; accepted 9 October 2004.

Address correspondence to:

Vladimir Korzh
Institute of Molecular and Cell Biology
Proteos, 61 Biopolis Drive, Singapore 138673
e-mail: vlad@imcb.a-star.edu.sg

Wnt signalling mediated by Tbx2b regulates cell migration during formation of the neural plate

Steven H. Fong[1,*], Alexander Emelyanov[1,*], Cathleen Teh[1] and Vladimir Korzh[1,2,†]

[1]Institute of Molecular and Cell Biology, 61 Biopolis Drive, Proteos, 138673 Singapore
[2]Department of Biological Sciences, National University of Singapore, 10 Kent Ridge Crescent, 119260 Singapore
*These authors contributed equally to this work
†Author for correspondence (e-mail: vlad@imcb.a-star.edu.sg)

Accepted 9 June 2005

Development 132, 3587-3596
Published by The Company of Biologists 2005
doi:10.1242/dev.01933

Summary

During gastrulation, optimal adhesion and receptivity to signalling cues are essential for cells to acquire new positions and identities via coordinated cell movements. T-box transcription factors and the Wnt signalling pathways are known to play important roles in these processes. Zebrafish *tbx2b*, a member of the TBX2 family, has previously been shown to be required for the specification of midline mesoderm. We show here that *tbx2b* transcripts are present during mid-gastrula before its expression is detected by whole-mount in situ hybridization. Isolated ectodermal cells deficient in Tbx2b have altered cell surface properties and the level of cadherins in these cells is lower. In chimaeric embryos generated by cell transplantation and single blastomere injections, Tbx2b-deficient cells are defective in cell movement in a cell-autonomous manner, resulting in their exclusion from the developing neural plate. Using this 'exclusion' phenotype as a screen, we show that Tbx2b acts within the context of Fz7 signalling. The exclusion of cells lacking T-box proteins in chimeras during development was demonstrated with other T-box genes and may indicate a general functional mechanism for T-box proteins.

Key words: T-box, Cell adhesion, Zebrafish, Frizzled 7, Dishevelled, DIX domain, β-catenin

Introduction

During gastrulation, concurrent cell movement and cell fate specification eventually lead to the formation of germ layers and axes in the embryo. Because zebrafish embryonic cells are pluripotent up to the early gastrula stages (Ho and Kimmel, 1993), alteration of cell movement can cause changes in fate specification by virtue of exposure to local signalling cues prevalent in the 'adopted' position. Conversely, a failure in fate specification can lead to changes in cell movement behaviour.

In the zebrafish ectoderm, individual cells lose their independence and integrate their behaviour to achieve a coherent movement over the yolk as a sheet (Concha and Adams, 1998), while the underlying mesodermal cells migrate as individuals or groups of cells. This is in contrast to *Xenopus*, where the ectoderm is tightly coupled to the mesoderm (Shih and Keller, 1994). Optimal cell adhesion is essential for proper cell movement (Nelson and Nusse, 2004). Cell-surface adhesion molecules such as cadherins control cell-cell adhesion and influence cell migration. Disparity in cell adhesion properties among neighbouring cells is known to lead to loss of integrity and cell sorting within the ectodermal sheet (Concha and Adams, 1998).

The embryonic ectoderm has the potential to acquire either epidermal or neural fates. According to the default model, neural induction depends on the suppression of bone morphogenetic protein (Bmp, vertebrate homologue of Dpp) signalling by organizer-derived inhibitors (Munoz-Sanjuan and Brivanlou, 2002). Mass cell movements during gastrulation, especially that of convergent extension (CE), eventually establish the neural plate, which can be differentiated from the remaining epidermal ectoderm by early neural markers such as *sox19* (Vriz and Lovell-Badge, 1995). CE movement is most extensively investigated at the molecular level within the context of mesoderm formation (Myers et al., 2002). As such, the molecular mechanism governing dorsal movement of the overlying ectoderm leading to the formation of the neural plate is not well understood.

In *Xenopus*, Wnt/β-catenin has been demonstrated to inhibit Bmp (Baker et al., 1999) and is required for the expression of secreted Bmp antagonists (Wessely et al., 2001). In the zebrafish, Wnt/β-catenin-dependent *bozozok* (*boz*) is sufficient to suppress expression of *bmp* (Fekany-Lee et al., 2000). This is consistent with the role of β-catenin-dependent Wnt signalling, or canonical Wnt signalling, in fate determination (Moon et al., 2002). β-Catenin-independent Wnt signalling, or non-canonical Wnt signalling, has been demonstrated to influence morphogenetic cell movement (Tada et al., 2000; Heisenberg et al., 2000) by controlling Dishevelled (Ds)-mediated polarity in a manner reminiscent of the *Drosophila* planar-cell-polarity (PCP) pathway. However, in addition to its function in the Wnt signalling pathway, β-catenin also binds to the cytoplasmic domain of type 1 cadherins and plays an essential role in the structural organization and function of cadherins in the actin cytoskeleton (Jamora et al., 2003). Different cadherins have been shown to stimulate directly the

Development

Development

differentiation of stem cells into specific tissues (Larue et al., 1996). As such, there is a possible convergence of Wnt, β-catenin and cadherin signalling in adhesion, morphogenetic movement and differentiation.

Transcription factors of the T-box family (Tbx) play important roles in vertebrate development (Smith, 1999; Wilson and Conlon, 2002). *Brachyury* (*T*) and the zebrafish orthologue *no tail* (*ntl*) are known to be essential for the specification of axial mesoderm (Smith, 1999). In addition, *T*, *Tbx16*/*spadetail* (*spt*) and *Xbra* have been shown to be required for mesodermal cell movement (Wilson and Beddington, 1997; Ho and Kane, 1990; Kwan and Kirschner, 2003). A number of human disorders have been linked to mutations in T-box genes, confirming their medical importance (Packham and Brook, 2003). Recently, a knockout of TBX2 in mice resulted in abnormal development of the heart (Harrelson et al., 2004).

Ntl is shown to function in parallel to Wnt5 signalling in the morphogenesis of the posterior body (Marlow et al., 2004) and Xbra is shown to regulate Wnt11 expression during gastrulation (Tada and Smith, 2000). The *Drosophila Tbx2*-related opto-motor blind (omb) is regulated by the Wingless (Wg), Decapentaplegic (Dpp) (Grimm and Pflugfelder, 1996) and Hedgehog (Hh) (Kopp and Duncan, 1997) signalling pathways; *Xenopus* Tbx2 is known to function within the Sonic hedgehog (Shh) pathway (Takabatake et al., 2002); in chick, Tbx2 is known to function through both Shh and Bmp signalling (Suzuki et al., 2004).

Zebrafish *tbx2b* was previously named *tbx-c*. Using a dominant-negative (dn) approach, it was shown to function downstream of Tgfβ signalling, of *ntl* and of *floating head* (*flh*) in the late-phase specification of the notochord and development of motoneurons (Dheen et al., 1999). In this report, we show that neural development is dependent on early Tbx2b activity during gastrulation. Using a combination of antisense morpholino oligonucleotide (MO) gene 'knockdown' (Nasevicius and Ekker, 2000) and in vivo analysis of chimaeric embryos generated by cell transplantation or single blastomere injection, we demonstrate that, during neural plate formation and neuronal specification, Tbx2b functions within the context of Wnt signalling to mediate cell migration.

Materials and methods

Reagents

MOs were obtained from Gene Tools (USA). Sequences were as follows (sequence complementary to predicted start codon is underlined): *tbx2b* MO, 5′-GGA AAG GGT GGT AAG CCA TCA CAG T-3′; *tbx2b* MOv2, used for all data generated in this study, 5′-GGT AAG CCA TCA CAG TCC CTG TAA A-3′; *fz7* MO, 5′-ATA AAC CAA CAA AAA CCT CCT CGT C-3′; *fz7a* MO, 5′-CCA ATC TGG AGC TCC AGA CGT GAC C-3′; *fz2* MO, 5′-ACA AAA TGA GTC CGG CAA ACT ATG C-3′; *axin1* MO, 5′-CAT AGT GTC CCT GCA CTC TGT CCC A-3′ phenocopies the mutant *masterblind*; *stbm* MO is as described (Park and Moon, 2002); *ntl* MO is as described (Nasevicius and Ekker, 2000); *b-jun* MO, 5′-ACT CAT AGA GTT GGA AAA CCG GTG G-3′; *c-jun* MO, 5′-TTT AGG CGC TGT TAA GCA CTG TCC G-3′. Stocks (1 mM) were made in Danieau's solution. Pertussis toxin was obtained from Sigma (P2980, 200 mg/ml).

Whole-mount in situ hybridization, immunohistochemistry, western blot and TOP-Flash assay

Whole-mount in situ hybridization and whole-mount immunohistochemistry with anti-fluorescein-POD were performed according to established techniques. Proteins were extracted from 20 embryos/lane for western blot, and detected with chemiluminescent detection kit (Cell Signalling Technology, USA). TOP-flash assay was performed as described (Korinek et al., 1997).

Dominant negative Fz7-EGFP/BAC construct

Dn-*fz7* targeting construct was generated from *fz7* cDNA by replacing the stop codon with an EGFP-kanamycin cassette using overlapping amplicons and primer extension. Primer sequences were as follows: 5′UTRF, 5′-AGG AAA CCG CAC TCT GTT CA-3′; *fz7*R, 5′-TAC CGT CGT CTC GCC CTG GTT-3′; *fz7*EGFPF, 5′-GGC GAG ACG ACG GTA ATG GTG AGC AAG GGC-3′; kanR, 5′-TCA GAA GAA CTC GTC AAG AAG GCG ATA GAA-3′; kan3′UTRF, 5′-CTT CTT GAC GAG TTC TTC TGA GAA AAA GAG CGA TCG TTT TCG-3′; and 3′UTRR, 5′-ACA AGT CCC CGG TTA AAA CAA GTG TTG G-3′. The resultant dn*fz7*-EGFP construct was co-transformed with pGETrec into *E. coli* DH10B carrying a BAC of the intronless *fz7* gene. Homologous recombination was then induced (Narayanan et al., 1999).

Transplantation

Donor embryos were injected at the one-cell stage with fluorescein dextran pre-mixed with MO or Danieau's solution. About 20 cells from each donor were transplanted into wild-type host embryo of the same stage. Chimaeric embryos were grown to 10 and 24 hpf. Location of transplanted cells at 10 hpf was visualized by a combination of immunohistochemistry with anti-fluorescein-POD and *sox19* whole-mount in situ hybridization. Images were taken using the Olympus AX70 (Olympus, Japan) microsope fitted with CCD camera. Fluorescent and bright-field images were superimposed with Photoshop 5.5 (Adobe) software.

Injections at 16 cell stage

Dechorionated 16-cell stage embryos were transferred to a Petri dish with moulded agar (1.5% agarose in egg water) injection wells and one central blastomere was injected with not more than 200 pl of reagents. Injected embryos were allowed to develop to 4 hpf, and then were inspected under a UV dissecting microscope. Embryos with labelled clones in the centre of the blasdoderm, when viewed from the animal pole, that represented a perfect cone when viewed from the side, were allowed to develop further. In this way only ectodermal derivatives were labelled.

Real time RT-PCR

Total DNA-free RNA (1 mg) was subjected to oligo(dT)15 primed RT with PowerScript Reverse Transcriptase (Clontech) according to the manufacturer's recommendations, and 1/20 of the reaction mix was used for PCR. Real-time semi-quantitative PCR assay was carried out using gene-specific primers for *tbx2b* (forward, 5′-AGG AAC CCG TTC TTG AGC AGC-3′; reverse, 5′-AGG CCG CTT GGC AAT CCG GTG-3′), EF1α (forward, 5′-AGA CTG GTG TCC TCA AGCC TG-3′; reverse, 5′-TGA AGT TGG CAG CCT CCA TGG-3′) and *fz7* (forward, 5′-TCA CTG TGG CTC TAC AAA CGA CC-3′; reverse, 5′-TGC ACT TCG AGA CCG GCG TCC-3′) in a DNA Engine Opticon System (MJ Research, USA). SYBR Green was used as the reporter for real-time PCR. Briefly, HotStart Taq (Qiagen) activation for 15 minutes, four segment amplification and quantification program repeated 35 times [95°C for 30 seconds; 62°C for 10 seconds with a single fluorescence measurement; 72°C for 30 seconds, melting curve program (78°C to 95°C)]. Serial dilutions of cDNA were used as standards for semi-quantitation. Correction for inefficiencies in RNA input or reverse transcriptase was performed by normalizing to EF1α

amplification. The comparative C(T) method, calculating relative expression levels compared to control, was used for quantification.

Hanging-drop culture

Hanging-drop cultures were carried out with animal caps from embryos at 50% epiboly as previously described (Steinberg and Takeichi, 1994). Fluorescent images were obtained with a Zeiss Axioplan2 equipped with Zeiss AxioCam HRc CCD camera (Zeiss, Germany).

Results

RT-PCR showed that *tbx2b* transcripts are not maternally supplied and appear only at 50% epiboly (5.5 hpf, Fig. 1A and data not shown). Real-time PCR measurements of the level of transcripts in the dorsal and ventral half of 5.5 hpf embryos (when the shield could be seen with confidence) indicated that *tbx2b* is present at a higher level in the ventral blastoderm than the dorsal blastoderm (Fig. 1E). By 8 hpf and later, the transcripts accumulate in the dorsal blastoderm and dorsal structures – the notochord and neural derivatives (Dheen et al., 1999). This shift in the distribution of *tbx2b* from ventral to dorsal coincides with the dorsal CE movement of cells during gastrulation.

The initial functional analysis on the role of *tbx2b* in development was performed with a dn-Tbx2b lacking the C-terminal transactivation domain (Dheen et al., 1999). For this study, a MO-mediated loss-of-function approach (targeted gene 'knockdown') was adopted. Two anti-*tbx2b* MOs were designed (see Materials and methods). Both straddle the start codon of *tbx2b*, but offset by 10 bases along the 5′-UTR. To establish their efficacy, the two MOs were injected into one-cell stage embryos (pan-embryonic injection). At the same concentration, *tbx2b* MOv2 was more effective in producing a phenotype than *tbx2b* MOv1 and was used for all experiments in this study (henceforth referred to as *tbx2b* MO).

When co-injected with *tbx2b* MO pan-embryonically, translation of a *myc*-tagged *tbx2b* containing the target site for *tbx2b* MO was blocked in a dose-dependent manner (Fig. 1B). The midline axial mesoderm of the morphants, as analyzed and compared with embryos obtained from overexpression of dn-Tbx2b with the marker *sonic hedgehog* (*shh*), had malformed notochord and lacked the floor plate (Fig. 1C). In the most severely affected morphants, only remnants of the notochord were present (Fig. 1D). This is reminiscent of the mutant *flh*, and is in agreement with our previous study (Dheen et al., 1999). These results suggest that the phenotype observed with *tbx2b* MO was indeed specific to the 'knockdown' of *tbx2b*.

Pan-embryonic 'knockdown' of *tbx2b* with *tbx2b* MO delayed the onset and progression of gastrulation by up to 2 hours and produced phenotypes at 24 hpf in a dose-dependent manner. In its most severe form (at 1 pmol/embryo), *tbx2b* morphants display phenotypes similar to *boz*$^{-/-}$ embryos (Fekany-Lee et al., 2000) – short AP axis, absent or malformed notochord, fused somites, small and/or cyclopic eyes, and small brain (Fig. 1F-G). Cross-sections of the morphants at the level of the eyes showed that the neural tube was severely malformed: the ventricle was absent and the eyes were underdeveloped (Fig. 1H,I). Injections of a sense MO up to 10 pmol showed no phenotype.

The disorganized forebrain of the *tbx2b* morphant supported a role for Tbx2b in neural development. However, the severity of the malformation rendered analyses of pan-embryonic morphants ambiguous. To circumvent this, we analyzed the behaviour of Tbx2b-deficient cells in chimaeric embryos. The chimaeras were generated by two complementary approaches aiming to target ectodermal derivatives – cell transplantation and single-blastomere injection.

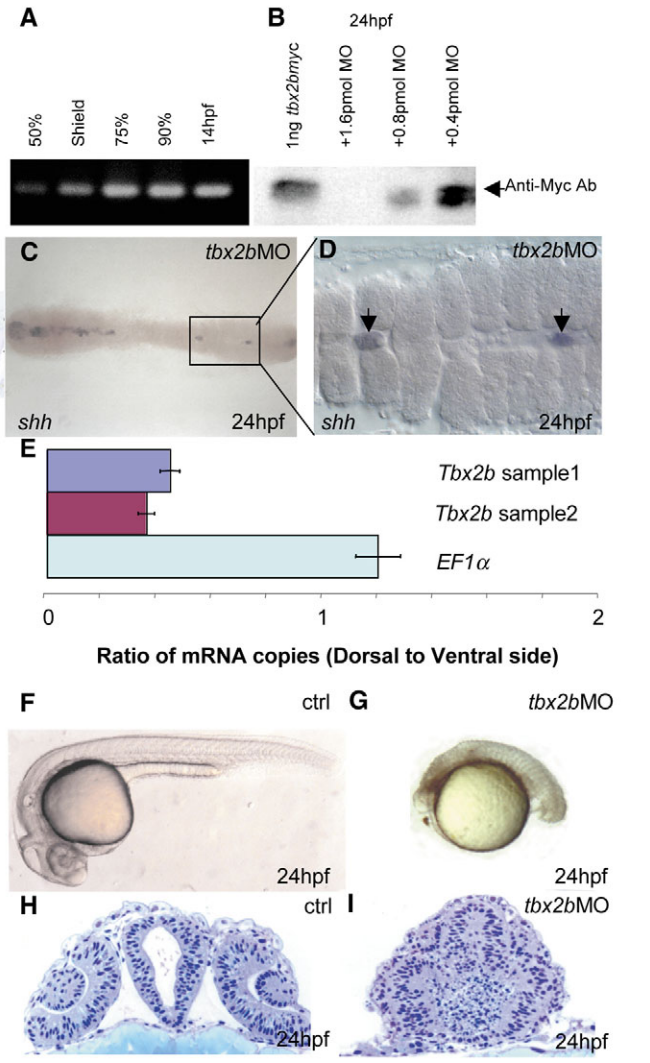

Fig. 1. *tbx2b* MO blocks translation of *tbx2b* and impairs normal development. (A) RT-PCR using primers specific to the 5′-UTR of *tbx2b* shows that this transcript was present as early as 50% epiboly. (B) Western blot with anti-Myc antibody shows that translation of recombinant *tbx2b-myc* was blocked in the presence of *tbx2b* MO in a dose-dependent manner. (C) Dorsal view of *tbx2b* morphant shows the almost complete loss of *shh* in the trunk region of the embryo. The boxed section is enlarged in D, showing the *shh*-positive cells as remnants of notochord (arrow). (E) Real-time PCR shows that *tbx2b* transcripts are present at a higher level in the ventral gastrula (5.5 hpf) when compared with *EF1α*. (F,G) Phenotype of *tbx2b* morphant (2 pmol) (G) when compared with control (F) (see text for description). (H,I) *tbx2b* is required for proper development of the eyes and forebrain. (H) Plastic cross-section through the forebrain of a 24 hpf control embryo at the level of the lens. (I) Cross-section of the *tbx2b* morphant shows severe disorganization of the forebrain and eyes.

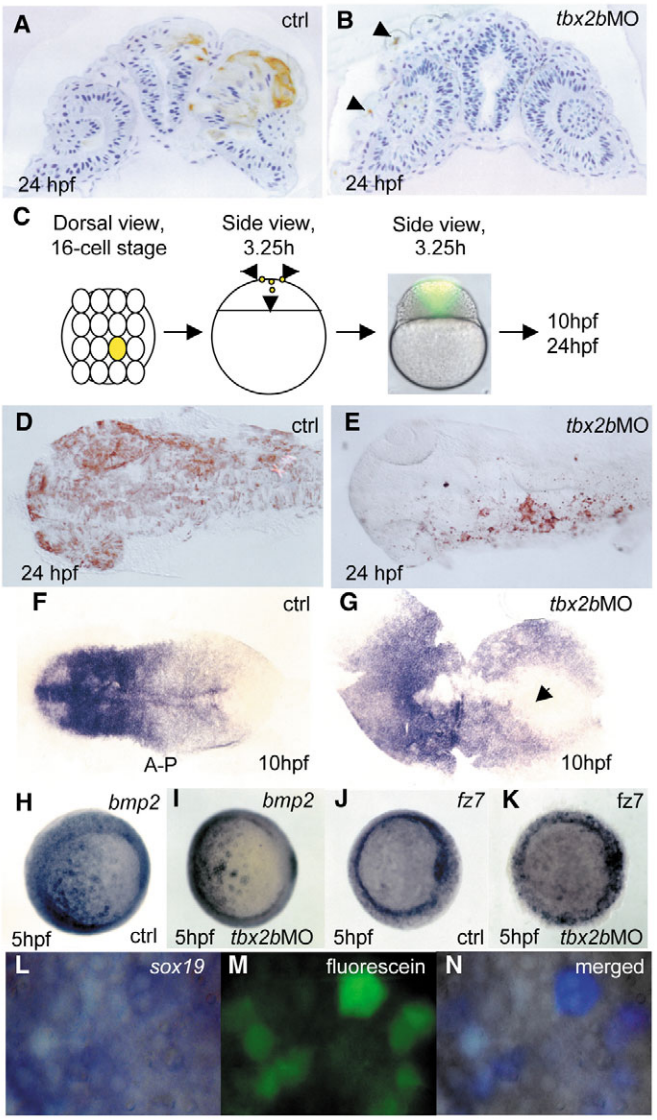

Fig. 2. Tbx2b is required for cells to adopt a neural fate. Deep cells from embryos co-injected with fluorescein-dextran (70 kDa) and *tbx2b* MO at 30% epiboly were transplanted into homochronic wild-type hosts. (A) Cross-section through the neuroretina and brain shows transplanted control labelled cells in the CNS. By contrast (B) transplanted Tbx2b-deficient cells were present only in the epidermis (arrowheads). (C) One central blastomere of 16-cell stage embryos was injected with fluorescein either with or without *tbx2b* MO, and embryos were allowed to develop to 24 hpf. Both control and *tbx2b* morphants developed normally and showed a similar distribution of labelled clones in vivo at 3.25 hours. (D) Dorsal view of 24 hpf control embryo shows labelled cells in neural plate and epidermis. (E) *tbx2b* morphant labelled cells were present only in epidermis. (F,G) Whole-mount in situ hybridization with the pan-neural marker *sox19* shows a delay in convergence of the neural plate in *tbx2b* morphant (arrow in G) compared with control (F). (H-K) Whole-mount in situ hybridization with *bmp2* (H,I) and *fz7* (J,K) show similar expression patterns in control and Tbx2b morphant at 5 hpf. (L-N) Transplanted fluorescein labelled Tbx2b-deficient cells continue to express *sox19* in 5 hpf wild-type host. (N) The merged photographs were enhanced in Adobe Photoshop such that only the simultaneous presence of blue (whole-mount in situ hybridization signal) and green (fluorescence) produced a purple signature. Otherwise, cells remain grey.

Fluorescein-dextran-labelled cells of the animal blastoderm were transplanted from 4 hpf wild-type donor embryos into the same location in homosynchronous wild-type hosts. By 24 hpf, labelled cells were found in the brain, eyes and epidermis (Fig. 2A). In similar transplants, when *tbx2b* morphant cells were placed in wild-type hosts, the labelled cells appeared only in the epidermis (Fig. 2B), supporting the suggestion that Tbx2b may be required during the formation of the neural plate. To confirm this, a single central blastomere of 16-cell stage embryos was injected (referred to as a 1/16 injection, Fig. 2C) with fluorescein, either with or without *tbx2b* MO, and the position of the labelled cells determined later. At 3.25 hpf, both control and *tbx2b* MO-injected embryos showed labelled clones in the ectoderm (Fig. 2C), suggesting that right up to this stage there were no discernible behavioural differences between control and *tbx2b* morphant cells. However, at 24 hpf, control embryos had labelled cells in the eyes, epidermis and CNS (Fig. 2D), while *tbx2b* MO injected embryos displayed labelled cells only in the epidermis (Fig. 2E), thus supporting the observations from transplantation experiments.

In both transplantation and single-blastomere injection experiments, there were reduced numbers of Tbx2b morphant cells compared with control. This could arise from an increase in cell death, from a decrease in cell proliferation or from cell loss. Staining of *tbx2b* morphants with Acridine Orange and TUNEL assay showed no significant increase in apoptosis (not shown). We also failed to observe cell loss because of sloughing during gastrulation, although we could not rule out this possibility later in development. Therefore the reduction in cell count was probably the result of impairment in cell proliferation. This is consistent with reports implicating human TBX2 in cell cycle control and oncogenesis (Jacobs et al., 2000; Prince et al., 2004).

sox19 encodes the early pan-neural transcription factor (Vriz and Lovell-Badge, 1995). It is expressed in the neural plate at 10 hpf (Fig. 2F). In *tbx2b* morphants the neural plate was broader, with a pronounced gap in expression around the midline (Fig. 2G, arrow). We asked if this was likely to be due to an early defect in specification, and thus focused on at early patterning. The expression patterns of *bmp2* and *fz7* in control and morphant 5 hpf embryos were similar (Fig. 2H-K), although expression in the morphants appeared to be more punctate than in control embryos. This could be the result of the delayed epiboly in *tbx2b* morphants. In addition, during gastrulation, transplanted donor cells from *tbx2b* morphants continue to express *sox19* in wild-type hosts at 5 hpf (Fig. 2L-N). These results suggest that early fate specification is not affected by the loss of Tbx2b function; instead, dorsal convergence cell movement was delayed in the morphants.

When 1/16 injected embryos were stained for both fluorescein and *sox19* at 10 hpf, control labelled cells were found in the neural plate and epidermis (Fig. 3A). By contrast, Tbx2b morphant cells were excluded from the neural plate (Fig. 3B). This suggested that the lack of labelled cells in the 24 hpf morphants observed in previous experiments was due to the absence of labelled cells in the neural plate at 10 hpf. 1/16 injection of *tbx2b* mRNA led to the appearance of labelled cells with normal morphology at the midline at 10 hpf, and in the notochord at 24 hpf, in about 10% of the injected embryos (n=30, Fig. 3C,D). Although this result is consistent with the role of Tbx2b in the formation of axial mesodermal structures

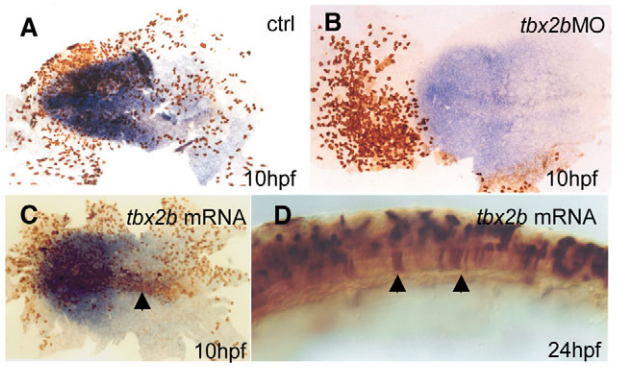

E

Phenotypes / Reagents	Exclusion	No Exclusion	In notochord
Control *n*=50	0%	100%	0
MO(0.05pmol) *n*=38	65%	35%	0
MO(0.05pmol)+ mRNA(0.5ng) *n*=23	61%	39%	0
MO(0.05pmol)+ mRNA(1ng) *n*=22	36%	55%	9% (2)
mRNA(1ng) *n*=30	0%	90%	10% (3)

Fig. 3. 'Exclusion' phenotype can be rescued by *tbx2b* mRNA. Compared with control (A), a 1/16 injection of *tbx2b* MO led to 'exclusion' phenotype (B) at 10 hpf. Neural plate highlighted with *sox19* in blue; fluorescein labelled cells in brown. By contrast, 1/16 injection of *tbx2b* mRNA (1.0 ng) led to (C) labelled cells with normal morphology in the midline (arrow) at 10 hpf and, (D) the notochord (arrows) at 24 hpf, consistent with the role of Tbx2b in axial mesodermal specification. (E) Exclusion phenotype at 10 hpf from *tbx2b* MO (0.05 pmol) was rescued with *tbx2b* mRNA lacking the target site in a dose-dependent manner. In the presence of *tbx2b* MO, 1.0 ng mRNA led to appearance of labelled cells in the midline similar to C and D, while significantly reducing the number of embryos with 'exclusion' phenotype. 0.5 ng mRNA was less effective in reducing the 'exclusion' phenotype but did not cause appearance of labelled cells in the midline.

(Dheen et al., 1999) it is nevertheless interesting and surprising because the clonal population derived from the injected blastomere were ectodermal in origin. This apparent re-specification of fate across germ layers by overexpression of *tbx2b* needs to be further investigated.

The percentage of embryos with an 'exclusion' phenotype, where labelled cells arising from 1/16 injection of *tbx2b* MO were excluded from the neural plate (as defined by *sox19* expression) at 10 hpf, was significantly reduced in a dose-dependent manner by co-injection of a *tbx2b* mRNA lacking the target site for *tbx2b* MO. This phenomenon was accompanied by the appearance of labelled cells in the midline and the notochord at 10 and 24 hpf, respectively, in about 10% of experimental embryos (Fig. 3E). In all, the results support the specificity of *tbx2b* MO and demonstrate the early requirement of Tbx2b in the formation of the neural plate.

The 'exclusion' phenotype points to aberrant cell migration within the embryonic ectoderm, suggesting that cell adhesion could be compromised. The surface of embryos undergoing gastrulation is smooth (Fig. 4A). By contrast, pan-embryonic injections of *tbx2b* MO (Fig. 4B) caused rounding of cells on the surface of morphants. As a result, the morphants acquired a 'rough' phenotype, suggesting that cell adhesion in vivo was affected. Currently, we do not know if there were other cell polarity defects associated with this 'rough' phenotype.

To test whether Tbx2b-depleted cells exhibited altered cell adhesion properties, cell re-association experiments were performed. Texas Red-labelled animal caps of 5 hpf embryos from wild-type or MO-depleted embryos were dissociated and mixed with fluorescein-labelled wild-type cells and cultured as hanging-drop. After 24 hours, the two control-derived populations formed a single aggregate (Fig. 4D), suggesting similar surface adhesion properties. By contrast, cells that were co-injected with fluorescein and *tbx2b* MO (Fig. 4E) formed shells around small aggregates of control cells. This is consistent with idea that aggregated control cells have higher level of the same cadherin than do morphant cells in the outer shells (Steinberg and Takeichi, 1994).

Cadherins are essential for cell adhesion. Indeed, supporting the observation from hanging-drop culture, the level of cadherins failed to increase during gastrulation in *tbx2b* morphants (Fig. 4G). This suggests that the deficiency in cadherins could be the proximal cause of the defects in cell adhesion and migration observed in vivo. It is known that during epiboly, cell-cell adhesion plays a crucial role in maintaining the integrity of the ectodermal sheet (Concha and Adams, 1998). Although *Xbra* is known to inhibit cell migration, it was shown to do so by inhibiting adhesion to fibronectin instead of affecting the level of cadherin directly (Kwan and Kirschner, 2003). The mutation in *parachute* (*pac*) eliminates N-cadherin. Similar to *tbx2b* morphants, this mutant is characterized by abnormal anterior neural tube (Lele et al., 2002). Indeed, cells transplanted from $pac^{-/-}$ into wild-type hosts failed to populate the anterior CNS by 24 hpf (9/9). By contrast, cells from heterozygous siblings were found in the CNS of hosts (10/10).

To demonstrate that migration of cells deficient in Tbx2 is also affected, morphant cells were co-transplanted with control cells into the ectoderm of wild-type embryos and observed in vivo (Fig. 4H-I). The morphant cells lagged behind control cells when migrating to the dorsal side of the embryo at 50% (Fig. 4J) and 80% epiboly (not shown). In addition, by the end of gastrulation, these cells did not express *sox19* and remained outside the neural plate at 10 hpf (Fig. 4L). Thus, an essential aspect of neural plate formation is the requirement of Tbx2b for optimal cell adhesion and consequent cell movement into the dorsal ectoderm destined to develop as the neural plate.

The appearance of 'exclusion' phenotype from 1/16 injection of *tbx2b* MO in neural plate stage embryos provided a quick assay to screen for genes that are potentially functioning in the same pathway as *tbx2b* (Table 1). Reagents (MOs or mRNAs) were injected in the 1/16 manner together with a fluorescein tracer, and the number of embryos exhibiting the 'exclusion' phenotype at 10 hpf was scored. A percentage similar to or higher than that obtained from *tbx2b* MO suggests a potential correlation of function. MOs and mRNAs used in the screen were previously tested in pan-embryonic injections

for efficacy and viability (data not shown). Where available, MOs were tested to phenocopy the respective mutants (see Materials and methods). The assay allowed us to narrow down quickly on a potential pathway.

Consistent with the role of Bmp suppression in neural induction, 1/16 injection of *bmp2* mRNA led to 'exclusion' phenotype in all experimental embryos. This is in contrast to injection of dn-BmpR, which blocked Bmp signalling (Neave et al., 1997). A 1/16 injection of *b-jun* and *c-jun*, known to be involved in CE movement through non-canonical Wnt signalling (Myers et al., 2002), led to complete exclusion, supporting the notion that the 'exclusion' phenotype arises from a cell movement defect. A 1/16 injection of PKA (Fig. 4N, a negative regulator of the Hh pathway) (Hammerschmidt et al., 1997) and XFD (Fig. 4O, which blocked FGF signalling) (Schulte-Merker et al., 1995) failed to recapitulate the exclusion phenotype and thus ruled out the involvement of the Hedgehog and FGF pathways upstream of Tbx2b. By contrast, interference of Wnt signalling by overexpression of a dn-Fz7 that lacked the C-terminal intracellular PDZ-binding domain led to the 'exclusion' phenotype (Fig. 4P). Detailed analyses showed that a similar effect could be obtained with anti-*fz7* MO (*fz7* MO, Fig. 4Q), but not with MOs against the closely related *fz7a* and the more distantly related *fz2* (Table 1).

Next, intracellular components downstream of Fz7 were analyzed (Table 1). Dishevelled (Ds) consists of three functional domains: the DIX domain is essential for β-catenin activity, whereas the PDZ and DEP domains are involved in non-canonical signalling (Topczewski et al., 2001). Constructs of *Xenopus* Ds (Xds) with domain deletions were injected in the 1/16 manner. Of these three constructs, only XdsΔDIX, which lacks DIX domain, phenocopied the exclusion phenotype, suggesting that a disruption of β-catenin signalling could contribute into the 'exclusion' phenotype. Indeed, TOP-flash assay of Fz7 morphant embryos indicated a marked decrease in the level of β-catenin-dependent Tcf activity (Fig. 5A). Although MOs against *b-jun* and *c-jun* led to exclusion, the inability of the XdsΔDEP (without DEP domain) and XdsΔPDZ (without PDZ domain) to induce exclusion is particularly interesting as the non-canonical pathway is known to function via corresponding domains to activate the JNK/SAPK cascade (Korinek et al., 1997). Owing to the pleiotropic nature of β-catenin and Jun, rescue experiments with *tbx2b* remain complicated. In summary, the screen showed that interfering with Wnt signalling consistently produced the same effect as depletion of Tbx2. These results led us to focus our analysis on *fz7*.

fz7 is expressed in the ectoderm during gastrulation (Fig. 5B); thus, it is present in the ectodermal cells at the time when they acquire neural fates. Ectopic overexpression (by intracellular injection of DNA construct into one-cell stage embryos) of a dn-Fz7-EGFP/BAC (with the EGFP inserted into the C terminus to replace the stop codon) caused the loss of *tbx2b* expression (Fig. 5C). Real-time PCR analysis of *tbx2b*- and *fz7*-morphants (MOs injected at 0.5 pmol and 0.2 pmol)

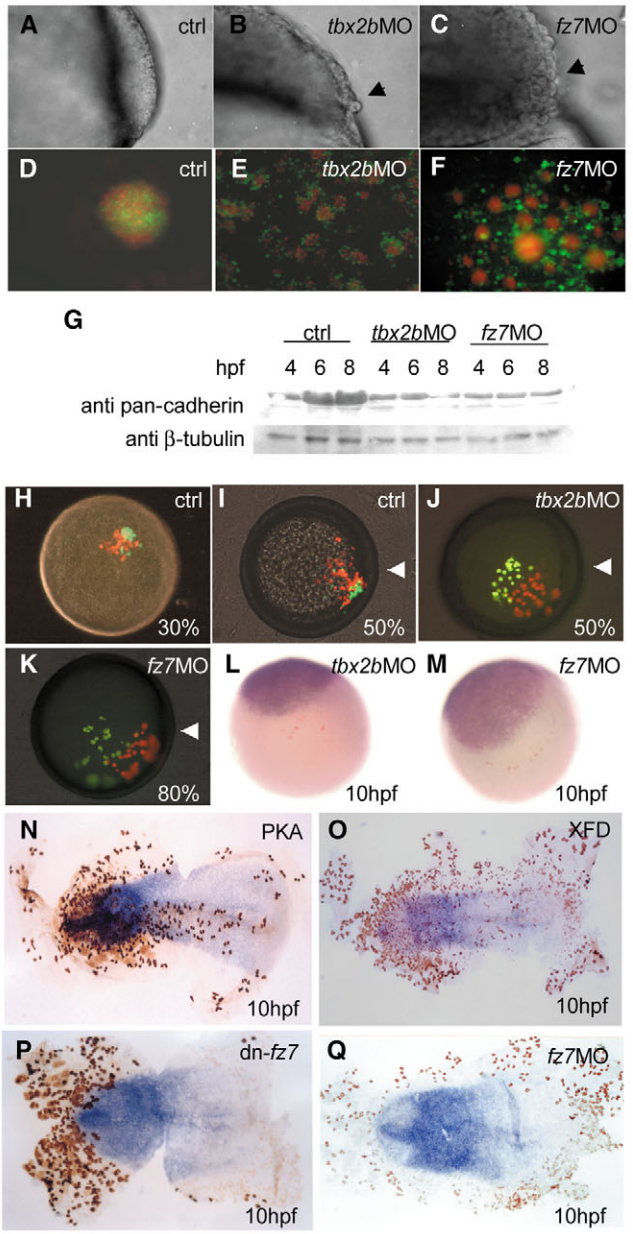

Fig. 4. (A-G) Early function of Tbx2b and Fz7 is required for cell adhesion. The smooth surface of (A) a wild-type gastrulating embryo, is in contrast to the 'rough phenotype' (black arrows) in (B) Tbx2b and (C) Fz7 morphants. (D) In control, dissociated 6 hpf cells labelled with fluorescein (green) and Texas Red (red) formed a single aggregate after 24 hours in hanging drop culture. By contrast, cells derived from fluorescein-labelled (E) Tbx2b- and (F) Fz7-morphant cells formed single layer shells around wild-type Texas Red-labelled aggregates. (G) Western blot with a pan-cadherin antibody showed that the level of cadherins in Tbx2b and Fz7 morphants remained the same or declined in contrast to the control. (H-M) Cell movement during gastrulation was affected in Fz7- or Tbx2b-deficient cells. Control cells with fluorescein and Texas Red transplanted into wild-type host at (H) 30% epiboly co-migrated towards the dorsal side by (I) 50% epiboly, but fluorescein labelled (J) Tbx2b and (K) Fz7 morphant cells were unable to migrate (white arrowheads indicate position of the shield). A 10 hpf embryo stained for fluorescein (brown) shows that transplanted (L) Tbx2b and (M) Fz7 morphant cells were excluded from the *sox19*-positive neural plate. (N-Q) Flat mounts of 10 hpf embryos, double stained for fluorescein (brown) and *sox19* (blue), after single cell injection at 16-cell stage with (N) PKA, (O) XFD, (P) dn-Fz7 and (Q) *fz7* MO.

Table 1. Screen shows the involvement of Fz7 and the Wnt pathway in the 'exclusion' phenotype

Reagent	Embryos with phenotype (%)	*n*
Control MO	0	50
tbx2b MO	65	38
aa+*tbx2b*	36	22
bmp2	100	26
dn-BMPR	8	25
PKA	0	25
dn-fz7	40	25
*fz7*MO	73	45
aa+*tbx2b*	42	26
*fz7a*MO	7	26
*fz2*MO	22	27
XdsΔDIX	62	26
XdsΔDEP	0	26
XdsΔPDZ	0	23
b-jun MO	100	21
c-jun MO	100	17
stbm MO	0	15
ntl MO	9	34
Pertussis toxin	17	24

showed that whereas *fz7* MO downregulates *fz7* and *tbx2b* transcription at 5 hpf, *tbx2b* MO has no effect on the transcription of *fz7* and its target mRNA (Fig. 5E).

Further analysis showed that *fz7* morphants displayed 'rough' phenotype during gastrulation (Fig. 4C), *fz7*-deficient cells failed to aggregate with control cells in hanging-drop cultures (Fig. 4F), *fz7* morphants failed to upregulate cadherins (Fig. 4G), and transplanted *fz7*-deficient cells did not co-migrate with control cells (Fig. 4K,M). A 1/16 co-injection of *tbx2b* mRNA with *fz7* MO led to the appearance of morphologically undifferentiated labelled cells in the eyes and forebrain at 24 hpf (Fig. 5D), suggesting that Tbx2b is able to rescue the cell movement, but not the fate specification function of Fz7. Owing to the pleiotropic nature of Fz7 function, attempts to rescue the 'exclusion' phenotype of *fz7* MO by co-injection of a *fz7* mRNA without the MO target site were unsuccessful. Together, these results suggest that Tbx2b may function as a downstream effector of Fz7-mediated cell movement during neural plate formation (Djiane et al., 2000).

Is the cell movement defect arising from Tbx2b 'knockdown' the direct cause of neuronal specification failure in these cells later in development? To answer this, cells from shield stage (6 hpf) of Tbx2b morphant donors were transplanted directly into the dorsal side of homochronic wild-type hosts at two locations: one that gives rise to the eyes and the other to the hindbrain by 24 hpf (Kimmel et al., 1990; Moens and Fritz, 1999). Whereas wild-type cells transplanted into wild-type hosts ended up in appropriate positions and differentiated according to neighbouring tissues (Fig. 5F-G), in both cases all transplanted morphant cells ended up in the intended locations at 24 hpf but could not acquire the typical morphology of cells in these tissues, suggesting that they were unable to differentiate properly (not shown).

However, owing to the delay in the onset and progression of gastrulation in morphants, the donors were not morphologically equivalent to wild-type shield stage embryos (they resembled 4 hpf embryos). To confirm that the failure in specification was not due to the delay in development, transplantation was repeated with cells from morphant donors at shield stage irrespective of the actual age (~8 hpf). Although

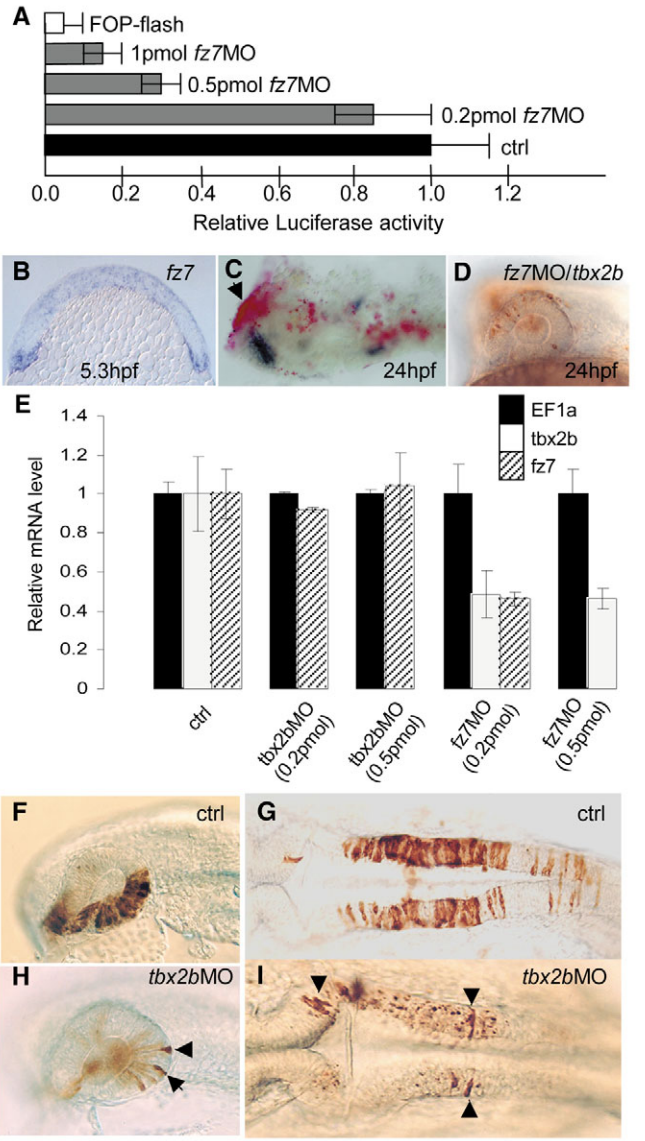

Fig. 5. (A-D) Tbx2b is regulated by Fz7. (A) TOP-flash assay shows a reduction of β-catenin-dependent Tcf activity in *fz7* morphants. (B) Expression of *fz7* at 5.3 hpf (cross-section). (C) Expression of a dn-fz7-EGFP/BAC (red, see Materials and methods) caused the loss of *tbx2b* expression (blue) in the eye (arrow). (D) The absence of *fz7* MO/fluorescein-injected cells in the eyes and CNS at 24 hpf is rescued by co-injection of *tbx2b* mRNA. (E) Real-time PCR analysis of Tbx2b and Fz7 morphants showed a decrease in *tbx2b* and *fz7* transcripts in the presence of *fz7* MO, but no effect from *tbx2b* MO at 5 hpf. *n*=15 for control, *n*=7 for *tbx2b* MO and *n*=4 for *fz7* MO. (F-I) Rescue of cell movement defect by transplantation into wild-type host at shield stage. Wild-type donor cells differentiated into morphologically distinct cells in the eye (F) and hindbrain (G) by 24 hpf. By contrast, only a few Tbx2b-deficient cells differentiated into distinct eye (H) and hindbrain (I) cells (arrowheads).

a few transplanted cells managed to regain the typical morphology of cells in these tissues (arrowheads, Fig. 5H,I), the majority did not. This result suggests that Tbx2b may have a later role in neuronal differentiation. Similarly, we demonstrated that in the absence of Fz7, overexpression of *tbx2b* could only rescue the cell movement defect but not the

Development

subsequent differentiation of transplanted cells (Fig. 5D). Altogether, these results suggest that, independent of its requirement in cell adhesion and cell movement, Tbx2b is necessary, but insufficient, for neuronal differentiation in the late neuroectoderm. *tbx2b* is expressed at high levels in sensory cells and other neuronal lineages later in development, and is therefore likely to play a role in their differentiation (Dheen et al., 1999).

Discussion

The previous loss-of-function study using dn-Tbx2b has shown a role for Tbx2b in the notochord (Dheen et al., 1999). In this study, we used morpholino antisense oligos (MO) to effect a 'knockdown' of Tbx2b to address its early function in development suggested by the presence of its transcripts as early as 50% epiboly, before they were detected by whole-mount in situ hybridization. The specificity of the MO used was established by its ability to block translation of myc-tagged Tbx2b and produce comparable phenotypes in the notochord demonstrated with dn-Tbx2b.

Pan-embryonic injection of *tbx2b* MO led to a delay in epiboly and malformed anterior forebrain at 24 hpf. In order to separate analyses in ectoderm from mesoderm, we focused on the behaviour of Tbx2b-depleted ectodermal cells in an otherwise normal wild-type embryo. We demonstrated that cells deficient in Tbx2b were consistently excluded from the neural plate at 10 hpf, and did not develop as neural cells by 24 hpf. Embryonic cells are pluripotent up to the early gastrula stages (Ho and Kimmel, 1993). Therefore, alteration of cell movement can cause changes in fate specification by virtue of exposure to local signalling cues prevalent in the 'adopted' position. Conversely, a failure in fate specification can cause a change in cell movement behaviour. Either mechanism could lead to exclusion of cells from the neural plate. However, analysis of expression of *bmp2*, *fz7* and *sox19* suggest that early fate specification is not affected by 'knockdown' of Tbx2b. Indeed, the neural plate is induced in the Tbx2b morphant. Our results thus indicate that Tbx2b functions in cell migration in the ectoderm during the formation of the neural plate.

It has been shown that strong intercellular adhesion plays a crucial role in maintaining the integrity of the gastrulating ectodermal sheet (Concha and Adams, 1998). In zebrafish null mutant for N-cadherin (*pac*), neuroectodermal cell adhesion is altered, leading to compromised convergent cell movements during neurulation (Lele et al., 2002). We show that cells depleted of Tbx2b have reduced cadherins, and this altered cell adhesion is likely to be the cause of migration defects leading to their exclusion from the neural plate in chimeras. As β-catenin binds tightly to the cytoplasmic domain of type 1 cadherins (Jamora et al., 2003), loss of cadherins in Tbx2b-depleted cells may lead to defects in β-catenin stabilization and localization, with subsequent consequences in differentiation. As such, there is a possible convergence of Tbx2b, Wnt, β-catenin and cadherin signalling in adhesion, morphogenetic movement and differentiation.

Although *spt* (Ho and Kane, 1990), *T* (Wilson and Beddington, 1997), *ntl* (Conlon and Smith, 1999) and *Tbx5* (Hatcher et al., 2004) have been implicated in cell movement, the roles demonstrated for them are confined within the context of mesoderm. Still, these studies showed that in chimeras with neighbouring wild-type and T-box-deficient cells, the movement of wild-type cells in their normal developmental context resulted in the exclusion of T-box-deficient cells similar to what we demonstrate here. It would seem that this is a common phenomenon and may indicate a general functional mechanism for T-box proteins in cell migration during development.

Interestingly, overexpression of Tbx2b in the ectoderm led to the appearance of cells in the notochord, a mesodermal structure. Although it is known that Tbx2b is required for the specification of axial mesodermal structures at the expense of lateral mesodermal tissues (Dheen et al., 1999), what we demonstrate here is its ability to transfate cells from ectoderm to dorsal mesoderm. We do not yet know the precise mechanism of this phenomenon. However, we show here that a low level of Tbx2b is needed for proper cell adhesion and cell movement within the ectodermal sheet. It is possible that dorsal mesoderm has higher levels of cell adhesion, and the affected cells move into the underlying mesoderm during gastrulation. Analysis with maternal-zygotic *one-eyed-pinhead* (MZ*oep*) mutant cells showed that internalization and mesendoderm formation in zebrafish can be attained autonomously by single cells (Carmany-Rampey and Schier, 2001). If so, it opens the possibility that differential activation of Tbx2b is a mechanism by which systematic differences in cell surface properties and cell segregation behaviour is modulated for the purpose of long-term effects on cell fate specification. More analysis is needed to better understand this observation.

The exclusion phenotype provided a rapid assay for screening signalling pathways that Tbx2b might be operating within. The screen suggests that Tbx2b functions within the context of Wnt signalling, specifically through the receptor Fz7. Zebrafish Fz7, like its homologue in *Xenopus*, has a broad range of functions from fate specification to cell movement, but it is the cell movement requirement for Fz7 that is mediated by Tbx2b. As *Drosophila* Omb also acts within the Wnt context in multiple developmental situations (Grimm and Pflugfelder, 1996), this developmental link may be conserved in evolution. Although Fz7 is shown to regulate *tbx2b* transcriptionally, a full analysis of the detailed molecular mechanism is beyond the scope of this study. Preliminary analysis of the 2.5 kb 5′ genomic sequence of *tbx2b* identified numerous Tcf-binding sites (not shown), hinting at the possibility of regulation of *tbx2b* transcription *via* β-catenin/Tcf.

The functional roles of the canonical and non-canonical Wnt pathways were thought to be quite different (Moon et al., 1997). In vertebrates, Wnt-dependent morphogenetic cell movements were linked to the non-canonical pathway (Tada et al., 2000; Heisenberg et al., 2000), which directly controls Ds-mediated cell polarity (Wallingford et al., 2000). The canonical Wnt pathway was associated with the initiation of CE movements, but not movement per se (Moon et al., 1997). Although β-catenin acts in both signalling and adhesion in insects and vertebrates (Moon et al., 2002), the involvement of the canonical Wnt pathway in cell movement has been shown only in invertebrates (Korswagen, 2002).

In the *Xenopus* blastula, β-catenin was proposed to regulate CE and mediate cell fate via two parallel pathways involving Nodal-related 3 and Siamois, respectively (Kuhl et al., 2001).

In zebrafish, β-catenin modulates Nodal signalling, to regulate both cell fate and cell movement (Myers et al., 2002); and *Boz*, to repress *bmp2b* (Leung et al., 2003). In this study, the ability of Fz7 to mediate Wnt signalling via the DIX-domain of Ds to effect cell adhesion and cell movement during gastrulation suggests that Ds may not function in a strictly modular manner. The current notion that cell movement events are mediated by the non-canonical pathway through the DEP- and PDZ-domains of Ds may need to be looked at afresh.

It has been shown recently that Tbx2 is required for patterning the atrioventricular canal and for morphogenesis of the outflow tract during heart development in mice (Harrelson et al., 2004). Cell migration plays an important role in heart formation in teleosts (Glickman and Yelon, 2002) and amniotes (Hatcher et al., 2004). Although *tbx2b* is expressed in the developing heart and the morphants display cardiac defects later in development (not shown), it remains to be seen if Tbx2b plays a role in the migration of cardiac cells.

Authors are indebted to members of V.K.'s laboratory, to W. Chia and to P. Singh for critical reading of this manuscript. We thank R. Moon, S. Vriz and U. Takeda for reagents and cDNA. We also thank W. Chia, S. H. Yang, E. Manser, D. Grunwald, C.-P. Heisenberg and D. Kimelman for discussion. We thank the anonymous reviewers for their invaluable comments that led to improvement of the manuscript. We apologise to many colleagues whose work was not referred to in this publication owing to space limitations. This work was supported by a research grant from the Agency for Science, Technology and Research of Singapore to V.K. Authors declare that they have no competing financial interests.

References

Baker, J., Beddington, R. and Harland, R. (1999). Wnt signaling in *Xenopus* embryos inhibits *Bmp4* expression and activates neural development. *Genes Dev*. **13**, 3149-3159.

Carmany-Rampey, A. and Schier, A. F. (2001). Single-cell internalization during zebrafish gastrulation. *Curr. Biol*. **11**, 1261-1265.

Concha, M. and Adams, R. (1998). Oriented cell divisions and cellular morphogenesis in the zebrafish gastrula and neurula: a time-lapse analysis. *Development* **125**, 938-994.

Conlon, F. L. and Smith, J. C. (1999). Interference with brachyury function inhibits convergent extension, causes apoptosis, and reveals separate requirements in the FGF and activin signalling pathways. *Dev. Biol*. **213**, 85-100.

Dheen, T., Sleptsova-Friedrich, I., Xu, Y., Clark, M., Lehrach, H., Gong, Z. and Korzh, V. (1999). Zebrafish tbx-c functions during formation of midline structures. *Development* **126**, 2703-2713.

Djiane, A., Riou, J., Umbhauer, M., Boucaut, J. and Shi, D. (2000). Role of frizzled 7 in the regulation of convergent extension movements during gastrulation in Xenopus laevis. *Development* **127**, 3091-3100.

Fekany-Lee, K., Gonzalez, E., Miller-Bertoglio, V. and Solnica-Krezel, L. (2000). The homeobox gene bozozok promotes anterior neuroectoderm formation in zebrafish through negative regulation of BMP2/4 and Wnt pathways. *Development* **127**, 2333-2345.

Glickman, N. S. and Yelon, D. (2002). Cardiac development in zebrafish: coordination of form and function. *Semin. Cell Dev. Biol.* **13**, 507-513.

Grimm, S. and Pflugfelder, G. O. (1996). Control of the gene optomotor-blind in Drosophila wing development by decapentaplegic and wingless. *Science* **271**, 1601-1604.

Hammerschmidt, M., Bitgood, M. and McMahon, A. P. (1997). Protein kinase A is a common negative regulator of hedgehog signalling in the vertebrate embryo. *Genes Dev.* **10**, 647-658.

Hatcher, C. J., Diman, N. Y., Kim, M. S., Pennisi, D., Song, Y., Goldstein, M. M., Mikawa, T. and Basson, C. T. (2004). A role for Tbx5 in proepicardial cell migration during cardiogenesis. *Physiol. Genomics* **18**, 129-140.

Harrelson, Z., Kelly, R. G., Goldin, S. N., Gibson-Brown, J. J., Bollag, R. J., Silver, L. M. and Papaioannou, V. E. (2004). Tbx2 is essential for patterning the atrioventricular canal and for morphogenesis of the outflow tract during heart development. *Development* **131**, 5041-5052.

Heisenberg, C. P., Tada, M., Rauch, G. J., Saude, L., Concha, M. L., Geisler, R., Stemple, D. L., Smith, J. C. and Wilson, S. W. (2000). Silberblick/Wnt11 mediates convergent extension movements during zebrafish gastrulation. *Nature* **405**, 76-81.

Ho, R. K. and Kane, D. A. (1990). Cell-autonomous action of zebrafish spt-1 mutation in specific mesodermal precursors. *Nature* **348**, 728-730.

Ho, R. K. and Kimmel, C. B. (1993). Commitment of cell fate in the early zebrafish embryo. *Science* **261**, 109-111.

Jacobs, J. J., Keblusek, P., Robanus-Maandag, E., Kristel, P., Lingbeek, M., Nederlof, P. M., van Welsem, T., van de Vijver, M. J., Koh, E. Y., Daley, G. Q. et al. (2000). Senescence bypass screen identifies TBX2, which represses Cdkn2a(p19ARF) and is amplified in a subset of human breast cancers. *Nat. Genet.* **26**, 291-299.

Jamora, C., DasGupta, R., Kocieniewski, P. and Fuchs, E. (2003). Links between signal transduction, transcription and adhesion in epithelial bud development. *Nature* **422**, 317-322.

Kimmel, C. B., Warga, R. M. and Schilling, T. M. (1990). Origin and organization of the zebrafish fate map. *Development* **108**, 581-594.

Kopp, A. and Duncan, I. (1997). Control of cell fate and polarity in the adult abdominal segments of Drosophila by optomotor-blind. *Development* **124**, 3715-3726.

Korinek, V., Barker, N., Morin, P. J., van Wichen, D., de Weger, R., Kinzler, K. W., Vogelstein, B. and Clevers, H. (1997). Constitutive transcriptional activation by a beta-catenin-Tcf complex in APC–/– colon carcinoma. *Science* **275**, 1784-1787.

Korswagen, H. C. (2002). Canonical and non-canonical Wnt signaling pathways in Caenorhabditis elegans: variations on a common signaling theme. *BioEssays* **24**, 801-810.

Kuhl, M., Geis, K., Sheldahl, L. C., Pukrop, T., Moon, R. T. and Wedlich, D. (2001). Antagonistic regulation of convergent extension movements in *Xenopus* by Wnt/beta-catenin and Wnt/Ca(2+) signaling. *Mech. Dev*. **106**, 61-76.

Kwan, K. M. and Kirschner, M. W. (2003). *Xbra* functions as a switch between cell migration and convergent extention in the *Xenopus* gastrula. *Development* **130**, 1961-1972.

Larue, L., Antos, C., Butz, S., Huber, O., Delmas, V., Dominis, M. and Kemler, R. (1996). A role for cadherins in tissue formation. *Development* **122**, 3185-3194.

Lele, Z., Folchert, A., Concha, M., Rauch, G. J., Geisler, R., Rosa, F., Wilson, S. W., Hammerschmidt, M. and Bally-Cuif, L. (2002). parachute/n-cadherin is required for morphogenesis and maintained integrity of the zebrafish neural tube. *Development* **129**, 3281-3294.

Leung, T., Bischof, J., Soll, I., Niessing, D., Zhang, D., Ma, J., Jackle, H. and Driever, W. (2003). bozozok directly represses bmp2b transcription and mediates the earliest dorsoventral asymmetry of bmp2b expression. *Development* **130**, 3639-3649.

Marlow, F., Gonzalez, E. M., Yin, C., Rojo, C. and Solnica-Krezel, L. (2004). No tail co-operates with non-canonical Wnt signaling to regulate posterior body morphogenesis in zebrafish. *Development* **131**, 203-216.

Moens, C. B. and Fritz, A. (1999). Techniques in neural development. *Methods Cell Biol*. **59**, 253-272.

Moon, R. T., Brown, J. D. and Torres, M. (1997). WNTs modulate cell fate and behaviour during vertebrate development. *Trends Genet.* **13**, 157-162.

Moon, R. T., Bowerman, B., Boutros, M. and Perrimon, N. (2002). The promise and perils of Wnt signaling through beta-catenin. *Science* **296**, 1644-1646.

Munoz-Sanjuan, I. and Brivanlou, A. H. (2002). Neural induction, the default model and embryonic stem cells. *Nat. Rev. Neurosci*. **3**, 271-280.

Myers, D. C., Sepich, D. S. and Solnica-Krezel, L. (2002). Convergence and extension in vertebrate gastrulae: cell movements according to or in search of identity? *Trends Genet.* **18**, 447-455.

Narayanan, K., Williamson, R., Zhang, Y., Stewart, A. F. and Ioannou, P. A. (1999). Efficient and precise engineering of a 200 kb beta-globin human/bacterial artificial chromosome in E. coli DH10B using an inducible homologous recombination system. *Gene Ther.* **6**, 442-447.

Nasevicius, A. and Ekker, S. C. (2000). Effective targeted gene 'knockdown' in zebrafish. *Nat. Genet*. **26**, 216-220.

Neave, B., Holder, N. and Patient, R. (1997). A graded response to BMP-4 spatially coordinates patterning of the mesoderm and ectoderm in the zebrafish. *Mech. Dev*. **62**, 183-195.

Nelson, W. J. and Nusse, R. (2004). Convergence of Wnt, beta-catenin, and cadherin pathways. *Science* **303**, 1483-1487.

Packham, E. A. and Brook, J. D. (2003). T-box genes in human disorders. *Hum. Mol. Genet.* **12**, R37-R44.
Park, M. and Moon, R. T. (2002). The planar cell-polarity gene stbm regulates cell behaviour and cell fate in vertebrate embryos. *Nat. Cell Biol.* **4**, 20-25.
Prince, S., Carreira, S., Vance, K. W., Abrahams, A. and Goding, C. R. (2004). Tbx2 directly represses the expression of the p21 WAF1 cyclin-dependent kinase inhibitor. *Cancer Res.* **64**, 1669–1674.
Schulte-Merker, S. and Smith, J. C. (1995). Mesoderm formation in response to Brachyury requires FGF signalling. *Curr. Biol.* **5**, 62-67.
Shih, J. and Keller, R. (1994). Gastrulation in Xenopus laevis: involution – a current view. *Semin. Dev. Biol.* **5**, 85-90.
Smith, J. (1999). T-box genes: what they do and how they do it. *Trends Genet.* **15**, 154-158.
Steinberg, M. S. and Takeichi, M. (1994). Experimental specification of cell sorting, tissue spreading, and specific spatial patterning by quantitative differences in cadherin expression. *Proc. Natl. Acad. Sci. USA* **91**, 206-209.
Suzuki, T., Takeuchi, J., Koshiba-Takeuchi, K. and Ogura, T. (2004). Tbx genes specify posterior digit identity through Shh and BMP signaling. *Dev. Cell* **6**, 43-53.
Takabatake, Y., Takabatake, T., Sasagawa, S. and Takeshima, K. (2002). Conserved expression control and shared activity between cognate T-box genes Tbx2 and Tbx3 in connection with Sonic hedgehog signaling during Xenopus eye development. *Dev. Growth Differ.* **44**, 257-271.
Tada, M. and Smith, J. C. (2000). Xwnt11 is a target of Xenopus Brachyury: regulation of gastrulation movements *via* Dishevelled, but not through the canonical Wnt pathway. *Development* **127**, 2227-2238.
Topczewski, J., Sepich, D. S., Myers, D. C., Walker, C., Amores, A., Lele, Z., Hammerschmidt, M., Postlethwait, J. and Solnica-Krezel, L. (2001). The zebrafish glypican knypek controls cell polarity during gastrulation movements of convergent extension. *Dev. Cell* **1**, 251-264.
Vriz, S. and Lovell-Badge, R. (1995). The zebrafish Zf-Sox 19 protein: a novel member of the Sox family which reveals highly conserved motifs outside of the DNA-binding domain. *Gene* **153**, 275-276.
Wallingford, J. B., Rowning, B. A., Vogeli, K. M., Rothbacher, U., Fraser, S. E., Harland, R. M. (2000). Dishevelled controls cell polarity during Xenopus gastrulation. *Nature* **405**, 81-85.
Wessely, O., Agius, E., Oelgeschlager, M., Pera, E. M. and De Robertis, E. M. (2001). Neural induction in the absence of mesoderm: b-catenin-dependent expression of secreted BMP antagonists at the blastula stage in Xenopus. *Dev. Biol.* **234**, 161-173.
Wilson, V. and Beddington, R. (1997). Expression of T protein in the primitive streak is necessary and sufficient for posterior mesoderm movement and somite differentiation. *Dev. Biol.* **192**, 45-58.
Wilson, V. and Conlon, F. (2002). The T-Box family. *Genome Biol.* **3**, 3008.1-3008.7.

Development